



National Library
of Canada

Acquisitions and
Bibliographic Services Branch

395 Wellington Street
Ottawa, Ontario
K1A 0N4

Bibliothèque nationale
du Canada

Direction des acquisitions et
des services bibliographiques

395, rue Wellington
Ottawa (Ontario)
K1A 0N4

Your file Votre référence

Our file Notre référence

NOTICE

The quality of this microform is heavily dependent upon the quality of the original thesis submitted for microfilming. Every effort has been made to ensure the highest quality of reproduction possible.

If pages are missing, contact the university which granted the degree.

Some pages may have indistinct print especially if the original pages were typed with a poor typewriter ribbon or if the university sent us an inferior photocopy.

Reproduction in full or in part of this microform is governed by the Canadian Copyright Act, R.S.C. 1970, c. C-30, and subsequent amendments.

AVIS

La qualité de cette microforme dépend grandement de la qualité de la thèse soumise au microfilmage. Nous avons tout fait pour assurer une qualité supérieure de reproduction.

S'il manque des pages, veuillez communiquer avec l'université qui a conféré le grade.

La qualité d'impression de certaines pages peut laisser à désirer, surtout si les pages originales ont été dactylographiées à l'aide d'un ruban usé ou si l'université nous a fait parvenir une photocopie de qualité inférieure.

La reproduction, même partielle, de cette microforme est soumise à la Loi canadienne sur le droit d'auteur, SRC 1970, c. C-30, et ses amendements subséquents.

Canada

**THE CONVERSION OF AMMONIA, PHENOL AND PYRUVATE
INTO TYROSINE BY THE USE OF THE TYROSINE PHENOL-
LYASE ACTIVITY OF MICROENCAPSULATED *ERWINIA*
*HERBICOLA***

IAN LLOYD-GEORGE

Department of Chemical Engineering

McGill University, Montreal

April, 1993

A thesis submitted to the Faculty of Graduate Studies and Research
in partial fulfillment of the requirements of the degree of Doctor of
Philosophy.

© Ian Lloyd-George

1993



National Library
of Canada

Acquisitions and
Bibliographic Services Branch

395 Wellington Street
Ottawa, Ontario
K1A 0N4

Bibliothèque nationale
du Canada

Direction des acquisitions et
des services bibliographiques

395, rue Wellington
Ottawa (Ontario)
K1A 0N4

Your file *Votre référence*

Our file *Notre référence*

The author has granted an irrevocable non-exclusive licence allowing the National Library of Canada to reproduce, loan, distribute or sell copies of his/her thesis by any means and in any form or format, making this thesis available to interested persons.

L'auteur a accordé une licence irrévocable et non exclusive permettant à la Bibliothèque nationale du Canada de reproduire, prêter, distribuer ou vendre des copies de sa thèse de quelque manière et sous quelque forme que ce soit pour mettre des exemplaires de cette thèse à la disposition des personnes intéressées.

The author retains ownership of the copyright in his/her thesis. Neither the thesis nor substantial extracts from it may be printed or otherwise reproduced without his/her permission.

L'auteur conserve la propriété du droit d'auteur qui protège sa thèse. Ni la thèse ni des extraits substantiels de celle-ci ne doivent être imprimés ou autrement reproduits sans son autorisation.

ISBN 0-315-91660-5

Canada

Submitted by: Ian Lloyd-George

Thesis Short Title:

Detoxification of ammonia and phenol by microencapsulated *Erwinia herbicola*

Thesis Full Title:

The conversion of ammonia, phenol and pyruvate into tyrosine by the use of the tyrosine phenol-lyase activity of microencapsulated *Erwinia herbicola*

This work is dedicated to my maternal grandparents

Mary Jane Dyer

and

Eldon A. Rose

Completed under the direction of T.M.S. Chang O.C. MD PhD FRCP(C)

Director, Artificial Cells and Organs Research Centre

Professor of Physiology, Medicine and Biomedical Engineering.

Associate of Chemistry and Chemical Engineering.

ABSTRACT

The tyrosine phenol-lyase (TPL) - E.C. 4.1.99.2 - activity of free and alginate-polylysine-alginate microencapsulated whole cells of *Erwinia herbicola*, was used to convert ammonia, pyruvate and phenol or catechol into L-tyrosine or dihydroxyphenyl-L-alanine (L-dopa). This conversion could serve as the basis of a novel system for the removal of toxic ammonia and phenol from the blood during liver failure.

It was found that there were endogenous modifiers in the whole cell TPL system, hence the kinetic parameters vary with the amount of cells in the system. However typically the apparent K_M for tyrosine varied from 0.2 mM to 0.28 mM, while that of phenol was 0.5 mM. Whole cell TPL can display kinetics of great complexity, suggesting that the enzyme is likely to be a tetramer.

The effect of process variables on the relative strength of alginate -PLL- alginate microcapsules can be conveniently assessed by entrapping blue dextran (Mwt 2.0×10^6) within the microcapsules and then agitating them within a rotary shaker.

RÉSUMÉ

L'activité enzymatique du tyrosine phenol-lyase (TPL) - E.C. 4.1.99.2 associée aux cellules entières d'*Erwinia herbicola* libres ou contenues dans les microcapsules alginate-polylysine-alginate (APA), a été utilisée afin de convertir soit l'ammoniaque, le pyruvate et le phénol, soit le catéchol, en L-tyrosine ou en dihydroxyphenyl-L-alanine (L-dopa). Cette conversion peut servir de base à un nouveau système ayant pour but l'élimination sanguine d'ammoniaque et de phénols toxiques, lors d'une crise hépatique.

Comme les agents modificateurs endogènes ont été localisés dans le système TPL de la cellule entière, les paramètres cinétiques varient avec le montant de cellules présentes dans le système. Pourtant, le K_M apparent a varié typiquement entre 0.2 mM et 0.28 mM pour le tyrosine, tandis que celui du phénol était 0.5 mM. Le TPL de la cellule entière peut faire preuve d'un caractère cinétique de grande complexité, suggérant qu'il est probable que l'enzyme soit un tétramère.

L'effet des variables du procédé sur la robustesse relative des microcapsules APA peut être convenablement évalué, en enfermant de la dextrine bleue (P.M. 2×10^6) à l'intérieur des microcapsules, assujetties aux secousses d'un agitateur rotatif.

ACKNOWLEDGEMENTS

First and foremost I would like to thank my supervisor Professor T.M.S. Chang O.C.; M.D.; C.M.; Ph.D.; FRCP (C) for the guidance, supervision and the many kindnesses that he has shown me during the course of this project. I consider it a tremendous honour to have been a part of his research group at the Artificial Cells and Organs Research Centre (ACORC).

I would also like to thank the staff of the Chemical Engineering workshop for constructing the droplet former used in this study. The technical staff of ACORC namely, Rahul Varma, Emma Resurrecion and Mr Colin Lister all helped me at one time or another. However a special note of thanks is owed to the chief technician Mr Lister for taking the time to teach me how to use the HPLC.

I was blessed to have had friends such as Dr Silvia Bruni, Maryam Mobed, Vaia Coromilli, Khaled Al-Sugair, Flavio Garafalo, Maurice Cataneo, Felice D' Agnillo and Harry Wong among others during my time at the laboratory. Maryam Mobed provided the French translation of the Abstract.

I would also like to thank Professors Ehud Ilan, Takako Nishiya and Rajendra Sipehia for providing an intellectually stimulating work environment.

The support and encouragement of my family is gratefully acknowledged.

TABLE OF CONTENTS

ABSTRACT	i
RÉSUMÉ	ii
ACKNOWLEDGEMENTS	iii
TABLE OF CONTENTS	iv
LIST OF FIGURES	ix
LIST OF TABLES	xiv
NOMENCLATURE	xvi
 1.0 INTRODUCTION	 1
1.1 GENERAL INTRODUCTION	1
1.2 CONCISE STATEMENT OF THE OBJECTIVES OF THE STUDY	1
 2.0 LITERATURE SURVEY AND BACKGROUND	 4
2.1 THE LIVER AND LIVER FAILURE	4
2.1.1 The Liver	4
2.1.2 Liver Failure	5
2.1.3 Conventional Artificial Liver Support	7
2.1.4. Immobilized Hepatocytes and Artificial Liver Support.	10
2.2 ALTERNATIVE ENZYME SYSTEMS FOR AMMONIA REMOVAL ...	12
2.2.1 Immobilized Enzyme Systems for Ammonia Removal	12
2.2.2 The Microbial Production of Amino Acids	14
2.3 TYROSINE PHENOL LYASE DEAMINATING (EC. 4.1.99.2)	17
2.3.1. Sources of TPL.	17
2.3.2 Reactions of TPL.	19
2.3.3. The Structure of TPL.	20
2.3.4. Kinetic Mechanism of Tyrosine Phenol Lyase.	22
2.3.5. Kinetic Parameters for Tyrosine Phenol Lyase.	25
2.3.6. The Immobilization of TPL Activity.	26
2.4 ARTIFICIAL CELLS	29

2.4.1. Artificial Cells: General Principles.	29
2.4.2. Artificial Cells with Living Cells and Tissues.	31
3.0 EXPERIMENTAL METHODS	35
3.1 MICROENCAPSULATION	35
3.1.1 General Procedure	35
3.1.2. The Droplet Former	38
3.1.3 Application of Treatment Solutions	39
3.1.4. Estimation of the Relative Strength of the Microcapsules	40
3.2 MATHEMATICAL SIMULATION OF SPORE DEATH DURING HEAT STERILIZATION	40
3.2.1. Simulation of Can Temperature During Heat Sterilization.	43
3.2.2. Simulation of Spore Death During Heat Sterilization	45
3.3 THE EFFECT OF STERILIZATION ON THE VISCOSITY AVERAGE MOLECULAR WEIGHT OF ALGINATE.	48
3.3.1. Sterilization Procedure.	48
3.3.2. Estimation of Alginate Molecular Weights.	48
3.4 GROWTH, ACTIVITY AND PRODUCTION STUDIES.	49
3.4.1. Culture Preservation	50
3.4.2. Biomass Versus Time Profiles in Nutrient Broth	50
3.4.2. Growth as a Function of Agitation and Temperature.	51
3.4.3. Enzyme Induction	51
3.4.4. Cell Harvesting	52
3.4.5. Protein Assay	52
3.4.6. Assay of Tyrosine Phenol Lyase (TPL) Activity	52
3.4.7. Assay of L-Tyrosine and L-Dopa	53
3.4.8. L-Tyrosine and L-Dopa Production	54
3.4.9. Data Analysis	54
4.0 RESULTS & DISCUSSION	55

4.1 MICROENCAPSULATION TECHNIQUE	55
4.1.1. Simulation of Spore Death During Sterilization	55
4.1.2. The Effect of Heat Sterilization on Depolymerization of Alginate ...	56
4.1.3. The Effect of Airflow on the Diameter of Alginate-PLL-Alginate Microcapsules.	57
4.1.4. The Effect of Liquid Flow on the Diameter of the Microcapsules ...	68
4.1.5. The Effect of Alginate Preparation and PLL Contact Time on the Relative Strength of the Microcapsules	74
4.1.6. Elution Profile of Blue Dextran 2000	80
4.1.7. Cell Protein in Microcapsules as a Function of Cell Protein in 1.5 % Alginate.	81
4.2 GROWTH STUDIES ON <i>ERWINIA HERBICOLA</i>	82
4.2.1 Absorbance Versus Biomass for <i>Erwinia herbicola</i>	82
4.2.2. Growth of <i>Erwinia herbicola</i> in Nutrient Broth	83
4.2.3. The Growth of <i>Erwinia herbicola</i> as a Function of Temperature. ...	84
4.2.3. TPL Activity Induction with Time Profile.	86
4.3 EXPLORATORY STUDIES OF THE KINETICS OF WHOLE CELL <i>ERWINIA HERBICOLA</i> TPL	88
4.3.1. TPL Activity Versus Biomass Profile	88
4.3.2. The Effect of the Buffer System Used for Activity Determination ...	89
4.3.3. The Effect of the Addition of PLP to the Assay Flasks	90
4.3.4. Initial Rate Kinetics of Whole Cell TPL for the Degradation of Tyrosine.	92
4.3.4a. Basic Features of Velocity versus Substrate Profiles of Initial Rate Data.	92
4.3.4b Kinetic Analysis of Initial Rate Data.	104
4.3.4b (i) Analysis by the Hill and Michaelis-Menten Equations	104
4.3.4b (ii). Analysis by the Model of Monod	113
4.3.4b (iii). Analysis by the Model of Adair.	118
4.3.4b (iv) Analysis by the Model of Koshland, Nemethy and Filmer	118

4.3.4b (v). Summary of the Preliminary Kinetic Analysis of the Initial Rate Data	119
4.4 MICROENCAPSULATED TPL ACTIVITY OF WHOLE CELL <i>E. HERBICOLA</i>	121
4.4.1. Effect of Shaking Speed on the TPL Activity of Free and Microencapsulated <i>Erwinia herbicola</i>	121
4.4.2. The Effect of Temperature on the TPL Activity of Free and Microencapsulated <i>Erwinia herbicola</i>	122
4.4.3. Comparative Study of TPL Activity Versus Substrate Profile for Free and Microencapsulated Whole Cell <i>E. herbicola</i>	124
4.5 PRODUCTION OF TYROSINE OR DOPA WITH THE TPL OF WHOLE CELL <i>ERWINIA HERBICOLA</i>	127
4.5.1. Conversion of Ammonia, Pyruvate and Phenol or Catechol into L-Tyrosine or L-dopa	127
4.5.2 Evaluation of an Approximate Kinetic Model for the Conversion of Ammonia, Phenol and Pyruvate into Tyrosine	129
4.6 GENERAL DISCUSSION	139
4.6.1. Significance of Microencapsulation-Technique Results	139
4.6.2 Significance of Growth-Studies Results.	141
4.6.3 Significance of the Exploratory Kinetic Studies	142
4.6.3a Activity Versus Total Cell Protein in the Assay Profile	142
4.6.3 (b) Significance of the Results Obtained During the External Addition of PLP.	142
4.6.3c. Significance of the Initial Rate Data for the Kinetics of Tyrosine Degradation by Whole Cell TPL of <i>E. herbicola</i>	143
4.6.3c (i) Background to the Initial Rate Experiments Conducted	143
4.6.3c (ii) Significance of the Initial Rate Data for the Degradation of Tyrosine	149
4.6.4. Significance of the Comparative Studies on the TPL Activity of Free and Microencapsulated Whole Cell <i>E. herbicola</i>	155

4.6.4 (a). Comparative Study of TPL Activity for Free and Microencapsulated Cells.	155
4.6.4(b). Significance of the Results Obtained in the Comparative Study for the Production of Tyrosine and Dopa	156
4.6.6. General Considerations and Suggestions for Further Work	160
5.0 CONCLUSIONS	162
6.0 CLAIMS TO ORIGINALITY	165
7.0 REFERENCES	167
8.0 APPENDICES	I
8.1 APPENDIX I	I
8.1.1. Source of And Purity of Chemicals.	I
8.1.2. Chemicals used in Microencapsulation	II
8.2 APPENDIX II	IV
8.2.1. Scans of Blue-Dextran and Alginate Solutions.	IV
8.3 APPENDIX III	VI
8.3.1 Development of Rapid Equilibrium Kinetic Models Used.	VI
8.4 APPENDIX IV	XIX
8.4.1. Photomicrographs of Microcapsules Prepared Similarly to Those Used in Comparative (Free Versus Microencapsulated) Kinetic Studies.	XXI
8.5 APPENDIX V	XXIV
4.5.2 Development of an Approximate Kinetic Model for the Conversion of Ammonia, Phenol and Pyruvate into Tyrosine	XXIV
8.6 APPENDIX VI	XXX
8.6.1 Data Obtained After Prolonged Reaction at 37 °C	XXXI

LIST OF FIGURES

Figure 1.	Schematic representation in the dimeric α_2 molecule of TPL. Domains are shown as circles. The molecular diads (+) are perpendicular to the page. Drawn after Antson et al (1992).	21
Figure 2.	Pyridoxal-5'-phosphate	23
Figure 3.	Summary of the mechanism of tyrosine degradation by TPL	24
Figure 4.	Schematic representation of an artificial cell (adapted from Chang (1972).	30
Figure 5.	Basic scheme of the steps in the formation of alginate-polylysine-alginate microcapsules.	37
Figure 6.	Schematic of the droplet former.	38
Figure 7.	Apparatus for the gelling of alginate drops, or the treatment of alginate gel beads.	40
Figure 8.	Mathematical simulation of spore death during heat sterilization of alginate.	56
Figure 9.	The effect of sterilization on the molecular weight of alginate. Stock solutions of alginate (3% Kelco H.V. or 4 % Kelco L.V. were heat sterilized at 255 °F.	57
Figure 10.	The effect of airflow and alginate concentration on the size of the microcapsules. Values are mean and standard deviation of the size distribution of diameters.	59
Figure 11.	Photomicrograph of microcapsules ($1185 \pm 197 \mu\text{m}$) made with Kelco-Gel HV alginate. The airflow was 2.0 l/min. The microcapsules are spherical and contain yellow <i>E. herbicola</i>	60
Figure 12.	Photomicrograph of microcapsules ($805 \pm 51 \mu\text{m}$) made with 1.5 % Kelco-Gel HV alginate. The airflow was 2.5 l/min. N.B. the yellow coloured bacteria in the microcapsules.	61
Figure 13.	Photomicrograph of microcapsules ($549 \pm 59 \mu\text{m}$) made with 1.5 % Kelco-Gel HV. The airflow 3.0 l/min. N.B. small empty microcapsules.	62
Figure 14.	Photomicrograph of microcapsules ($331 \pm 59 \mu\text{m}$) made with 1.5 % Kelco-Gel HV. The airflow was 3.5 l/min.	63

Figure 15.	Photomicrograph of microcapsules ($796 \pm 54 \mu\text{m}$) made with 0.75 % Kelco-Gel HV alginate. The airflow was 2.0 l/min. Lots of microcapsules are stuck together.	64
Figure 16.	Photomicrograph of microcapsules ($544 \pm 33 \mu\text{m}$) made 0.75 % Kelco-Gel HV. The airflow was 2.5 l/min. N.B. empty capsules, many not well formed.. . . .	65
Figure 17.	Photomicrograph of "microcapsules" made with 0.75 % Kelco-Gel HV. The airflow was 3.0 l/min. N.B. microcapsules are not well formed . . .	66
Figure 18.	Photomicrograph of "microcapsules" made with 0.75 % Kelco-Gel HV alginate. The airflow was 3.5 l/min. N.B. microcapsules are empty or broken.	67
Figure 19.	The effect of liquid flow on the size of the microcapsules made with 1.5 % Kelco-Gel HV.	68
Figure 20.	Size distribution of the microcapsules as a function of liquid flow (L.F. = 0.389 or 0.763 ml/min) and airflow (A.F. in l/min). N.B. the more bimodal distribution when A.F. = 3.0.	70
Figure 21.	Size distribution of microcapsules made with a liquid flow of 1.07 and 1.49 ml/min. The distributions are more bimodal at an airflow of 3.0 l/min than at 2.5 l/min.	71
Figure 22.	Photomicrograph of microcapsules made with 1.5 % Kelco HV alginate. The liquid flow was 1.07 ml/min and the airflow was 2.5 l/min.	72
Figure 23.	Photomicrograph of microcapsules made with 1.5 % Kelco-Gel HV. The liquid flow was 1.07 ml/min and the airflow was 3.0 l/min.	73
Figure 24.	Blue dextran 2000 (MW 2 million) containing microcapsules made with Kelco HV heat sterilized for 5 minutes and PLL reaction time of 10 minutes.	75
Figure 25.	Blue dextran 2000 (Mwt 2 million) containing microcapsules made with Kelco LV alginate sterilized for 5 minutes and a PLL reaction time of 10 minutes.	76
Figure 26.	Breakage of microcapsules made with 1.5 % Kelco HV alginate. . . .	77
Figure 27.	The effect of agitation on the breaking of microcapsules made with Kelco LV alginate sterilized for 5 minutes.	79

Figure 28.	Elution profile for blue dextran 2000, dextran 500 and dextran 150 (d 2000, d500 and d150 respectively).	80
Figure 29.	The amount of whole cell <i>E. herbicola</i> protein encapsulated per ml of microcapsules plotted as a function of the amount of protein in 1.5 % Kelco HV alginate.	81
Figure 30.	The absorbance of <i>Erwinia herbicola</i> cell suspensions in nutrient broth as function of the biomass.	82
Figure 31.	Growth of <i>Erwinia herbicola</i> in nutrient broth as a function of agitation (as rpm) and time.	84
Figure 32.	The Effect of temperature on the growth of <i>E. herbicola</i> in nutrient broth. The shake speed was 180 rpm.	85
Figure 33.	The induction of Tyrosine Phenol-Lyase activity per mg of cell protein in <i>Erwinia herbicola</i> . Biomass as (cell protein per ml) of medium is also shown.	86
Figure 34.	The TPL activity of whole cell <i>E. herbicola</i> as a function of the total protein in the assay and the duration of cell growth in induction medium.	88
Figure 35.	The degradation of tyrosine by the TPL activity of whole cell <i>Erwinia herbicola</i> . N.B. that the addition of excess PLP decreases the rate. . .	91
Figure 36.	Some linearizations of the Michaelis-Menten Equation.	93
Figure 37.	Whole cell TPL activity for the degradation of tyrosine. Note sigmoidal behaviour and intermediate plateaux. Lines are a spline fit and are not meant to indicate a mathematical model.	95
Figure 38.	Lineweaver-Burk plots of the data in Figure 37. N.B. the curvature in the plots.	96
Figure 39.	Eadie and Scatchard plots of the initial rate data shown in Figure 37. Note the clear departure from Michaelis-Menten behaviour.	98
Figure 40.	Hanes plot of the data in Figure 41. Note that at low S the data departs markedly from Michaelis-Menten data.	99
Figure 41.	Velocity versus substrate profiles obtained with relatively high amounts of total cell protein in the assay. Lines are a spline fit and do not imply a mathematical model.	100

Figure 42.	Lineweaver-Burk plot of the data in Figure 41. Note these plots are also non-linear indicating non-Michaelis-Menten behaviour.	101
Figure 43.	Eadie and Scatchard plots of the data in Figure 41. Note the serpentine shape of the plots.	103
Figure 44.	Hanes plot of the data in Figure 41. These plot do not emphasise the departure from Michaelis-Menten behaviour as clearly as the Eadie or Scatchard plots.	104
Figure 45.	The effect of shaking speed on the TPL activity (initial rate) of free and microencapsulated whole cell <i>Erwinia herbicola</i> . (Temperature = 37 °C, pH = 8.0, n = 2.)	122
Figure 46.	The effect of temperature on the TPL activity of free and microencapsulated whole cells of <i>Erwinia herbicola</i>	123
Figure 47.	Velocity (TPL activity) versus substrate profile for free and microencapsulated <i>E. herbicola</i>	125
Figure 48.	The conversion of ammonia, pyruvate and phenol or catechol into L-tyrosine or L-dopa respectively by the TPL activity of whole cell <i>E. herbicola</i>	128
Figure 49.	The Conversion of ammonia, phenol and pyruvate to tyrosine by the TPL activity of whole cell <i>E. herbicola</i>	133
Figure 50.	Plots showing the fit of the integrated equation (4.20) to data for the conversion of ammonia, pyruvate and phenol to tyrosine by whole cells (1.6 mg total cell protein).	137
Figure 51.	Plots showing the fit of the integrated equation (4.20) to data for the conversion of ammonia, pyruvate and phenol to tyrosine by whole cells (6.6 mg total cell protein).	138
Figure 52.	Replot of the data from Brot (1965) showing deviations from Michaelis-Menten behaviour. N.B. the curve of the Scatchard plot.	145
Figure 53.	Replot of the data of Kumagai and Yamada (88) for cell free TPL. Note the curvature of the Scatchard plot.	147
Figure 54.	Scan of 0.1 percent alginate in HEPES buffered saline.	IV
Figure 55.	Scan of blue dextran 0.2 mg per ml in HEPES buffered saline (pH 7.4).	V
Figure 56.	Equilibria visualized in the allosteric model of Monod, Wyman and Changeux.	XIV

Figure 57.	Scheme of subunit interactions which occur in the sequential interaction model of Koshland, Nemethy and Filmer for the square arrangement.	XVIII
Figure 58.	Freshly prepared microcapsules made with Kelco-Gel® HV alginate .	XXII
Figure 59.	Microcapsules from the same batch as those shown in Figure 58 after 2 months of storage at 4°C.	XXIII
Figure 60.	Scheme of the steps in the formation of tyrosine from ammonia, phenol and pyruvate by tyrosine phenol lyase (assuming the enzyme has identical and equivalent active sites).	XXIV
Figure 61.	A simple mechanism which accounts for the mixed type inhibition of TPL by phenol reported by Kumagai (1972).	XXVII
Figure 62.	One example of the conversion of ammonia, phenol and pyruvate to tyrosine (Initial phenol concentration 50mM).	XXXI

LIST OF TABLES

Table I.	Literature K_M Values for free TPL (Tyrosine Synthesis and Degradation)	26
Table II.	Literature K_i values for free TPL	26
Table III.	Value of the Constants Used in the Simulation of Spore Death During Sterilization	47
Table IV.	The Initial Rate of Phenol Degradation by TPL in Comparative Buffer Study.	90
Table V.	Effect of PLP Addition on the Activity of Whole Cell TPL . . .	91
Table VI.	Parameters of the Hill Equation for Data in Figure 37 [†]	106
Table VII.	Parameters of the Hill Equation for Data in Figure 41 [†]	107
Table VIII.	The Value of the Parameters of the Michaelis-Menten Equation for the Data in Figure 37	109
Table IX.	The Value of the Parameters of the Michaelis-Menten Equation for the Data in Figure 41	110
Table X.	V_{max} and K_M (or $K_{0.5}$) Values Obtained by Different Procedures (Original Data in Figure 31).	111
Table XI.	V_{max} and K_M ($K_{0.5}$) Values Obtained by Different Procedures (Original Data in Figure 41)	112
Table XII.	Best Fit Parameters for the Exclusive Binding Model of Monod (Original Data in Figure 37)	116
Table XIII.	Best Fit Parameters for the Exclusive Binding Model of Monod (Original Data in Figure 41)	117
Table XIV.	Initial TPL Activity of Free and Microencapsulated <i>E. herbicola</i>	126
Table XV.	The Effect of Catechol and Illumination on the Production [#] of L-Dopa by Microencapsulated <i>E. herbicola</i>	129
Table XVI.	Kinetic Parameters for Whole Cell Tyrosine Phenol Lyase .	135

Table XVII. Components of the Tyrosine Phenol-Lyase Induction	
Medium	II

NOMENCLATURE

A	Effective heat transfer area
A	The conformation of a subunit of a multisubunit protein that is able to bind substrate S (in the Koshland, Nemethy and Filmer model)
A	The first substrate molecule which binds to the enzyme in an ordered enzyme kinetic mechanism (usually ammonia in this work).
Abs	Absorbance ($\lambda = 616.1 \text{ nm}$) of the blue dextran 2000 solution produced after blue dextran 2000 containing microcapsules are broken by agitation for 60 minutes in a rotary shaker.
Abs ₀	Absorbance of the blue dextran 2000 solution produced when blue dextran containing microcapsules are suspended in buffered saline (before shaking).
Abs _∞	Absorbance of the blue dextran 2000 solution produced when blue dextran containing microcapsules are completely broken by agitation with glass beads in a rotary shaker overnight.
B	The conformation of a subunit in a multisubunit protein to which substrate is bound in the Koshland, Nemethy and Filmer model.
B	The second substrate molecule which binds to the enzyme in an ordered mechanism (usually pyruvate in this work).
c	The ratio K_R/K_T . (Used in the model of Monod, Wyman and Changeux).
C	The third substrate molecule which binds to the enzyme in an ordered mechanism (usually phenol in this work).
C	Heat capacity.
DP	Degree of polymerization of a polymer (usually of alginate in this work)
E	Enzyme, usually in the form free of substrate or ligand.
E _a	Activation energy, in Arrhenius type relationships.

$[E]_t$	Total enzyme concentration -all species of enzyme considered- (used in kinetic expressions or in mass balance relationships).
G	Guluronic acid, one of the constituent monomers of alginate. (See M below).
Gr_f	The Grashof number evaluated at the film temperature.
h_o	Heat transfer coefficient for the outside of a container (from saturated steam to the wall in the context of this work).
h_i	Heat transfer coefficient for the inside of a container (from the wall to the bulk fluid).
k	Thermal conductivity of steel
k	Spore inactivation (or death) constant in Arrhenius type expression.
K_A	A pseudo Michaelis-Menten constant; an equilibrium constant which measures the tendency of substrate A to dissociate from the EA complex.(Used in ordered enzyme mechanism.
K_B	A pseudo Michaelis-Menten constant; an equilibrium constant which measures the tendency of a substrate B to dissociate from the EAB complex. (Used in ordered enzyme mechanisms).
K_C	A pseudo Michaelis-Menten constant; an equilibrium constant which measures the tendency of a substrate C to dissociate from the EABC complex. (Used in ordered enzyme mechanisms).
K_P	A pseudo Michaelis-Menten constant; an equilibrium constant which measures the tendency of product P to dissociate from the EP complex. (Used in enzyme mechanisms).
K_R	A pseudo Michaelis-Menten constant; an equilibrium constant which measures the tendency of a substrate molecule to dissociate from a subunit in the R state. (Used in the model of Monod, Wyman and Changeux).
K_T	A pseudo Michaelis-Menten constant; an equilibrium constant which measures the tendency of a substrate molecule to dissociate from a

	subunit in the T state. (Used in the model of Monod, Wyman and Changeux).
K_{AA}	Equilibrium constant which measures the strength of interaction between 2 subunits in the A conformation; nominally set to 1 in the model of Koshland, Nemethy and Filmer.
K_{AB}	Equilibrium constant which measures the strength of interaction between one subunit in the A conformation and another in the B conformation. (Used in the model of Koshland, Nemethy and Filmer).
K_{BB}	Equilibrium constant which measures the strength of interaction between two subunits when both are in the B conformation. (used in the model of Koshland, Nemethy and Filmer).
K_i	Inhibition constant; equilibrium constant which is a measure of the tendency for an inhibitor to dissociate from its inhibitory site on an enzyme.
K_M	The Michaelis-Menten constant; equilibrium constant (in rapid equilibrium systems) which is a measure of the tendency of substrate to dissociate from the active site of an enzyme.
L	The allosteric constant; an equilibrium constant which measures the tendency of oligomers in the R conformation to change to the T conformation. (Used in the models of Monod, Wyman and Changeux).
M	Mannuronic acid; one of the constituents of alginate (see G above).
N	Number of spores in a medium to be sterilized.
Nu_i	The Nusselt number evaluated at the film temperature.
n	Number of subunits. (Used in models relating enzyme kinetics to enzyme structure).
n_H	The Hill coefficient. A measure of the degree of cooperativity between enzyme subunits.
PB	Phosphate buffer (usually 0.1 M, pH 7.0 or pH 8.0).

PBSG	Phosphate buffer saline plus gelatin (general purpose diluent for bacterial systems).
Pr_f	The Prandtl number evaluated at the film temperature.
R	The conformation of the subunits in a multisubunit protein when it is in the relaxed (R) state. (used in the model of Monod, Wyman and Changeux). (See T below).
rpm	Revolutions per minute.
S	Substrate concentration or substrate depending on the context.
T	The conformation of the subunits in a multisubunit protein when it is in the tense or taut (T) state.
T_s	Saturated steam temperature in an autoclave.
T_0	Initial temperature.
T	Temperature at time t.
t	Time.
U	Overall heat transfer coefficient.
v	Velocity (rate) or initial velocity (of an enzyme reaction).
v_0	Velocity (rate) or initial velocity (of an enzyme reaction).
V_{max}	Maximum reaction rate which would occur if all active sites on an enzyme were saturated with substrate.
Y_s	Fractional saturation of all enzyme molecules with substrate.

Greek Symbols Used

α	S/K_R ; specific concentration of substrate in the model of Monod, Wyman and Changeux.
B	Constant in the Arrhenius expression relating the death constant to temperature.
∇	Nabla, a measure of the degree of sterilization.
η	Viscosity.

[η]

The intrinsic viscosity, the limiting viscosity number or the Strau-
dinger index.

λ

Wavelength.

1.0 INTRODUCTION

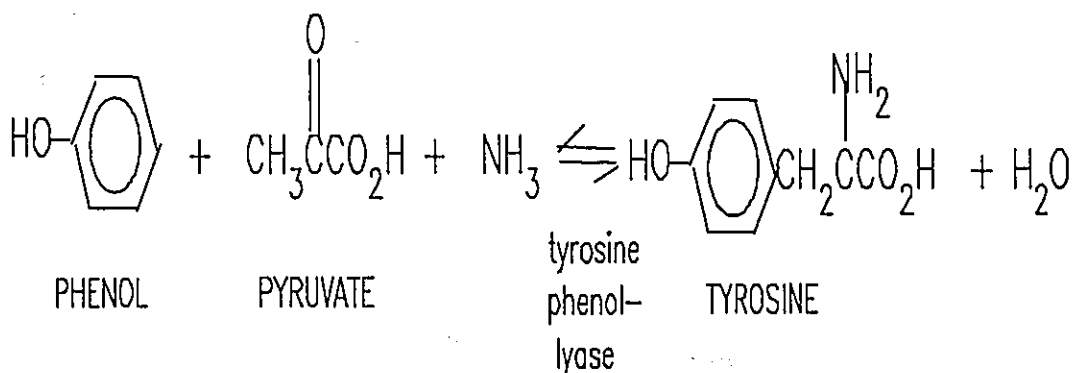
Daring ideas are like chessmen moved forward; they may be beaten, but they may start a winning game.

-Goethe

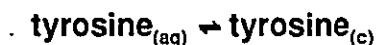
1.1 GENERAL INTRODUCTION

The essence of the project is to use the tyrosine phenol lyase (E.C. 4.1.99.2) activity of *Erwinia herbicola* to convert ammonia, phenol and pyruvate into tyrosine. The reaction is:

ammonia + phenol + pyruvate \rightarrow tyrosine.



The tyrosine produced by this reaction can then be adsorbed onto charcoal.



It is hoped that the results of this project can be applied in the development of a treatment for liver failure; in particular, for lowering the levels of ammonia and phenol that are present in the blood during liver failure. The intended use of the

reaction requires that the cells of *Erwinia herbicola* be microencapsulated and so a portion of the project was dedicated to an analysis of the encapsulation process and its effect upon the properties of the whole cell tyrosine phenol lyase (TPL) activity of *Erwinia herbicola*.

Initial growth studies were done to observe how the cells grew as a function of temperature and RPM. This data was used to choose a suitable temperature and agitation rate for the growth of *Erwinia herbicola* cells. The cells were then grown in a medium which caused them to induce TPL activity.

The kinetic data obtained with whole cell TPL enzyme were analyzed by using nonlinear regression. Models investigated included the Michaelis Menten, the Hill, Adair, Monod and the Koshland-Nemethy Filmer models of enzyme action. This is the first detailed kinetic study of whole cell TPL activity.

The first detailed study of the effects of alginate molecular weight on the relative strength of alginate-polylysine microcapsules was also done. This study was necessary to produce capsules which could withstand high shear. These microcapsules could then be used in a bio-reactor to convert ammonia, pyruvate and phenol into tyrosine.

A review of the relevant information on the liver and liver failure with some emphasis on the effects of ammonia and its removal during liver failure is also presented. Studies on micro-encapsulation systems for the immuno-isolation of cells or enzymes from biological fluids are also discussed.

1.2 CONCISE STATEMENT OF THE OBJECTIVES OF THE STUDY.

"What is to be done?"

Vladimir Ilyich Lenin.

The objectives of the study can be summarised briefly as follows:

- 1) To investigate the growth of *Erwinia herbicola* sufficiently, to obtain conditions suitable for the growth of the organism and the induction of tyrosine phenol-lyase (TPL) activity;

- 2) To characterise the kinetics of the whole cell TPL to such a degree that the effects of microencapsulation on the kinetics can be assessed;
- 3) To investigate the variables involved in the production of alginate-poly-L-lysine-alginate microcapsules. The resulting information will then be used produce microcapsules which can be shaken vigorously enough to minimise the resistance to mass transfer due to the external Nernst layer;
- 4) Prepare microcapsules with entrapped whole cells of *Erwinia herbicola* with the ability to convert ammonia, pyruvate and phenol or catechol into L-tyrosine or di-hydroxy-phenyl-L-alanine (L-dopa).

2.0 LITERATURE SURVEY AND BACKGROUND.

"..... And he (Zeus) bound devious and wily Prometheus with hard and inescapable bonds, after driving a shaft through his middle; and roused up a long-winged eagle against him that used to eat his immortal liver. But all the long-winged bird would eat during the whole day would be completely restored in equal measure during the night....."

From the Theogony

-Hesiod @ 800 B.C

2.1 THE LIVER AND LIVER FAILURE

2.1.1 The Liver.

The liver is a vitally important organ for the normal functioning of the body. This importance was surmised by the ancient Babylonians who considered the liver to be seat of the soul. Indeed if the soul is that which "animates and gives life", then the Babylonian perspective is not without merit, since life cannot long continue without a properly functioning liver.

The Greeks called the liver "hepar", and from this word comes the common adjectival form for things pertaining to the liver "hepatic". Thus the principal cells of the liver, i.e. its parenchymal cells are called hepatocytes.

The hepatic circulation lies between the venous drainage of the intestinal tract and the systemic circulation. Therefore almost all substances absorbed from the intestinal tract pass through the liver via the portal blood before reaching the systemic circulation (1). The substances in the blood coming from the gastrointestinal (GI) tract are altered chemically by the liver into forms that are suitable for direct use or for further processing by other specialized tissues or organs. For example ammonia in the blood from the GI is converted to urea by the Krebs cycle

enzymes in the liver (2,3). The kidneys are then able to excrete ammonia as urea with the urine.

The liver produces many peptides and hormones and discharges them directly to the bloodstream. It produces the bile which is then secreted through a system of ducts into the duodenum. The bile aids in digestion, and is also used as a medium for the excretion of certain detoxified compounds and waste materials; and for their eventual elimination from the body with the faeces. Bilirubin is only one of many substances conjugated in the liver and excreted in the bile.

In addition, the liver is a metabolic factory, which performs a number of important biochemical and other functions. It manufactures several of the plasma proteins and coagulation factors, notably factor II (prothrombin) and factor V (pro-accelerin). The metabolic detoxification of many compounds and drugs also occur in the liver.

If the liver is severely compromised, metabolic disturbances follow. These disturbances are such that they prevent the proper functioning of the body including the brain and can lead to death (4,5,6).

2.1.2 Liver Failure

Liver failure is the inability of the liver to carry out its normal functions. Jaundice and disturbed mental functioning including coma, characterise liver failure.

There are several degrees of liver failure; and an important criterion in its characterization is the presence or absence of hepatic encephalopathy (5, 6).

Hepatic encephalopathy is a disorder of mentation, neuromuscular functioning and consciousness occurring in patients with liver disease (7). This disorder may be graded in order of increasing severity from I to IV (7, 8).

Fulminant Hepatic failure (FHF) is acute liver failure complicated by hepatic encephalopathy, and it has mortality of 80 percent (6, 8, 9).

The major causes of liver failure are acute viral hepatitis and acute drug induced hepatitis (5, 6).

There are at least 14 categories of metabolic disturbances which occur during liver failure (10). The complexity of the disturbances have not allowed the identification of the precise metabolic event or events which cause hepatic encephalopathy. However since liver failure complicated by encephalopathy has such a high mortality the question of what causes the encephalopathy has received a lot of attention (5).

The concentration of all amino acids are elevated during liver failure. However the concentrations of the aromatic amino acids (AAA) increases more than that of the branched chain amino acids (BCAA). Some amino acids such as tryptophan are toxic in large concentrations (10). Therefore the imbalance in the amino acids concentrations has been suggested as a possible cause of hepatic encephalopathy (11, 12).

Bilirubin is normally excreted with the bile, however during liver failure this toxic substance accumulates in the blood (13).

Middle molecular weight substances (from 400 to 1500 Daltons), which are not usually present in normal plasma, are present in increased amounts during liver failure (14, 15). These middle molecular weight substances have been suggested as having a role in hepatic encephalopathy (15).

Ammonia and mercaptans in the hepatic portal blood from the GI are usually trapped by the liver. In liver failure these substances accumulate in the blood. Toxins which precipitate coma, such as ammonia, mercaptans, and fatty acids, act synergistically. When they are present together much smaller amounts are required to induce coma (16). The increase in the concentrations of ammonia, mercaptans and fatty acids have been suggested as a likely cause of the encephalopathy which occurs during liver failure (10, 16).

Inhibitory neurotransmitter substances such as γ -amino-butyric acid (GABA) are present in increased amounts in the blood during liver failure. GABA comes from the GI tract as a result of bacterial action (17, 18). Tyrosine and Phenylalanine (and other AAA) are elevated in the blood (11). This elevation leads to an increase in the concentration of phenolic compounds such as phenols and

tyramine (4-hydroxyphenethylamine). False neurotransmitters which resemble dopamine (hydroxy-tyramine) are produced from the catabolism of these phenolic compounds. The presence of increased amounts of inhibitory neurotransmitters such as GABA, and of false neurotransmitters from phenolic compounds, could cause the cerebral dysfunction that is typical of hepatic encephalopathy (19).

Organic acids such as pyruvate, α -ketoglutarate (α -kg), lactic and citric acids are present in increased amounts during liver failure. However they are considered to be a consequence of severe liver function impairment (7, 10).

With such a wide range of metabolic disturbances it is likely that the cause of the encephalopathy and the concomitant high mortality is multifactorial (20, 21).

The complexity of liver failure has meant that few successful approaches to hepatic support are available.

2.1.3 Conventional Artificial Liver Support

In the Theogony, Hesiod described the nightly regeneration of Prometheus's liver after its daily partial destruction. Even in these modern times the approach to treating acute liver failure relies on the enormous capacity of the liver to regenerate. Indeed after a 90 percent hepatectomy the human liver can regenerate (22, 23).

The philosophy underlying artificial liver support (ALS) is that certain toxins ought to be removed from, and or certain critical factors ought to be provided to the liver failure patient. If this is done then the patient's life can be prolonged until his liver regenerates and he will survive (20, 24). There are 4 areas where ALS is applicable. These are:

- 1) for the treatment of liver failure due to poisonings or idiosyncratic drug reaction;
- 2) for the treatment of viral hepatitis;
- 3) for terminal liver failure due to other long term conditions;
- 4) for the improvement of the clinical picture in preparation for transplantation or for temporary replacement after transplantation (24).

In both viral and drug induced hepatitis the liver has the ability to regenerate; however in viral hepatitis steps to maximise viral suppression are also necessary (20). In cirrhosis the liver will not regenerate, since normal tissue has been replaced by fibrotic tissue, and the pockets of functional hepatocytes may be few and isolated (25). If a suitable artificial liver support device was available the life of a cirrhotic could be prolonged until a suitable donor liver was obtained.

The conventional therapy for FHF attempts to:

- 1) eliminate toxic compounds;
- 2) maintain fluid and electrolyte balance;
- 3) provide glucose etc;
- 4) supply essential metabolites missing during liver failure;
- 5) control the increased bleeding tendency;
- 6) use nonabsorbable antibiotics such as neomycin to control the amount of nitrogenous material from the gut due to bacterial action (6, 26).

The overall survival rate in grade IV encephalopathy using these methods is 20 percent (5, 6).

Prior to 1972 **whole blood exchange** and or **plasma exchange (plasmapheresis)** were unsuccessful for treating liver failure (27, 28). In 1972 Chang treated a cirrhotic liver failure patient by **polymer coated charcoal haemoperfusion** (29). The patient was in coma but regained consciousness after the treatment. In charcoal haemoperfusion (CH) the blood from the patient is percolated through a column packed with polymer coated activated charcoal. The blood from the column, now partially cleared of toxins, is returned to the body.

Charcoal's capacity to remove water soluble toxins was well known, however its *in-vivo* use with blood was not possible; since charcoal releases microemboli which can block blood vessels. The direct contact between charcoal and blood causes the loss of platelets (thrombocytopenia) and leucocytes. These problems were solved by coating the charcoal particles with nitrocellulose polymer (20, 24, 29). A variety of other polymers including cellulose acetate and its

derivatives, nylon and polyethylene-glycols have since been investigated for their suitability to coat charcoal (30).

The ability of charcoal haemoperfusion to return consciousness, extend survival time and reduce mortality is now well established (13, 20, 31). Charcoal haemoperfusion is particularly effective when it is used in grade III coma or earlier (32, 33). It is not effective for long term survival in grade IV coma since irreversible damage may have already occurred (20). Charcoal haemoperfusion is not a complete artificial liver. Hence, it cannot replace all the functions of the liver.

Charcoal haemoperfusion clears the blood of a wide variety of toxins including mercaptans, phenols, aromatic amino acids, and toxic middle molecular weight substances (13, 20). Hence the detoxification functions of the liver can be partially replaced by charcoal haemoperfusion. Some essential substances can be provided by a partial blood exchange (31). A great advantage of charcoal haemoperfusion is its simplicity and straight forwardness. A disadvantage of charcoal haemoperfusion is that it does not clear the blood of ammonia (29, 31).

The deleterious effects of ammonia during FHF are not limited to its ability to precipitate coma. Ammonia also increases the permeability of the blood brain barrier and so it is partially responsible for the cerebral oedema which accompanies liver failure (34). Another deleterious effect of ammonia is that it inhibits the regeneration of the liver (35).

Other approaches at artificial liver support which remove ammonia have been attempted. Adsorbents such as oxystarch (36, 37) or zirconium phosphates (38) can be taken orally, but they have a low capacity *in vivo* and they are mainly applicable for conscious patients.

Ion-exchange resins in particular cation-exchange resins can remove ammonia and they have been incorporated into haemoperfusion devices. These resins can cause thrombocytopenia and the loss of leucocytes if they are not coated with a biocompatible membrane (13, 20, 24). Charged resins will give up an equivalent amount of cation for each mole of ammonia removed. They may also remove K^+ and Ca^{2+} and thus perturb unfavourably the electrolyte balance of a

FHF patient (39). Uncharged resins are not as effective for the removal of ammonia; however they are effective for the removal of lipophilic substances (13, 20). Ion-exchange resins have not been shown to be better for the treatment of liver failure than charcoal haemoperfusion.

The methods of artificial liver support discussed above were based on the direct removal of ammonia, either by adsorption, exchange of body fluids or by dialysis. An alternative approach would be to remove the ammonia after it has been converted to another form. Ideally the ammonia would be converted to a less toxic form or to a form that is adsorbable by charcoal. The reaction to be used for the conversion of ammonia, if it is to be applied *in-vivo*, must be able to proceed under approximately physiological conditions. Therefore as a minimum it should be kinetically feasible at 37 °C and at pH close to 7.4. Enzymes are ideally suited for effecting such a conversion of ammonia. The precedent for this approach is Nature herself, since in health ammonia detoxification occurs by the use of the urea cycle enzymes of the hepatocytes (3, 40, 41).

2.1.4. Immobilized Hepatocytes and Artificial Liver Support.

Given the structural complexity of the liver and its many functions, it is perhaps not surprising that haemoperfusion, haemodialysis or plasmapheresis cannot provide a complete artificial liver system. Theoretically an improved system could be developed which incorporated the principal functional cells of the liver, the hepatocytes. Such a system should be able to provide both detoxification functions and synthetic functions. Extracorporeal perfusion of the blood through stirred tank reactors containing liver slices and cubes has been done (42, 43). These systems can marginally lower the concentrations of certain toxins and produce liver synthesized factors. The inefficiency of the liver slices or liver cubes systems, is at least partially owed to the inability of oxygen or nutrients to diffuse to the interior of the liver slices. The lack of oxygen and nutrients reduces the viability of the cells. There is also no immuno-isolation between the treated blood and the liver slices or cubes.

Immuno-isolation can be provided by using either hollow fibre or microencapsulated hepatocyte systems. In hollow fibre systems, hepatocytes are placed on the exterior of semipermeable hollow fibres. The blood or plasma being treated flows in the lumen of the hollow fibres (44, 45). In microencapsulated systems the hepatocytes are entrapped within microcapsules with semipermeable membranes (46, 47, 48, 49). Microencapsulated hepatocytes could be incorporated into a bioreactor rather than using (immunologically) exposed hepatocytes. The use of microencapsulation for immunoisolation is a well developed field in its own right and it will be discussed later (50, 51, 52).

Some of the enzymes inside dead hepatocytes can continue to work for a while (42, 43). However for maximum effect the hepatocytes should be viable and this means that oxygen and other nutrients need to be supplied to the hepatocytes. Yarmush *et al* analyzed the oxygen demand of an artificial liver support system based on hepatocytes (25). They concluded that an artificial liver support system, which contains 10 percent of the total number of hepatocytes of the liver, *i.e.* roughly 25 billion immobilized hepatocytes, will require 10 m² of exchange surface area. Immobilised hepatocytes are often implanted in the peritoneal cavity, however the peritoneal cavity can only supply 1.5 m² of exchange surface area (25). The analysis of Yarmush *et al* is not supported by certain animal studies (46, 49).

The implantation of 15 million microencapsulated hepatocytes within the peritoneal cavity of liver failure rats show an increase in survival time (46). When 50 million microencapsulated hepatocytes were implanted intraperitoneally in liver failure rats there was also a significant increase in the survival rate (49). As the size of the animal increases the number of hepatocytes required for treatment increases substantially (53). Therefore, notwithstanding the early encouraging results with microencapsulated hepatocytes, it is worthwhile investigating other approaches for ammonia removal during liver failure.

The paucity of detailed knowledge required for successful long-term culture of hepatocytes make it worthwhile investigating other enzyme methods for ammonia removal during liver failure.

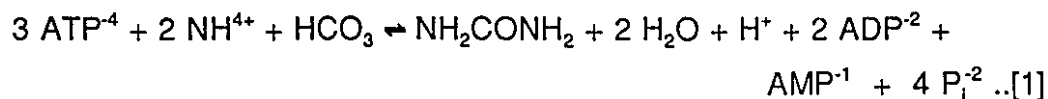
2.2 ALTERNATIVE ENZYME SYSTEMS FOR AMMONIA REMOVAL

"Extreme remedies are very appropriate for extreme diseases."

-Hippocrates

2.2.1 Immobilized Enzyme Systems for Ammonia Removal.

Ammonia is converted to urea by the urea cycle enzymes of the liver. Urea (NH_2CONH_2) is formed from ammonia and CO_2 as one of the last products of a cycle which involves at least five enzymes (3, 40). The process is energy intensive and requires the consumption of ATP. The net result of the complicated series of reactions described by the urea cycle are shown as reaction [1] below.



The conversion of the ammonia in the blood to amino acids could reduce the encephalopathy of liver failure. Some multienzyme systems for the production of amino acids from ammonia have been developed (54, 55, 56). There are also enzyme systems for the detoxification of compounds other than ammonia. The *in-vivo* conversion of ammonia to an amino acid during liver failure has the immediate advantage of converting a toxic component to a less toxic or even beneficial substance. The nitrogen load of the body would remain high since only the form of the ammonia nitrogen would be changed. This means that there is a possibility that the disturbed metabolism of the body would once again reconvert the amino acid to ammonia and ketoacids. Indeed the infusion of amino acids such as glycine, serine, threonine, glutamine, histidine, lysine or asparagine induced hyperammonemia in patients with hepatic encephalopathy (57). It is therefore desirable to convert ammonia to branched chain amino acids (BCAA), which are

present in relatively lower concentrations, or to other amino acids that are adsorbable by charcoal.

Enzyme systems, immobilized within semipermeable microcapsules, have been developed for the conversion of ammonia to BCAA (58, 59, 60). The process of converting ammonia to BCAA requires expensive co-substrates such as NADH or NADPH. The NADH or NADPH could be regenerated by another enzyme reaction which utilises the energy of a cheap substrate such as glucose, however the NADH would still leak from the enzyme system. The problem of cosubstrate leakage was solved by linking the NADH to a high molecular weight dextran (58, 59, 60, 61). The semipermeable membrane was then able to retain both the enzymes and the Dextran-NAD⁺.

This system is attractive conceptually; however there are limitations to its use. The viscosity of a Dextran-NAD⁺ solution increases rapidly with concentration. This limits greatly the amount of Dextran-NAD⁺ that can be incorporated in the system, and so rather low rates of reaction occur with these immobilized enzyme systems.

The conversion of the ammonia to BCAA, without their subsequent removal, may not be enough to correct liver failure. The parenteral infusion of solutions of amino acids at concentrations which corrected the ratio of AAA to BCAA has been shown not to increase the survival rate in humans (62) or in experiments with rabbits (63). Therefore the conversion of ammonia to amino acids that could be subsequently removed by charcoal haemoperfusion may be better. This approach would not only reduce the ammonia concentration, it would also reduce the total nitrogen load of the body.

Tyrosine, tryptophan, phenylalanine, lysine and arginine, (in that order), are adsorbed preferentially by charcoal. Aspartate and alanine are hardly adsorbed (64). Multi-enzyme systems for the conversion of ammonia to tyrosine, tryptophan, phenylalanine, lysine or arginine are not available, but could theoretically be developed. The necessity of retaining cofactors and or coenzymes in the system, would perhaps ensure that these systems would be of limited efficiency. Microbial

systems are able to produce amino acids from ammonia and other simple substrates. Perhaps some of the problems encountered with artificial multi-enzyme systems could be overcome by using an immuno-isolated microbial system ?

2.2.2 The Microbial Production of Amino Acids.

"...The thin sturdy envelope of the living cell consists of lipid, phosphate and protein. The proteins act as both gatekeepers and active carriers, determining what passes through the membrane...."

-C. Fred Fox.

The use of micro-organisms for the production of amino acids from ammonia and other substrates has several advantages over the use of immobilized enzyme systems. The problem of coenzyme and or cofactor retention within the system becomes less of a problem. The cell membrane of micro-organisms is selectively permeable, hence the cell retains its coenzymes and its cofactors as well as other valuable components. The problem of coenzyme or cofactor retention in the system is therefore less problematic with a microbial system. The overall system could also be cheaper, since the intermediate steps of enzyme isolation and purification are not required.

There are bacteria, yeasts, filamentous fungi and actinomycetes which cause the accumulation of amino acids in culture medium; however bacteria are the best producers (65). Initially the only commercially important amino acid was glutamic acid. It was used extensively as a flavour enhancer. Amino acids are now used as food additives, animal feed additives, therapeutic agents, and as raw materials for chemical processes (66). Aspartame, the artificial sweetener aspartyl-phenylalanine-methyl ester, is made by reaction between the constituent amino acids.

Amino acids are essential components of the microbial cell, and their biosynthesis is regulated to maintain optimum levels in the cell. For the

overproduction of an amino acid to occur there is typically a mutation in the cell. This mutation leads either to a defective repressor protein or to a defective regulatory site on a key enzyme. Consequently, there is the over production of a particular enzyme (66, 67). The over production of the enzyme then leads to higher synthetic reactions for the corresponding amino acid. There could also be defect in the cell wall of the microbe. In this situation because the cell wall is leaky, some amino acids escape from the cell. The optimum concentration of a key amino acid is never attained; and so the cell continues to overproduce the amino acid. This mechanism is often critical to the successful microbial production of glutamic acid (68).

In amino acid production, based on the mechanisms described above the cells are alive and in a sense it could be claimed that the amino acids are produced by a process of fermentation. The best amino acid producers are either aerobes or facultative anaerobes cultured under aerobic conditions (65); therefore the adaptation of these processes for *in-vivo* use would require the design of a system to provide sufficient oxygen to support the cells. The problem of oxygen and nutrient supply has not been adequately solved for hepatocyte use in ALS systems (25). The metabolic rate (*i.e.* amount of substrate or oxygen per hour per unit cell mass) for bacteria is typically 10 - 100 fold higher than that of eucaryotic cells (69). This indicates that the problem of nutrient and oxygen supply, to an *in-vivo* system for ALS using aerobic microbes, will not be solved in the near future.

For those amino acid producers that have defects in the cell wall, the leakiness of the cell is often related to how much biotin is in the media. Biotin is essential for the construction of the cell wall of these bacteria. If there is too little biotin, the cells will not grow. If there is too much biotin, the cell wall will not allow the escape of the amino acids and so there is no overproduction of amino acids. In the industrial production of amino acids, it is often found that substrates such as sugar cane molasses have too much biotin. This problem is solved by including penicillin or ampicillin, antibiotics which incorporate themselves within the cell wall, in the culture media. This ensures that the cell walls of the microbes are weak

even if there is an excess of biotin (68). Detergents such as cetylpyridinium chloride (CPC) may also be used to modify membrane permeability and allow the excretion of amino acids into the media. Very careful control over membrane permeability is required for successful amino acid production with these bacteria.

Cells that are actively growing are able to escape from the usual polymer gel matrices used to immobilize bacteria. This escape occurs even if the pore size of the membrane which retains the microbes, is smaller than the microbe (70, 71, 72). There could then be a problem with immuno-isolation if live actively growing cells are used. The problems associated with oxygen supply, the maintenance of the proper amount of biotin in the media, and immuno-isolation suggest that actively growing cells should not be the first choice for the conversion of ammonia to amino acids during liver failure.

The alternative to the fermentative mode of production is the enzymatic mode. In the enzymatic mode an enzyme is induced in the bacteria with the ability to transform substrates into amino acids. The bacteria is then merely a "bag" which contains the necessary enzyme and cofactors. This method has been used for the production of aspartate, tryptophan and tyrosine (66).

In the production of aspartate the enzyme aspartate ammonia lyase, is induced in microorganisms such as *Bacillus megaterium*, *Escherichia coli* and *Pseudomonas trifolii* (66). This enzyme catalyses the conversion of fumarate and ammonia to aspartic acid. Aspartate is not adsorbed strongly by charcoal (64).

In the production of tryptophan the enzyme tryptophanase is induced in microorganisms such as *Proteus rettgeri*. The enzyme catalyses the conversion of indole, pyruvate and ammonia to tryptophan (66). Tryptophan is strongly adsorbed by charcoal (64), and further the concentration of both indole, ammonia and pyruvate are elevated during liver failure. Apparently tryptophanase, suitably immobilized, could be used to remove both ammonia and indole from the blood during liver failure.

The enzyme tryptophanase requires pyridoxal-5'-phosphate (PLP) as coenzyme at the active site (73). It is worthwhile investigating the use of micro-

organisms with tryptophanase activity, for use in systems for ammonia detoxification during liver failure. However tryptophan, in high concentrations, is one of the more toxic amino acids (10).

In the production of tyrosine, the enzyme tyrosine phenol-lyase (TPL) can be induced in organisms such as *Erwinia herbicola* (66). This enzyme, which requires PLP, converts ammonia, phenol and pyruvate into tyrosine (73). Tyrosine is strongly adsorbed by charcoal (64), therefore if ammonia and phenol are converted to tyrosine by the use of TPL we could remove these toxins from the blood during liver failure.

TPL also converts catechol, ammonia and pyruvate to dihydroxyphenyl-L-alanine (L-dopa). The infusion of L-dopa into FHF patients has caused them to regain consciousness (10). L-dopa is, incidentally, also useful in the treatment of Parkinson's Disease. The study of whole cell tyrosine phenol lyase activity and its immobilization could lead to a system for the removal of ammonia and phenol from the blood during liver failure. It could also lead to the development of new approaches for the production of tyrosine and L-dopa.

2.3 TYROSINE PHENOL LYASE DEAMINATING (EC. 4.1.99.2).

2.3.1. Sources of TPL.

Interest in L-tyrosine phenol-lyase deaminating (EC 4.1.99.2) was first aroused when it was discovered that *Bacterium coli phenologenes* liberated phenol from L-tyrosine. The enzyme was initially called β -tyrosinase (74). TPL is however quite distinct from tyrosinase. Tyrosinase degrades tyrosine by oxidising its phenolic ring irreversibly; TPL lyses tyrosine into phenol, ammonia and pyruvate.

TPL is widely distributed among several species of the family Enterobacteriaceae. TPL activity has been found in the *Escherichia*, *Proteus*, *Erwinia*, *Citrobacter*, *Salmonella*, *Pseudomonas*, and *Xanthomonas* genera. Yeast, fungi and the actinomycetes have no TPL activity (74). Enei found that especially high

TPL activity could be induced, by tyrosine, in *Erwinia herbicola* strains ATCC 21434 and ATCC 21433. Strains of *Escherichia intermedia* are also good sources of the enzyme (74). *Escherichia intermedia* was renamed *Citrobacter intermedius* (75). For the sake of consistency with the original literature both names will be used in this report.

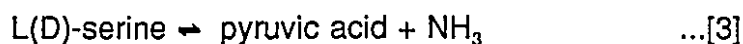
Clostridium tetanomorphum has an enzyme with the ability to convert tyrosine to ammonia, phenol and pyruvate (76). However whole cell preparations of this enzyme also degraded pyruvate to acetate and CO₂. This implies that undesirable side reactions could occur if the whole cell TPL activity of *C. tetanomorphum* was used for tyrosine production.

When *Erwinia herbicola* is grown in yeast and meat extract, medium maximal TPL activity appears in the early stationary-phase of growth (74). A tyrosine rich medium which allows the induction of high TPL activities in some micro-organisms was developed by Enei (77). However the induction of TPL activity with time in *E. herbicola* (the best source of the enzyme), with this medium was not reported. The effect of aeration on the development of TPL activity in *E. herbicola* was studied by varying the volume of medium in 500 ml shake flasks. It was found that somewhat higher specific activity was obtained when the volume of medium was 60 ml; however the growth of the cells was limited under these conditions (77).

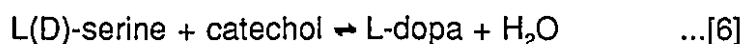
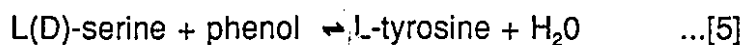
2.3.2 Reactions of TPL.

Tyrosine phenol-lyase catalyses a broad variety of reactions including α,β -elimination, β -replacement, and racemization (73, 78) as shown in selected examples below:

1. α,β -elimination;



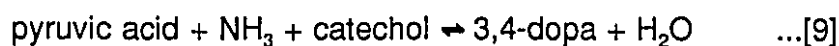
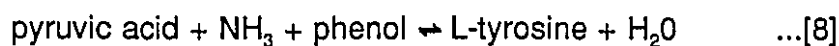
2. β replacement;



3. Racemization;



Tyrosine is produced in high yield by reaction [8], *i.e.* the reverse of reaction [2], and by reaction [5]. L-dopa is produced by reactions [6], [9] and [10]. Both crystalline TPL (78, 79, 80, 81) and whole cell TPL (78, 82, 83, 84, 85) have been used for the production of L-tyrosine and L-dopa.



2.3.3. The Structure of TPL.

"...The processes of life are turned on and off by means of a universal control mechanism that depends on the ability of protein molecules to bend flexibly from one shape to another under external influences..."

-Daniel E. Koshland Jr.

The group of Yamada and Kumagai crystallized TPL from *Escherichia intermedia*, and reported that the enzyme had a molecular weight of 170,000 (78, 86). They also stated that two moles of pyridoxal-5'-phosphate (PLP) were bound per mole of enzyme (78, 87). The same group reported that the TPL from *Erwinia herbicola* had a molecular weight of 259,000; and bound 2 moles of PLP per mole of enzyme (78, 88). Recently the results of Yamada and Kumagai, on the number of moles of PLP bound per mole of TPL, have been challenged (89, 90).

The tyrosine phenol-lyase from *Citrobacter intermedius* was crystallized and analyzed by X-ray crystallography. The results show that TPL is a tetramer made up of 2 dimers with weaker contacts than those between the monomers in a dimer (89). The tetramer binds 4 moles of pyridoxal phosphate (PLP) per mole of enzyme. Each polypeptide chain is folded into a small and a large hydrophobic domain. Each active site of the dimer is composed of amino acid residues from both the large and small domains of one subunit, and the large domain of the neighbouring subunit. The PLP is located at this interface as shown in Figure 1 (89).

Gene fragments which code for tyrosine phenol-lyase activity has recently been prepared from *Citrobacter freundii* (90, 91) and *Escherichia intermedia* (92). These fragments code for proteins with a molecular weight of about 50,000. This further strengthens the view that TPL is a tetramer built up of 4 monomers of 50000 Daltons each (90). The current thought is that TPL is a tetramer of four identical subunits, which binds 4 moles of PLP per mole of enzyme (89, 90, 91).

The clarification of the structural relationship of the subunits, and the number of active sites on TPL is critical for the interpretation of kinetic data obtained using the enzyme. The quaternary structure of protein molecules affect the ability of protein molecules to bind substrates and other ligands. Many multisubunit enzymes are known to display kinetic and binding behaviour that is profoundly non-Michaelis-Menten because of the subunit interactions which occur during substrate binding (93, 94, 95, 96).

All pyridoxal-5'-phosphate requiring enzymes probably evolved from a common ancestor (97). However TPL (EC 4.1.99.2) and tryptophanase (EC 4.1.99.1) differ from other PLP enzymes in that the PLP is easily resolved from these enzymes (87). If tryptophanase (TNA) is crystallized in the presence of high concentrations PLP the resulting enzyme will not contain its full complement of PLP. The dissociation of the PLP was attributed to conformation changes in the

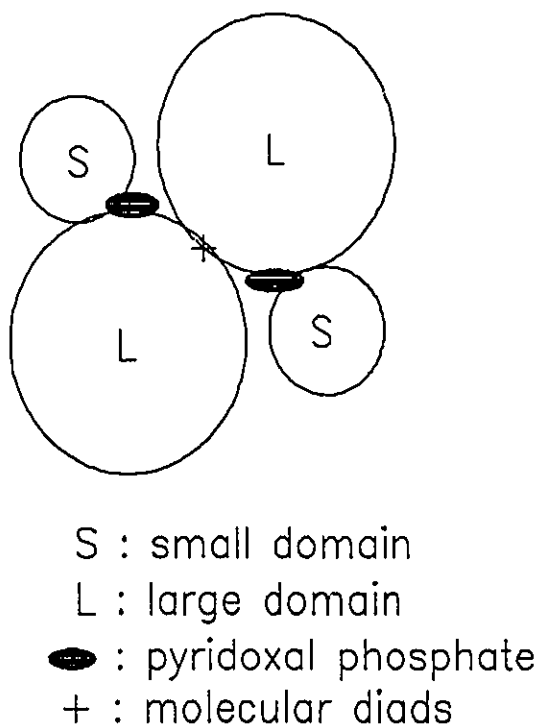


Figure 1. Schematic representation in the dimeric α_2 molecule of TPL. Domains are shown as circles. The molecular diads (+) are perpendicular to the page. Drawn after Antson et al (1992).

quaternary structure which reduced its affinity for PLP during the crystallization process. The lack of PLP causes the dissociation of tetrameric TNA to nonfunctional dimers (73). There is a high degree of homology between TPL and TNA (90) and so it is possible that PLP has a similar stabilising effect on quaternary structure of TPL.

Monovalent cations (NH_4^+ , K^+ , or Rb^+) are required for activity, the tight binding of PLP, and the stabilization of the apoenzyme-pyridoxal phosphate complex in both TPL and TNA (73).

2.3.4. Kinetic Mechanism of Tyrosine Phenol Lyase.

Tyrosine phenol lyase has pyridoxal-5'-phosphate (PLP) (Figure 2) at its catalytic centre. PLP will readily form a Schiff base with an amino acid to produce an aldimine. The reactions which can then occur in the amino acid or keto acid moieties of these Schiff bases and their metal chelates are influenced by several constitutional factors. These are:

- 1) the electron withdrawing effect of the pyridine ring, especially if the pyridine nitrogen has been protonated;
- 2) the electron-withdrawing effect of the azomethine nitrogen containing a covalently bound protein;
- 3) the electron-withdrawing influence of a metal ion coordinated to the azomethine nitrogen of the Schiff base, as well as the phenolic oxygen of the pyridine ring and to the carboxylate group of the amino or keto acid (98).

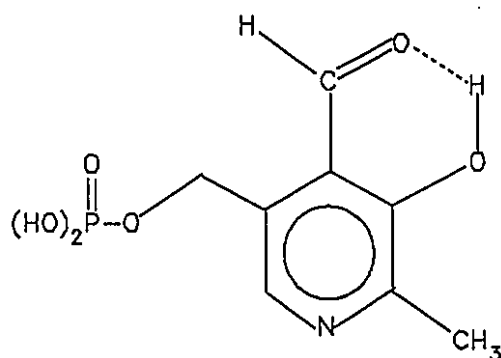


Figure 2. Pyridoxal-5'-phosphate

in PLP enzymes pyridoxal phosphate is usually bound to the ϵ -nitrogen of a lysine residue (73, 87). In the presence of an amino acid substrate such as tyrosine, an aldimine is formed between the substrate and PLP. "The substrate's α -proton is abstracted by an enzyme-bound base (B1) to form the quinoid structure (I) shown in Figure 3. Another base (B2) abstracts the hydroxyl proton, and the first base (B1) returns a proton to the aromatic C-4 position with the formation of a cyclohexadienone moiety (II). The activated carbon-carbon bond now breaks with simultaneous electron push from the PLP, and electron pull when the hydroxyl proton is returned by the base B2. Phenol is released, and after transamination and hydrolysis, pyruvic acid and ammonia are released from the enzyme" (99). The exact nature of all enzyme intermediates and the stereochemistry of the intermediate steps is still being investigated (73, 99, 100, 101, 102, 103).

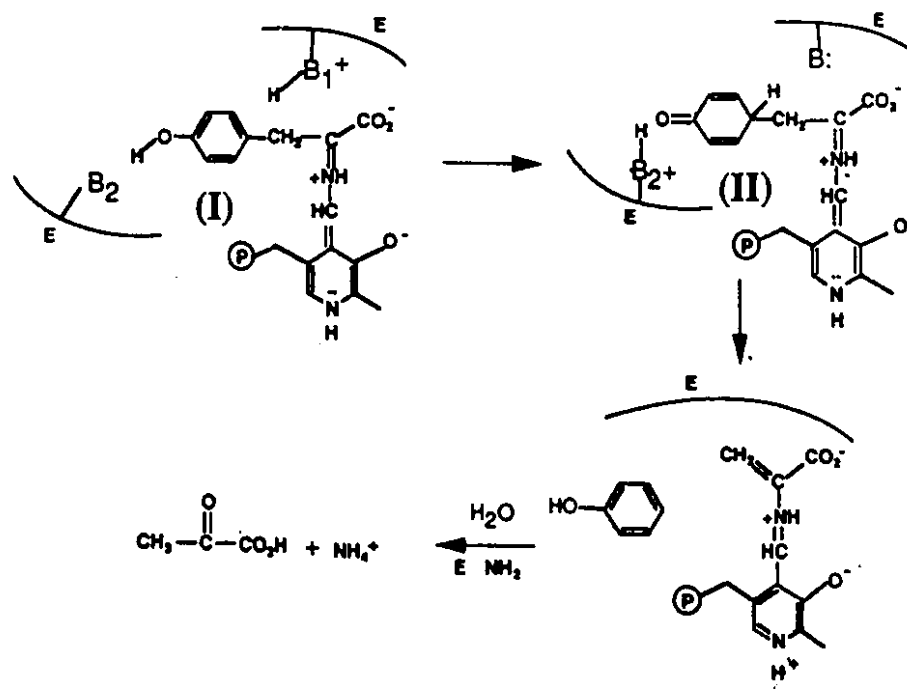


Figure 3. Summary of the mechanism of tyrosine degradation by TPL

In the degradation of tyrosine, the order of product release is phenol, pyruvate then ammonia (73, 99, 100, 101, 102, 103, 104). This suggests that the production of tyrosine with these products as substrate should occur by the *ter-ti* mechanism of Cleland (105). In this ordered mechanism ammonia would bind the

enzyme first, pyruvate second and phenol third with the subsequent release of tyrosine (78, 106).

2.3.5. Kinetic Parameters for Tyrosine Phenol Lyase.

Detailed kinetic studies of velocity versus substrate profiles of TPL have not appeared. Indeed the majority of the recent literature on TPL is focused on the nature of the intermediate steps and of the complexes formed as the degradation of tyrosine proceeds. Table I list the information that is available on the K_M of some substrates of the crystallized enzyme.

In the production of tyrosine from phenol, ammonia and pyruvate, high concentrations of phenol inhibited the free enzyme at high concentrations. The inhibition constants for some substances are given in Table II. Kumagai and Yamada reported that the inhibition of purified TPL by phenol was of the mixed type (78, 86, 88). However Para *et al* found that phenol inhibited whole cell TPL with "classical" inhibition kinetics (107).

It is perhaps prudent to mention that some of the kinetic constants in Tables I and II were obtained from the studies (78, 86, 87) that suggested that only 2 moles PLP were bound per mole of TPL. It is now thought there are likely to be 4 moles of PLP per mole of TPL (89, 90). Is it possible that the enzyme that was used in the earlier study was either partially inactive or partially denatured?

There are no published values for the equilibrium constant for the production of tyrosine from the substrates of TPL.

Table I. Literature K_M Values for free TPL (Tyrosine Synthesis and Degradation)			
Substrate	K_M (mM)	Reference	Reaction
tyrosine	0.59	Brot (1965)	[2] α,β -elim.
tyrosine	0.23	Kumagai (1970)	[2] α,β -elim.
phenol [†]	1.1	Yamada (1975)	[8] [#]
pyruvate [†]	12	Yamada (1975)	[8] [#]
ammonia [†]	20	Yamada (1975)	[8] [#]
[†] cosubstrate [#] synthetic reaction, reverse of [2]			

Table II. Literature K_i values for free TPL			
Inhibitor	K_i (mM)	Inhibition	reference
Phenol	0.04	mixed type	Yamada (1975)
Pyrocatechol	0.46	mixed type	Yamada (1975)
L-alanine	6.53	competitive	Yamada (1975)

2.3.6. The Immobilization of TPL Activity.

Several studies on the production of tyrosine by either crystalline or whole cell TPL have appeared (78, 79, 80, 81, 82, 83, 84, 85). However only few studies have used immobilised TPL activity (107).

Sepharose-bound-TPL may be prepared by using the cyanogen bromide method to link the enzyme to the sepharose. The activity of the bound enzyme is 30 percent of that of free enzyme (108). In a system for the continuous tyrosine production the immobilized enzyme is inefficient unless PLP is supplied continuously. The enzyme loses activity (but more gradually) with repeated use in a batch system if fresh PLP is not supplied.

Sepharose-bound-TPL may also be prepared by linking the enzyme to pyridoxal phosphate previously bound to sepharose (108). The link between the PLP and the sepharose is then made firm by reduction with NaBH_4 . The optimum pH range (7.5 to 8.5) of the enzyme was shifted by 0.5 to 1.0 pH unit towards the alkaline side by the immobilization process. Since sepharose is uncharged the shift of 1 pH unit probably indicates a distortion of the active site by the immobilization process (108).

Whole cells of *Escherichia intermedia* with TPL activity have been immobilized in polyacrylamide gel (107). The activity of the immobilised cells was 60 percent of that of the free cells. It was found that at concentrations of ammonia and pyruvate of 145 mM and 80 mM respectively, the K_M of phenol for free cells was 40 mM, and that for immobilized cells was 28 mM. Phenol concentrations above 55 mM were inhibitory, with a K_i of 73 mM and 128 mM respectively for free and immobilized cells. The Michaelis constants for ammonia and pyruvate for whole cell TPL were not reported.

Whole cells of *Citrobacter freundii* with TPL activity have been immobilized in carrageenan gel, and used for tyrosine production (109). In this study TPL activity was only observed after the cells were permeabilised by phenol. The duration of this "induction" period was a function of the "growth batch" and the initial phenol concentration. The "plastic strength" of the gel was low when the concentration of carrageenan in the gel was low. The plastic strength of the gel was high when the carrageenan concentration was high. The diffusion of phenol was restricted in the high strength gels. The gel also adsorbed a significant

amount of phenol. Intense mixing improved the reaction rate of the free cells by 60 to 70 percent.

The current experience with immobilised TPL suggest that whole cell TPL enzyme is better than free crystalline TPL (107). Cell free immobilized TPL enzyme has low activity, or else requires the resupply of pyridoxal phosphate. The previous methods used for the immobilization of whole cell TPL enzyme can not provide immuno-isolation. Indeed when cells are used in gels often they are alive and in systems designed for continuous production a steady state can be established, where the new cell growth in the gel balances the loss of cells from the gel (70). This approach is not suitable for the development of a system that may contact biological fluids such as blood or plasma. Gels can be strengthened by adding materials such as locust bean gum, or by crosslinking with glutaraldehyde (110). However these composite gels merely "suppress", they do not eliminate the loss of cells from the gel.

Micro-encapsulation (50, 51, 52) immuno-isolates cells or other biologically active material, and this concept will be introduced formally in the next section on "artificial cells".

2.4 ARTIFICIAL CELLS

"..artificial cell" is not a "specific physical entity. It is an idea involving the preparation of artificial structures of cellular dimensions for possible replacement or supplement of deficient cell functions.".."

-T.M.S. Chang

2.4.1. Artificial Cells: General Principles.

Many substances including enzymes, cell organelles, whole cells, detoxicants, antigens, antibodies, adsorbents and resins have useful biological activity. In 1964, Chang pioneered the concept that these substances could be configured as "artificial cells" (50, 51, 52).

Even the simplest of biological cells are very complex. Artificial cells only employ a few of the many properties of biological cells. An artificial cell may be considered to be a semipermeable microcapsule with biologically active material inside. One of the most important properties of the artificial cell is its selectively permeable ultra-thin membrane. This allows rapid equilibration of permeant molecules across the membrane (50, 52, 111).

The membrane of the artificial cell can be formed by precipitation or interfacial polymerization techniques. In these techniques a membrane is formed at the surface of a liquid that has been emulsified in another liquid.

When enzymes are immobilised inside semipermeable microcapsules with a high concentration of protein, such as haemoglobin, increased stability of the enzymes at 37 °C has been observed. This information is consistent with the fact that in most biological cells the protein concentration is in excess of 100 mg of protein per ml. The many protein-protein interactions help to stabilise the enzymes.

Artificial cells have made and will continue to make a tremendous impact in the treatment of disease. In the enzyme deficiency disease acatalasaemia, there is a defect in the enzyme catalase. Normally, this enzyme localised in the red blood cells breaks down hydrogen peroxide to water and oxygen. If the red blood

I: Intracellular impermeant materials
 E: Extracellular impermeant materials
 s,p: Permeant molecules

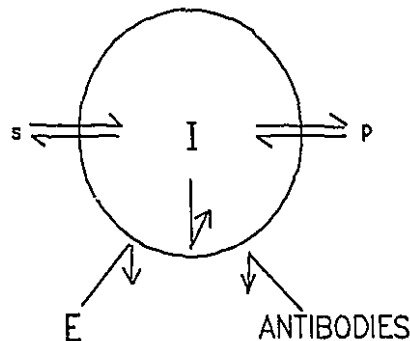


Figure 4. Schematic representation of an artificial cell (adapted from Chang (1972)).

cells have a defect in catalase, hydrogen peroxide reacts with haemoglobin to form methaemoglobin (112, 113). The usefulness of artificial cells in the treatment of enzyme deficiency diseases was illustrated by encapsulating catalase in artificial cells and injecting the cells into the peritoneal cavity of acatalasaemic mice. When these mice were injected with perborate (a substance which is removed by catalase) they recovered within half an hour. Acatalasaemic mice that were not protected with catalase containing artificial cells were incapacitated (113).

Acatalasaemia is only one of many in-born error diseases for which artificial cells have been developed. Microcapsules with phenylalanine ammonia lyase can lower the levels of phenylalanine in rats with phenylketonuria (PKU) (114).

Artificial cells increase the range in which biologically active material may be used for in-vivo applications because it protects the material from the immune system. Normally foreign proteins are rapidly deactivated by the body's immune system. When material is microencapsulated the antibody molecules are prevented from interacting with the foreign molecules (52).

One of the most notable applications of the artificial cell concept was in the coating of charcoal beads with collodion. The resulting microcapsules were then coated with albumin. The coating of the charcoal with nitrocellulose and then albumin makes the microcapsules "blood biocompatible". It was mentioned earlier that the blood can be perfused through a column packed with the coated charcoal.

This process is now used routinely to remove water soluble toxins such as theophylline or paracetamol from the blood (115, 116).

2.4.2. Artificial Cells with Living Cells and Tissues.

Cells can be immobilized by:

- 1) adsorbing them onto the surfaces of substances such as kaolin or woodchips; by
- 2) crosslinking them into pellets with bifunctional agents such as glutaraldehyde; by
- 3) entrapping them within a crosslinked matrix or gel; and by
- 4) entrapping them behind a barrier, such as the semipermeable membrane of a microcapsule or the outer surfaces of a tubes of hollow fibre devices (117, 118).

Microencapsulation is one of the more convenient barrier method available. In the future better hollow fibre devices which can withstand higher pressures, may challenge microencapsulation.

For encapsulating viable cells such as hepatocytes or islets, cross-linked protein (51, 52), alginate-polylysine (119, 120, 121), chitosan-alginate (122), cellulosesulphate-poly(dimethyldiallyl)-ammonium chloride (123), hydroxyethyl methacrylate-methyl methacrylate (124), and chitosan-carboxymethyl-cellulose (125) have been used as membrane forming compounds.

The reaction between polylysine and alginate is often used to form the membranes of microcapsules, the method is simple and no harsh solvents are required. Briefly, the cells are suspended in a (1.5 to 2.0 %) sodium alginate solution, droplets of this cell suspension are then gelled by contact with CaCl_2 . The calcium alginate beads with entrapped cells are then coated with a 0.05 to .1 percent polylysine solution. The polycationic polylysine then interacts with the polyanionic alginate to form a polylysine-alginate membrane. A further coat with a low concentration alginate solution may be applied. This results in the formation of an alginate-polylysine-alginate membrane around a calcium alginate infra-

structure. The interior of the bead is then liquefied by treating the beads with a sodium citrate solution. The citrate sequesters the calcium from the gel and the gel is liquified. The calcium citrate is removed by washing with saline (119, 120, 121). This process will be described in more detail in the experimental section.

Microcapsules made by this process have been used to encapsulate islets which have been used in the treatment of experimental diabetes in rats (119, 120, 121). Microencapsulated hepatocytes for the treatment of experimental liver failure in rats (46, 49) was mentioned earlier.

Alginate-PLL-alginate microcapsules can also be used for the culturing of hybridomas in bioreactors. A small concentration of hybridomas are encapsulated. If the conditions are suitable the hybridomas multiply and produce monoclonal antibodies (MoAb). The molecular weight of the monoclonal antibody is larger than the molecular weight cut off of the membrane and so it is trapped inside the microcapsule. The microcapsules can be easily separated from the culture medium and then broken to release the entrapped protein. This process for making monoclonal antibodies is cheaper since the MoAb is easily separated from the media constituents. The MoAb from the microcapsules is also partially purified and concentrated.

Several improvements to the basic microencapsulation procedure have been made. Goosen *et al*/ examined the effect of the molecular weight of the polylysine on the molecular weight "cut-off" of microcapsules and found that low molecular weight PLL increased the strength and reduced the permeability of the microcapsule membrane. It was felt that small molecular weights PLL could penetrate into the alginate bead and cross link the alginate and produce a more compact membrane (126, 127).

The polylysine step can be done in 2 stages. In the first stage a high molecular weight polylysine is used in the initial membrane forming stage. This leads to microcapsules that are very permeable. Therefore in the internal liquefaction stage some of the alginate within the microcapsules will leak out. The microcapsules are then treated with a low molecular weight PLL to reinforce the

membrane of the microcapsules. When hybridomas were cultured in these microcapsules they accumulated more MoAb protein (127, 128).

The biocompatibility of PLL-alginate microcapsules is improved when an additional coat of alginate is applied (129, 130, 131). This improvement is owed to the fact that the positively charged PLL is immunogenic, while the combination of alginate and PLL is neutral and thus less immunogenic. Alginate is a linear polysaccharide composed of 1,4 linked β -D-mannuronic acid (M) and α -L-guluronic acid (G) units (129). It was found in one study that a final coat with a high G alginates caused less fibrosis around the microcapsules (129). In another study different researchers reported that a final coat with a high M alginate would reduce the amount of fibrosis around peritoneally implanted microcapsules (130, 131).

A microcapsule membrane infiltrated with cells will be discontinuous and could consequently be weak. If these cells protrude from the microcapsule they could trigger the immunological rejection of implanted microcapsules (132).

In order to further improve their biocompatibility a "two-step" procedure for making alginate polylysine microcapsules was developed by Wong and Chang (133). Calcium alginate beads with entrapped hepatocytes were suspended in a 1.5 % sodium alginate solution. This suspension was then extruded as droplets which were then microencapsulated. In the internal liquefaction step the beads within the microcapsule are also liquified. This "two-step" procedure then produces microcapsules with cells inside, however there are no cells in the membrane of these microcapsules (133). Wong and Chang have shown that there is less fibrosis around intra-peritoneally implanted microcapsules, if they are made by the two-step procedure, as opposed to those made by the traditional approach (133).

The consequence of subtle differences in the preparation of alginate-PLL-alginate microcapsules were underlined in a report by Goosen *et al*, who mentioned that the permeability of the microcapsules to a protein could vary from batch to batch, even if the "same" conditions were used in the preparation of the microcapsules (127). This result on permeability, and the conflicting reports on the role of high G or high M alginates on biocompatibility, show that the conditions

during microencapsulation must be carefully controlled. If this is not done it is difficult to determine the exact effect of changes in process variables.

The variation in the biocompatibility of different types of alginate-PLL-alginate microcapsules partially explains the great variation in the results obtained when they are intra-peritoneally implanted. For instance some continue to work for only a few weeks, others for months to years (46, 47, 49, 117, 134).

3.0 EXPERIMENTAL METHODS

*"No facts are to me sacred; none are profane; I simply experiment,
an endless seeker with no past at my back."*

-Ralph Waldo Emerson

3.1 MICROENCAPSULATION

3.1.1 General Procedure

Alginate-polylysine-alginate microcapsules were prepared. The method used was essentially that of Lim and Sun (119, 120, 121) with modifications. All treatment solutions were kept in an ice-water bath until they were ready for use. The pH was controlled to 7.4 by buffering with N-2-Hydroxyethyl piperazine-N-2-ethanesulfonic acid (HEPES). The source and quality of the chemicals used are in Appendix I.

Droplets of an *Erwinia herbicola* cell suspension in a solution of sodium alginate were gelled as they fell in a 1.4 % calcium chloride bath. The concentration of the sodium alginate was typically 1.5 %, but it was varied for certain experiments. The "gelation" time in the calcium bath was at least 6 minutes. The calcium alginate gel beads with entrapped cells were retrieved from the calcium chloride bath and washed with saline.

In the next stage in the process, the calcium alginate beads were placed in a 0.05 % polylysine (PLL) in saline bath. The polylysine treatment was usually for 6 or 10 minutes as indicated in the results section. The polycationic polylysine crosslinked the polyanionic alginate to form PLL-alginate coated calcium alginate beads. The saline washed PLL-alginate beads were then treated with a 0.1% sodium alginate (NAG) solution for 4 minutes. The 0.1 % NAG was always made from Kelco Gel® low viscosity alginate that had been heat sterilized for 5 minutes as described below. This process "mops up" polylysine residues that are not complexed by the alginate near the surface of the beads. The beads are now alginate-PLL-alginate coated.

The final stage in the formation of the microcapsules requires that the interior of the beads be liquified. This liquefaction occurs when the beads are placed in a sodium citrate (3 %, diluted 50:50 with saline) bath. The citrate sequesters the calcium in the bead and breaks up the gel. After this stage the beads have been transformed into microcapsules with an alginate-PLL-alginate membrane with a liquid core. The citrate treatment was done twice. The overall process is shown schematically in Figure 5.

The size of the microcapsules were obtained by sizing with an eye piece micrometer attached to a microscope. Generally 400 or more microcapsules were examined and the frequency of the diameters observed used to determine the size distributions for the microcapsule population.

Effects due to systematic error or bias was minimised by varying each element of the experimental designs for airflow and alginate concentration *et cetera* in random order.

- 1- Cells in sodium alginate (1.5 %).
- 2- Gellation in CaCl_2 (1.3 %) for at least 6 minutes.
- 3- Gelled beads are washed with saline (1.0 minute).
- 4- Gelled beads are coated with 0.05 % PLL (6 or 10 minutes).
- 5- Washed PLL coated beads are coated with 0.1 % NAG (4 minutes).
- 6- Alginate-PLL-alginate coated beads are washed with saline (1.0 minute). Done twice.
- 7- Internal liquefaction of the beads by treatment with 1.5 % citrate in saline (7 minutes). Done twice.
- 8- The resulting alginate-PLL-alginate membrane microcapsules are washed with saline (1 minute). Done thrice.

Figure 5. Basic scheme of the steps in the formation of alginate-polylysine-alginate microcapsules.

3.1.2. The Droplet Former

The droplet former was made of 2 concentric cylinders with extensions for "luer locks" to connect tubing for air and liquid flow. The cell suspension in alginate was pumped by a syringe pump through the inner cylinder. An airflow was maintained in the annulus formed by the inner and outer cylinder. This airflow helped to break up the liquid jet from the inner cylinder and sheared off the droplets. The size of the microcapsules could be partially controlled by varying the airflow. The inner cylinder was made from a 24 gauge needle. The outer cylinder had a diameter of 2.1 mm. The droplet former is shown below in Figure 6.

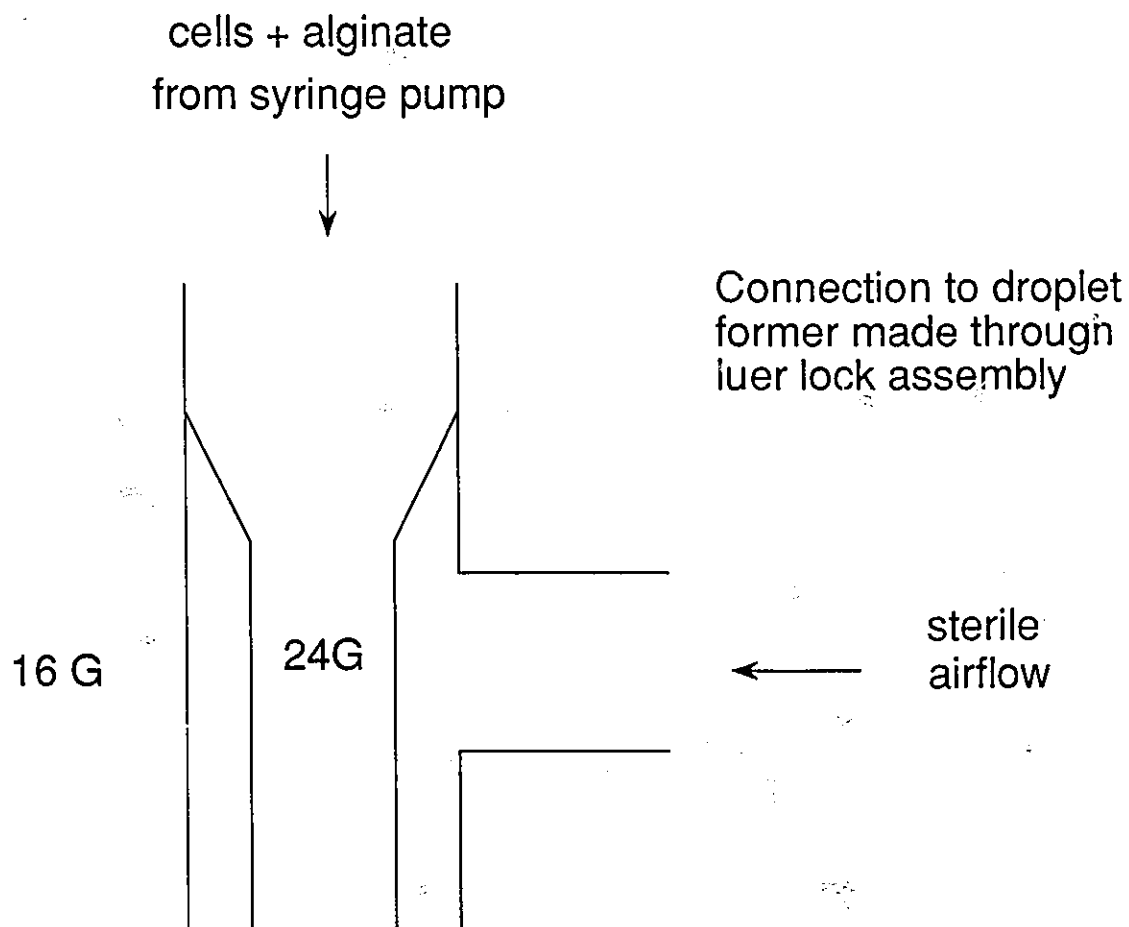


Figure 6. Schematic of the droplet former.

3.1.3 Application of Treatment Solutions

Microcapsules were made in 5.0 ml batches. The volume of the 1.4 % calcium chloride bath was 900 ml. In effect this bath was "infinite" since it was more than enough to completely gel 5.0 ml of 1.5 or 2.0 percent sodium alginate. The large bath was used to ensure gelation and to capture all the droplets from the droplet former. The droplets from the droplet former did not fall vertically, but were dispersed in a cone with its apex at the droplet former. If a large diameter bath was not used many of the droplets would have been lost when high air-flowrates were used.

The volume of all other treatment solutions, except for the PLL, was 200 ml. The volume of the PLL solution was 100 ml, this smaller volume was used because PLL is very expensive.

For the gelation stage a polypropylene beaker was modified by replacing its bottom with a 170 μm nylon grid. This modified beaker was then placed in a 1.0 litre beaker which contained the 1.4 % CaCl_2 solution and a magnetic stir bar. The alginate droplets fell in the modified beaker and were supported on the grid. In this way the CaCl_2 solution was constantly stirred with a minimum of disturbance to the beads as they gelled. The system is shown in Figure 7.

A similar procedure was used for the application of all other solutions. However the alginate gel beads were transferred to a smaller beaker (that was also modified to have a perforated bottom) to facilitate the use of smaller volumes of solution.

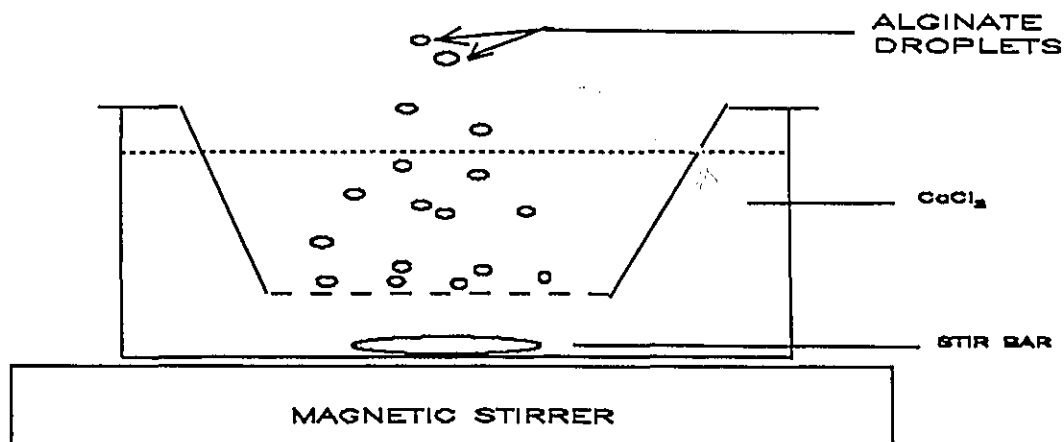


Figure 7. Apparatus for the gelling of alginate drops, or the treatment of alginate gel beads.

3.1.4. Estimation of the Relative Strength of the Microcapsules.

General Procedure

The effect of changes in alginate molecular weight and PLL reaction time on the relative strength of the microcapsules was evaluated by monitoring the fraction of the microcapsules broken, while they were shaken at various speeds. Blue dextran 2000 (Pharmacia, Mwt 2×10^6) and cells were entrapped in the microcapsules, and samples of the microcapsules in buffer were shaken at various revolutions per minute (rpm). The increase in the absorbance of the blue dextran in the supernatant was monitored after 60 minutes of shaking. Scans of absorbance versus wavelength were used to show that alginate does not interfere at ($\lambda = 616.1$ nm or $\lambda = 257.9$) the absorbance maxima of blue dextran. The scans are shown in Appendix II. Typically 0.5 ml of "blue-dextran microcapsules" and 4.5 ml of HEPES buffered saline (pH 7.4) were placed in a 20 ml scintillation vial (diameter 2.8 cm). The vials were shaken at 37 °C in an incubator with a 2 inch throw.

The fraction of the microcapsules that were broken was estimated as:

$$f_{60} = \frac{Abs - Abs_0}{Abs_{\infty} - Abs_0} \quad \dots 3.1$$

where f_{60} is the estimate of the fraction of the microcapsules broken after 60 minutes of shaking; Abs is the absorbance (measured at 616.1 nm) of the blue dextran in the supernatant after shaking; Abs_0 is the absorbance before shaking and Abs_{∞} is the absorbance when the microcapsules are all broken by shaking the microcapsules with glass beads at high rpm. Plots of f_{60} versus rpm were used to determine the rpm that was required to break the microcapsules.

Preparation of Blue Dextran Microcapsules

A solution of blue dextran was prepared by mixing 50 mg (of blue dextran) per ml of saline and stirring overnight. The resulting blue dextran solution was then mixed in a 70 to 30 ratio with a cell suspension stock (8.374 mg/ml total cell protein). This mixture was then mixed with an equal volume of a 3 % alginate solution. After thorough mixing, the combination of cells and blue dextran in the resulting 1.5 % alginate solution was then microencapsulated as described above.

The liquid flow and airflow to the droplet former in these experiments were 1.07 ml/min and 2.5 l/min respectively.

Kelco-Gel® LV (i.e. the low viscosity gelling grade alginate) and Kelco-Gel® HV the high viscosity gelling grade alginate were used in these studies. The alginates were sterilized for 5 minutes and 15 minutes. The polylysine "reaction time" (really the contact time with the PLL solution) was varied from 6 to 10 minutes except in one case which will be discussed in the Results section.

Examination of the Size Distribution of Blue Dextran 2000

The molecular weight of blue dextran 2000 is nominally given as 2 million by the manufacturer (Pharmacia). However the size distribution is not provided and the polydispersity of the blue dextran could be significant. An idea of the size distribution of blue dextran 2000 was obtained by passing it through a sepharose

CL-6B gel column. This sepharose gel resolves dextrans with molecular weights from 10,000 to 1,000,000. The elution profile of the blue dextran 2000 was compared to that of dextran 150 (Pharmacia) and dextran T500 (Pharmacia). Dextran 150 and dextran T500 have molecular weights of 150,000 and 500,000 respectively.

3.2 MATHEMATICAL SIMULATION OF SPORE DEATH DURING HEAT STERILIZATION

3.2.1. Simulation of Can Temperature During Heat Sterilization.

Alginate was initially sterilized in pyrex bottles, but the results indicated that there was considerable depolymerization of the alginate in the autoclave. It was therefore critical to determine the minimum time required to autoclave the alginate. Solutions of sodium alginate were subsequently sterilized in a thin walled steel can. The heat capacity of this can was small relative to the 100 ml of alginate stock that was to be sterilized in the autoclave. The assumption that the contents of the can would be reasonably well mixed (especially at temperatures above 70 °C) was used to facilitate the mathematical analysis. Once the can's temperature, as a function of time was known, the relationship of spore death as a function of temperature and time was used to determine the proportion of cells that would die during the sterilization cycle. This procedure is similar to that described by Humphrey *et al* (135, 136).

The temperature in the autoclave was assumed to be constant at T_s , the temperature of saturated steam during the heating cycle of the autoclave. This assumption was assured in practice, by preheating the autoclave to reduce the time of the initial "conditioning" stage during the autoclave cycle.

A heat balance around the can in a time period $\delta\theta$ gives:

heat in = rate of accumulation

$$UA(T_s - T)\delta\theta = MC\left(\frac{\partial T}{\partial t}\right)\delta\theta \quad \dots 3.2$$

$$\therefore \ln\left(\frac{T_s - T}{T_s - T_0}\right) = - \frac{AU}{MC}t \quad \dots 3.3$$

$$\text{or } T = T_s - (T_s - T_0)e^{-\frac{AU}{MC}t} \quad \dots 3.4$$

where **A** is the effective heat transfer area to the can; **U** is the overall heat transfer coefficient; **C** is the heat capacity of can and contents, T_s is the steam temperature; T_0 is the initial temperature of the can and contents; and T is the temperature of the can at time t .

The overall heat transfer coefficient (**U**) was estimated as :

$$U = \frac{1}{\frac{1}{h_o} + \frac{\Delta x}{k} + \frac{1}{h_i}} \quad \dots 3.5$$

where h_o is the heat transfer coefficient for steam condensing on the outside of the can; h_i is heat transfer coefficient for the inside of the can; k is the thermal conductivity of steel; and Δx is the thickness of the wall of the can.

The heat transfer coefficient of condensing steam at 398 K is large, about 10,000 W/m²K (137), therefore the major resistances to heat transfer are owed to the can's wall and to the low value of the heat transfer coefficient for the inside of the can, hence:

$$\frac{1}{h_o} < \frac{\Delta x}{k} + \frac{1}{h_i} \quad \dots 3.6$$

and

$$U \approx \frac{1}{\frac{\Delta x}{k} + \frac{1}{h_i}} \quad \dots 3.7$$

A value for h_i was estimated by the correlation for free convection in enclosed spaces from the work of Evans and Stefany (138)

$$\left(\frac{h_i L}{k}\right) = Nu_i = 0.55(Gr_i Pr_i)^{1/4} \quad \dots 3.8$$

where h_i is the internal heat transfer coefficient, L is the length of the container (involved in heat transfer), k is the thermal conductivity of the liquid, Nu_i is the film Nusselt number, Gr_i is the film Grashof number, Pr_i is the film Prandtl number. The values of the physical properties of the water-alginate mixture were taken from tables in the text by Geankoplis (137). Additional properties for alginate solutions were obtained from the alginate manufacturer Kelco (New Jersey).

3.2.2. Simulation of Spore Death During Heat Sterilization

Once the can temperature as a function of time was known, the relationship of spore death as a function of temperature was used to determine the proportion of cells that would die as a function of temperature and time. The rate of spore death is first order:

$$\frac{dN}{dt} = -kN \quad \dots 3.9$$

where k is the death constant, and N is the number of spores at time t . The relationship between k and temperature is given by an Arrhenius type relationship:

$$k = B \left(e^{-\frac{E_a}{RT}} \right) \quad \dots 3.10$$

with a constant B and "activation energy" E_a . A general discussion of B and E_a can be found in the work of Deindoerfer and Humphrey (136). During sterilization the viable spore population is reduced from its initial value to some predetermined level adequate for the degree of sterilization desired. This design criterion is often called Nabla (∇), and it is equal to $\ln (N_0/N)$. N_0 and N represent the number of viable spores at the start of the sterilization, (i.e. at t equal 0), and at time t respectively.

In general ∇ is given by the integration of equation 3.9 over a time period t .

$$\nabla = \ln \frac{N_0}{N} = \int_0^t k dt \quad \dots 3.11$$

$$\nabla = \int_0^t B e^{-\frac{E_a}{RT}} dt \quad \dots 3.12$$

The expression for ∇ is complicated because the temperature in the can is not a constant. However if the relationship for T is substituted, ∇ can be evaluated by numerical integration. The trapezoidal rule was used to evaluate the integral with values of Δt of 15 s. Values for B and E_a (the constants in the expression for the specific death rate) were taken from data for *Bacillus stearothermophilus*, since spores of this organism is one of the most difficult to kill by heat.

A typical criterion for ∇ is the "12-D" kill, where $\log_{10} (N_0/N)$ is equal to 12. This is equivalent to the reduction of the number of spores from 1×10^7 to 1×10^{-5} . Since fractional viable spores do not exist, 1×10^{-5} spores is considered to be the probability that only 1 sterilization per 10^5 would fail.

Table III lists the values of the constants used in the simulation.

Table III. Value of the Constants Used in the Simulation of Spore Death During Sterilization.		
A	Can's heat transfer area	0.000841 m
U	Overall heat transfer coefficient	1336 W/(m ² K)
M	Mass of can and contents	0.104 kg
C	Heat capacity of can and contents	4185 J/K
T _s	Autoclave steam temperature	397 K
T ₀	Initial temperature of the can and contents	298 K
B	Constant in the expression for death rate	$7.94 \times 10^{38} \text{ min}^{-1}$
E _a	"Activation Energy in the expression for death rate	$68.7 \times 10^3 \text{ cal/gmol}$

3.3 THE EFFECT OF STERILIZATION ON THE VISCOSITY AVERAGE MOLECULAR WEIGHT OF ALGINATE.

3.3.1. Sterilization Procedure.

The effect of sterilization on the viscosity average molecular weight of alginate was determined by sterilizing 100 ml samples of either 3 or 4 % sodium alginate stock solutions for 5, 10, 15 and 20 minutes. The alginate solutions were prepared in HEPES buffered saline (pH 7.4). Both Kelco low viscosity (L.V.) and Kelco high viscosity (H.V.) gelling grade alginates were sterilized by this procedure. The temperature was 255 °F (123.8 °C) and the sterilization was done in a can vented through a foam plug. (The simulation of spore death as a function of time was done for a similar container.)

3.3.2. Estimation of Alginate Molecular Weights.

Molecular weights were determined by using the correlation of Donnan and Rose (139, 140) :

$$DP = 58[\eta] \quad \dots 3.13$$

where $[\eta]$ is the limiting viscosity number or the intrinsic viscosity and DP is the degree of polymerization. It was assumed that the monomeric weight of alginate was 216; therefore the molecular weight (Mwt) of alginate is given by:

$$Mwt = 12,528[\eta] \quad \dots 3.14$$

A monomeric weight of alginate of 216 includes the water of hydration which is normally bound to the monomers of alginate (139, 140).

The following relationships are used to calculate $[\eta]$:

$$i) \quad \eta_r = \frac{\eta}{\eta_0} \quad \dots 3.15$$

$$ii) \quad \eta_{sp} = \frac{\eta - \eta_0}{\eta_0} \quad \dots 3.16$$

$$iii) \quad [\eta] = \lim_{c \rightarrow 0} \frac{\eta_{sp}}{c} \quad \dots 3.17$$

where the relative viscosity η_r is the ratio of the viscosity of the polymer (alginate) solution, η , to that of the solvent (saline), η_0 . The specific viscosity η_{sp} is the relative increase in the viscosity which occurs when a polymer is dissolved in a solvent. The viscosity number (η_{sp}/c) measures the average contribution of the solute molecules at concentration c to the viscosity. The limiting viscosity number or the Straudinger index $[\eta]$ is also called the intrinsic viscosity (141).

The alginate stock solutions after sterilization were diluted with saline to concentrations from 0.0375 to 0.25 g per 100 ml. The viscosity of these solutions were measured by a Cannon-Ubbelohde semi-micro viscometer at 28 °C. Plots of the viscosity number versus concentration were extrapolated to zero concentration. The intercept of these plots with the viscosity number axis was taken to be the intrinsic viscosity.

3.4 GROWTH, ACTIVITY AND PRODUCTION STUDIES.

Erwinia herbicola ATCC 21434 was obtained from the American Type Culture Collection (ATCC).

3.4.1. Culture Preservation.

Lyophilized cells of *Erwinia herbicola* were resuspended into nutrient broth (Difco) and grown up to the late exponential phase. The cells were then divided into aliquots and mixed with glycerol to aid cryo-preservation (142) and stored in a -70 °C freezer. This provided a permanent stock of the original culture. In routine work, cells freshly grown in Ehrlenmeyer flasks were stored in a cold room at 4 °C. Cells from these flasks were used as preinocula for the inoculum flasks. Cells used as inocula were always freshly grown and were in the late exponential phase. After 1 month of culture maintenance by using inoculum from cultures stored in the cold room, a fresh culture was started from the stock in the -70 °C. This reduced the chance that contaminated cultures or cultures that had mutated could be inadvertently used.

All experiments in the same design block or group were done with cultures grown from the same stock from the -70 °C freezer.

3.4.2. Biomass Versus Time Profiles in Nutrient Broth

Dry weight or biomass per millilitre of cell suspension were determined by filtering, under vacuum, measured volumes of cell suspension through tared nylon 0.2 µm filters. The filters were obtained from Millipore. The filters were then dried to constant weight in an oven at 105 °C. Standard curves of the "absorbance" of the cell suspension versus the biomass as dry weight were constructed. Absorbance was measured at 610, 490 and 410 nm. Biomass as a function of time in growing cultures were then obtained by relating the absorbance of the cell suspension to the standard curve at 610 nm since this curve was most linear. Growth was quenched before each absorbance determination by diluting with cold nutrient broth which contained chloramphenicol at 175 µg/ml as recommended by

Koch (143). The low temperature and the chloramphenicol stopped the growth of the cells without killing them. The use of "absorbance" to measure biomass is based on the "light scattering turbidimetric" method discussed by Koch (144).

3.4.2. Growth as a Function of Agitation and Temperature.

Growth as a function of agitation was conducted in 250 ml shake flasks with an amount of medium equal to 20 % of the volume of the flask. The inoculum was 10 % of the volume of the medium. Nutrient broth (Difco) was used as medium. The amount of agitation was varied by adjusting the shake speed from 60 to 220 revolutions per minute (rpm). Experiments were conducted at 32 °C in an incubator with a 2 inch (5.08 cm) throw. Cells that had been grown at 140 RPM and 30 °C were used for the inoculation of the flasks. The cells of the inocula were in the late exponential to early stationary phase of growth.

The effect of temperature and time on the development of biomass was followed as above in the agitation studies, except that the shake rate was kept constant at 180 rpm. The shaker (a Labline Junior Orbit Incubator) was also modified by attaching an external cooler via the cooling tubes at the rear. The external cooler's bath temperature was set at -1 °C. By using the combination of the cooler and the "Labline" shaker temperature controller steady temperatures with a deviation of ± 0.5 °C could be maintained.

3.4.3. Enzyme Induction.

TPL activity was induced by growing the cells in a tyrosine rich medium that was similar to that of Enei *et al* (77), however 12.0 g/l hydrolysed soy protein was substituted for the soy liquor. The results of the growth studies (described above) suggested that the cells could be successfully grown at 32 °C and at an rpm of 180 in a shaker with a 2 inch throw. These conditions were used for the growth of the cells in the induction medium with an initial pH of 7.0.

Growth was conducted in 500 ml Ehrlenmeyer shake flasks with 100 ml of TPL induction medium. The inoculum was 10 % of the medium and was prepared

from cells grown in nutrient broth at 180 rpm and 32 °C. The cells were in the late exponential to early stationary-phase.

3.4.4. Cell Harvesting

Cells were harvested by centrifugation at 10,000 g for 10 minutes. The supernatant was discarded and the cells washed twice by resuspension in 0.1 M phosphate buffer (PB) followed by centrifugation. The resulting cell pellet was then reconstituted in PB. All cell harvesting was done at 4 °C.

3.4.5. Protein Assay

For activity studies total cell protein was used as a measure of biomass. Total cell protein was analyzed by the coomassie blue method (145) with bovine serum albumin as the protein standard. Coomassie blue was obtained from BioRad. Typically 100 µl of cell suspension was mixed with 500 µl of 3.0 M NaOH in a pyrex test tube. The tube was then heated for 10 minutes in a water bath at 90 °C to solubilise the bacterial cell protein. The sample was neutralised with 500 µl of 3.0 M HCl. The sample was then centrifuged at 16,500 g for 3 minutes to precipitate cell wall debris and other insoluble components. A sample of the resulting supernatant was then analyzed for its protein concentration with the aid of a calibration curve produced with bovine serum albumin (Bio-Rad) as standard.

For the assay of the amount of protein entrapped within microcapsules, 200 µl of microcapsules was mixed with 500 µl of 3.0 M NaOH and heated at 90 °C for 10 minutes. This process dissolved the microcapsules and solubilised the bacterial protein. The rest of the assay was carried out as described above for free cells.

3.4.6. Assay of Tyrosine Phenol Lyase (TPL) Activity

TPL activity was determined by measuring the amount of phenol produced with time by the degradation of tyrosine in the reverse of reaction 1. The assay flasks contained 18 ml of 2.0 mM tyrosine in PB (0.1 mM pH 8.0). The temperature

was 37 °C and the stir rate was 180 rpm unless otherwise stated. Reaction was initiated by adding 2.0 ml of cell suspension or 1.0 ml of microcapsules and 1.0 ml of buffer. Samples were removed at various times and assayed for phenol by the method of Porteous and Williams (146). The amount of cells in the assay is given as total amount of cell protein in mg, rather than on a per unit volume basis. This is done to stress the fact that the protein is in the form of whole cells during the assay, and not in a solubilised or homogenised form.

The initial slope of the plot of phenol concentration versus time was considered to be the initial rate or the activity. To remove bias from the determination of the initial slope, a best fit polynomial in time (such as equation 3.18) was fitted to the data as suggested by various authors (147, 148). Differentiation of the equation (3.18) with time shows that the initial rate is given by the value of parameter a_1 in equation 3.18. The minimum degree of the polynomial that could fit the phenol production with time data was determined by the sequential F-test (149).

Typically a polynomial in time of degree 2 or less was adequate to fit the data.

$$[phenol] = a_0 + a_1t + a_2t^2 \dots + a_it^i + \dots + a_nt^n \quad \text{..3.18}$$

3.4.7. Assay of L-Tyrosine and L-Dopa

L-Tyrosine and L-dihydroxyphenyl-L-alanine (L-dopa) were analyzed by high performance liquid chromatography (HPLC). Tyrosine and dopa have low solubility in aqueous systems at pH values close to neutrality. Therefore the product tyrosine or dopa could be partially solid depending on the extent of the production reactions 8 or 9 (C₁ section 2.3.2). For tyrosine assay the total product of the reaction was solubilised by mixing with an equal volume of 1.5 M NaOH. The high pH assured the solubilization of the product tyrosine (and the microcapsules if

present). 40 μ l of this solution was made up to 2000 μ l with 20 % (v/v) methanol. The 20 % methanol caused the precipitation of cell protein that could foul the HPLC column. The deproteinized tyrosine solution was then diluted with pure methanol (1:4, v/v). This final sample was then analyzed by HPLC with the method of Hill (150).

3.4.8. L-Tyrosine and L-Dopa Production

For the production of tyrosine or dopa, 8 ml of PB (0.1 M, pH 8.0) at the required concentrations of ammonia, pyruvate and phenol or catechol respectively were placed in flasks. Two millilitres of cell suspension were added to initiate reaction in free cell studies. For immobilised cell studies 1.0 ml of microcapsules plus 1.0 ml of PB was added to initiate reaction. The reactions were carried out in an incubator at temperatures as indicated and shaken at 240 rpm.

3.4.9. Data Analysis

The fit of kinetic data to some of the classical models of enzyme kinetics were analyzed by the use of nonlinear least squares regression. In these models, the algorithm of Marquardt (151) was usually used when the number of parameters were less than 3 or 4 (151).

The production data was analyzed by fitting the data to the integrated form of likely rapid equilibrium mechanisms. The equations were nonlinear. The values of the parameters which gave a minimum of the residual sums of squares of each model were determined by using the algorithm of Ralston and Jennrich (152). This algorithm was used because the derivatives of the resulting models with respect to each parameter were calculated numerically. The complexity of these models makes the explicit determination of the required derivatives time consuming and tedious. The best model was considered to be the one with the smallest value for the residual sums of squares due to the regression and with all parameters significant at the level of $p \leq 0.05$.

4.0 RESULTS & DISCUSSION

4.1 MICROENCAPSULATION TECHNIQUE

I pass with relief from the tossing sea of Cause and Theory to the firm ground of Result and Fact.

-Sir Winston S. Churchill.

4.1.1. Simulation of Spore Death During Sterilization.

The results of the simulation of spore death during the heat sterilization of 100 ml of alginate in a thin walled can are shown in Figure 8. These results indicate that adequate sterilization occurs in approximately 4.8 minutes. This degree of sterilization corresponds to $\nabla = 27.63$ and represents a theoretical reduction in the number of spores from 1×10^7 to 1×10^{-5} . The simulation gives conservative results because it does not consider the additional death which occurs as the autoclave cools down. On the liquid cycle the autoclave releases the steam pressure by a slow exhaust cycle which lasts about 7 minutes. In this period the temperature in the autoclave drops from 255 °F to 212 °F (123.8 °C to 100 °C).

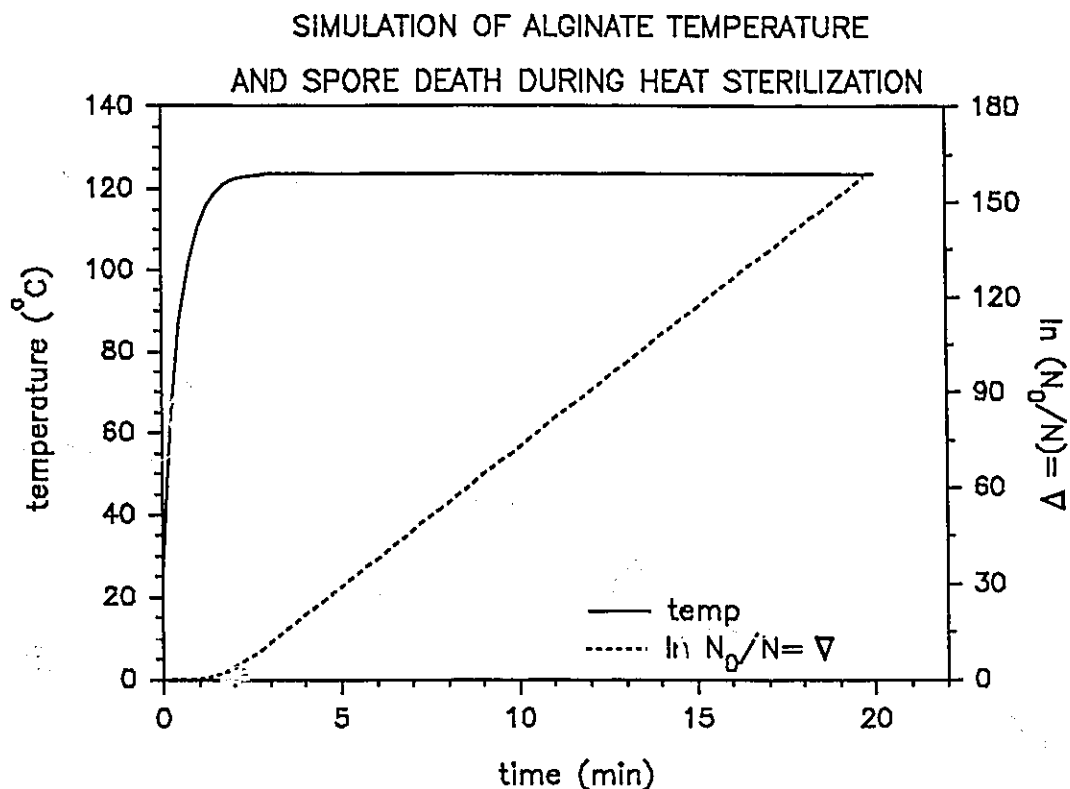


Figure 8. Mathematical simulation of spore death during heat sterilization of alginate.

4.1.2. The Effect of Heat Sterilization on Depolymerization of Alginate.

The alginate (in alginate in buffered saline solutions (pH 7.4)) depolymerised when it was heated to the sterilization temperature. After 20 minutes of sterilization at 255 °F the viscosity average molecular weight of Kelco-Gel® LV alginate (*i.e.* the low viscosity alginate) decreases by 19 percent (from 55,800 ± 7,400 to 45,100 ± 2,200 Daltons). The molecular weight of Kelco-Gel® HV alginate (*i.e.* the high viscosity alginate) decreases by 42 percent (from 113,600 ± 5,400 Daltons to 65,700 ± 1,200 Daltons) when it is heat sterilized for 20 minutes. The molecular weight of alginate as a function of the duration of heat sterilization is shown in Figure 9.

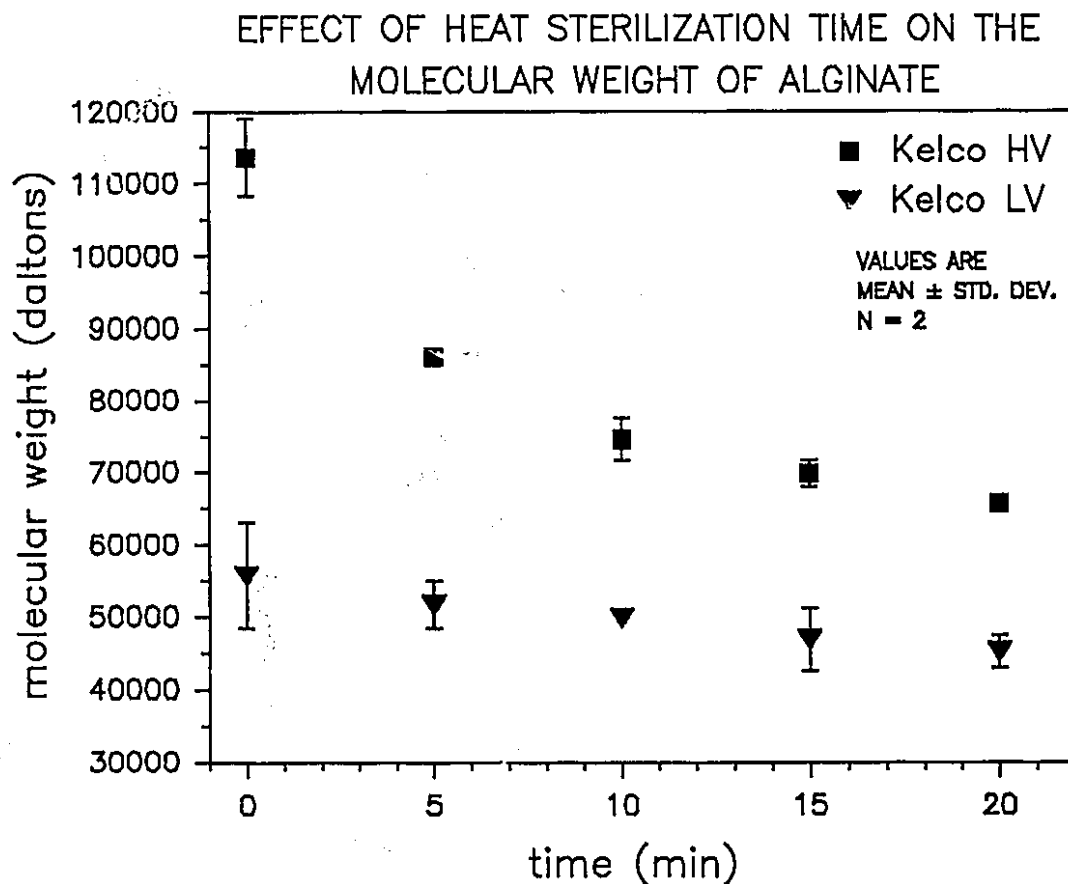


Figure 9. The effect of sterilization on the molecular weight of alginate. Stock solutions of alginate (3% Kelco H.V. or 4 % Kelco L.V. were heat sterilized at 255 °F.

4.1.3. The Effect of Airflow on the Diameter of Alginate-PLL-Alginate Microcapsules.

The effect of airflow and alginate concentration on the diameter of microcapsules made with Kelco-Gel® HV alginate in the bead formation stage is shown as Figure 10. The alginate was sterilized as a 3 percent stock in HEPES buffered saline (pH 7.4). The alginate concentration was varied in 0.25 percent increments from 0.75 to 1.5 percent. The flow of the cell suspension (of *Erwinia herbicola*) in alginate to the droplet former was 0.389 ml/min. The airflow was varied from 2.0 to 3.5 l/min. The number of cells in the cell suspension was measured as total cell protein was 3.11 mg/ml. The diameter of the microcapsules

decreased by an average of 590 microns for each 1.0 l/min increase in the airflow to the droplet former. However at the higher flowrates the alginate drops emerged as a fine spray. The fine droplets did not enter the calcium chloride solution. They deposited on the air-water interface. This tendency was most pronounced when the alginate concentrations was 0.75 or 1.00 percent and the airflow was 3.5 l/min.

Microcapsules were examined by light microscopy. Well prepared microcapsules have a size distribution that is unimodal. An alginate concentration of 1.5 percent produced good microcapsules if the airflow was 2.0 or 2.5 l/min. At higher airflows the microcapsules were of smaller diameter, however some of these microcapsules appeared empty.

At lower alginate concentrations the microcapsules were either not spherical, or they were stuck together or else they were fragmented and broken. The fragmented microcapsules occurred at the higher airflows (*i.e.* at 3.0 or 3.5 l/min).

EFFECT OF AIRFLOW ON THE SIZE OF ALGINATE-POLYLYSINE-ALGINATE MICROCAPSULES

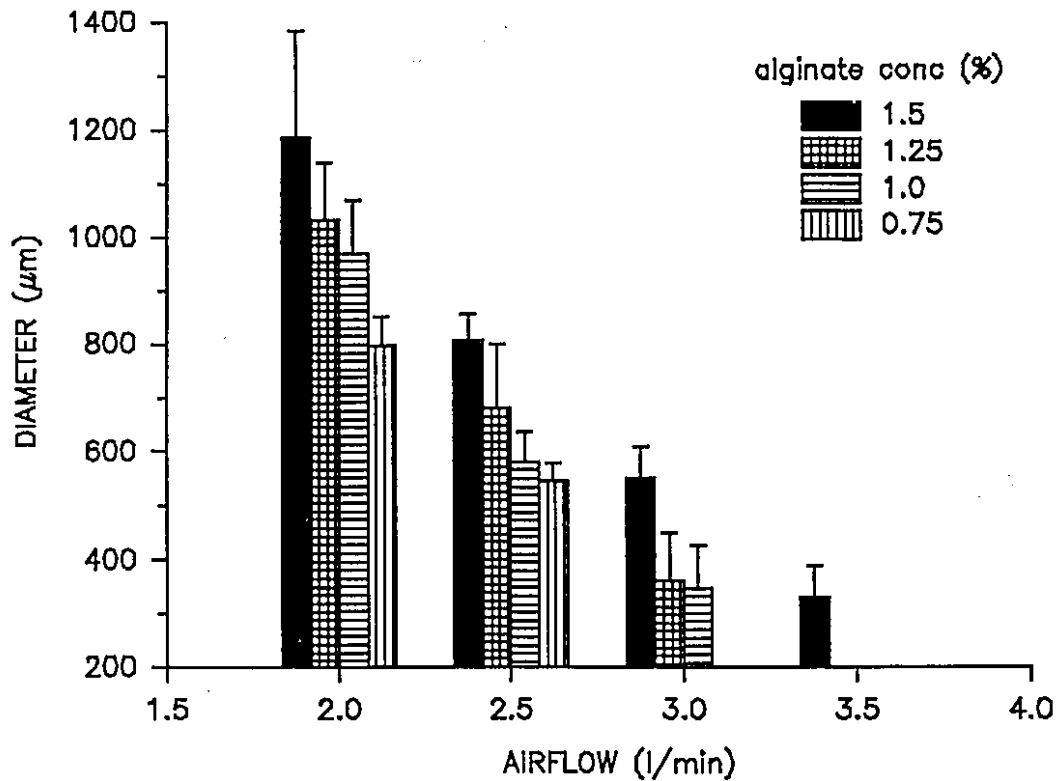


Figure 10. The effect of airflow and alginate concentration on the size of the microcapsules. Values are mean and standard deviation of the size distribution of diameters.

Figures 11, 12, 13 and 14 show photomicrographs of microcapsules prepared with 1.5 percent Kelco-Gel® HV (high viscosity) alginate and various airflows. Figures 15, 16, 17 and 18 show photomicrographs of microcapsules prepared with 0.75 percent Kelco-Gel® HV alginate. The inability to make good microcapsules at low alginate concentrations and high airflows is shown in these latter Figures.

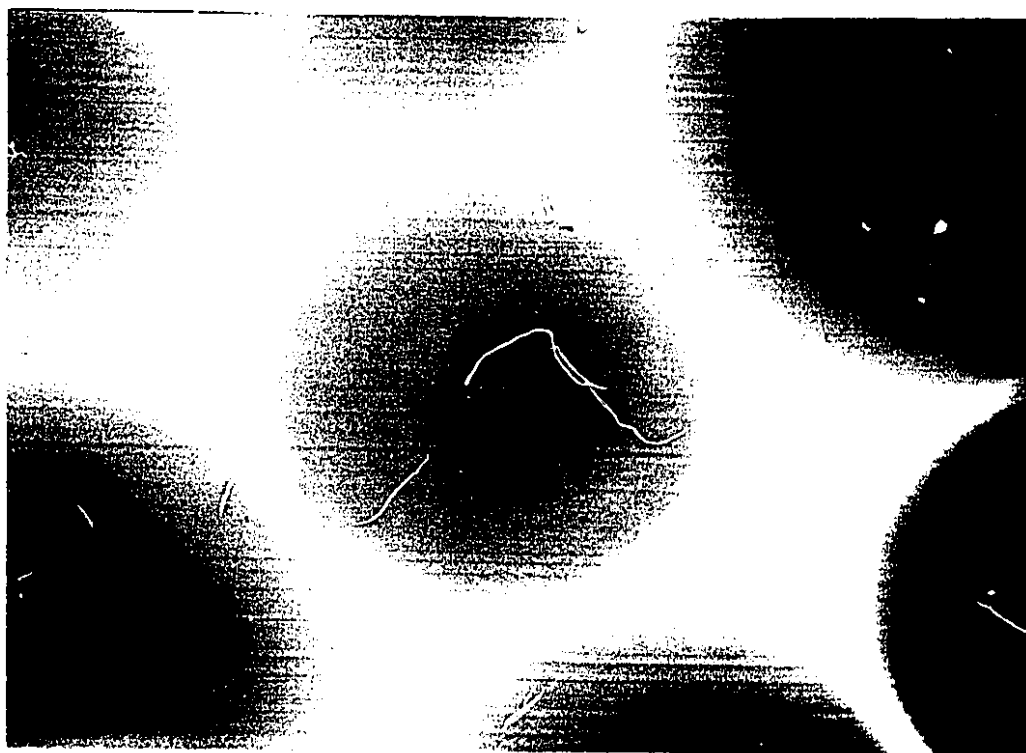


Figure 11. Photomicrograph of microcapsules ($1185 \pm 197 \mu\text{m}$) made with Kelco-Gel HV alginate. The airflow was 2.0 l/min. The microcapsules are spherical and contain yellow *E. herbicola*.

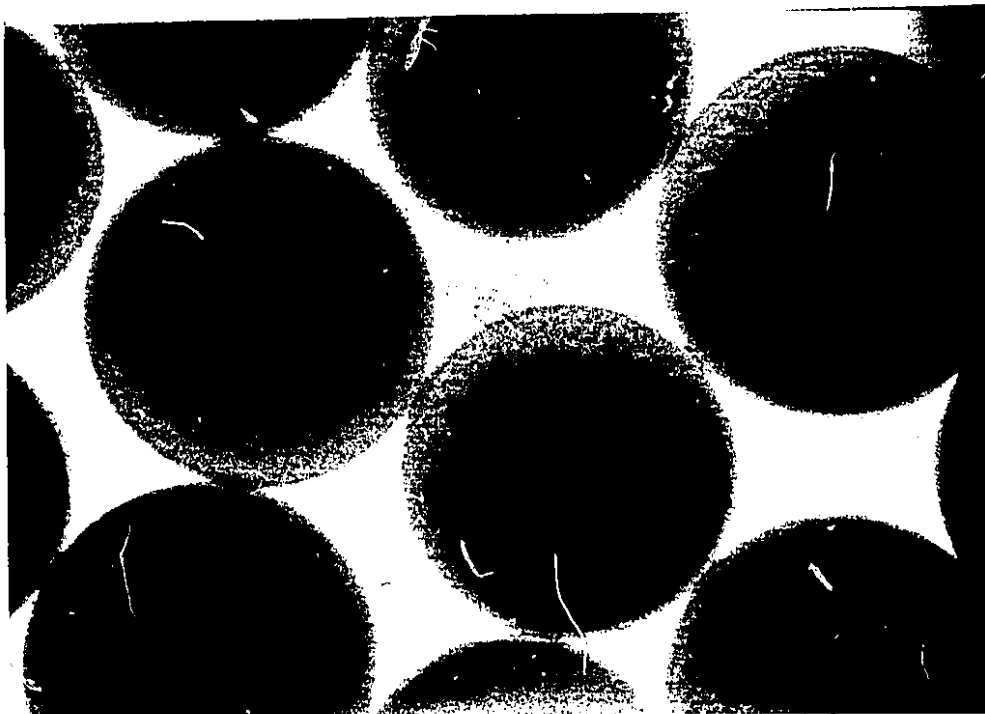


Figure 12. Photomicrograph of microcapsules ($805 \pm 51 \mu\text{m}$) made with 1.5 % Kelco-Gel HV alginate. The airflow was 2.5 l/min. N.B. the yellow coloured bacteria in the microcapsules.

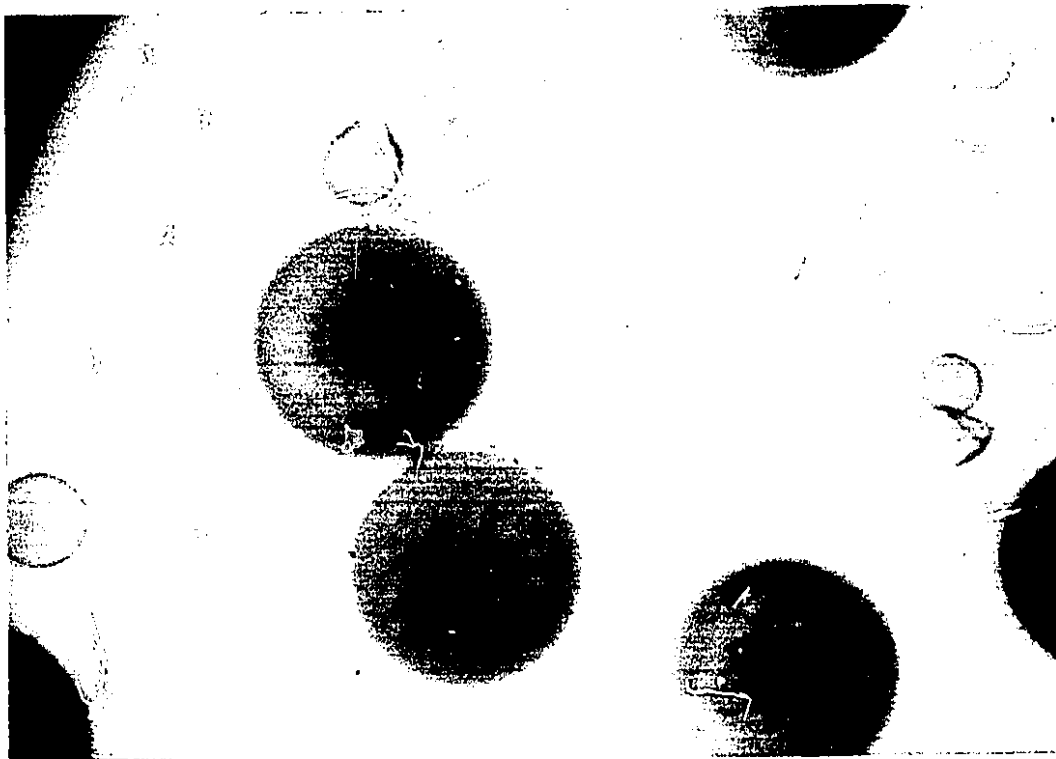


Figure 13. Photomicrograph of microcapsules ($549 \pm 59 \mu\text{m}$) made with 1.5 % Kelco-Gel HV. The airflow 3.0 l/min. N.B. small empty microcapsules.

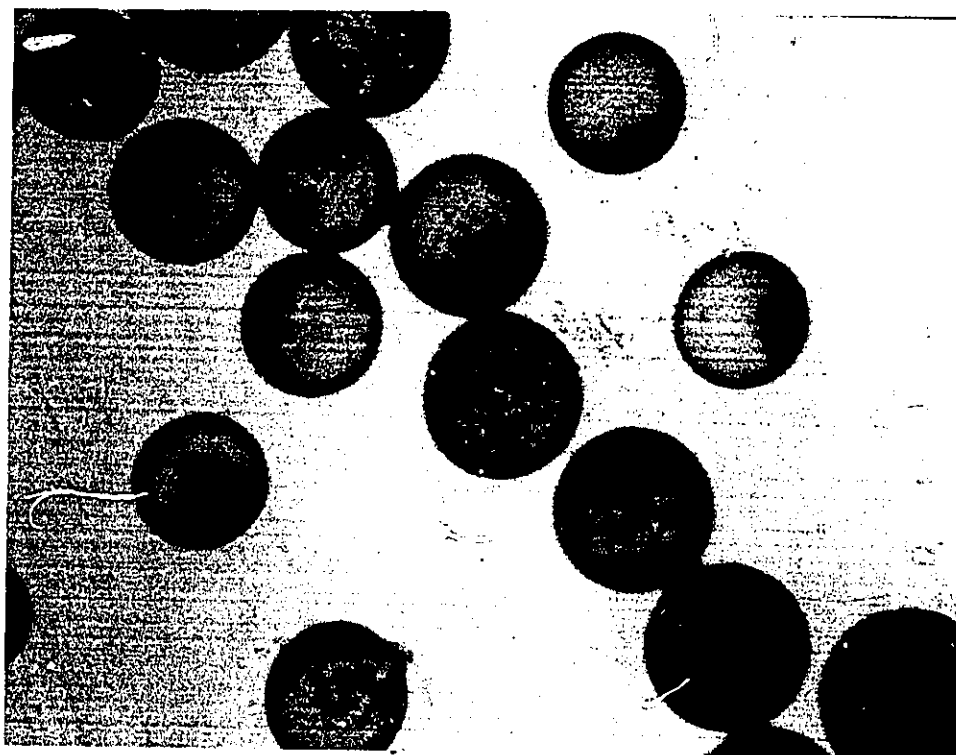


Figure 14. Photomicrograph of microcapsules ($331 \pm 59 \mu\text{m}$) made with 1.5 % Kelco-Gel HV. The airflow was 3.5 l/min.



Figure 15. Photomicrograph of microcapsules ($796 \pm 54 \mu\text{m}$) made with 0.75 % Kelco-Gel HV alginate. The airflow was 2.0 l/min. Lots of microcapsules are stuck together.

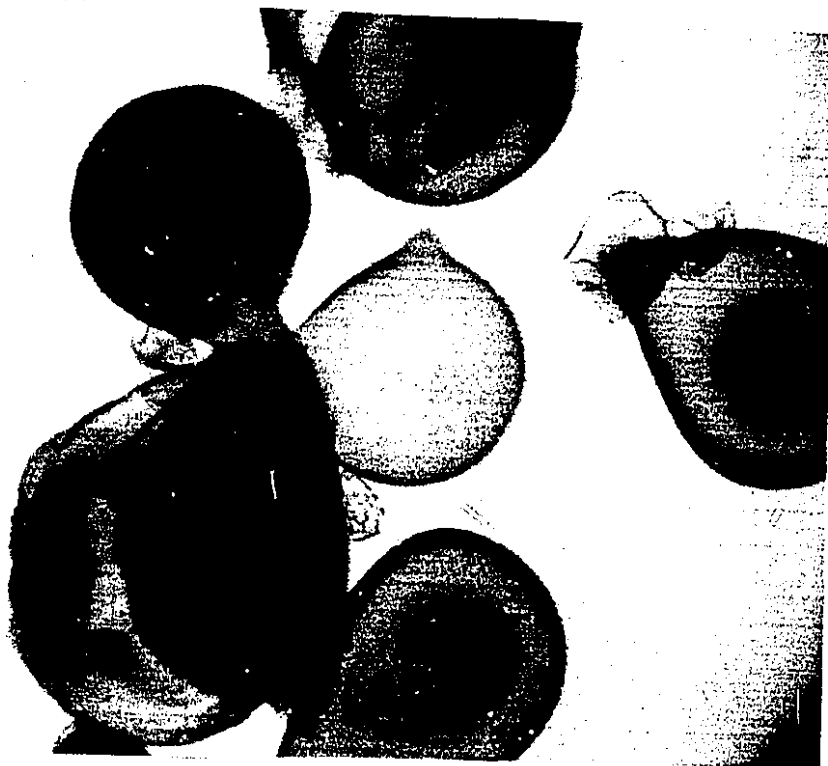


Figure 16. Photomicrograph of microcapsules ($544 \pm 33 \mu\text{m}$) made 0.75 % Kelco-Gel HV. The airflow was 2.5 l/min. N.B. empty capsules, many not well formed..

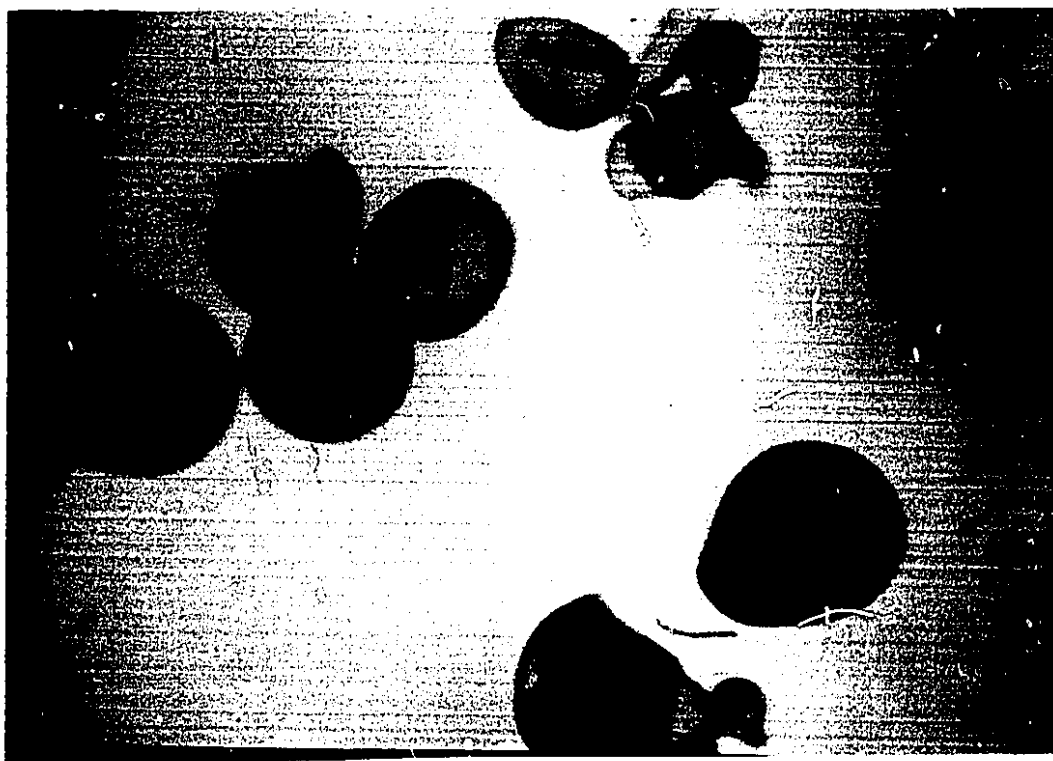


Figure 17. Photomicrograph of "microcapsules" made with 0.75 % Kelco-Gel HV. The airflow was 3.0 l/min. N.B. microcapsules are not well formed

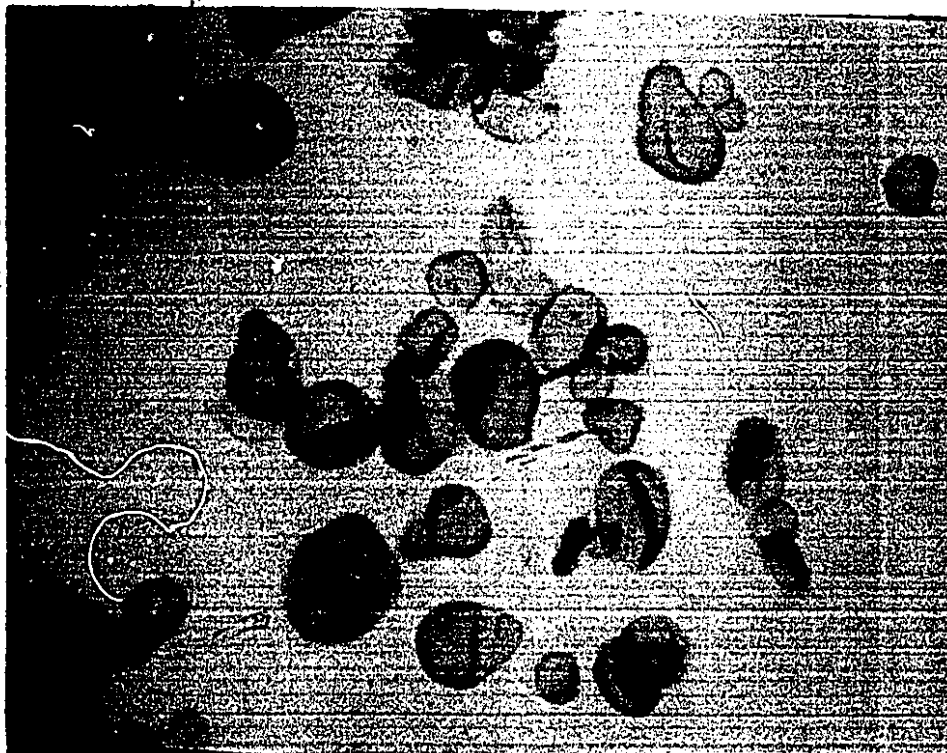


Figure 18. Photomicrograph of "microcapsules" made with 0.75 % Kelco-Gel HV alginate. The airflow was 3.5 l/min. N.B. microcapsules are empty or broken.

4.1.4. The Effect of Liquid Flow on the Diameter of the Microcapsules.

The effect of liquid flow on the diameter of microcapsules made with 1.5 % Kelco-Gel® HV is shown graphically in Figure 19. The PLL reaction time was 10 minutes. The airflow to the droplet former was either 2.5 or 3.0 l/min as indicated in the figure; the flow of the cell suspension was set at either 0.389, 0.763, 1.07 or 1.49 ml/min. These liquid flowrates corresponded to settings on a syringe pump of 10, 8, 7 and 6. The amount of cells in the cell suspension in alginate (measured as total cell protein) was 3.31 ± 0.24 mg/ml. There was no significant change in the size of the microcapsules with increases in liquid flow (under these conditions).

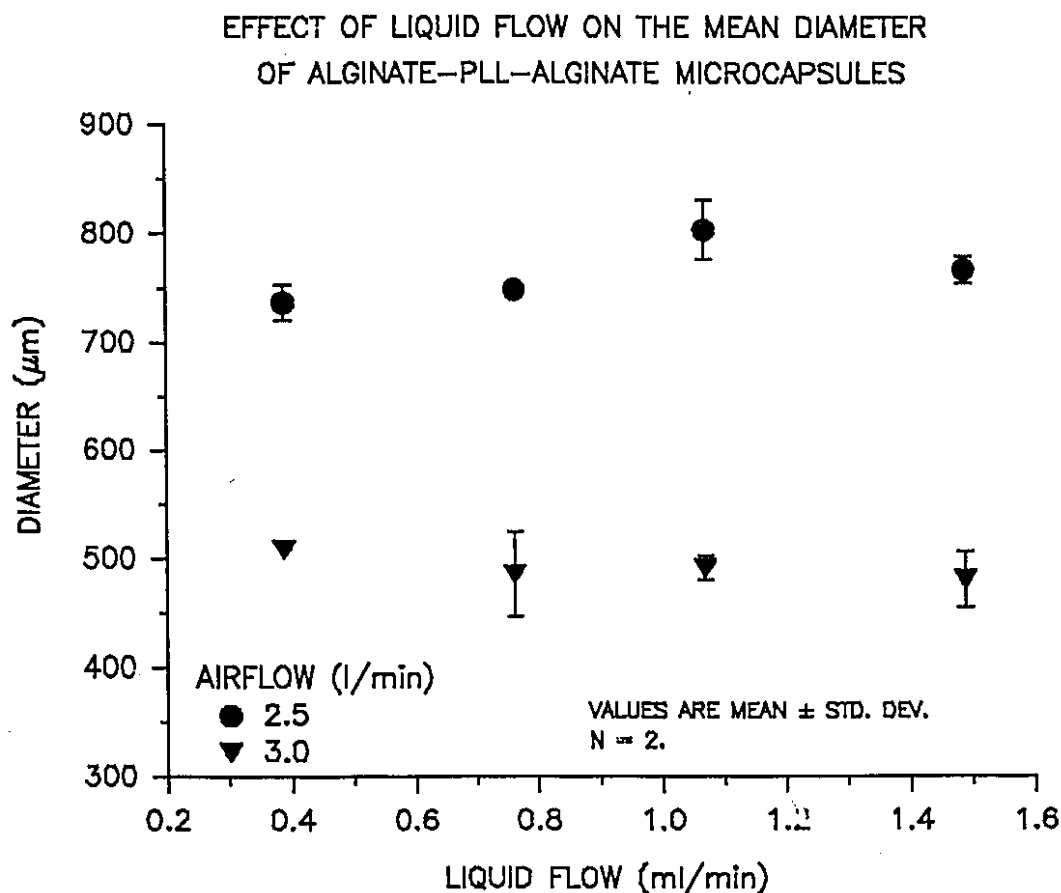


Figure 19. The effect of liquid flow on the size of the microcapsules made with 1.5 % Kelco-Gel HV.

The increase in the airflow from 2.5 to 3.0 l/min resulted in the formation of a great number of satellite microcapsules. These results are similar to those described earlier in the airflow experiment, in that the satellite microcapsules also appeared empty in this case. Typical size distributions obtained are shown in Figures 20 and 21. They show the increased tendency to form a bimodal distribution as the airflow is increased from 2.5 to 3.0 l/min. Microcapsules made at a liquid flow of 1.07 ml/min and an airflow of 2.5 and 3.0 l/min are shown in Figures 22 and 23.

Thus while a high airflow to the droplet former produces microcapsules of smaller mean diameter, the size distribution will be pronouncedly bimodal. In addition defective satellite microcapsules will also be produced.

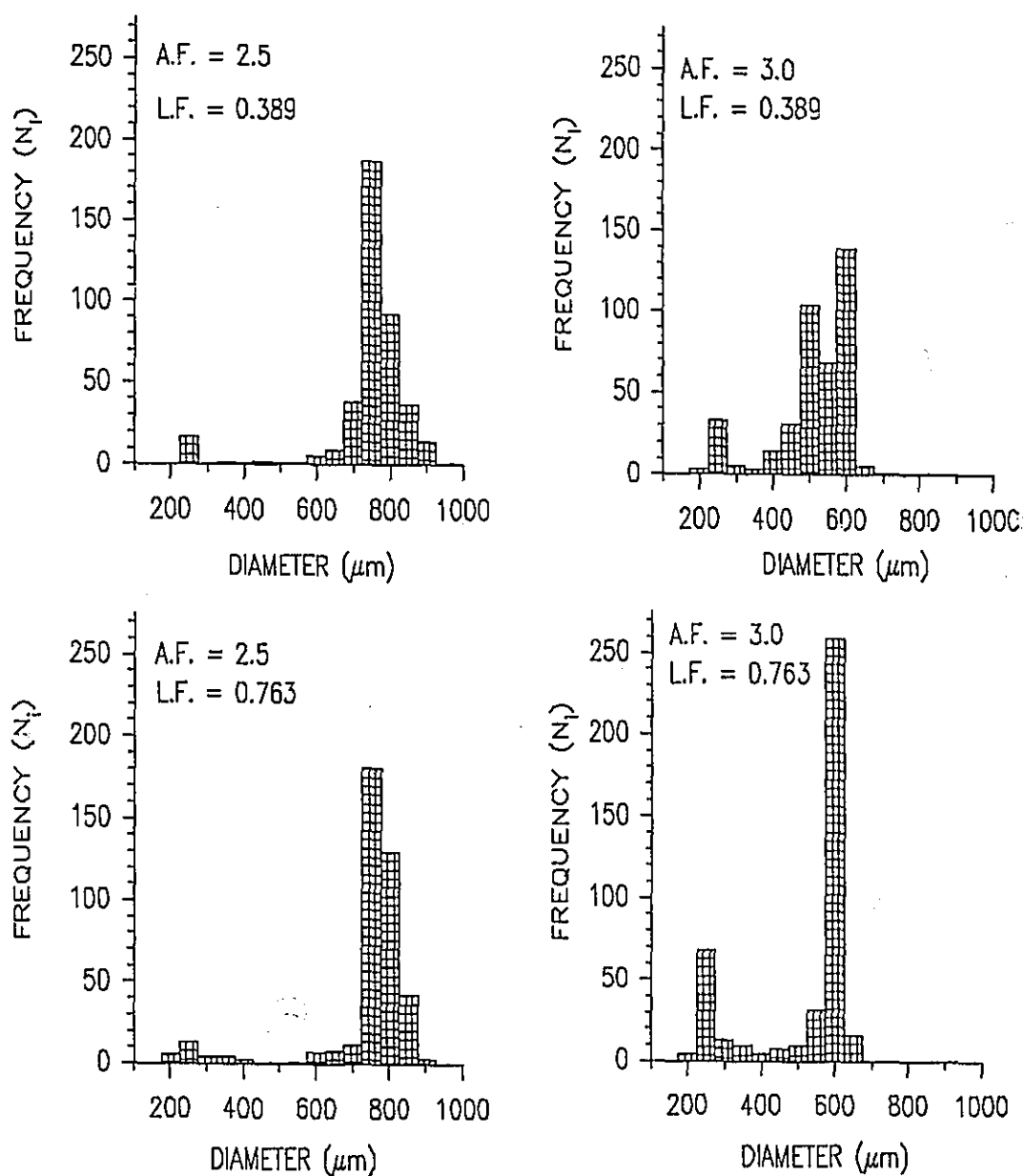


Figure 20. Size distribution of the microcapsules as a function of liquid flow (L.F. = 0.389 or 0.763 ml/min) and airflow (A.F. in l/min). N.B. the more bimodal distribution when A.F. = 3.0.

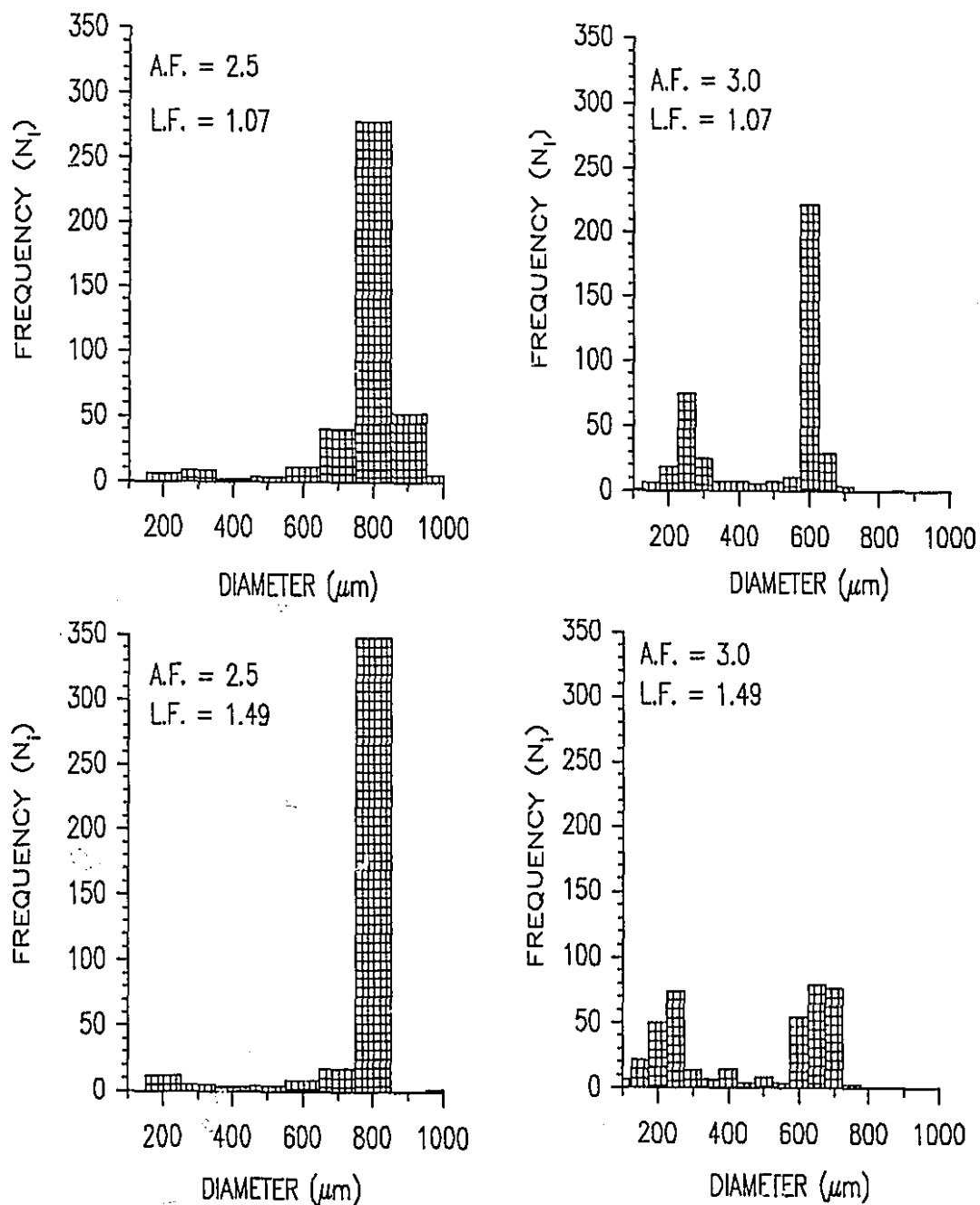


Figure 21. Size distribution of microcapsules made with a liquid flow of 1.07 and 1.49 ml/min. The distributions are more bimodal at an airflow of 3.0 l/min than at 2.5 l/min.

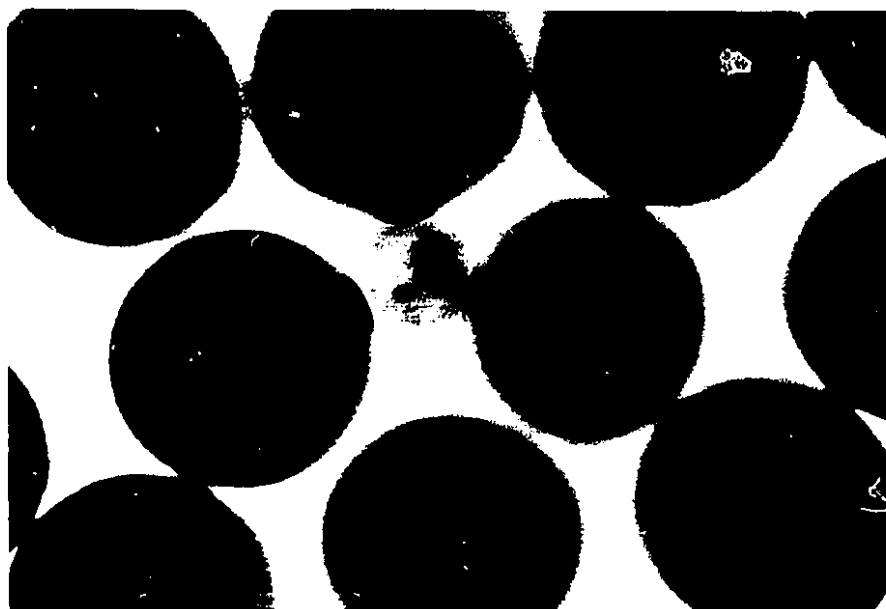


Figure 22. Photomicrograph of microcapsules made with 1.5 % Kelco HV alginate. The liquid flow was 1.07 ml/min and the airflow was 2.5 l/min.

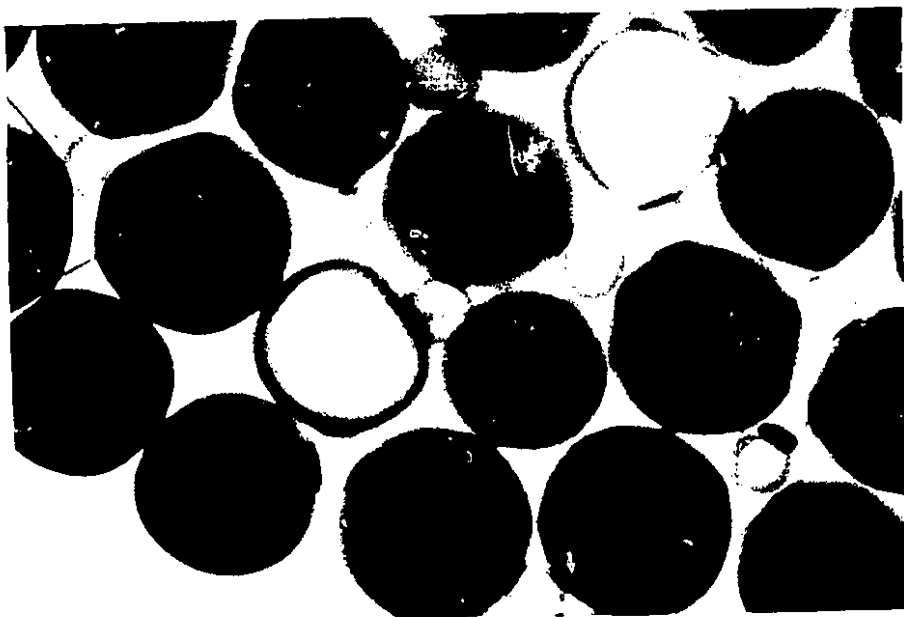


Figure 23. Photomicrograph of microcapsules made with 1.5 % Kelco-Gel HV. The liquid flow was 1.07 ml/min and the airflow was 3.0 l/min.

4.1.5. The Effect of Alginate Preparation and PLL Contact Time on the Relative Strength of the Microcapsules.

Microcapsules which contained blue dextran 2000 (Pharmacia, Mwt 2.0×10^6) and *Erwinia herbicola* cells were shaken at speeds from 150 up to 400 rpm. The fraction broken after 60 minutes was assessed. They were prepared using a liquid flow of 1.07 ml/min and an airflow of 2.5 l/min to the droplet former. The presence of blue dextran in the microcapsules aided in the visual assessment of the quality of the microcapsules. Broken microcapsules were almost transparent under light microscopy, however intact microcapsules appeared as uniformly dark blue spheres.

Figure 24 shows blue dextran containing microcapsules made with Kelco-Gel[®] HV alginate sterilized for 5 minutes and a PLL reaction time of 10 minutes. Figure 25 shows microcapsules made under identical conditions except that they were made with Kelco-Gel[®] LV alginate. The microcapsules made with Kelco-Gel[®] HV alginate are all blue, because of the entrapped blue dextran. Some of those made with Kelco-Gel[®] LV do not contain blue dextran.

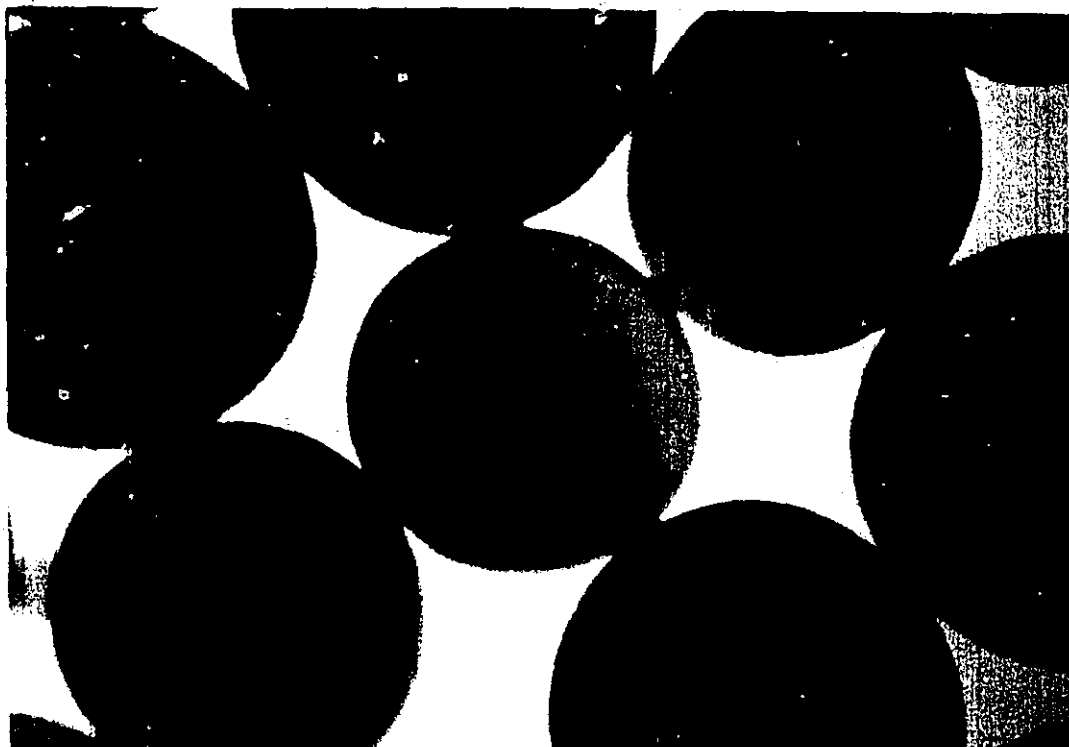


Figure 24. Blue dextran 2000 (MW 2 million) containing microcapsules made with Kelco HV heat sterilized for 5 minutes and PLL reaction time of 10 minutes.

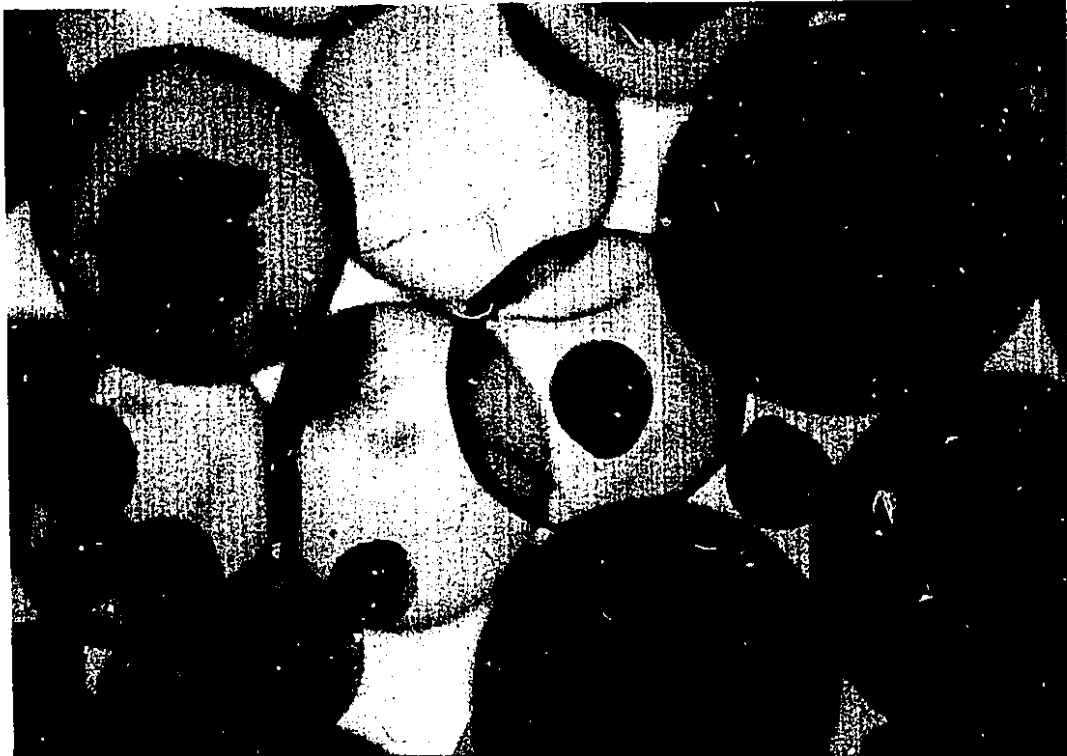


Figure 25. Blue dextran 2000 (Mwt 2 million) containing microcapsules made with Kelco LV alginate sterilized for 5 minutes and a PLL reaction time of 10 minutes.

Microcapsules made with Kelco-Gel® HV alginate sterilized for 5 minutes, did not release blue dextran into the supernatant if the shaking speed was less than 300 rpm. At 400 rpm the microcapsules started to release blue dextran, this indicates that they started to break at this rpm.

Microcapsules made with Kelco-Gel® HV alginate that was sterilized for 15 minutes started to release blue dextran at a shake speed of 150 rpm. The amount of released blue dextran increased as the shake speed was increased. This suggests that either the microcapsules, made under these conditions, are highly permeable to blue dextran 2000 (MW 2×10^6) or else they are very fragile, hence

they break at a lower RPM. Microcapsules made with a PLL contact time (or reaction time) of 6 minutes released more blue dextran than those made with a PLL contact time of 10 minutes. These results are shown graphically in Figure 26. This indicates that an increase in PLL reaction time increases the strength of these microcapsules (or reduces their permeability to blue dextran 2000).

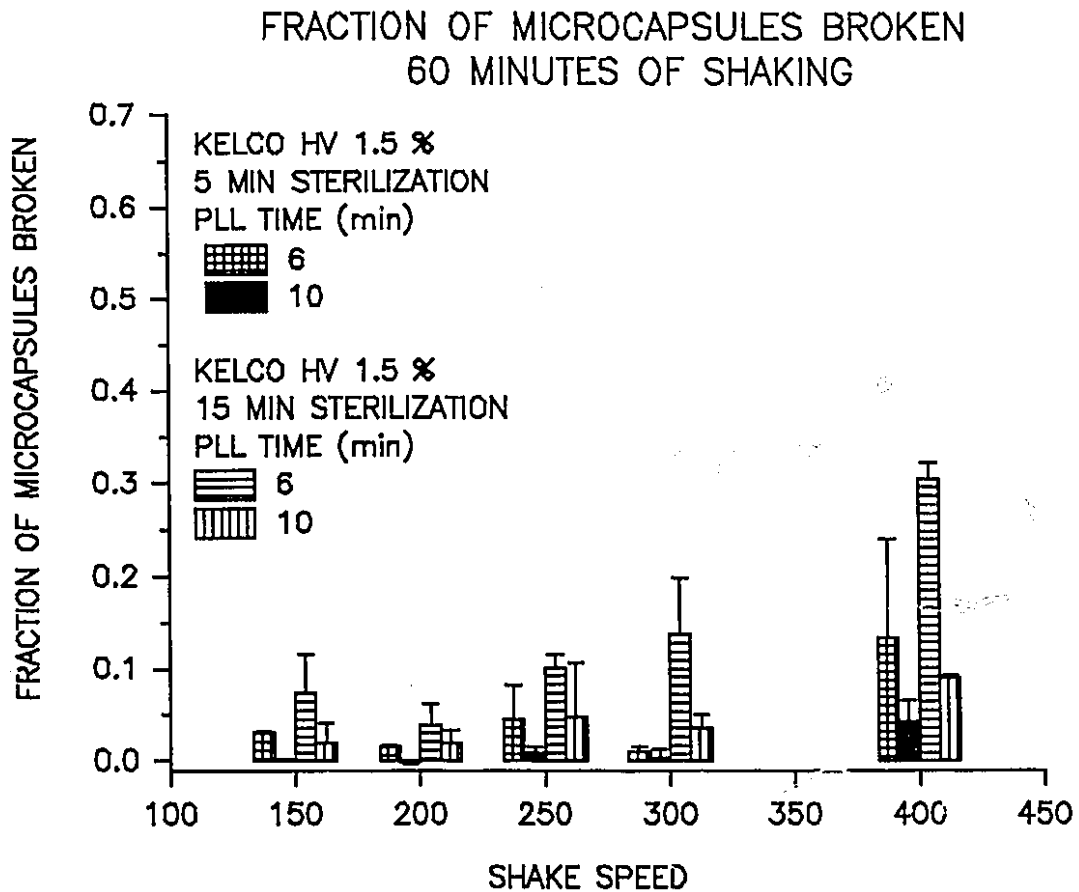


Figure 26. Breakage of microcapsules made with 1.5 % Kelco HV alginate.

The fraction of microcapsules broken was not assessed when they were made from 1.5 % Kelco-Gel® LV alginate that had been sterilized for 15 minutes, and the PLL reaction time was 6 minutes. These microcapsules were too fragmented. If the polylysine reaction time is increased to 15 minutes, Kelco-Gel® LV alginate sterilized for 15 minutes will produce some microcapsules containing blue dextran, however many of them will not contain any blue dextran. The microcapsules without entrapped blue dextran may appear to be undamaged; since they can appear as intact spheres under light microscopy.

One half of the microcapsules made with Kelco-Gel® LV alginate, that had been sterilized for 5 minutes, and with a PLL reaction time of 6 minutes, broke after being shaken at 300 rpm. One third of the microcapsules made with a PLL reaction time of 10 minutes broke after being shaken at 400 rpm. The results are shown in Figure 27.

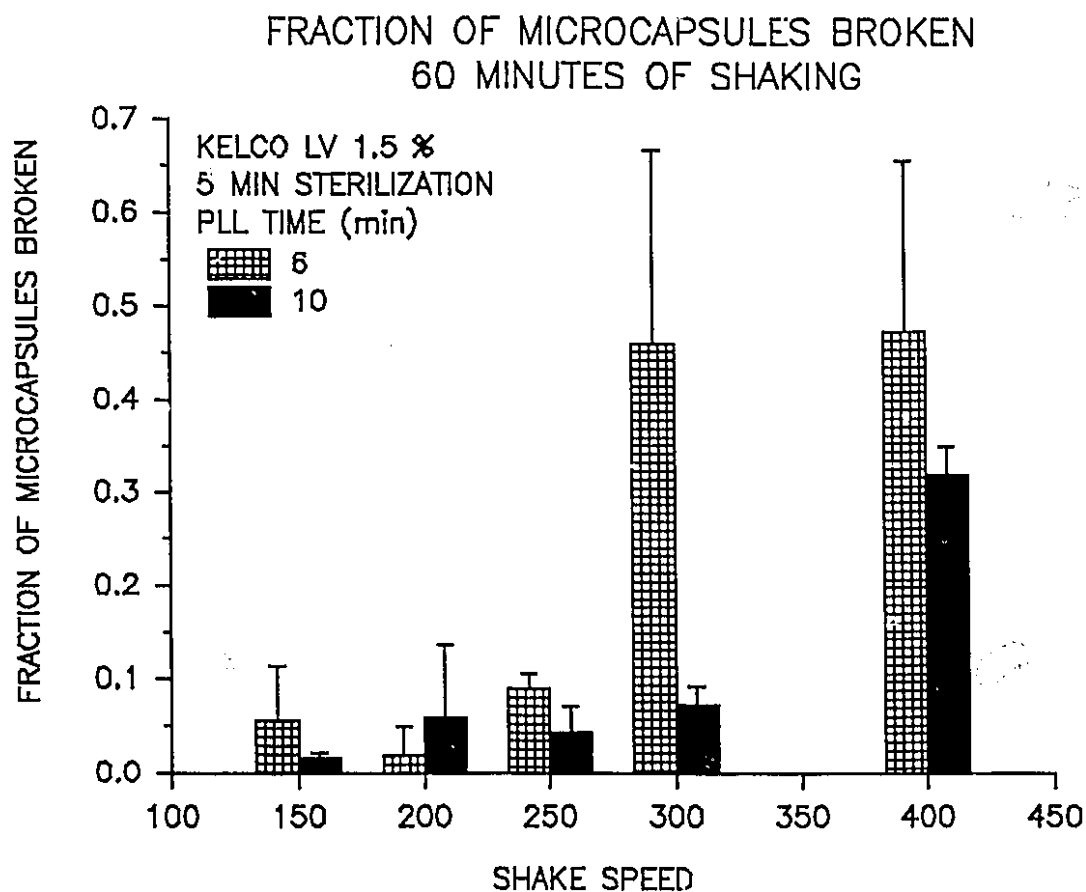


Figure 27. The effect of agitation on the breaking of microcapsules made with Kelco LV alginate sterilized for 5 minutes.

The results with blue dextran microcapsules taken altogether indicate that microcapsules made with high viscosity alginate, *i.e.* the high molecular weight alginate, are stronger than those made with low molecular weight alginate. Longer polylysine reaction times increase the strength of the microcapsules.

4.1.6. Elution Profile of Blue Dextran 2000

The elution profile of blue dextran 2000 (MW 2.0×10^6) from sepharose CL6B was compared to that of a 150,000 and a 500,000 molecular weight dextran. The resulting elution profile is represented in Figure 28. The data shows that blue dextran 2000 is polydisperse, nevertheless most of the polymer chains have a molecular weight above 150,000.

ELUTION PROFILE FOR DEXTRANS ON CL6B SEPHAROSE GEL

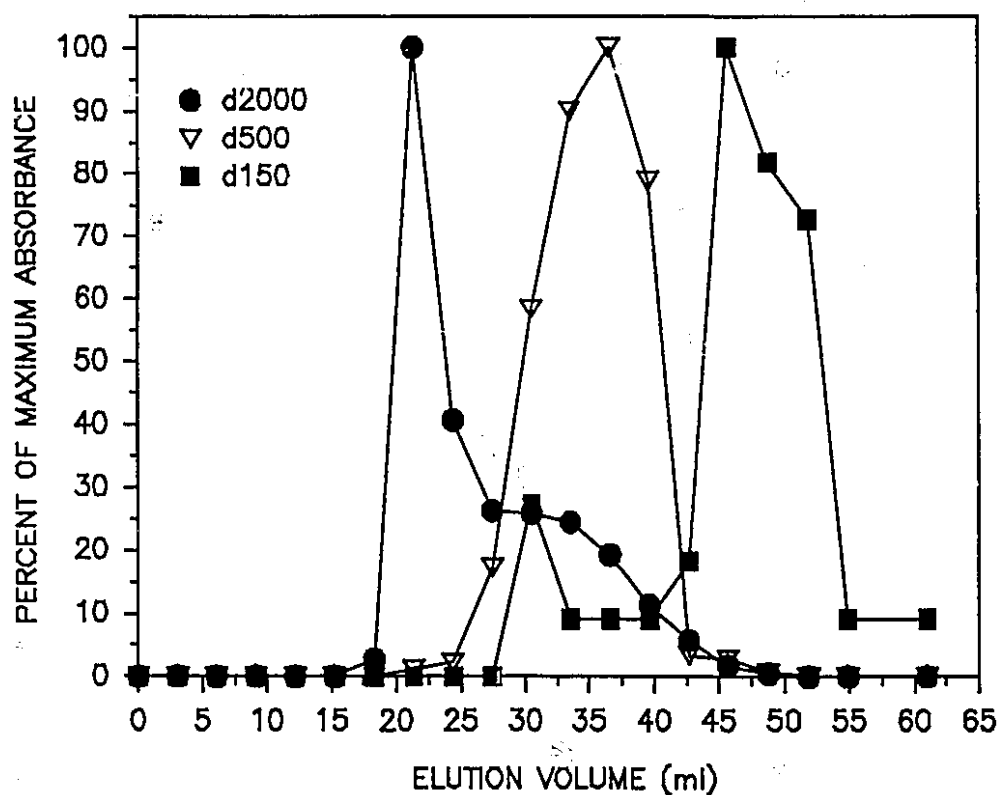


Figure 28. Elution profile for blue dextran 2000, dextran 500 and dextran 150 (d 2000, d500 and d150 respectively).

4.1.7. Cell Protein in Microcapsules as a Function of Cell Protein in 1.5 % Alginate.

The amount of total *Erwinia herbicola* cell protein encapsulated per ml of microcapsules was determined as a function of the amount of protein per ml of the cell suspension in 1.5 percent Kelco-Gel® HV alginate. The airflow to the droplet former was 2.5 l/min, and the liquid flow was 0.389 ml/min. The results are shown in Figure 29. The amount of protein encapsulated per ml of microcapsules was linearly related to the amount of protein in the cell suspension (slope = 0.831, R = 0.999). This calibration curve was used to determine how much free cell suspension was equivalent to a given amount of microcapsules.

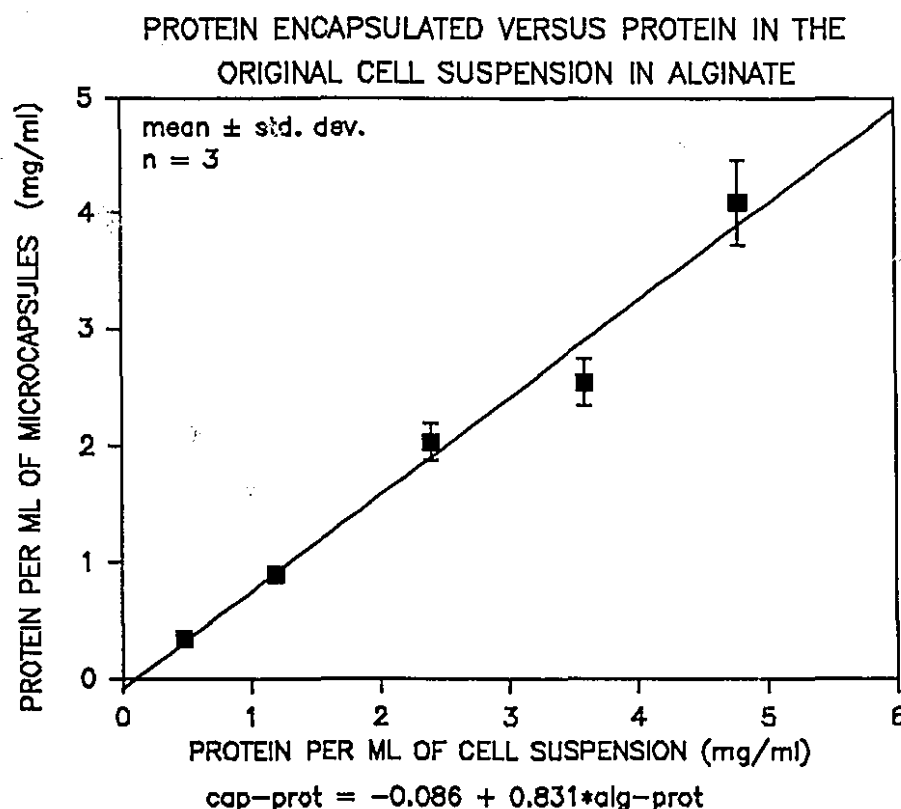


Figure 29. The amount of whole cell *E. herbicola* protein encapsulated per ml of microcapsules plotted as a function of the amount of protein in 1.5 % Kelco HV alginate.

4.2 GROWTH STUDIES ON *ERWINIA HERBICOLA*

4.2.1 Absorbance Versus Biomass for *Erwinia herbicola*.

The absorbance (at 400, 490 and 610 nm) of an *Erwinia herbicola* cell suspension versus its dry cell mass (biomass) is shown in Figure 30. The absorbance was a function of the wavelength, however the absorbance measured at 610 nm was most linearly related to the biomass. The absorbance at 610 nm was used to monitor the growth of *Erwinia herbicola* as a function of agitation (measured as rpm) and temperature.

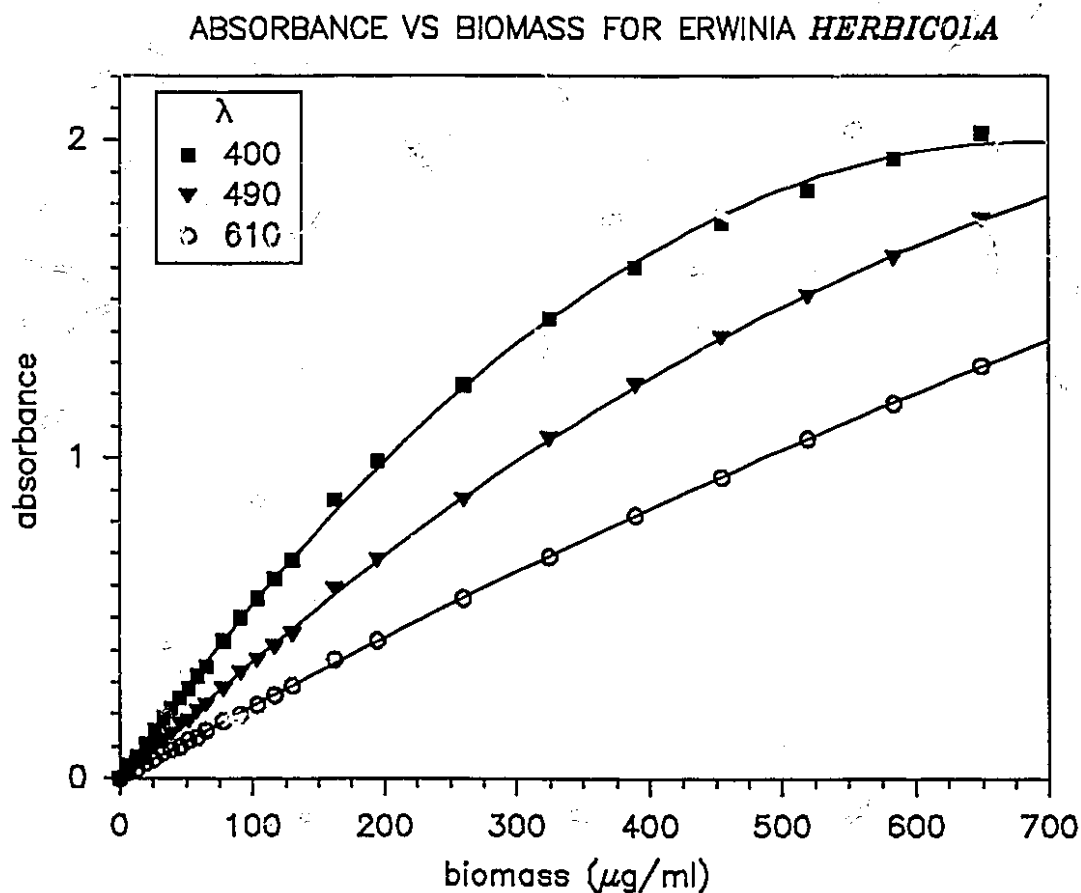


Figure 30. The absorbance of *Erwinia herbicola* cell suspensions in nutrient broth as function of the biomass.

4.2.2. Growth of *Erwinia herbicola* in Nutrient Broth.

The growth of *Erwinia herbicola* (in nutrient broth) at 32 °C was observed as a function of the shaking speed and time. At 60 rpm the cells grew up slowly to the stationary phase. After 5 hours of growth, cells grown at 60 rpm were present at a biomass concentration of 300 µg/ml. Cells grown at 100 rpm or more were present at a concentration of at least 600 µg/ml. After 16 hours whether the cells were grown at 60, 100, 140, 180 or 220 rpm, the amount of biomass was about 500 µg/ml. These results, shown in Figure 31, indicate that *Erwinia herbicola* tolerates vigorous shaking.

A shake rate of 180 rpm was used as the shake speed in subsequent growth of *Erwinia herbicola*. This rpm was partly chosen because the activity of whole cell tyrosine phenol lyase (TPL) has to be assessed at an rpm of 180 or more. This rpm was shown in preliminary work to produce an almost constant rate of product formation over 16 minutes, with 1.8 mM tyrosine as substrate. It was reasoned that if the cells were grown under a certain condition of shear perhaps they would be better able to withstand similar shear stresses in the activity or production studies. In the TPL induction medium of Enei *et al* (77) there are tyrosine crystals, because the solubility of tyrosine is low. A high shake rate would also promote the dissolution of the tyrosine crystals as the tyrosine in solution was consumed by the growing cells. This fact also contributed to the decision to use an rpm of 180 as the shake speed in subsequent work.

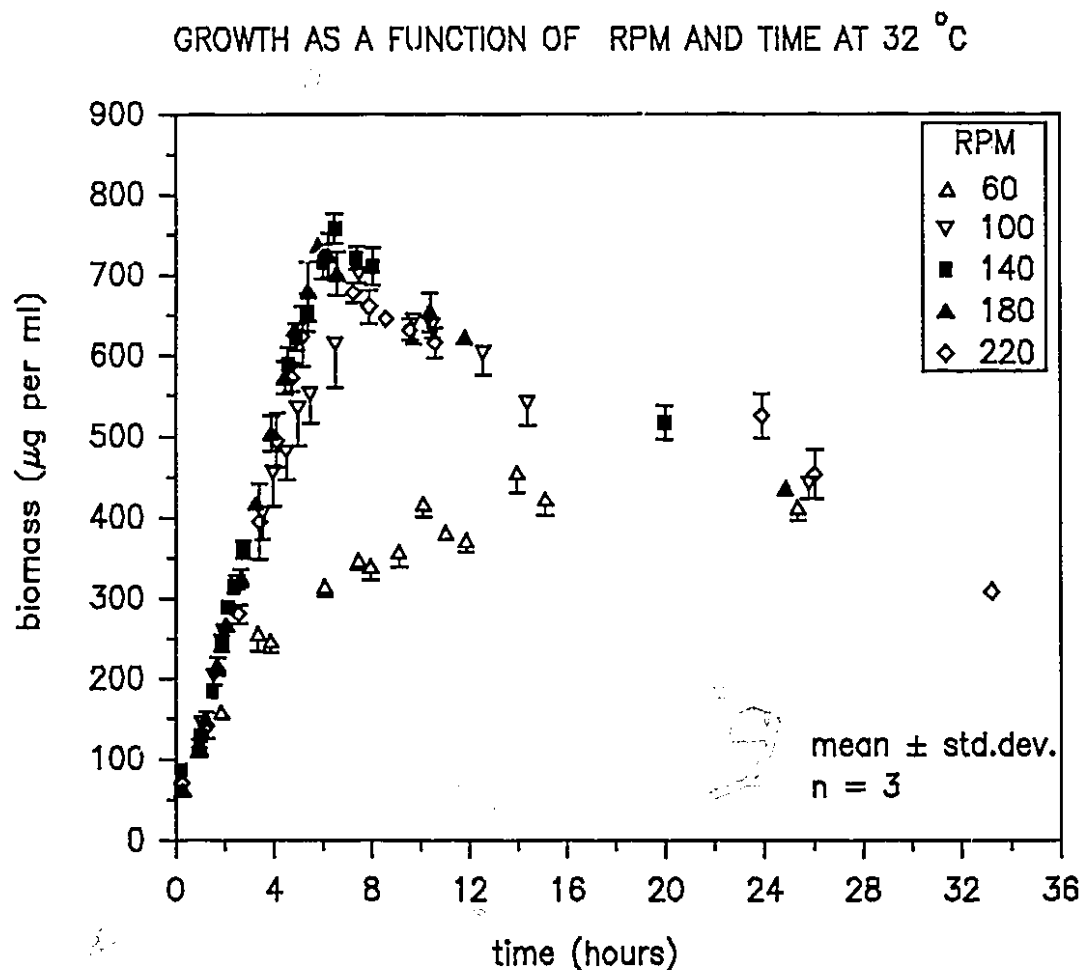


Figure 31. Growth of *Erwinia herbicola* in nutrient broth as a function of agitation (as rpm) and time.

4.2.3. The Growth of *Erwinia herbicola* as a Function of Temperature.

The effect of temperature on the growth *E. herbicola* as function of time was studied from 22 °C to 42 °C at a shake speed of 180 rpm. At 22 °C and 25 °C the cells grew up to the stationary phase and remained there for 10 hours or more. At 37 °C the cells grew more rapidly then started to die more rapidly. There was limited growth at 42 °C (Figure 32).

The results of the growth in nutrient broth studies suggested that the inocula for the tyrosine phenol lyase induction flasks could be suitably prepared by growing

GROWTH WITH TEMPERATURE AT 180 RPM

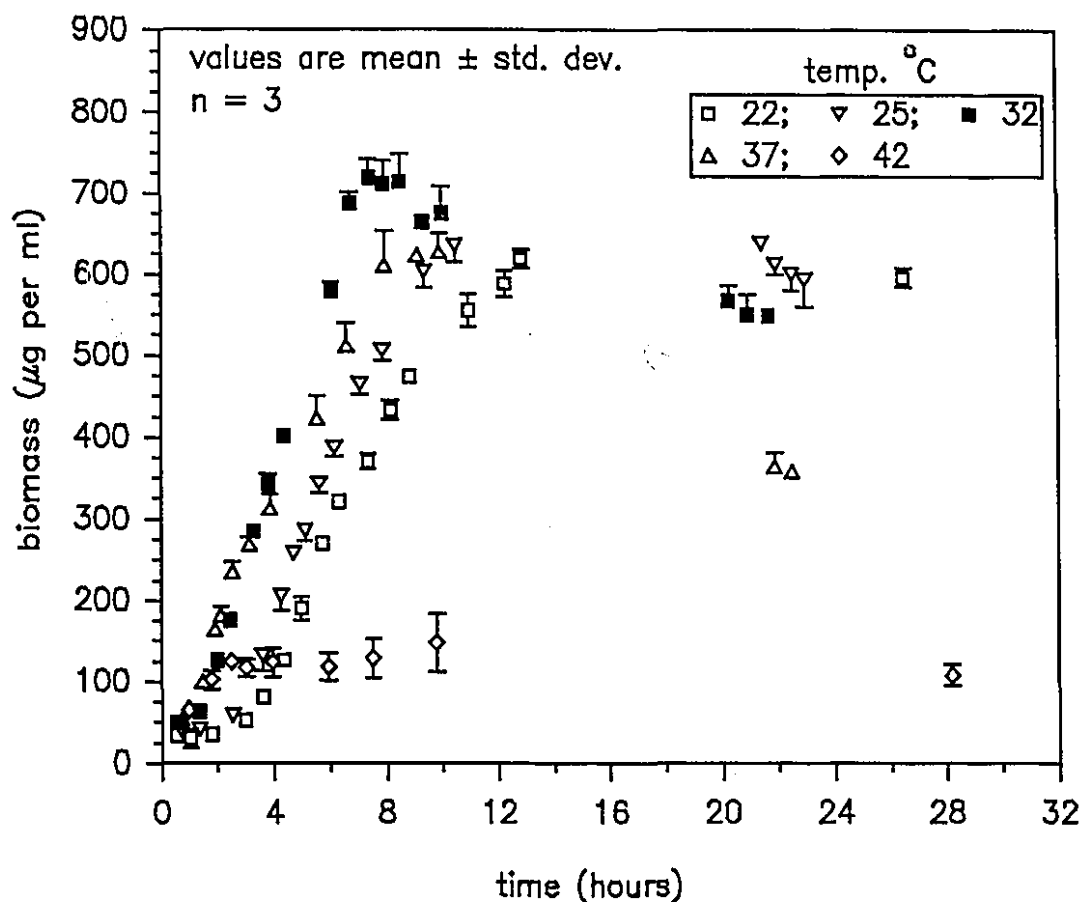


Figure 32. The Effect of temperature on the growth of *E. herbicola* in nutrient broth. The shake speed was 180 rpm.

E. herbicola at 180 rpm and 32 °C. These cells were kept for at most 2 days at 4 °C before being used as pre-inocula for the inoculum flasks. The inoculum was always cells freshly grown in nutrient broth for 8 hours. If these steps were adopted the duration of the lag phase in the enzyme induction medium was zero, and the batch to batch variation from one fermentation to the next was minimised. The detailed temperature profile studies were done in a shaker that was modified to give a variation in temperature of ± 0.5 °C. However routine work was done in a shaker in which the temperature occasionally drifted up or down by 2 °C. The

drifting of the temperature was due to the fact that the controller was of the on-off variety and the temperature in the McIntyre Building (Mc Gill University) fluctuates widely. This fluctuation in temperature could contribute to batch to batch variation in the properties of the cells.

4.2.3. TPL Activity Induction with Time Profile.

When the enzyme induction medium was used to grow cells - at 180 rpm and 32 °C - the cells grew to the stationary phase after 10 hours. The cells remained at the stationary phase for at least 20 hours.

The Tyrosine Phenol-Lyase specific activity of the cells was obtained by plotting the TPL activity of the cells as a function of the total protein in the cells in mg. The initial slope of this plot was considered as the specific activity. The TPL activity per milligram of total cell protein increased during the stationary phase (Figure 33).

Cells were harvested after 24 hours of growth in all subsequent investigations unless indicated otherwise.

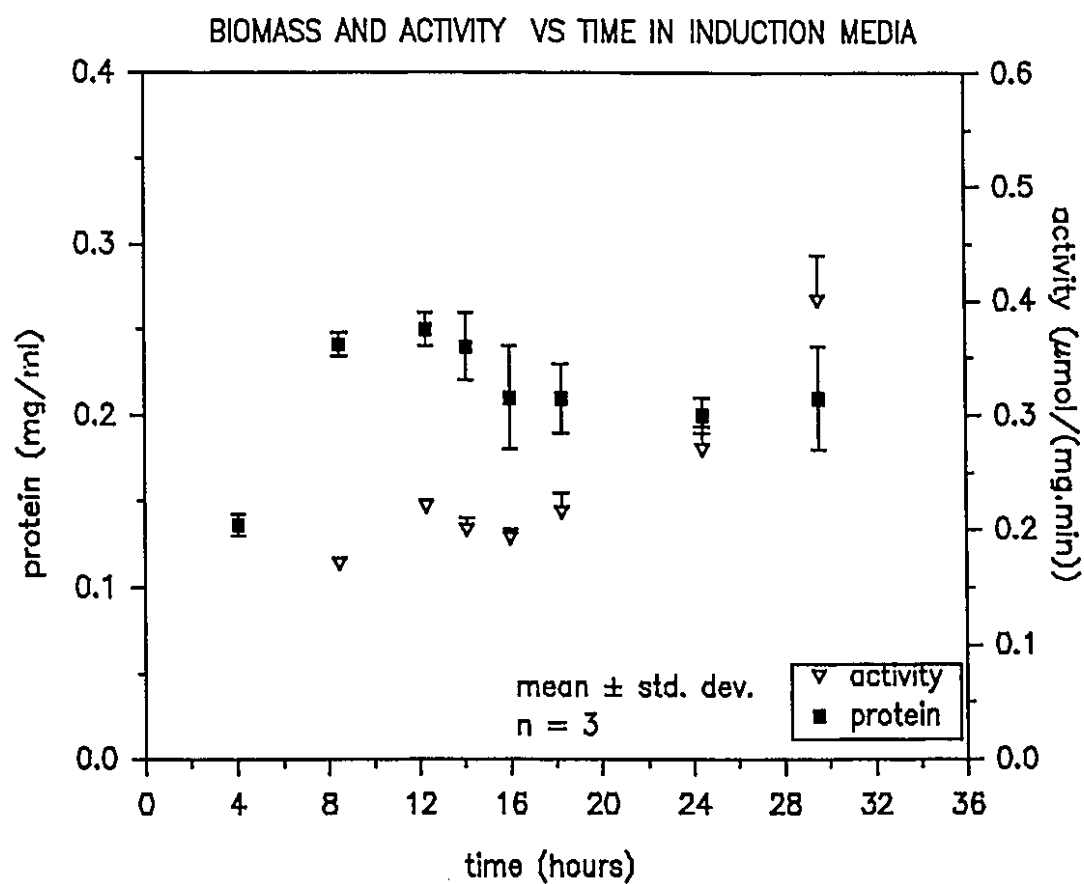


Figure 33. The induction of Tyrosine Phenol-Lyase activity per mg of cell protein in *Erwinia herbicola*. Biomass as (cell protein per ml) of medium is also shown.

4.3 EXPLORATORY STUDIES OF THE KINETICS OF WHOLE CELL *ERWINIA HERBICOLA* TPL.

4.3.1. TPL Activity Versus Biomass Profile.

The Tyrosine Phenol-Lyase activity of the cells was plotted as a function of the amount of cells in the assay. The amount of cells was measured as the total cell protein in the assay flask. The resulting plot was nonlinear whether the cells were grown for 12, 24 or 36 hours. The results in Figure 34 show that the specific TPL activity (*i.e.* the TPL activity per mg of total cell protein) decreases as the total amount of cells in the system increases. These results also show an increase in specific activity with the duration of cell growth between 12 and 36 hours.

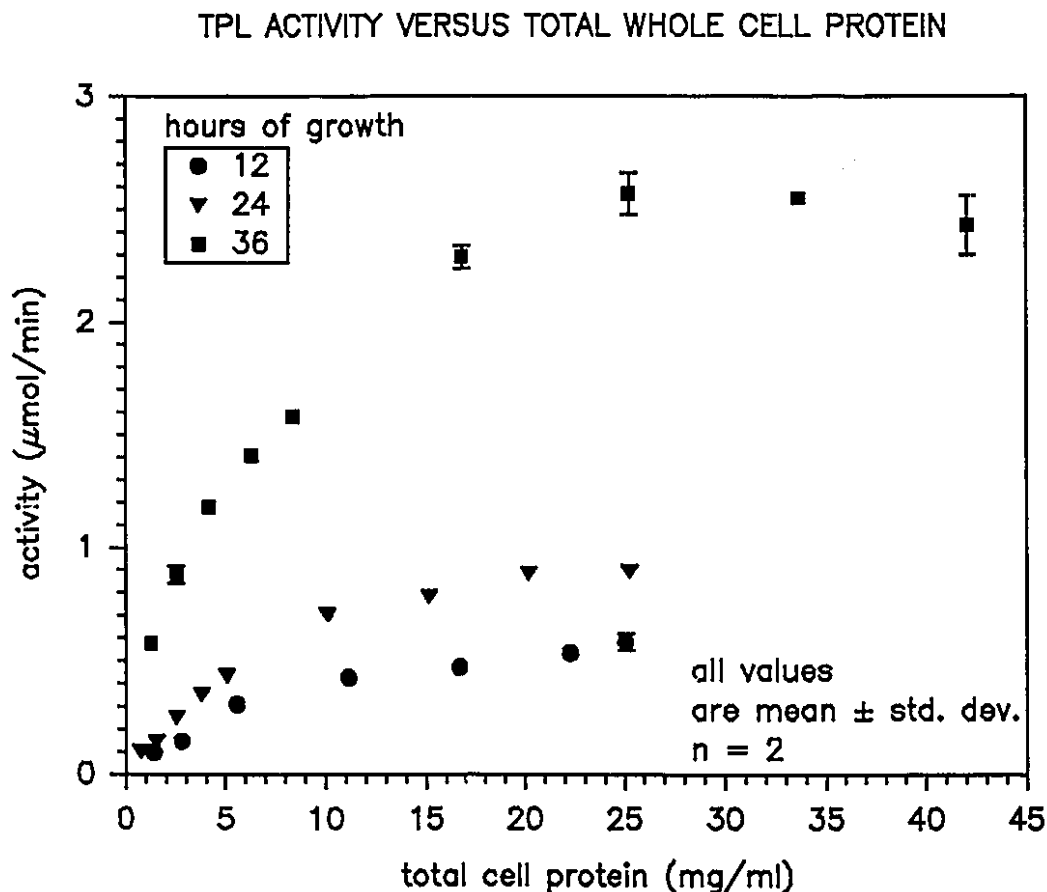


Figure 34. The TPL activity of whole cell *E. herbicola* as a function of the total protein in the assay and the duration of cell growth in induction medium.

4.3.2. The Effect of the Buffer System Used for Activity Determination.

It is possible that the cells could break down during the assay because the buffer used for cell washing and the re-suspension of the cell pellet after harvesting and for cell storage afterwards was not suitable.

In order to check if the 0.1 M PB (phosphate buffer) was an appropriate buffer for the whole cell TPL system, the degradation of tyrosine by whole cell TPL was examined in 0.1 M PB and in phosphate buffered saline plus gelatin (PBSG). The results for the 0.1 M PB and the PBSG (8.5 g of NaCl, 0.3 g of anhydrous KH_2PO_4 , 0.6 g of Na_2HPO_4 , and 0.1 g of gelatin per litre of distilled water) system are summarised in Table IV. The initial rate of phenol production from tyrosine by the TPL activity of whole cell tyrosine phenol lyase was obtained by fitting phenol production data with polynomials in time. No significant difference in activity was observed when the buffer was changed to the general purpose diluent PBSG. Therefore 0.1 M PB is as suitable as PBSG for the washing and suspension of *Erwinia herbicola* cells, when they are being used for their TPL activity.

These results show that extra protein in the form of gelatin does not need to be added to the whole cell TPL system to stabilise the walls of the cell.

The remainder of the activity studies on TPL were done in 0.1 M PB at pH 8.0. It was convenient to use a buffer which contained potassium since TPL requires K^+ (or Rb^+ or NH_4^+) for its activity.

Magnesium ions can be added to the diluents or the buffers used for bacterial storage, since this ion contributes to cell membrane integrity. A potassium based buffer was desired (for reasons explained above), and Mg^{2+} complexes with potassium phosphate at about pH 8.0 so the effects of Mg^{2+} addition were not investigated.

Table IV. The Initial Rate of Phenol Degradation by TPL in Comparative Buffer Study.		
Total Cell Protein in Assay (mg)	Activity	
	0.1 M PB	PBSG
2.216 [#]	0.01204 ± 0.0011	0.0121 ± 0.0001
4.432	0.0236 ± 0.0033	0.0221 ± 0.0003
8.864	0.0246 ± 0.004	0.0277 ± 0.0012
# n = 2		

4.3.3. The Effect of the Addition of PLP to the Assay Flasks.

If sufficient pyridoxal phosphate (PLP) is added to the assay flasks to give a concentration of 4.5 mM, the rate of degradation of tyrosine decreases relative to an assay without added PLP (Figure 35). This shows that the external addition of excess PLP may inhibit the Tyrosine Phenol-Lyase system; and suggests that the cells have manufactured and accumulated sufficient pyridoxal phosphate (PLP) for their needs. The initial rate of phenol production in the two systems is shown in Table V. These results show that when the amount of whole cell protein in the assay is 8.40 mg, the activity in the presence of added PLP is lower than when there is no externally added PLP. The results in Table V suggest that as the amount of whole cell protein in assay increases the inhibition by externally added PLP is stronger.

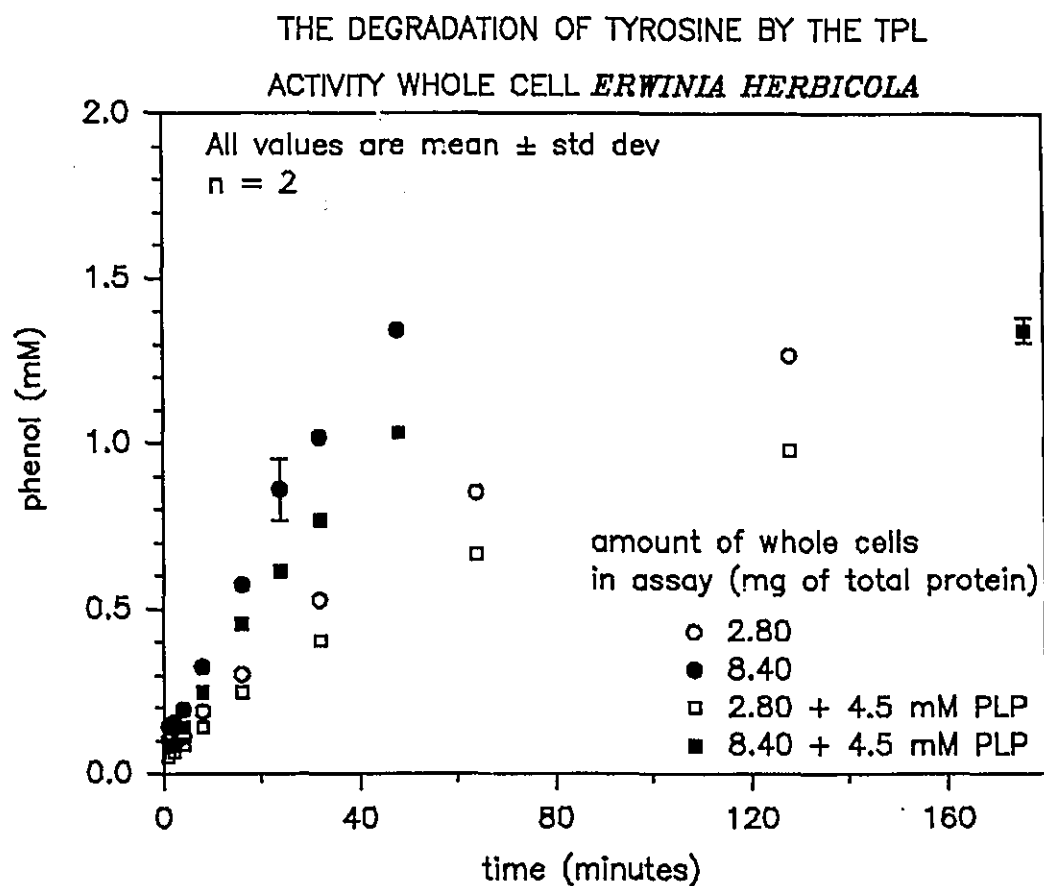


Figure 35. The degradation of tyrosine by the TPL activity of whole cell *Erwinia herbicola*. N.B. that the addition of excess PLP decreases the rate.

Table V. Effect of PLP Addition on the Activity of Whole Cell TPL			
Total Cell Protein in Assay (mg)	Initial Rate of Phenol Production (mM/min)		p Value for Comparison
	PB	PB + PLP	
2.80	0.0155 \pm 0.0004	0.0124 \pm 0.0003	< 0.075
8.40	0.0354 \pm 0.0023	0.0256 \pm 0.0004	< 0.005

4.3.4. Initial Rate Kinetics of Whole Cell TPL for the Degradation of Tyrosine.

4.3.4a. Basic Features of Velocity versus Substrate Profiles of Initial Rate Data.

The initial rate or velocity of tyrosine degradation was studied by observing the initial rate of phenol production from the tyrosine in an assay mixture (0.1 M PB, pH 8.0, 37 °C). The concentration of the tyrosine was varied from 0.1 to 1.8 mM. It was not convenient to use higher concentrations because the solubility of tyrosine is low in most aqueous systems at pH 8.0. The limits of reliable phenol detection prevented the observation of initial velocities at substrate concentrations less than 0.05 mM. The Lineweaver-Burk plots (153) of early results were nonlinear; and the determined values of the apparent K_M of tyrosine were a function of the amount of cell protein the system. Hence velocity versus substrate profiles were obtained at different amounts of total cell protein, to further investigate this phenomenon. The cells were harvested after 24 hours of growth in the TPL enzyme induction medium and they were used immediately after harvesting. The data was plotted according to 3 different linearizations of the Michaelis-Menten (154) equation:

$$v_0 = \frac{V_{\max} S}{K_m + S} \quad \dots(4.1)$$

where V_0 (or V) is the initial velocity or reaction rate; V_{\max} is the maximum reaction rate upon saturation with substrate; S is the concentration of substrate and K_M is the half saturation constant or the dissociation constant for the enzyme-substrate (ES) complex.

Each of these plots will emphasize different aspects of the data if the data is not Michaelis-Menten. The linearizations used were the Lineweaver-Burk plot (153), the Eadie plot (155) which is the inverse of Scatchard plot (156) and the Hanes plot (157). The required transforms of the data are shown as Figure 36.

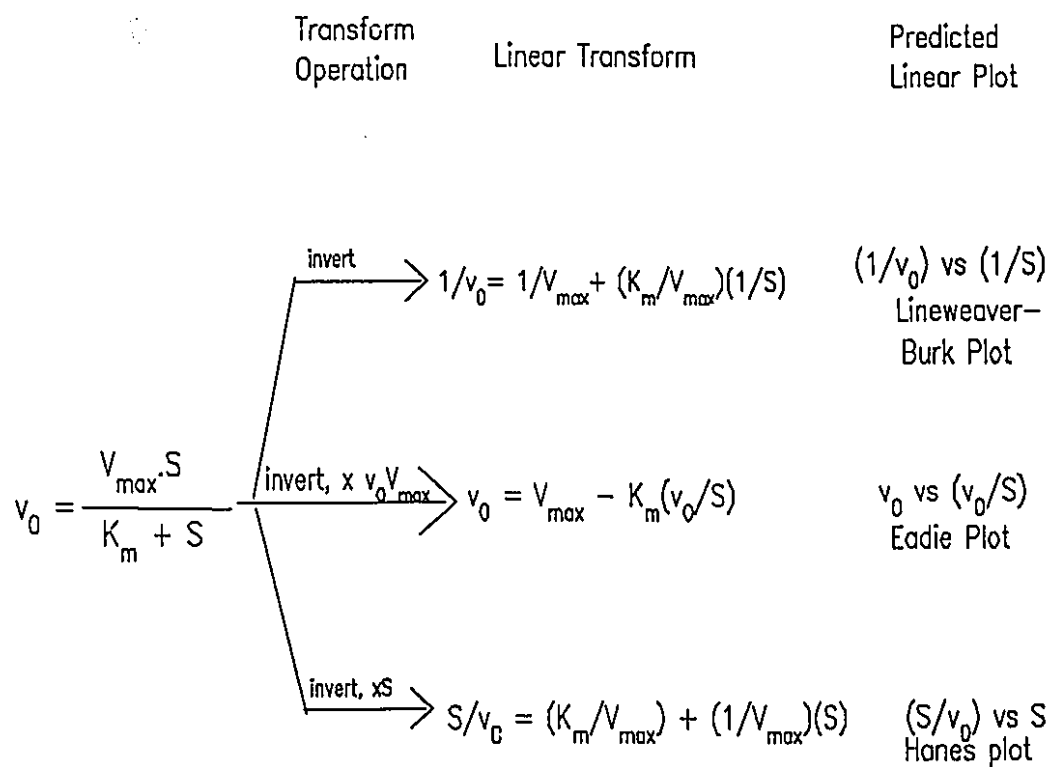


Figure 36. Some linearizations of the Michaelis-Menten Equation.

Figure 37 show the velocity versus substrate profiles obtained when the amount of whole cell *Erwinia herbicola* protein in the system is relatively small. The plots of velocity versus substrate are initially sigmoidal. In the set of data at 0.680 mg of protein, there is an intermediate concentration range in which the data plateaus markedly. This indicates non-Michaelis-Menten behaviour.

Earlier work (Figure 34) shows that the specific activity varies with the amount of cells in the assay. The data in Figure 37 also show that the general shape of the velocity versus substrate profile can vary with the amount of cells in the assay. The complexity shown by the velocity versus substrate profiles in Figure 37 predict non-linear Lineweaver-Burk plots for the data (Figure 38).

VELOCITY VS SUBSTRATE PROFILE

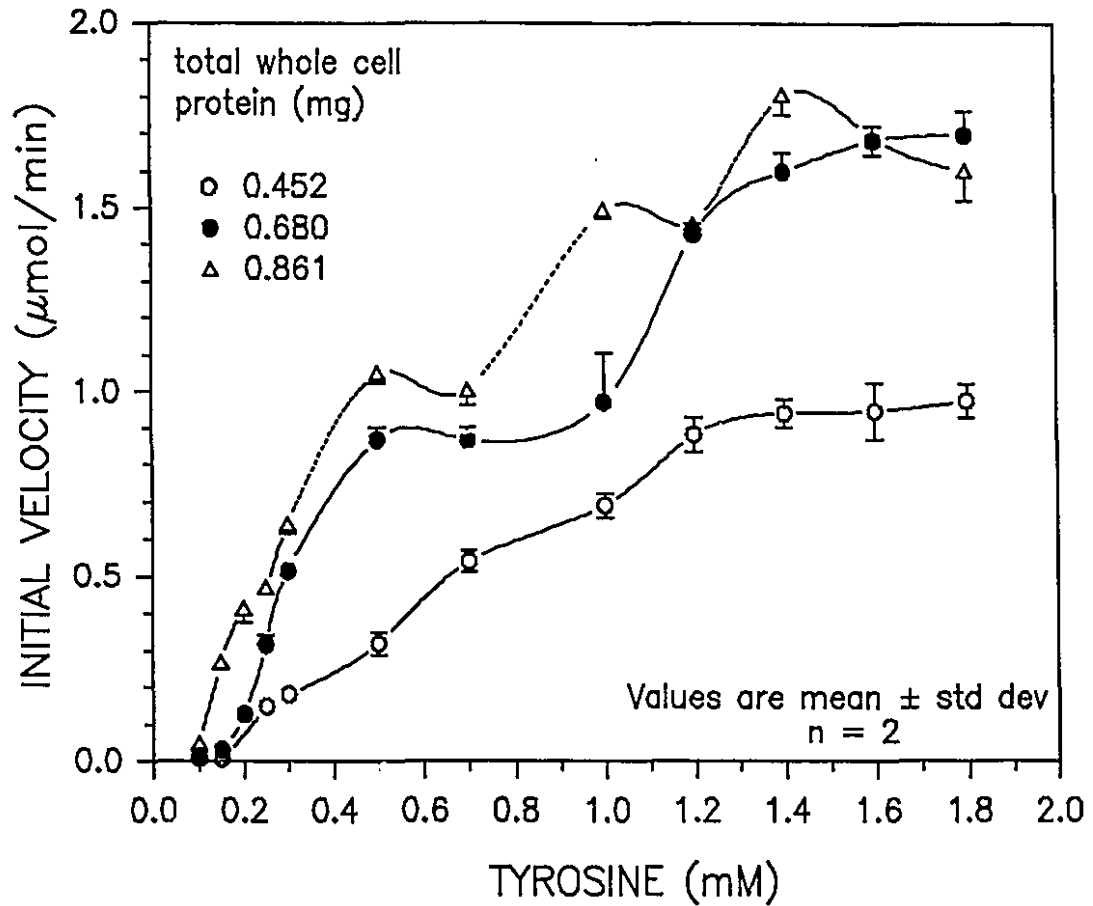


Figure 37. Whole cell TPL activity for the degradation of tyrosine. Note sigmoidal behaviour and intermediate plateaux. Lines are a spline fit and are not meant to indicate a mathematical model.

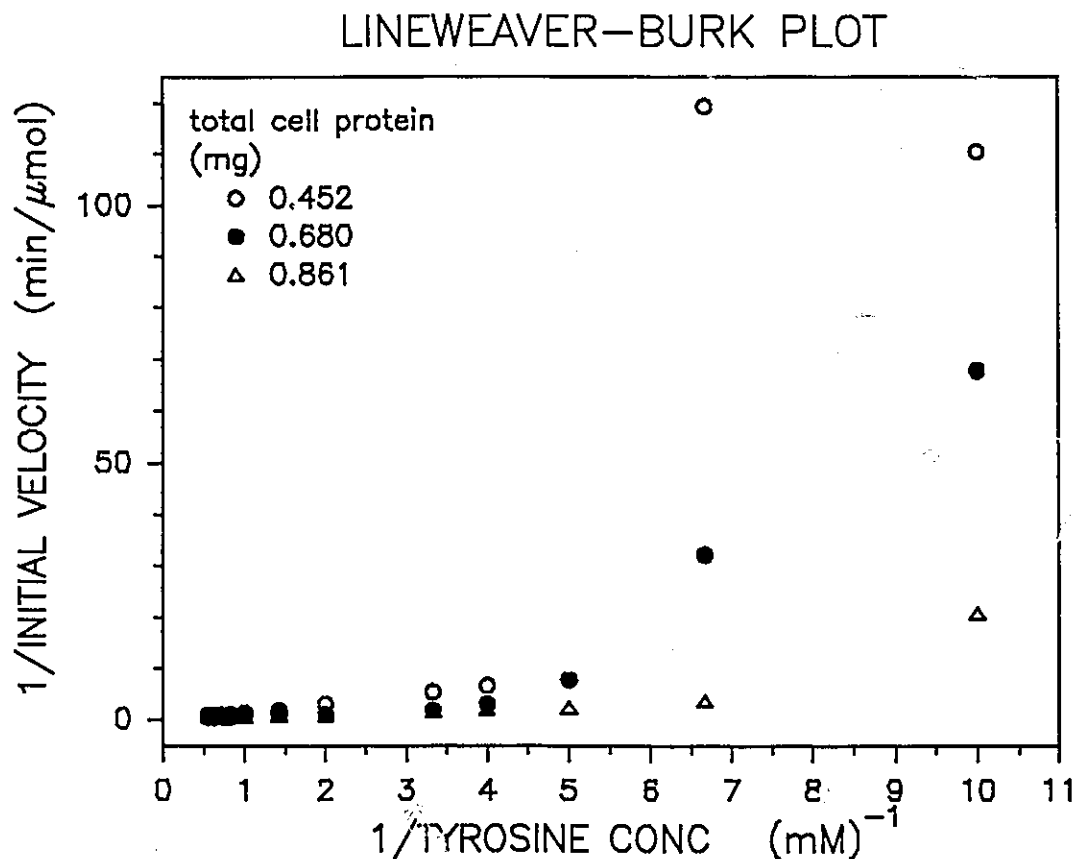


Figure 38. Lineweaver-Burk plots of the data in Figure 37. N.B. the curvature in the plots.

The Eadie and Scatchard plots of the data in Figure 37 is shown as Figure 39. The downward concavity of the Scatchard plots indicate that there is positive cooperativity at low values of velocity (and therefore low values of S) (96). Positive cooperativity being defined as the enhancement in the binding of a second substrate molecule, because of the previous binding of a molecule of substrate or some other ligand. Thus after the first substrate molecule has bound to the enzyme the affinity of the enzyme for the second molecule increases and there is sigmoidal increase in reaction rate. These results indicate that there are subunit effects in the kinetics of the whole cell TPL system. Note however that there are

also areas of upward concavity in the Scatchard plots, thus these systems also indicate negative cooperativity (96). These systems then indicate a region of positive cooperativity followed by negative followed by positive cooperativity (*i.e.* mixed cooperativity). Negative cooperativity can be defined as a reduction in the affinity for binding of a substrate molecule because of the previous binding of a ligand, or a substrate molecule.

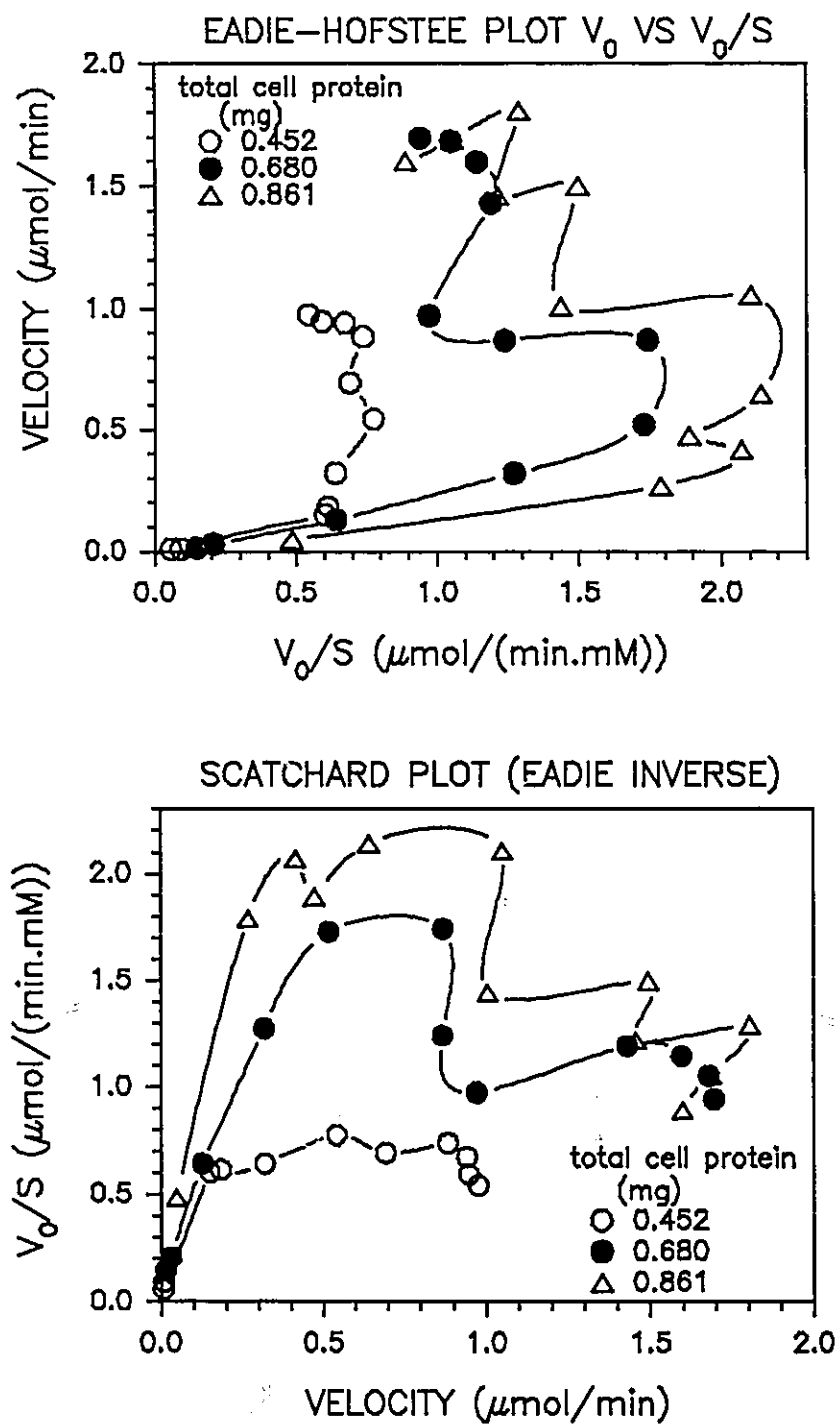


Figure 39. Eadie and Scatchard plots of the initial rate data shown in Figure 37. Note the clear departure from Michaelis-Menten behaviour.

The Hanes plot of the data in Figure 37 show that at low S the value of S/V decreases indicating that V is increasing rapidly relative to S. This initial region that is concave upwards indicates an initial sigmoidal increase in reaction rate. However as the total amount of whole cell protein in the assay system increases, from 0.452 mg to 0.861 mg, the region indicating sigmoidal behaviour decreases. The Hanes plot of the data in Figure 37 is shown as Figure 40.

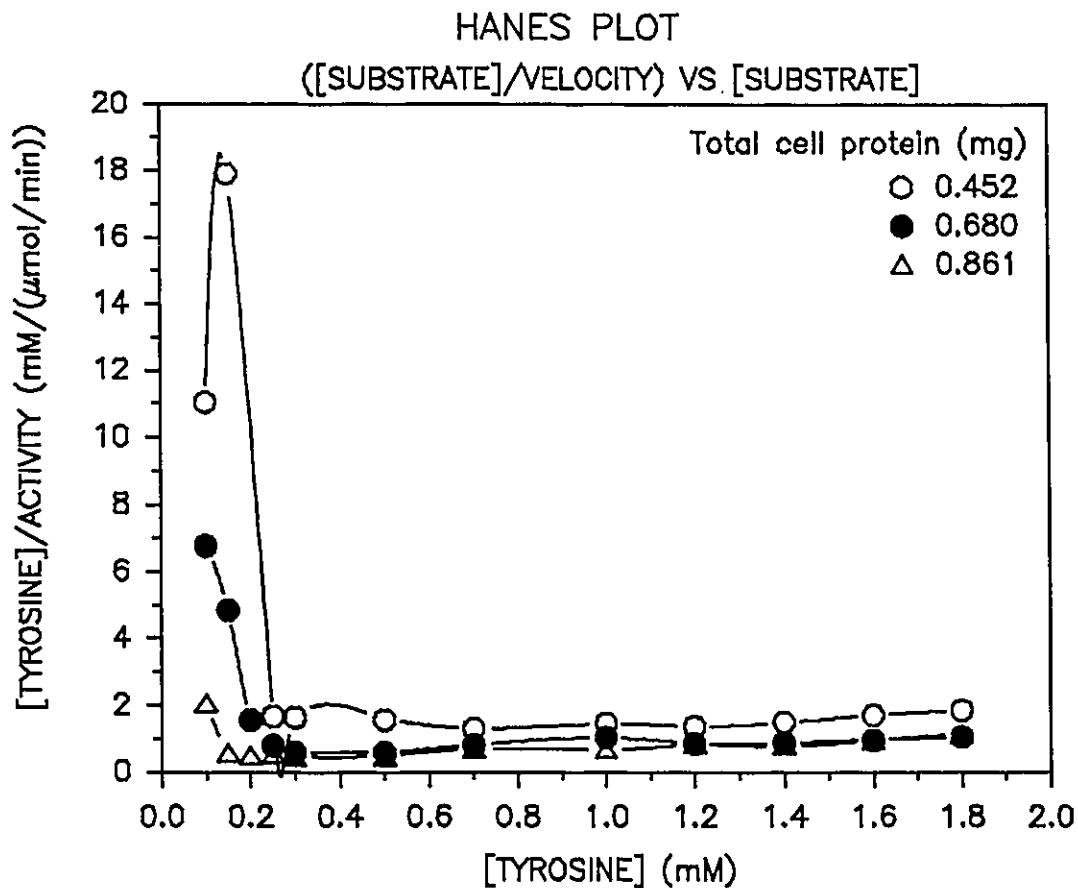


Figure 40. Hanes plot of the data in Figure 41. Note that at low S the data departs markedly from Michaelis-Menten data.

Figure 41 shows the velocity versus substrate profiles obtained with higher concentrations of *Erwinia herbicola* cells (relative to those used to obtain the data in Figure 37). These cells were harvested from a different batch than those used in Figure 37). There are differences in the apparent enzyme activity from batch to batch. Therefore the velocity versus substrate profiles in Figure 41 differ from those in Figure 37 because the amount of cells are different and because of the batch to batch variation in TPL activity. Since the cells were harvested from different batches they have been analyzed separately.

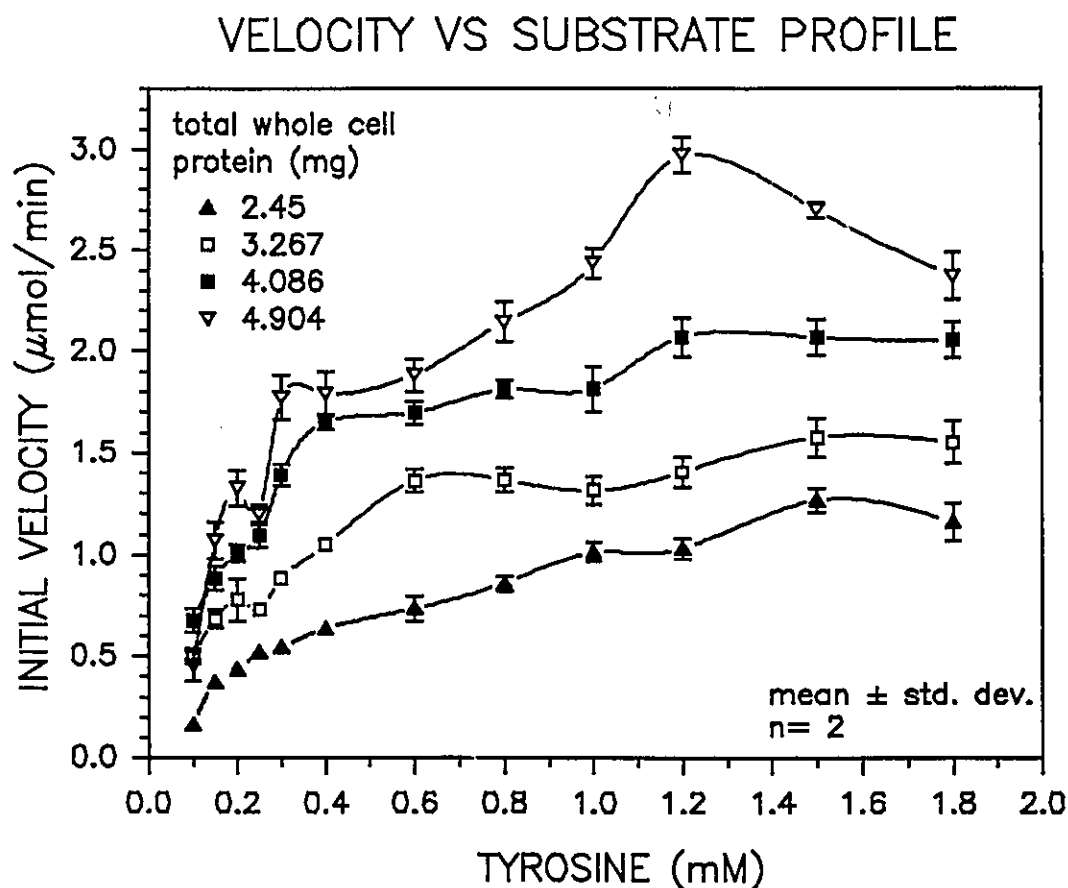


Figure 41. Velocity versus substrate profiles obtained with relatively high amounts of total cell protein in the assay. Lines are a spline fit and do not imply a mathematical model.

The behaviour of the system is less sigmoidal at low values of substrate, when higher amounts of protein are present in the system; however the intermediary plateaux are evident. This data confirms the trend that the initial sigmoidal region decreases as the amount of whole cell protein in the system decreases.

The Lineweaver-Burk plot of the data in Figure 41 is shown in Figure 42. The plots are nonlinear indicating departures from Michaelis-Menten behaviour. In particular both ends of the Lineweaver-Burk plots are curved. However the departures from Michaelis-Menten behaviour are not recognised as being pronounced in this plot.

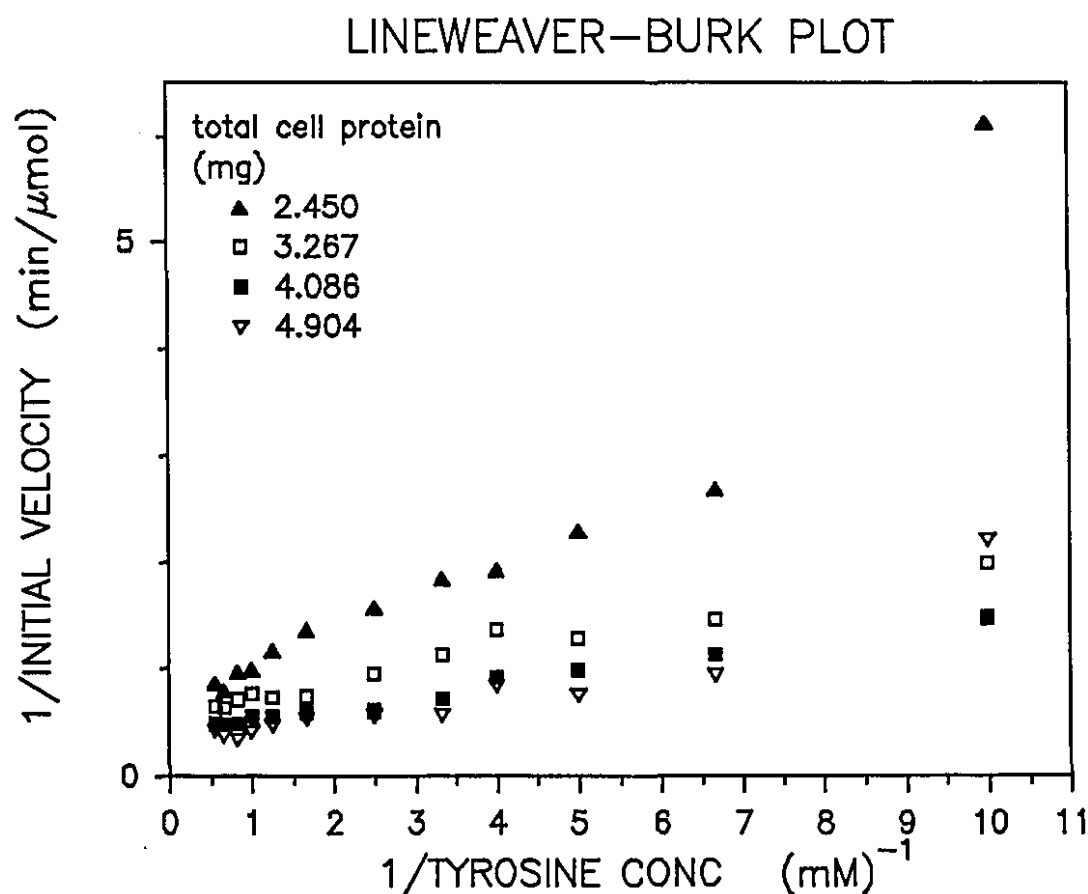


Figure 42. Lineweaver-Burk plot of the data in Figure 41. Note these plots are also nonlinear indicating non-Michaelis-Menten behaviour.

The Eadie and Scatchard plots of the data in Figure 41 are shown in Figure 43. These plots are nonlinear, indeed when the amount of total cell protein in the system is 3.267, 4.086 or 4.904 mg the curves are almost serpentine. These curves suggest regions of positive followed by negative cooperativity.

The Hanes plot of the data in Figure 41 is shown as Figure 44, these plots do not show the pronounced non-linearity of the Eadie or Scatchard plots.

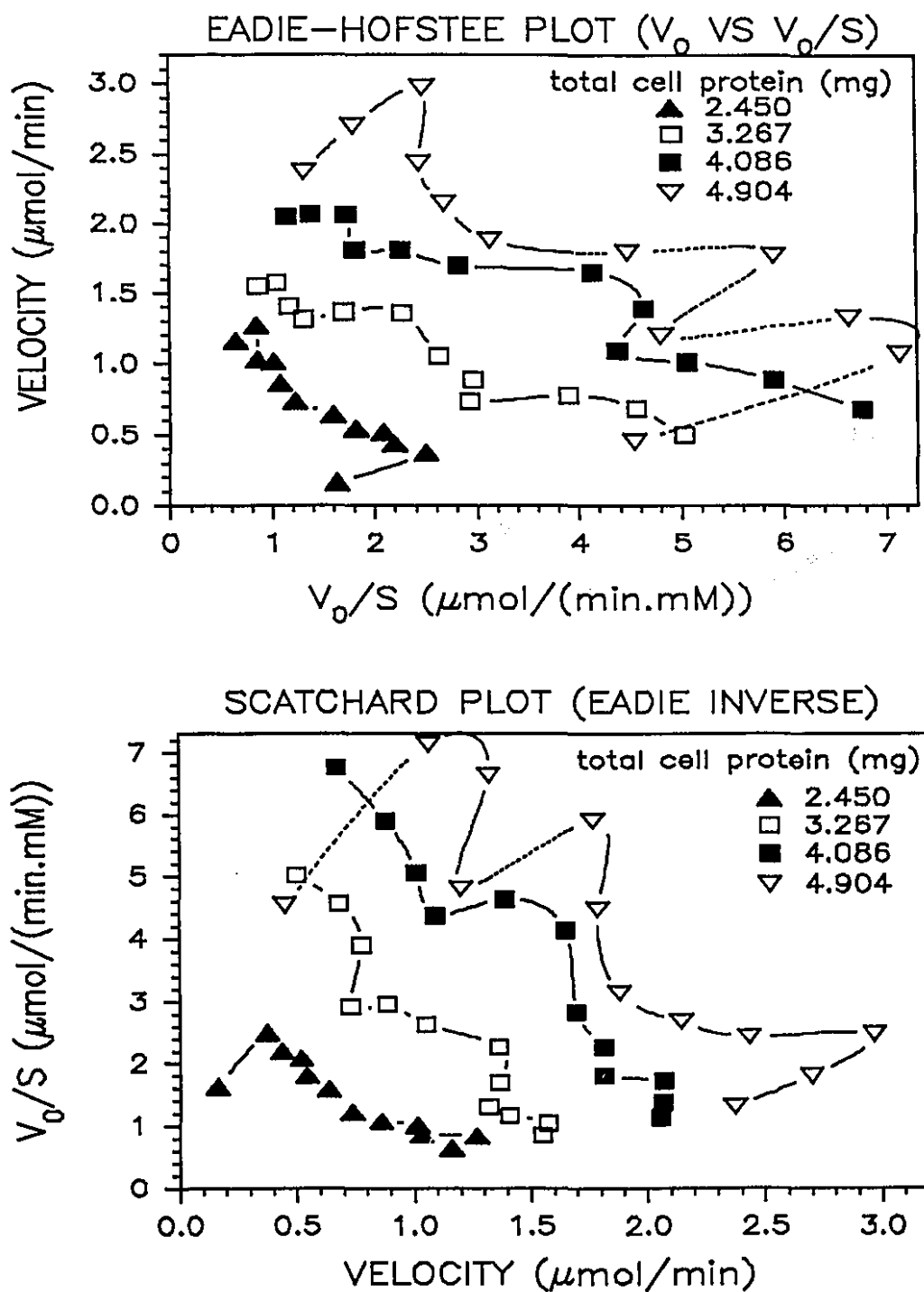


Figure 43. Eadie and Scatchard plots of the data in Figure 41. Note the serpentine shape of the plots.

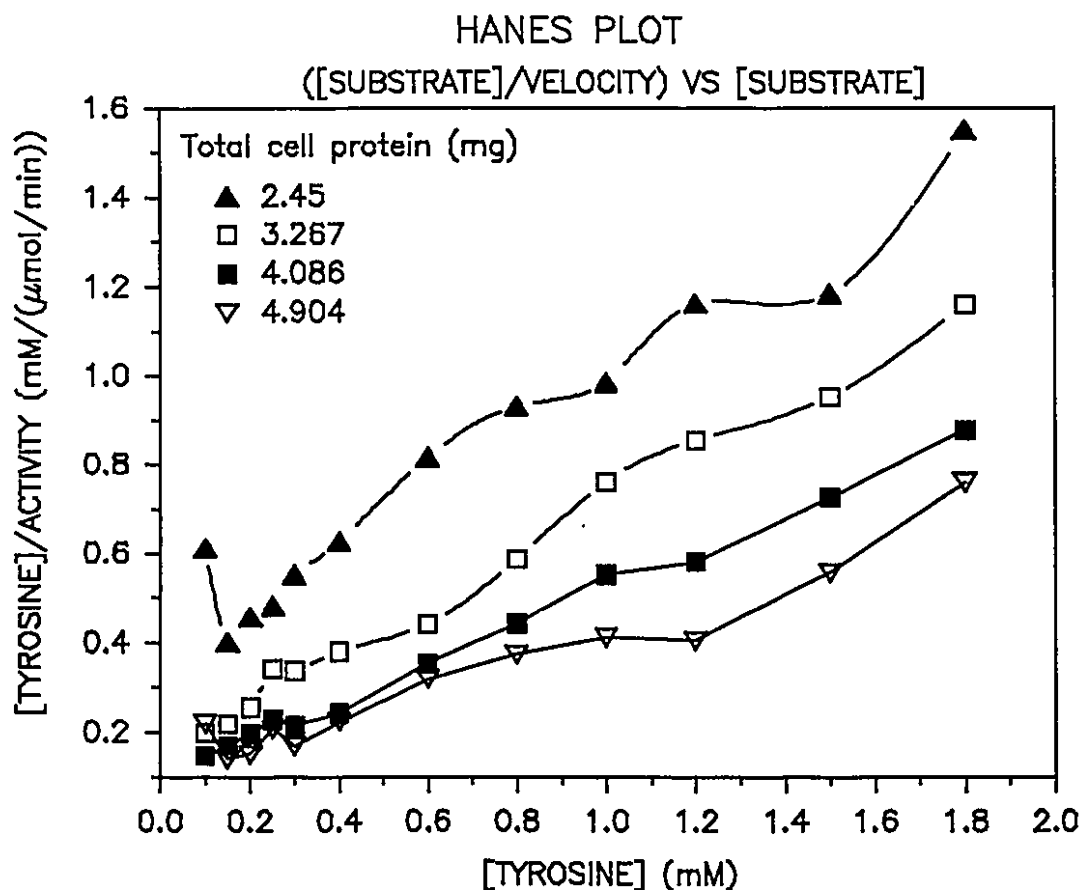


Figure 44. Hanes plot of the data in Figure 41. These plot do not emphasise the departure from Michaelis-Menten behaviour as clearly as the Eadie or Scatchard plots.

4.3.4b Kinetic Analysis of Initial Rate Data.

4.3.4b (i) Analysis by the Hill and Michaelis-Menten Equations

The Hill coefficient (n_H) is a general measure of the degree of cooperativity in enzyme systems, or in other systems where protein-ligand interactions occur. The value of the Hill coefficient for each profile in Figures 37 and 41 was determined by fitting the velocity substrate profiles to the Hill (158) equation as modified for kinetic data:

$$\frac{v}{V_{\max}} = \frac{S^{n_H}}{(K_{0.5} + S^{n_H})} \quad \dots(4.2)$$

where v is the initial velocity of the reaction ; V_{\max} is the velocity at saturating enzyme concentrations; $K_{0.5}$ is the dissociation constant of the ES_n complex to free E and S, it is also the concentration which produces a velocity that is one half of V_{\max} ; and n_H is the Hill coefficient. The equation is developed in Appendix III.

The values obtained for the parameters of the Hill equation are shown in Tables VI and VII. The data in Table VI show that the value of n_H -the Hill coefficient- decreases as the amount of protein in the system is increased, starting from a value of 2.0 (1.96 ± 0.13) it decreases to 1.5 (1.5 ± 0.1). The data in Table VII show that when the total amount of cell protein was 2.45 mg the value of the Hill coefficient was 1.00 ± 0.13 , (*i.e.* a value not significantly different from 1.0). If the Hill coefficient is equal to 1.0 then the system could approximate Michaelis-Menten behaviour, since under this circumstance the Hill equation collapses into the Michaelis-Menten equation. However, it must be remembered that the n_H is only measuring the average cooperativity, and so a value of 1.0 for n_H does not preclude an area of positive cooperativity followed by one of negative cooperativity (or vice versa). At higher protein concentrations the Hill coefficient again starts to increase. If the results of the Tables VI and VII are combined the following general conclusions can be reached:

- 1) with low amounts of cells (as measured by total cell protein) in the system, its kinetics can be sigmoidal with the value of the Hill coefficient close to 2;
- 2) as the amount of protein in the system is increased the value of the Hill coefficient decreases and tends towards a value of 1.0.

The data in Tables VI and VII also show that the value of $K_{0.5}$ decreases as the amount of protein in the system increases. These results reveal the complexity of the whole cell TPL system.

Table VI. Parameters of the Hill Equation for Data in Figure 37 [†]				
Total Protein in Assay (mg)	parameters	Value	Std dev	significance at 95 % C.I.
0.452	V_{max}	1.193	0.08	s
	$K_{0.5}$	0.610	0.10	s
	n_H	1.96	0.13	s
0.680	V_{max}	1.814	0.16	s
	$K_{0.5}$	0.419	0.13	s
	n_H	1.90	0.19	s
0.861	V_{max}	1.98	0.11	s
	$K_{0.5}$	0.38	0.08	s
	n_H	1.50	0.10	s
[†] The specific activity of these cells is different from those used in Figure 41. Therefore only limited comparison of both sets of data is possible. (Please see Table VII also)				

Table VII. Parameters of the Hill Equation for Data in Figure 41 [†]				
Total Protein in Assay (mg)	Parameters	Value	Std dev	significance at 95 % C.I.
2.45	V_{max}	1.60	0.11	s
	$K_{0.5}$	0.60	0.09	s
	n_H	1.00	0.13	s
3.267	V_{max}	1.71	0.08	s
	$K_{0.5}$	0.22	0.06	s
	n_H	1.11	0.04	s
4.086	V_{max}	2.21	0.08	s
	$K_{0.5}$	0.144	0.035	s
	n_H	1.25	0.02	s
4.904	V_{max}	3.27	0.37	s
	$K_{0.5}$	0.31	0.13	s
	n_H	1.12	0.11	s
† Note the specific activity of the cells used in this study (Figure 41) was different from those used in Figure 37.				

The kinetic data was also fitted by the equation of Michaelis and Menten and the values obtained for the parameters with non-linear least squares regression are shown in Tables VIII and IX. At low total amount of whole cell protein in the system, the values obtained for the parameters were not all significant. At higher protein concentrations the nonlinear regression routine could converge to statistically significant values of the parameters. However the pattern of the distribution of the residuals showed that the model was inappropriate. If non-linear regression is used to evaluate K_M and V_{max} they are always realistic, *i.e.* they

are greater than zero even if they are not significant. If the Lineweaver- Burk, Eadie or Hanes linearization is used for the evaluation of V_{\max} and K_M , the values obtained for the parameters can be physically unrealistic in that negative values for the parameters can occur (Tables X and XI).

If the Hanes linearization is used for the determination of the values of V_{\max} and K_M when the amount of cells in the assay is relatively large, the values obtained can be statistically the same as those obtained by non-linear regression. This occurred when the amount of cells in the assay was 2.45 mg of protein or more (Table XI). The Lineweaver-Burk linearization gave values for V_{\max} and K_M different from those obtained by non-linear regression when the amount of protein was 2.45 mg or 4.904 mg (Table XI). The Eadie plot detected the deviations from Michaelis-Menten behaviour most clearly as measured by square of the regression coefficient R . R for the Lineweaver-Burk linearization was 69 percent when that for the Eadie plot was 0 percent (Table X).

The K_M values obtained by using nonlinear least squares to fit the Michaelis-Menten equation to the data show the same trend as the $K_{0.5}$ values obtained with the Hill Equation. If low amounts of protein are in the system, the apparent K_M for tyrosine degradation can be large (4.55 mM); if larger amounts of protein are present the apparent K_M varies from 0.25 to about 0.3 mM. Note however that when the amount of protein in the assay was 2.45 mg, the value obtained for K_M was 0.6 mM a value different from the 0.25 to 0.30 mM which occurs at higher protein levels.

These results show clearly that the value obtained for the apparent K_M of the whole cell TPL system depends on the amount of whole cell protein in the system. However the marked non-linearity of the Eadie plots show that even when the values obtained for K_M and V_{\max} are statistically significant, the system is not truly Michaelis-Menten.

Table VIII. The Value of the Parameters of the Michaelis-Menten Equation for the Data in Figure 37 [†]				
Total Cell Protein in Assay (mg)	Parameters	Value	std dev	Significance at 95 % C.I.
0.452	V_{max}	3.74	1.81	n.s*
	K_M	4.55	2.86	n.s
0.680	V_{max}	4.73	1.56	s
	K_M	2.93	1.40	ns
0.861	V_{max}	2.87	0.39	s
	K_M	1.09	0.30	s
[†] The data in Figure 37 is being analyzed separately from that in Figure 41 because they were harvested from different batches; * "s" indicates that the value of the parameter is statistically significant at the $p \leq 0.05$ level; "ns" indicates a lack of significance at this level.				

Table IX. The Value of the Parameters of the Michaelis-Menten Equation for the Data in Figure 41. [†]				
Total Protein in Assay (mg)	Parameters	Value	std dev	Significance at 95 % C.I.
2.45	V_{max}	1.61	0.10	s
	K_M	0.60	0.09	s
3.267	V_{max}	1.80	0.07	s
	K_M	0.28	0.03	s
4.086	V_{max}	2.39	0.08	s
	K_M	0.25	0.03	s
4.904	V_{max}	3.02	0.20	s
	K_M	0.30	0.06	s
[†] Note the data in Figure 41 is analyzed separately from that in Figure 41, because the cells were harvested from different batches; "s" indicates that the value of the parameter is statistically significant at the $p \leq 0.05$ level; "ns" indicates a lack of significance at this level.				

Table X. V_{max} and K_M (or $K_{0.5}$) Values Obtained by Different Procedures (Original Data in Figure 31).*						
Protein	Parameter	Lineweaver	Eadie	Hanes	N.L. [†] of M.M.	N.L. of Hill
0.452	$V_{max}^{\#}$	-0.07	-0.03	-0.21	3.74	1.19
	K_M^{**}	-0.89	-1.00	-1.65	4.55	0.61
	Rsq(%)	78.6	31.6	19.5		
0.680	V_{max}	-0.11	0.30	-0.66	4.73	1.81
	K_M	-0.70	-0.53	-1.91	2.93	1.81
	Rsq(%)	80.3	8.6	14.3		
0.861	V_{max}	-0.53	1.46	13.99	2.87	1.98
	K_M	-0.85	0.31	10.44	1.1	0.38
* The Data for Figure 37 is analysed separately from that in Figure 41 because there are batch to batch variations; # V_{max} is in $\mu\text{mol}/\text{min}$; ** K_M is in mM; Rsq is the square of the correlation coefficient for a linear model; N.L. Non Linear Regression.						

Table XI. V_{max} and K_M ($K_{0.5}$) Values Obtained by Different Procedures (Original Data in Figure 41). [*]						
Protein	Parameter	Lineweaver	Eadie	Hanes	N.L. [†] of M.M.	N.L. of Hill
2.45	$V_{max}^{\#}$	2.62	1.44	1.64	1.61	1.6
	K_M^{**}	1.25	0.49	0.64	0.60	0.60
	Rsq(%)	89.3	70.5	94.8		
3.267	V_{max}	1.71	1.74	1.80	1.80	1.71
	K_M	0.24	0.25	0.29	0.28	0.22
	Rsq(%)	96.2	88.7	99.0		
4.086	V_{max}	2.43	2.40	2.37	2.39	2.21
	K_M	0.26	0.25	0.24	0.25	0.14
	Rsq(%)	98.3	91.0	99.4		
4.904	V_{max}	5.28	2.96	3.16	3.02	3.01
	K_M	0.86	0.28	0.35	0.30	0.24
	Rsq(%)	84.8	51.0	93.1		
[*] Data analysed separately from that in Figure 37 because the cells were harvested from different batches; [#] V_{max} is in $\mu\text{mol/min}$; ^{**} K_M is in mM; [†] Rsq is the correlation coefficient for a linear model; ! N.L. Non Linear Regression						

4.3.4b (ii). Analysis by the Model of Monod.

The Eadie or Scatchard plots of the initial rate kinetic data at relatively low amounts of total cell protein show that the systems can have mixed cooperativity. The most general model of Monod, Wyman and Changeux (159) is able to fit systems which display complex cooperativity. The basic assumption of this model is that the enzyme (indeed proteins in general) exist in at least 2 conformations; a relaxed (**R**) conformation with high affinity for substrate and a tense (**T**) conformation with lower affinity for substrate. The general equation of Monod is :

$$v = \frac{nk_T[E]_t L c \alpha (1 + c \alpha)^{n-1} + nk_R[E]_t \alpha (1 + \alpha)^{n-1}}{L(1 + c \alpha)^n + (1 + \alpha)^n} \quad \dots 4.3$$

with parameters k_T , k_R , L , K_R , K_T and n . Where n is the number of substrate binding sites; k_T and k_R are the respective rate constants for product formation from the tense (**T**) conformation and the relaxed (**R**) conformation of the enzyme; L is the equilibrium or allosteric constant for the transition of the enzyme from the R state to the T state; α equal S/K_R is a normalised measure of the substrate concentration with K_R as the dissociation constant of substrate from the R state; c is the ratio K_R/K_T and K_T is the dissociation constant of substrate from the T state; $[E]_t$ is the total concentration of enzyme. The development of equation 4.3 is presented in Appendix III.

Since $[E]_t$ is not known explicitly for a whole cell system equation 4.3 was modified by setting:

$$nk_T[E]_t = V_{\max(T)} \quad \text{and}$$

$$nk_R[E]_t = V_{\max(R)}$$

In initial fits of the general equation of Monod, Wyman and Changeux, n was allowed to vary. The best fit values of this parameter was from 4 to 5, and never less than 2.5. This suggests that the number of subunits (or active sites) is

more than 2 and is probably equal to 4. The literature suggests that the number of subunits of TPL is either 2 (78, 86, 87, 88) or 4 (89, 90, 91), however in the light of these results it was considered that 4 subunits was more likely. Therefore n was set explicitly to 4 for further fits of the data.

The asymptotic correlation matrix of the parameters (160) had elements that were almost all equal to 1. This suggested that a simpler model could fit the data as well (or else enough data was not present to allow the accurate estimation of each parameter). Therefore the model was simplified by assuming that the rate constant for product formation was the same for both the T state and the R state. This simplified form of the model is the more common form of the Monod allosteric model and gives as a mathematical description of the initial velocity of the system:

$$\frac{v}{V_{\max}} = \frac{L\alpha(1 + \alpha)^{n-1} + \alpha(1 + \alpha)^{n-1}}{L(1 + \alpha)^n + (1 + \alpha)^n} \quad \dots 4.4$$

This equation can only describe Michaelis-Menten systems (*i.e.* $L = 0$ or $K_R = K_T$) or positively cooperative systems. The best fit value of the parameters obtained upon fitting equation 4.4 to the data indicated values of K_T that were much larger than K_R . This suggested that the binding to the T state could be ignored, hence equation 4.4 can be further simplified to:

$$\frac{v}{V_{\max}} = \frac{\alpha(1 + \alpha)^{n-1}}{L + (1 + \alpha)^n} \quad \dots 4.5$$

This equation is the exclusive binding allosteric model of Monod *et al* (159). If L is set to zero in this model it is identical to the Michaelis-Menten equation. Since equation 4.5 becomes after substitution for α as S/K_R equation 4.6, which gives immediately a Michaelis-Menten type equation as shown below.

$$v = \frac{V_{\max} \left(\frac{S}{K_R} \right) \left(1 + \frac{S}{K_R} \right)^{n-1}}{\left(1 + \frac{S}{K_R} \right)^n}$$

$$v = \frac{V_{\max} S}{K_R + S} \quad \dots 4.6$$

The Monod equation for exclusive binding (equation 4.5) converged to the same value for the residual sum of the squares as the complete Monod model (equation 4.3). The exclusive binding model was therefore considered to be as good a fit to the data as the complete Monod model.

The values of the parameters which best fit the data are presented in Tables XII and XIII. Typically only 2 (*i.e.* V_{\max} and K_R) of the 3 parameters of the model were statistically significant. At the higher concentrations of total protein in the assay, a value of L not significantly different from zero implies that a Michaelis-Menten fit to the data is just as good a fit to the data. If the total amount of cell protein in the assay is low and hence there is sigmoidal behaviour, a value for L that is not significant implies that this model is inferior to the model of Hill (158) since that model converged to a similar residual sum of squares with all parameters significant.

The values obtained for K_R and V_{\max} are identical to those obtained for K_M and V_{\max} with the Michaelis-Menten fit when the amount of cell protein in the system is 2.45 mg or more. For the data obtained at lower amounts of protein in the assay (0.452, 0.680 and 0.861 mg) the values obtained for V_{\max} do not increase (or decrease) monotonously, this result is anomalous and indicates that the model is inferior to the Hill model as a description of the data.

Weighting the data with the reciprocal of the square of the standard deviation of the velocity did not improve the precision of the parameters for the exclusive binding model of Monod.

Table XII. Best Fit Parameters for the Exclusive Binding Model of Monod (Original Data in Figure 37)*				
Total Amount of Protein in Assay (mg)	Parameter	Value	Std. Dev. of Parameter	Significance at 95 % C.I.
0.452	V_{max}	1.33	0.12	s
	K_R	0.52	0.15	s
	L	13.31	9.70	n s
0.680	V_{max}	2.89	0.96	s
	K_R	1.11	0.82	n s
	L	1.59	2.52	n s
0.861	V_{max}	2.17	0.25	s
	K_R	0.47	0.19	s
	L	3.09	3.68	n s
* The data in Figure 37 is analyzed separately than that in Figure 41 because the cells were harvested from different batches. Cf Table XIII				

Table XIII. Best Fit Parameters for the Exclusive Binding Model of Monod (Original Data in Figure 41)*				
Total Amount of Protein in Assay (mg)	Parameter	Value	Std. Dev. of Parameter	Significance at 95 % C.I.
2.450	V_{max}	1.61	0.02	s
	K_R	0.60	0.23	s
	L	0.00	0.61	n s
3.267	V_{max}	1.80	0.17	s
	K_R	0.28	0.10	s
	L	0.00	0.00	n s
4.086	V_{max}	2.33	0.10	s
	K_R	0.21	0.04	s
	L	0.85	1.22	n s
4.904	V_{max}	3.01	0.30	s
	K_R	0.24	0.11	s
	L	1.59	3.40	n s
* The data in Figure 41 was analyzed separately from that in Figure 37 because the cells were harvested from different batches.				

4.3.4b (iii). Analysis by the Model of Adair.

The Adair model for the rapid equilibrium binding of a ligand to a tetrameric protein (161), when applied to kinetic data (162) is :

$$v_0 = \frac{E_t [4k_1K_1'S + 12k_2K_1'K_2'S^2 + 12k_3K_1'K_2'K_3'S^3 + 4k_4K_1'K_2'K_3'K_4'S^4]}{1 + 4K_1'S + 6K_1'K_2'S^2 + 4K_1'K_2'K_3'S^3 + K_1'K_2'K_3'K_4'S^4} \dots 4.7$$

where v_0 is the initial velocity; $[E]_t$ is the total concentration of enzyme; S is the concentration of substrate; k_i is the average rate constant for product formation when i substrate molecules are bound to the enzyme; K_i is the inherent affinity constant for substrate binding to form ES_i from ES_{i-1} and S (162). If $k_1 = k_2 = k_3 = k_4 = k_p$ and $4k_p[E]_t$ is set to V_{\max} then the Adair equation for kinetic data becomes:

$$\frac{v_0}{V_{\max}} = \frac{[K_1'S + 3K_1'K_2'S^2 + 3K_1'K_2'K_3'S^3 + K_1'K_2'K_3'K_4'S^4]}{1 + 4K_1'S + 6K_1'K_2'S^2 + 4K_1'K_2'K_3'S^3 + K_1'K_2'K_3'K_4'S^4} \dots 4.8$$

The general Adair equation is developed in Appendix III.

The Adair equation is able to fit systems with complicated mixed cooperativity (162) and therefore its fit to the initial rate kinetic data in Figures 37 and 41 was examined. The values of the parameters which best fit the data did not result in an improved fit relative to that obtained with the Hill equation. In other words the intermediary plateaux were not fitted by the data. Also in general while the value for V_{\max} was statistically significant the values for K_1 , K_2 , K_3 and K_4 respectively were usually not significant.

4.3.4b (iv) Analysis by the Model of Koshland, Nemethy and Filmer.

The general sequential interaction model of Koshland, Nemethy, and Filmer (KNF) (163) with restricted interactions between sites, assumes that the subunits of an enzyme will interact with each other. The strength of the interaction varies

depending on whether the active sites of the subunits are free, and thus they are in the A conformation, or else the active sites are occupied and the subunits are in the B conformation. Depending on the degree of saturation of the enzyme there can be AA, AB or BB interactions. The geometry or spatial arrangement of the subunits will also affect the types and the number of possible interactions.

The complexity of the velocity versus substrate plots, and the result of the Monod *et al* fit which gave better results when n equals 4 suggest that TPL is probably a tetramer. This result is also supported by the literature (89, 90, 91), indeed X-ray crystallography suggests that TPL is a tetrameric protein whose subunits are arranged as a square or rectangle (89). Therefore the KNF model for a square was fitted to the initial rate data. This model is more versatile than the simple allosteric model of Monod *et al* (159) since it predicts positive cooperativity, negative cooperativity and mixed cooperativity depending on the relative strengths of the AB, or BB interactions (93, 162). The mathematical description of the model is given by equation 4.9 below:

$$\frac{V_0}{V_{\max}} = \frac{K_{AB}^2(K_S K_I S) + (2K_{AB}^2 K_{BB} + K_{AB}^4)(K_S K_I S)^2 + 3K_{AB}^2 K_{BB}^2(K_S K_I S)^3 + K_{BB}^4(K_S K_I S)^4}{1 + 4K_{AB}^2(K_S K_I S) + (4K_{AB}^2 K_{BB} + 2K_{AB}^4)(K_S K_I S)^2 + 4K_{AB}^2 K_{BB}^2(K_S K_I S)^3 + K_{BB}^4(K_S K_I S)^4} \quad \dots 4.9$$

where v_0 is the initial velocity, V_{\max} is the maximum velocity which occurs when the enzyme is saturated with substrate **S** and is equal to $4k_p[E]_t$, the product of the rate constant for product formation and the total concentration of active sites; K_S is the binding constant for substrate **S** to the active site; K_I represents the transformation constant of the enzyme from conformation A (which occurs when the active site is vacant) to conformation B (which occurs when the active site is occupied); K_{AB} is the equilibrium constant reflecting the strength of the interaction between a subunit in the A conformation and a subunit in the B conformation; K_{BB} is the equilibrium constant reflecting the strength of the interaction between 2 subunits in the B conformation. K_{AA} which measures the interaction between 2 subunits in the A conformation is set equal to 1.

If equation 4.8 is fitted to the initial rate data obtained with relatively low amounts of whole cell protein (Figure 37), the only parameter that is consistently significant is V_{\max} . The value obtained for V_{\max} was essentially the same as that obtained when the data was fitted with the exclusive binding model of Monod (*i.e.* the results of Tables XII and XIII). The values of the other parameters have not been presented since they were not statistically significant.

4.3.4b (v). Summary of the Preliminary Kinetic Analysis of the Initial Rate Data.

Models based on the structural rate steady state analysis developed by Ricard *et al* (93) will be discussed in the General Discussion and are not presented at this time. However a comprehensive analysis of the initial rate data by the more common models of enzyme kinetics have been done. These analyses show that the system can display very complex kinetic patterns especially when the cell concentration, as measured by total cell protein, is low. At higher cell concentrations however where intermediary plateaus are not as prominent the data is still not truly Michaelis-Menten since Eadie or Scatchard plot of the data show pronounced curvature. In section 4.6.3 the way in which the kinetics displayed by a system can be affected by the amount of enzyme in the system will be discussed in some detail.

The Hill model is the most parsimonious model which gives a reasonable fit to all the initial rate data. This model can fit - with significant value for the parameters - both the sigmoidal behaviour of the data which occurs with low concentrations of cells, as measured by total cell protein, and the approximate Michaelis-Menten behaviour which occurs with higher amounts of protein. The Hill model is still only an approximation however since it cannot fit an intermediary plateau.

4.4 MICROENCAPSULATED TPL ACTIVITY OF WHOLE CELL *E. HERBICOLA*

4.4.1. Effect of Shaking Speed on the TPL Activity of Free and Microencapsulated *Erwinia herbicola*.

The effect of stirring speed on the observed TPL activity of microencapsulated *Erwinia herbicola* was studied at 37 °C in PB (0.1 M, pH 8.0). The activity was determined by assay of the phenol produced by the degradation of tyrosine. The activity of free and microencapsulated cells were compared. The microcapsules were made from a 100 ml stock of 3.0 % Kelco-Gel® HV alginate that had been sterilized for 5.0 minutes in a can as described above (in section 3.3.1). The degree of sterilization provided by this procedure was adequate to kill all spores in the alginate. The stock of alginate was diluted with cell suspension to give a cell suspension in 1.5 percent alginate in buffered saline. The airflow and liquid flow to the droplet former were 2.5 litre/minute and 0.389 ml/minute respectively. The PLL (mol. wt. 25,000) reaction time was 10.0 minutes. The final microcapsules ($751 \pm 68 \mu\text{m}$, mean \pm std. dev.) contained 5.6 mg of total cell protein per millilitre. They were kept in PB (pH 7.0, 100 mM) until they were ready for use.

Microcapsules with entrapped *Erwinia herbicola*, when made in this way, were stable and could maintain their integrity during storage for at least 2 months when kept in buffer supplemented with chloramphenicol (CAM). The CAM inhibited bacterial growth. Comparative photomicrographs of before and after two months of storage are shown in Appendix IV. The cells have settled (presumably under gravity) but the microcapsule membrane is intact.

At low shake rates the activity of the microencapsulated cells is very low. At a shake speed of 120 rpm the activity of the microencapsulated cells is almost zero. When the shake speed is increased to 240 rpm or more the activity of free and of microencapsulated cells is the same (Figure 45). For subsequent studies of microencapsulated enzyme a shaking speed of at least 240 rpm was used.

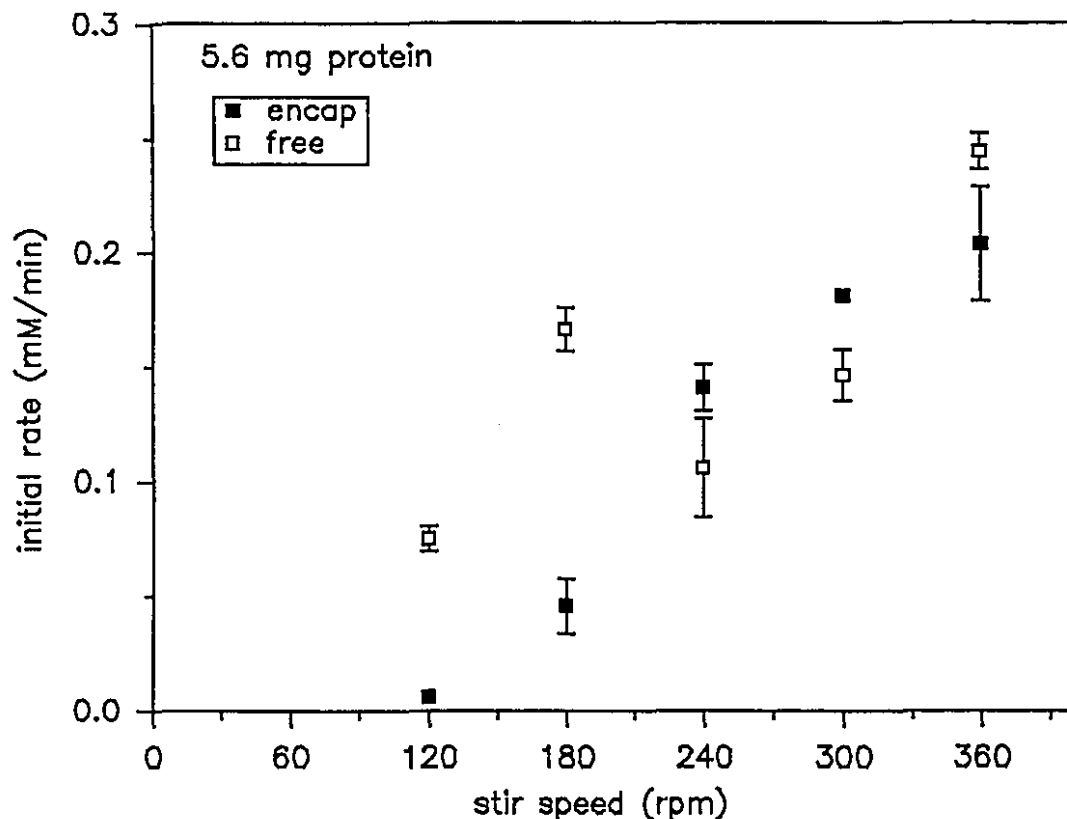


Figure 45. The effect of shaking speed on the TPL activity (initial rate) of free and microencapsulated whole cell *Erwinia herbicola*. (Temperature = 37 °C, pH = 8.0, n = 2.)

4.4.2. The Effect of Temperature on the TPL Activity of Free and Microencapsulated *Erwinia herbicola*.

The activity of free and microencapsulated cells as a function of temperature is shown in Figure 46. The shake speed was 240 rpm. The TPL activity of free and microencapsulated cells are almost the same at 37 °C, but at lower temperatures the free cells have a higher activity than the microencapsulated cells. The pseudo Arrhenius plot ($\log_e(\text{activity})$ versus reciprocal temperature) - not shown - for both free and encapsulated cells was approximately linear ($r = 0.78$ and 0.84 respectively).

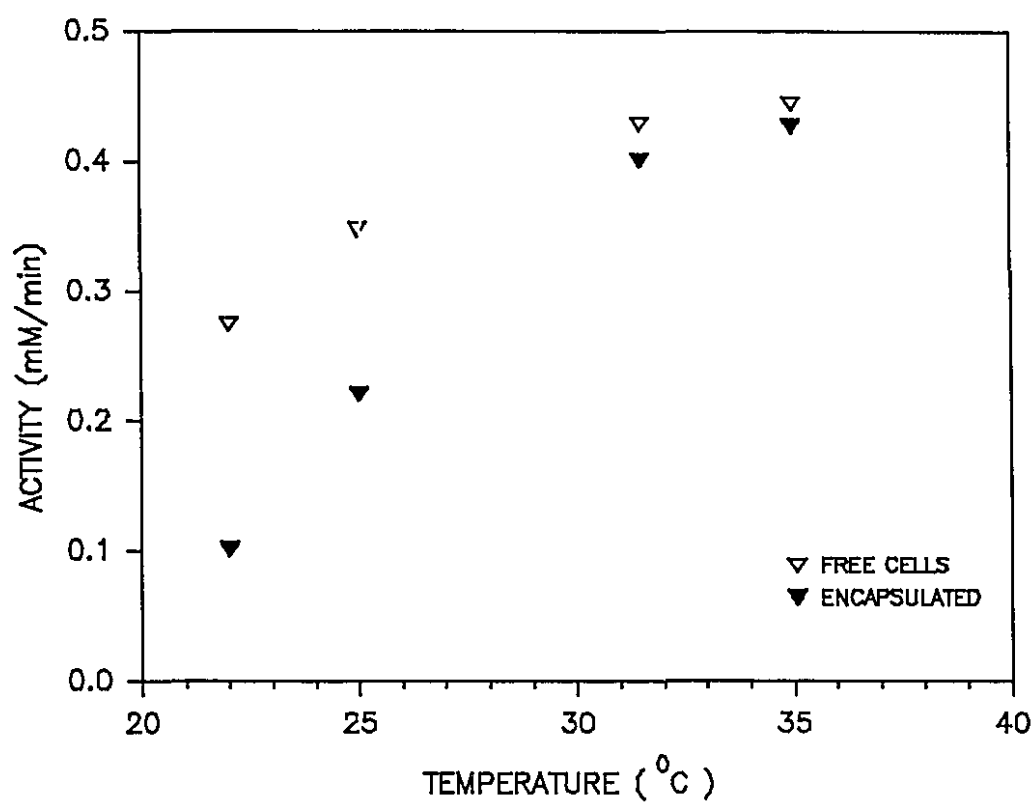


Figure 46. The effect of temperature on the TPL activity of free and microencapsulated whole cells of *Erwinia herbicola*.

4.4.3. Comparative Study of TPL Activity Versus Substrate Profile for Free and Microencapsulated Whole Cell *E. herbicola*.

The TPL activity of microencapsulated and free *E. herbicola* was compared at pH 8.0 and 37 °C, the assay flasks were stirred at 240 rpm. The microcapsules ($821 \pm 83 \mu\text{m}$, mean \pm std. dev.) containing 0.5 mg of protein per ml were prepared with Kelco-Gel® HV alginate that had been heat-sterilized for 5 minutes as described previously. The airflow and liquid flow to the droplet former were 2.5 l/min and 1.07 ml/min, respectively. A liquid flow of 1.07 ml/min to the droplet former is convenient since it reduces the time required to make a batch of microcapsules. However previous studies (Section 4.1.4) have shown that differences in the liquid flow rate (at constant airflow) do not change significantly the size distribution of the resulting microcapsules so it was assumed that an rpm of 240 was adequate for stirring the microcapsules.

The TPL activity versus tyrosine concentration profiles for free and microencapsulated cells are shown in Figure 47. The Michaelis-Menten equation was used to fit the data; and both the value for V_{max} and K_M were significantly different -in a statistically sense- from zero (Table XIV); however this equation does not fit the data well. These constants are more properly considered as apparent Michaelis-Menten constants; since they refer to whole cells and there may be endogenous inhibitors, activators and diffusional resistances *et cetera* in the system. Each of these effects could modify the value calculated for the parameters of the Michaelis-Menten equation.

As shown earlier the kinetics of the whole cell TPL system is very complicated and none of the simpler kinetic models are able to fit the data well. The residuals of the Michaelis fit are also shown in Figure 47. The pattern is clearly not random and indicate an intermediary area where the actual velocity values are lower than predicted by the equation. This suggests an intermediary plateau area, however this plateau is not as pronounced as those obtained in some sets of data (*vide supra* Figure 37 for example). The residuals of the Michaelis fit for the encapsulated data shows a similar pattern to that obtained for

the free data. These results provide further confirmation that the whole cell TPL enzyme does not truly display Michaelis-Menten kinetics, although some authors (76, 78, 86, 88) have made this claim. This point will be discussed further in Section 4.6.3.

The apparent value obtained for the V_{max} for the free and the encapsulated system are statistically identical; however the apparent value for the K_M of the encapsulated cells is significantly higher than that for the free cells. This indicates

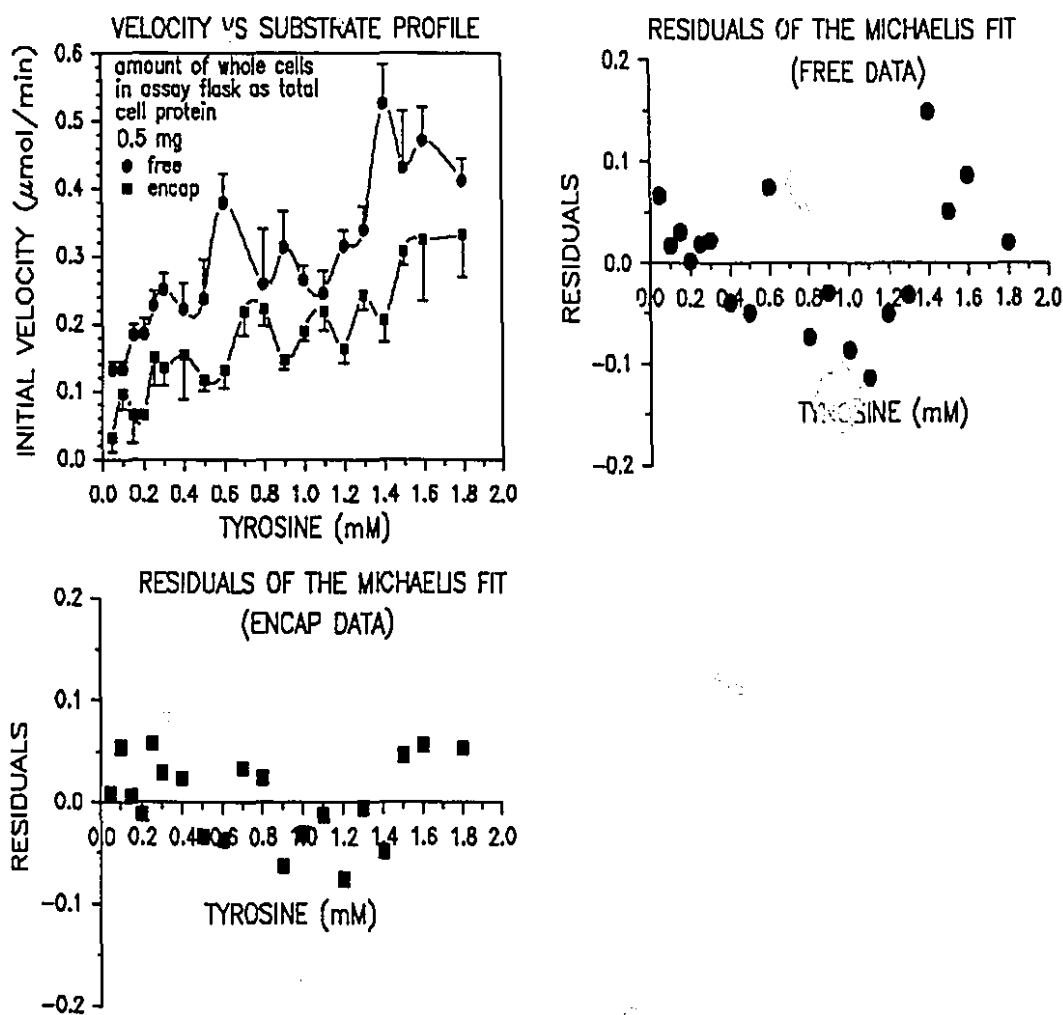


Figure 47. Velocity (TPL activity) versus substrate profile for free and microencapsulated *E. herbicola*.

that there may be some mass transfer resistance in the system that would become noticeable at low concentrations of substrate.

Table XIV. Initial TPL Activity of Free and Microencapsulated <i>E. herbicola</i> .			
	Parameter	Value	Std. dev.
free	V_{max}	0.46	0.05
	K_M	0.30	0.12
encapsulated	V_{max}	0.41	0.08
	K_M	0.86	0.38

4.5 PRODUCTION OF TYROSINE OR DOPA WITH THE TPL OF WHOLE CELL *ERWINIA HERBICOLA*.

4.5.1. Conversion of Ammonia, Pyruvate and Phenol or Catechol into L-Tyrosine or L-dopa.

The conversion of ammonia, pyruvate and phenol, or catechol into L-tyrosine or L-dopa at 27 °C by the TPL activity of *Erwinia herbicola* is shown in Figure 48. The reaction medium (10 ml) contained whole cells of *Erwinia herbicola* (5.6 mg total cell protein). For the microencapsulated study the cells were entrapped in 1.0 ml of microcapsules ($916 \pm 103 \mu\text{m}$, mean \pm std. dev.). The initial concentration of phenol was 50 mM in the experiment for tyrosine production. In the experiment for L-dopa the initial catechol concentration was also 50 mM. The initial concentrations of both ammonia and pyruvate were 80 mM. The shake speed was 240 rpm.

The data for conversion to tyrosine suggests that for the first 5 hours of the reaction free cells and microencapsulated cells perform equally well. However with prolonged reaction encapsulated cells achieved a higher conversion of reactants to tyrosine (Figure 48).

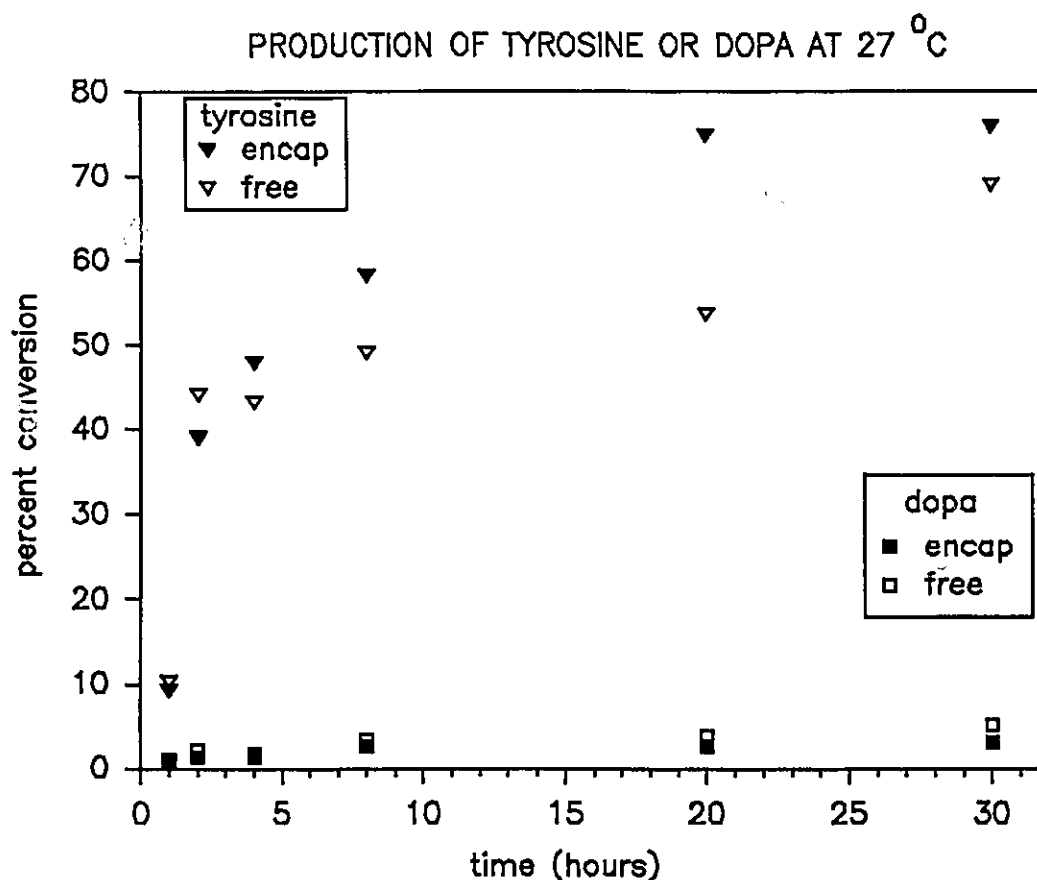


Figure 48. The conversion of ammonia, pyruvate and phenol or catechol into L-tyrosine or L-dopa respectively by the TPL activity of whole cell *E. herbicola*.

After 5 hours of reaction, the conversion (with respect to phenol) of reactants to tyrosine in the flasks was 50 percent. This compares with a conversion of reactants to L-dopa in flasks which contained catechol of only 3 percent (Figure 48).

It was possible that the TPL was inhibited by the catechol or else the product L-dopa and or the catechol was destroyed by light. An experimental design was done to observe the effects of catechol concentration and of light on the production of L-dopa. The experiments in the design were conducted at 37 °C for 6 hours with microencapsulated cells of *Erwinia herbicola* (6.6 mg total protein in 1.0 ml of microcapsules, $898 \pm 101 \mu\text{m}$). The results of the design are shown

in Table XV. An analysis of the variance (ANOVA) of the data in the Table was done. As the concentration of catechol increased from 10 mM to 40 mM there was a reduction in the amount of L-dopa produced but the effect was not significant ($p > 0.05$). More L-dopa was produced when the reaction was done in the light as opposed to when it was performed in the dark ($p < 0.05$).

Table XV. The Effect of Catechol and Illumination on the Production* of L-Dopa by Microencapsulated <i>E. herbicola</i>.			
	conc of catechol (mM)		
	10	25	40
light [†]	1405 ± 490	1221 ± 489	692 ± 57.5
dark	584 ± 32	546 ± 6	634 ± 49
# production = μmoles of L-Dopa produced			
† n = 2 for each cell of the factorial design			

4.5.2 Evaluation of an Approximate Kinetic Model for the Conversion of Ammonia, Phenol and Pyruvate into Tyrosine.

Model Development

The postulated mechanism for the degradation of tyrosine by tyrosine phenol-lyase implies that the production of tyrosine from ammonia, phenol and pyruvate occurs by an ordered ter-uni mechanism (73, 99) (Section 2.3.4). The scheme of the process is shown in **Appendix V**, in which ammonia, phenol and pyruvate are bound by the enzyme in that order, before the release of tyrosine.

If rapid equilibrium assumptions are applied and subunit effects are

assumed to be minimal and the system is sufficiently far from its thermodynamic equilibrium, then an integrated form of the ter-uni mechanism can be readily derived. The circumstances under which subunit effects can be minimal are discussed in the General Discussion and will not be presented here.

The integrated form of the kinetic equation can be applied to data obtained during the production of tyrosine from ammonia, pyruvate and phenol. The equations were derived as shown in **Appendix V** for 3 conditions. In the first condition, inhibition by phenol is not considered explicitly. In the second condition, it is assumed that phenol inhibits TPL with mixed type inhibition kinetics. In the third condition, it is assumed that phenol inhibits TPL with simple competitive inhibition kinetics. Mixed type inhibition by phenol was considered because Kumagai and Yamada (78, 86) reported that phenol inhibits TPL with mixed type kinetics. Simple competitive inhibition by phenol was considered because Para et al (107) reported that phenol inhibits whole cell TPL with "classical" inhibition kinetics. The well known notation of Cleland (105) was utilised in the derivation of the equations.

The integrated form of the ter-uni mechanism when inhibition by phenol is not explicitly considered is:

$$t = \frac{1}{V_{\max}} \left(C_1(S_0 - S) + (C_2 + \frac{C_3}{H} + \frac{C_4}{H^2}) \ln \frac{S_0}{S} - (\frac{C_3}{H} + \frac{C_4}{H^2}) \ln \frac{H+S_0}{H+S} + \right. \\ \left. (C_5 + \frac{C_4}{H}) (\frac{1}{(H+S_0)} - \frac{1}{(H+S)}) \right) \quad \dots(4.10)$$

with:

$$C_1=1; C_2=K_C; C_3=K_B K_C; C_4=K_A K_B K_C \left(1 + \frac{S_0}{K_P}\right)$$

$$\text{and } C_5 = K_A K_B \frac{K_C}{K_P}$$

where H is equal to $[A]_0 - [C]_0$, the difference between the initial concentrations of substrates A and C. The concentration of substrate C has been replaced by S. A, B, C and P are respectively the first, second and third substrates and the product in a ter-uni mechanism, hence they designate ammonia (A), pyruvate (B), phenol (C), and tyrosine (P) in this analysis. K_A , K_B , K_C and K_P are the dissociation constants of ammonia, pyruvate, phenol and tyrosine from the relevant enzyme complex as shown in Appendix V; hence they are pseudo Michaelis-Menten constants. V_{max} is the maximum enzyme velocity which occurs when the enzyme is saturated with substrates, i.e. when all the enzyme is in the form EABC (enzyme-ammonia-pyruvate-phenol). In order to obtain more manageable equations the simplification that $[A] = [B] > [C]$ was invoked. The pertinent experimental data used for parameter estimation during tyrosine production were therefore obtained under circumstances such that the initial concentrations of ammonia (80 mM) and pyruvate (80 mM) were equal to each other and greater than the initial concentration of phenol (40 mM).

Solubility Considerations.

The solubility of tyrosine is low in aqueous systems. This means that the concentration of tyrosine can become constant as the reaction proceeds and ammonia, phenol and pyruvate are converted to product tyrosine. This point would occur when the concentration of the tyrosine is equal to its solubility, since any additional tyrosine produced by the reaction would precipitate (unless some type of supersaturation phenomenon occurred). This means that the production of tyrosine by TPL from the substrates ammonia, phenol and pyruvate will have 2 regions. In region 1 the tyrosine concentration is less than its solubility, in region 2 the tyrosine concentration is constant and equal to its solubility.

The exact solubility of tyrosine in this system (water, tyrosine, phenol, pyruvate, ammonia, *et cetera*) is not known, since the presence of phenol in the system will probably increase the solubility of tyrosine above what it would be in an aqueous system lacking phenol. The solubility of tyrosine in water at 25 °C is

2.5 mM (165), and at 37 °C can be predicted to be about 4.5 mM. However these solubilities only give a guide to the minimum solubility of tyrosine in an aqueous system when phenol is present.

For a microencapsulated system the effect of tyrosine precipitation is more complex, since tyrosine could precipitate within the microcapsules. The precipitation of tyrosine within the microcapsules will introduce effects that are not easily accounted for in kinetic or mass transfer terms. The equations are therefore not meant to apply to the region in which tyrosine precipitates.

Equilibrium Considerations

The equation presented above and the others developed in Appendix V ignore the reverse reaction, i.e. the catalytic reconversion of tyrosine to ammonia, pyruvate and phenol, this is reasonable provided the system is far from equilibrium. Data obtained with an initial phenol concentration of 40 mM and pyruvate and ammonia concentrations at 80 mM show that a near 100 percent conversion of phenol is possible after 24 hours of reaction (at 37 °C). Therefore the effects of the equilibrium can be ignored under these conditions if the duration of the reaction is about 10 hours. The data is shown in Appendix VI. These data have not been analyzed with the data used in the model evaluation (see below) because they were obtained with encapsulated cells; and the emphasis here is on a comparative study of the activity of free and encapsulated cells under contemporaneous conditions.

Evaluation of the Parameters of the Model.

Two different levels of cells (total cell protein 1.6 mg and 6.6 mg) were used for the conversion of ammonia, pyruvate and phenol into tyrosine at 37 °C. The initial concentrations of pyruvate were equal at 80 mM and that of phenol was 40 mM. Both free and microencapsulated cells were used. Microencapsulated cells were contained in 1.0 ml of microcapsules (diameter $898 \pm 101 \mu\text{m}$, mean \pm std. dev.). The data for the conversion to tyrosine of ammonia, phenol and pyruvate is

shown in Figure 49.

The data at 37 °C was analyzed because the solubility of tyrosine is higher at 37 °C than at room temperature. This means that the reaction could be followed for a longer time without having to account for the possible precipitation of tyrosine within the microcapsules. At the higher cell concentration tyrosine visibly precipitated after 8 hours of reaction. No precipitation occurred at the lower cell concentration used during the time course of the reaction.

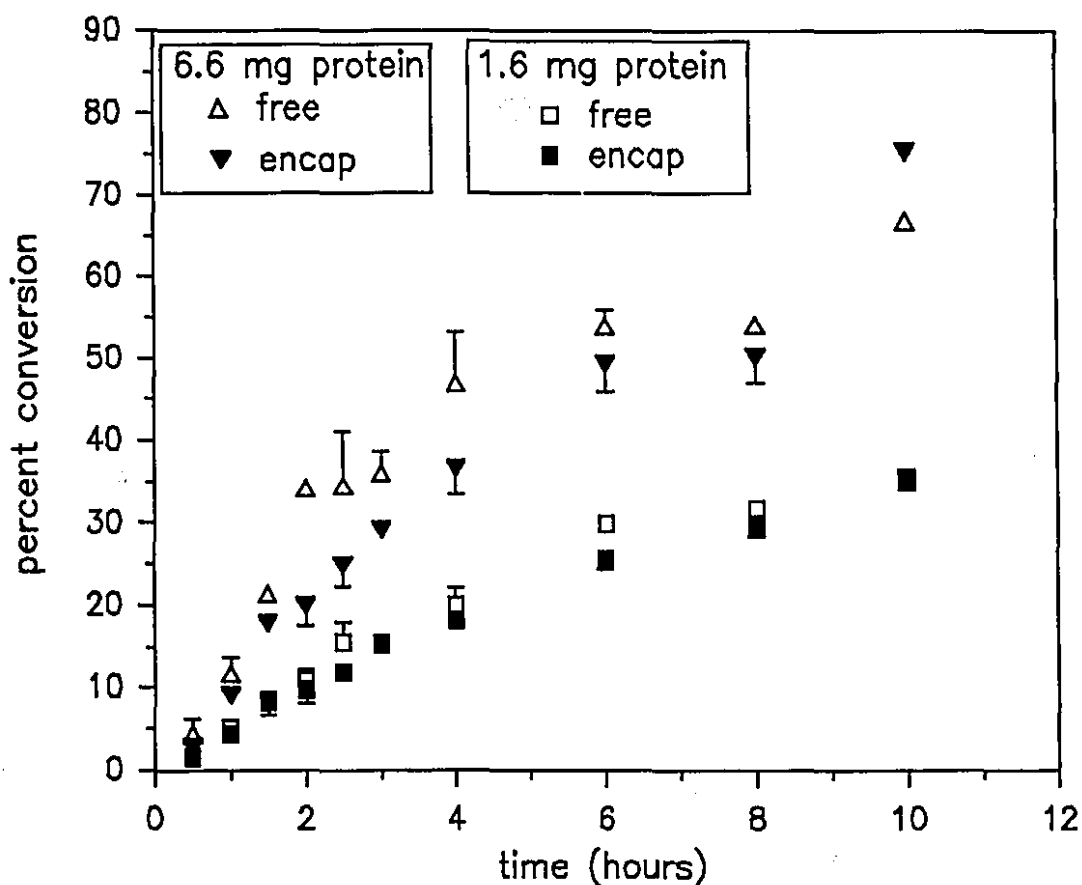


Figure 49. The Conversion of ammonia, phenol and pyruvate to tyrosine by the TPL activity of whole cell *E. herbicola*.

The fitting of the data at the lower cell concentration suggested apparent K_M values for ammonia, phenol, pyruvate and tyrosine -the K_A , K_B , K_C , and K_P of the

integrated form of the kinetic equation- of 134, 46, 0.52 and 0.2 mM respectively for free whole cells. The large value of the apparent K_M for ammonia (K_A) suggested that the system could be considered approximately saturated with phenol and tyrosine. That is $[E]$ and $[EA]$ are small relative to $[EAB]$, $[EABC]$ and $[EP]$. Therefore equation 4.10 could be approximated by equation 4.11. The basis for the simplification is shown in Appendix V in the subsection "Saturation by Phenol Considerations".

$$t = \frac{1}{V_{\max}} \left(C_1(S_0 - S) + \left(C_2 + \frac{C_4}{H^2} \right) \ln \frac{S_0}{S} - \left(\frac{C_4}{H^2} \right) \ln \frac{H+S_0}{H+S} + \left(C_5 + \frac{C_4}{H} \right) \left(\frac{1}{(H+S_0)} - \frac{1}{(H+S)} \right) \right) \quad \dots(4.11)$$

$$\text{with } C_1 = 1; C_2 = K_C; C_4 = (K_A K_B) K_C \frac{S_0}{K_P}; C_5 = (K_A K_B) \frac{K_C}{K_P}$$

Equation 4.11 does not allow the explicit determination of either K_A or K_B since they always occur together as the product $K_A K_B$. Analysis of the data with the integrated form of the equations modified to account for partial saturation by phenol (*i.e.* 4.11), yielded apparent K_M and V_{\max} values as shown in Table XVI. The data indicates that the process of microencapsulation does not significantly affect the apparent K_M values if the stirring speed is adequate and substrate concentrations are high. The data in Table XVI also suggests that $K_A K_B$ the apparent K_M for the dissociation of the enzyme-ammonia-pyruvate complex (EAB) to free enzyme, ammonia and pyruvate is a function of the amount of cell protein. V_{\max} seems smaller for encapsulated cells than for an equal amount of free cells, however the difference was not statistically significant at the level of $p \leq 0.05$.

Table XVI. Kinetic Parameters for Whole Cell Tyrosine Phenol Lyase				
	1.6 mg total protein		6.6 mg total protein	
PARAMETER	FREE	ENCAP	FREE	ENCAP
K_P^\dagger (mM)	0.179 ± 0.004	0.20 ± 0.03	0.221 ± 0.04	0.28 ± 0.03
K_C (mM)	0.76 ± 0.24	0.513 ± 0.018	0.50 ± 0.11	0.47 ± 0.04
$K_A K_B$ (mM ²)	4433 ± 85	4875 ± 174	3191 ± 567	1871 ± 375
V_{\max} (mM/hr)	2.91 ± 0.41	2.27 ± 0.14	6.98 ± 1.35	4.34 ± 0.28

$\dagger K_P \equiv K_M \text{ NH}_3$; $K_C \equiv K_M \text{ Phenol}$; $K_A K_B \equiv (K_M \text{ NH}_3)^*(K_M \text{ Pyruvate})$

The data in Figure 49 is replotted in the form of time versus phenol concentration in Figures 50 and Figure 51. The best fit line obtained with the parameters of Table XVI is also shown in these plots. The distribution of the residuals for the data obtained with the encapsulated cells is reasonably random; however the distribution for the free cells is not as random. However considering the fact that the system is not truly Michaelis-Menten, and the complexity of the whole cell TPL system as revealed by the earlier results, equation 4.20 represents a reasonable approximation of the system. It should be borne in mind that the intermediary plateau effects, *et cetera* that were observed could not be fit by any simple extension to the Michaelis-Menten model, which accounted for the fact that TPL is a multiple subunit enzyme. Therefore an improved model would be extremely complex and require many more parameters.

Analysis of the data with the models that also accounted for inhibition (see Appendix V) did not significantly reduce the sums of the squares of the residuals relative to the model (equation 4.11) which did not explicitly account for inhibition. This shows that K_i the dissociation constant of phenol from an inhibitory site is large relative to the dissociation constants for other enzyme species. Hence the

putative inhibitory effects of phenol would only be significant at higher concentrations of phenol. The simpler inhibition model was sufficient to account for the inhibition effects observed. The mixed type inhibition model did not improve the fit of the data. The value of K_i obtained from fitting the data with the simpler inhibition model was 200 mM at low concentrations of protein.

The integrated ter-uni mechanism is considered to be an adequate fit to the data, since for concentrations of phenol less than 50 mM the inhibition model did not improve the fit to the data. This model can be simplified somewhat when the concentration of ammonia is low since the value of the apparent K_M for ammonia is large relative to the concentrations of ammonia used and the apparent K_M values for phenol and tyrosine are small relative to their concentrations.

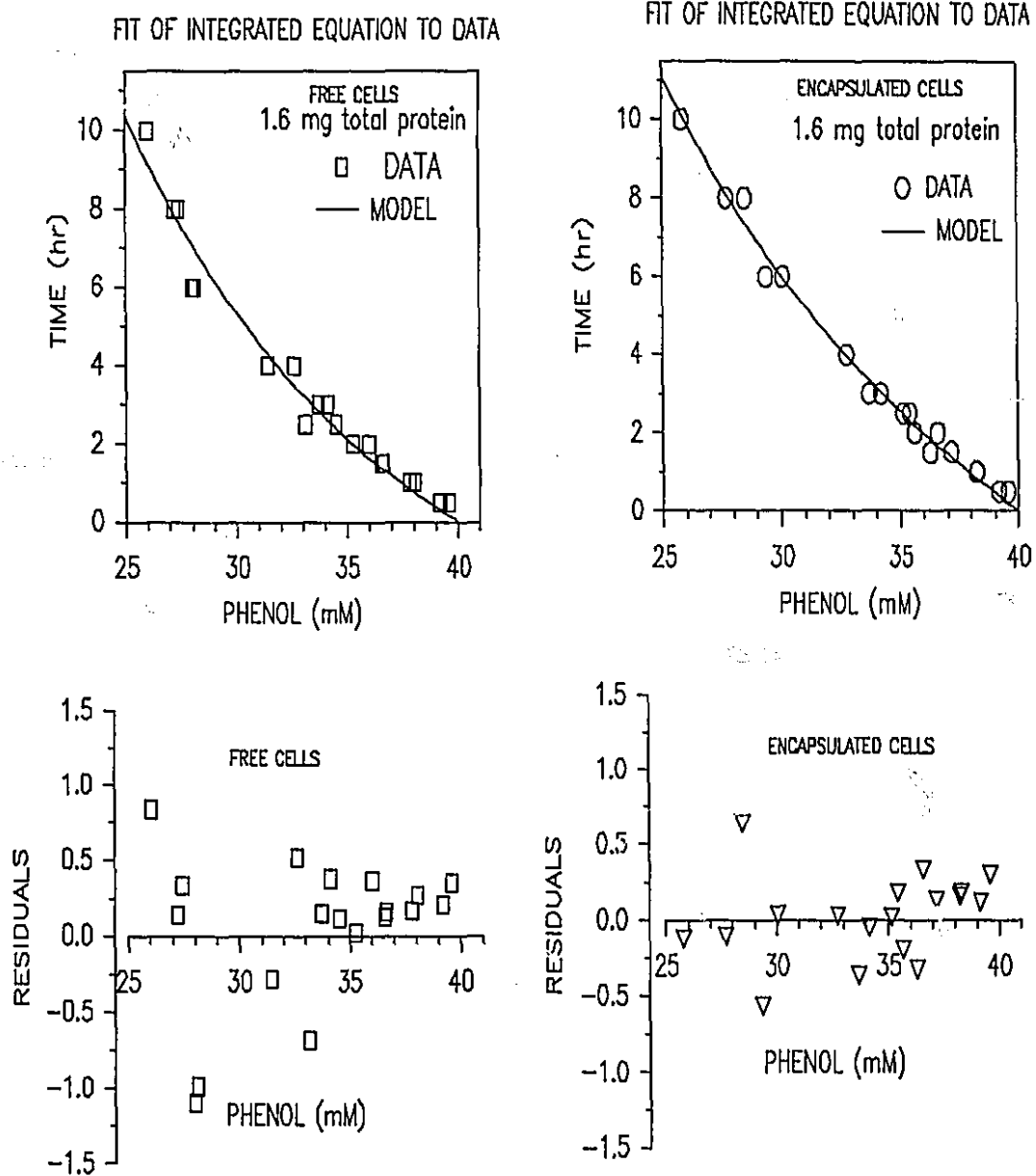


Figure 50. Plots showing the fit of the integrated equation (4.20) to data for the conversion of ammonia, pyruvate and phenol to tyrosine by whole cells (1.6 mg total cell protein).

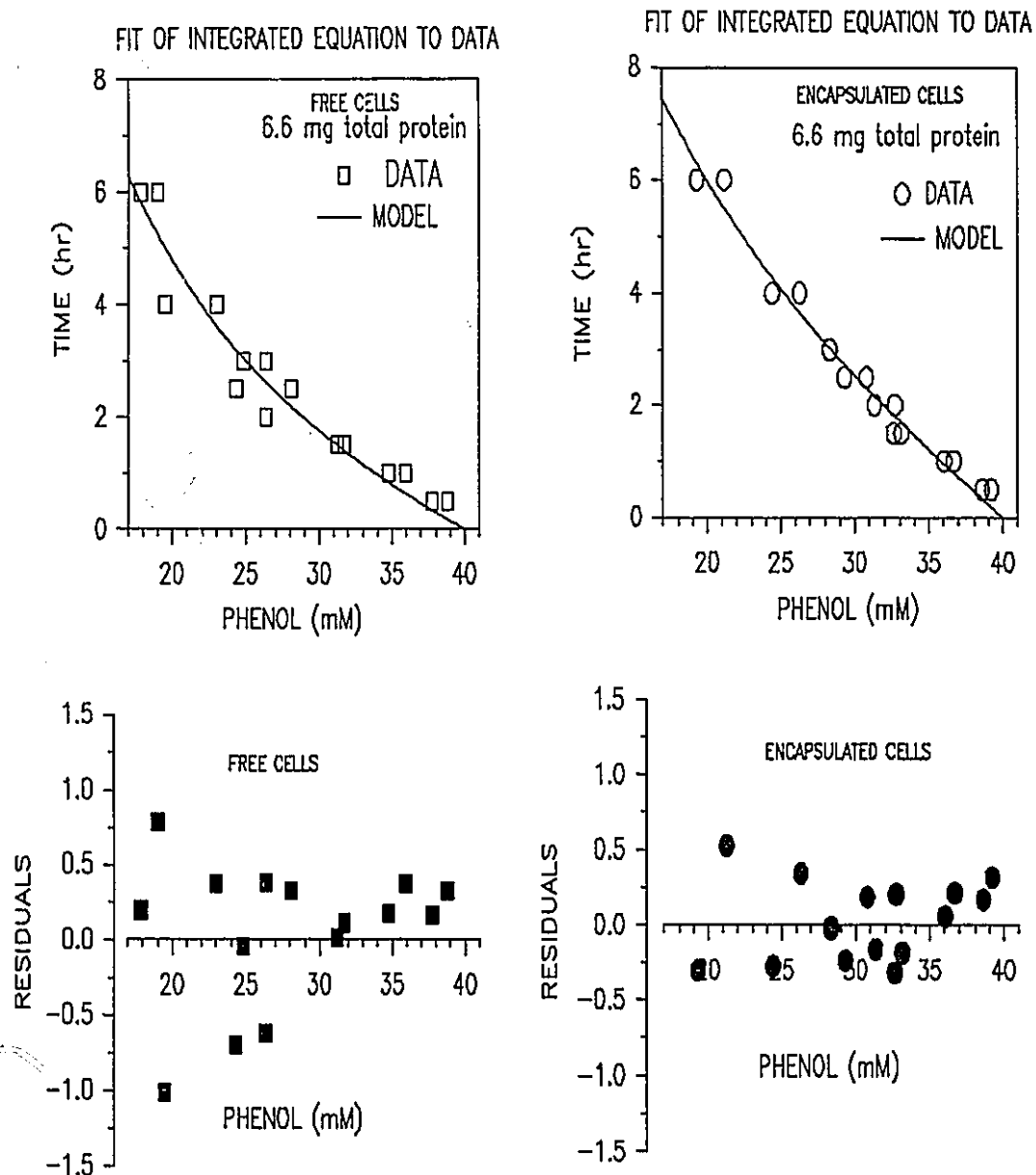


Figure 51. Plots showing the fit of the integrated equation (4.20) to data for the conversion of ammonia, pyruvate and phenol to tyrosine by whole cells (6.6 mg total cell protein).

4.6 GENERAL DISCUSSION

*"What are the roots that clutch, what branches grow
Out of this stony rubbish?"*

T. S. Elliot

4.6.1. Significance of Microencapsulation-Technique Results.

The results show that there is significant depolymerization of alginate during the heat sterilization of its solutions. These results are supported by the work of Leo *et al* (166), who showed that the viscosity of alginate solutions decrease with increasing temperature. The reduction in solution viscosity was attributed to the depolymerization of the alginate. However the change in molecular weight of the alginate as a function of time during sterilization was not reported by the authors.

If the degree of polymerization of the alginate is too low, the properties of the gel beads are affected. Indeed, below a certain critical molecular weight alginate solutions cannot form gels (167, 168). The trend in alginate bead preparation is to use low molecular weight alginates because they can be sterilized by filtration through a 0.2 μm filter (167). Solutions of high molecular weight alginates cannot be readily filter sterilized because of their high viscosity. Since alginates are depolymerised by heat, heat sterilization of alginates does not seem popular.

The results obtained in the present study show that a high molecular weight alginate can be adequately heat-sterilized and still have a molecular weight that is high enough to gel well. If the alginate beads are of good quality then it is likely that the polylysine (PLL) coat will be more even and the eventual microcapsules will be better able to maintain their integrity under shear.

The molecular weight of Kelco-Gel® L.V. alginate is about 50,000 Daltons according to the supplier, this value agrees with that obtained in this study. Microcapsules made with alginate of this molecular weight do not withstand shear as well as those made with a higher molecular weight alginate. Thus microcap-

sules made with Kelco-Gel® L.V. alginate may be suitable for implantation, however they are less suitable for use in bioreactors in which vigorous stirring is required.

There are correlations that describe the diameter of alginate beads produced by 2 fluid atomizers (169, 170). However these correlations are not directly applicable to microcapsule data. They are best at predicting the diameter of alginate droplets as they leave the droplet-former or atomizer. The final size of the microcapsule is also related to the initial shrinking during the gelling process and a final swelling after the liquefaction of the core.

The more important result of the effect of airflow on the quality of the microcapsules experiments, is the fact that as the airflow is increased the microcapsule size distribution becomes more bimodal and many of the microcapsules become empty. This suggests that the range of airflows that are suitable for microcapsule preparation is quite narrow.

The strength of the microcapsules increased when the PLL reaction time was increased. The longer polylysine reaction time probably allows more time for the diffusion of the PLL into the surface of the gel beads. This would provide a membrane with more PLL-alginate crosslinks. This is consistent with the results of Goosen (128), who showed that microcapsule membranes became more compact and less permeable as the PLL reaction time is increased or PLL molecular weight is reduced.

The entrapment of blue dextran 2000 ($MW\ 2.0 \times 10^6$) within the microcapsules proved to be a useful device. It allows the determination of the qualitative changes in the shear strength of the microcapsules with changes in alginate molecular weight or PLL reaction time. It also serves as a visual guide to the quality of the microcapsules. Damaged microcapsules made with Kelco-Gel® L.V. alginate were often observed as intact spheres. The only visual clue that these microcapsules were defective was the fact that they were not blue.

A rigorous analysis of the breakage of nylon microcapsules by shear in a turbine reactor has been done (171). A similar analysis was not applied to the data

in this study since the goal of the study is not to ascertain the exact breakage strength of the microcapsules.

4.6.2 Significance of Growth-Studies Results.

Certain characteristics of cells such as the permeability vary with the stage of growth of the cells (172), therefore if cells of reasonably constant properties are to be used the effect of basic variables such as agitation and temperature should be assessed.

The agitation partially controls the amount of oxygen available to the cell. High agitation rates will reduce the Nernst layer around the cells allowing more rapid transport of oxygen into the cells. High agitation can also cause the entrainment of air within the medium, and this will markedly increase the surface area for oxygen transport from the air into the medium. The results show that increasing the available oxygen in the medium by increasing the rate of agitation did not inhibit the growth of *E. herbicola*.

At 37 °C the cells grow up rapidly and then die. Therefore temperatures above 37 °C are not really suitable for the growth of *E. herbicola*. The results in this study show that temperatures from 22 °C to 32 °C are the most suitable for the growth of *E. herbicola*. This conclusion was also reported by Enei *et al* (77).

The data indicate that the decision to grow the cells at 32 °C and 180 rpm and then harvest after 24 hours of growth during TPL induction is probably a good one. Under these conditions the cells are well into the stationary phase, but not yet close to the death phase. The batch to batch variations could therefore be much less pronounced under these circumstances. However the slow increase in TPL activity (per mg of protein) during this period suggests that if a pure cell free enzyme was desired better yields of TPL would be obtained if growth was prolonged until 36 hours.

4.6.3 Significance of the Exploratory Kinetic Studies.

4.6.3a Activity Versus Total Cell Protein in the Assay Profile

The TPL activity versus the total amount cells in the assay indicates that the specific activity of whole cell TPL decreases with increasing amounts of total cell protein (Figure 34). This is symptomatic of the presence of endogenous inhibitor(s) in the whole cell TPL system (173, 174). As the amount of cells in the system increases the concentration of the inhibitors also increase and so the apparent specific activity of the pertinent enzyme decreases.

The presence of endogenous inhibitors and effectors or activators in complex biological systems such as whole cells or partially purified enzyme systems is a common phenomena (173, 174). Although the results show that there is at least one endogenous inhibitor in the whole cell TPL system, it does not preclude the possibility of several inhibitors and possibly some effectors.

The tyrosine degradative reaction is known to be inhibited by phenolic compounds and amino acids such as phenylalanine, alanine and serine (78, 86, 88). The amino acids are all likely to be present in the whole cell system, since they are such common metabolites in the cell.

The addition of ammonium ions to a whole cell TPL system increased the yield of L-dopa from serine and pyrocatechol (82). Ammonia is an important metabolite in the cell and so sufficient quantities of it could remain in the system for it to exercise an effect as an endogenous effector.

4.6.3 (b) Significance of the Results Obtained During the External Addition of PLP.

If PLP is added to the whole cell TPL system there is a reduction in the activity of the system. This indicates that the cells have accumulated sufficient PLP, hence adding extra amounts could be inhibitory. There would then be no advantage in adding PLP to a whole cell TPL system.

This conclusion is consistent with the observation of Enei *et al* (82), who reported that the addition of pyridoxine, pyridoxal and pyridoxal phosphate (PLP)

to a whole cell system for the production of L-dopa from serine and pyrocatechol only marginally increased the yield.

4.6.3c. Significance of the Initial Rate Data for the Kinetics of Tyrosine Degradation by Whole Cell TPL of *E. herbicola*.

".... if there is anything that the enzymologist has learned, it is that enzymes are more complex than one might expect..."

-Kenneth E. Neet.

4.6.3c (i) Background to the Initial Rate Experiments Conducted.

The production of tyrosine by Tyrosine Phenol-Lyase (TPL) from ammonia, pyruvate and phenol is an ordered ter-uni reaction. One of the concerns of a project of this type is the characterization of the system such that the effects of microencapsulation on the properties of free cells can be determined. The most straight-forward way of doing this is to evaluate the apparent K_M and V_{max} of the degradative reaction since the analysis of the one substrate reaction would be simpler. There is also information in the literature on the degradative reaction with the free TPL and this allows some comparisons to be made with the work of other groups.

Preliminary results obtained on the degradative reaction of TPL suggested that the apparent K_M of the whole cell TPL system was a function of the amount of cells in the assay. This situation is often encountered in the analysis of biological systems which contain whole cells or partially purified enzyme rather than ideal "purified enzymes" (172), and is usually indicative of the presence of endogenous modifiers (173).

In a Michaelis-Menten system in which endogenous modifiers are present, the true K_M can be estimated by determining the apparent K_M at low concentrations of enzyme protein and then extrapolating to the value of K_M at zero concentration of protein (173). Therefore once it was established that there were endogenous

modifiers in the system, velocity versus substrate profiles were obtained with low amounts of cells in the assay. (The reliability of the accurate detection of product phenol places a limit on how small the amount of cells in the assay can be.) However these detailed velocity versus substrate profiles revealed clearly that the whole cell TPL system was not truly Michaelis-Menten.

The analysis of TPL data with the assumption that it truly displays Michaelis-Menten kinetics has been done by Brot, Smit and Weisbach (76) and the group of Kumagai and Yamada (78, 86, 88). The results in this study challenge the Michaelis-Menten assumption.

A close reexamination of the data of these workers indicate that their original published data showed deviations from Michaelis-Menten behaviour. In Figure 52 the original data of Brot *et al* is presented. The data point at 5.0 mM tyrosine has been included in the profiles because it was present in the original data, but the solubility of tyrosine in an aqueous system is less than 5.0 mM under these conditions. The Lineweaver-Burk plot and the Scatchard plot of the data have been constructed and are also shown in Figure 52. The velocity versus substrate profile superficially appears to be Michaelis-Menten, and the Lineweaver-Burk plot seems linear except for the points at high tyrosine concentration. The Hanes plot indicates that at high values of substrate there is some deviation from linearity and thus from Michaelis-Menten behaviour. The Scatchard plot of the data however, indicates systematic deviations from Michaelis-Menten kinetics both at low velocities and at higher velocities.

A region of downward concavity in the Scatchard plot reveals that the rate is higher than would be predicted by the hyperbolic velocity versus substrate profile of a Michaelis-Menten system (95, 96, 175). There is also some evidence of negative cooperativity at high velocities, but there are not enough data points to definitely confirm this trend. Thus while the present study is the first to report that there is mixed cooperativity in the TPL system, a more detailed analysis of the early work of Brot would have revealed the non-Michaelis-Menten nature of the TPL system.

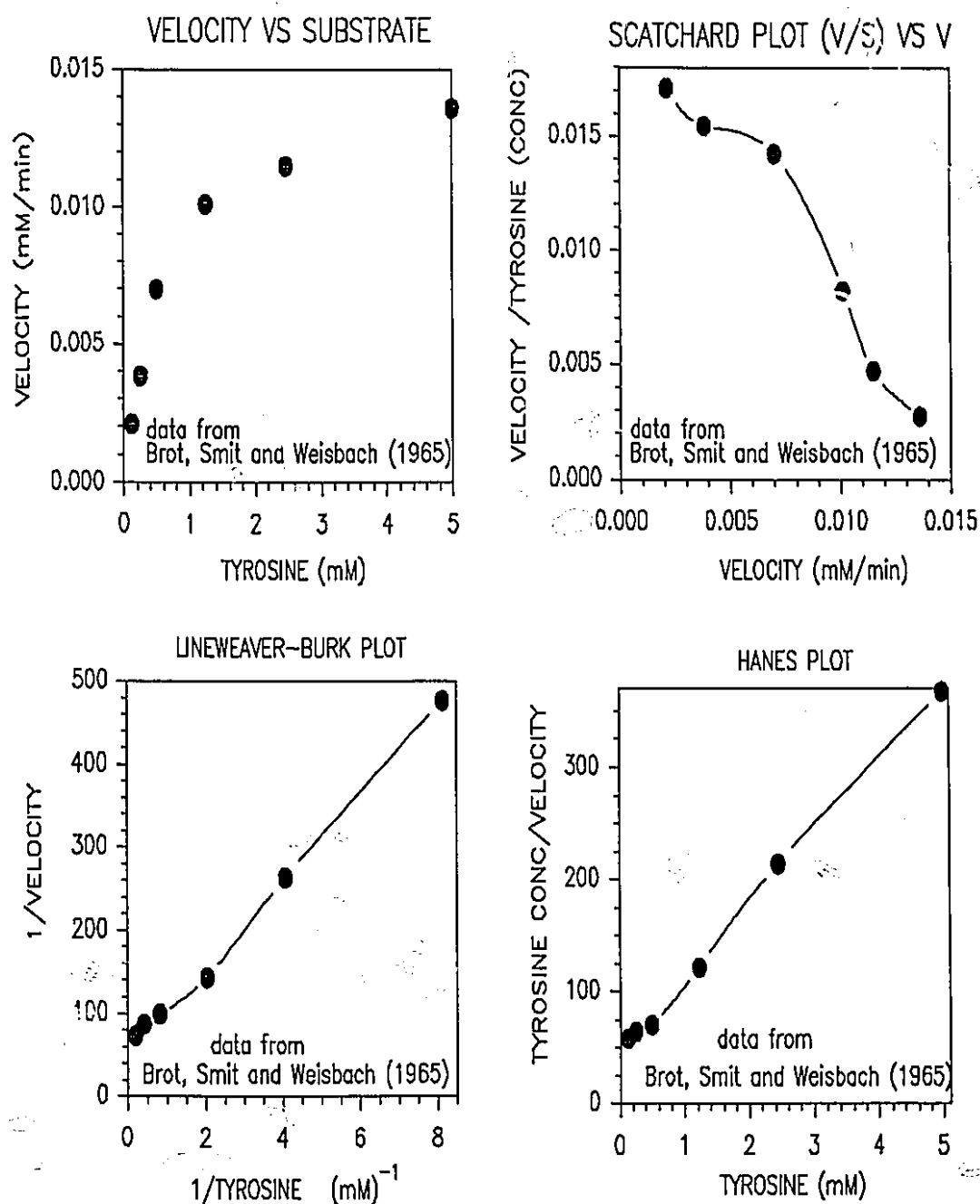


Figure 52. Replot of the data from Brot (1965) showing deviations from Michaelis-Menten behaviour. N.B. the curve of the Scatchard plot.

The data of Kumagai and Yamada for cell free TPL crystallized from *E. herbicola* protein is shown in Figure 53. In the original paper (88), only the Lineweaver-Burk plot of the data was shown. In Figure 53 the velocity versus substrate profile, the Scatchard plot and the Hanes plot of the data have been constructed. This data also shows definite curvature in the Scatchard plot, and indeed the velocity versus substrate profile does not indicate the hyperbolic rise expected from the Michaelis-Menten equation. The Hanes plot also reveals that the data is more likely to fit a curve, rather than the expected linear behaviour of a Michaelis-Menten system.

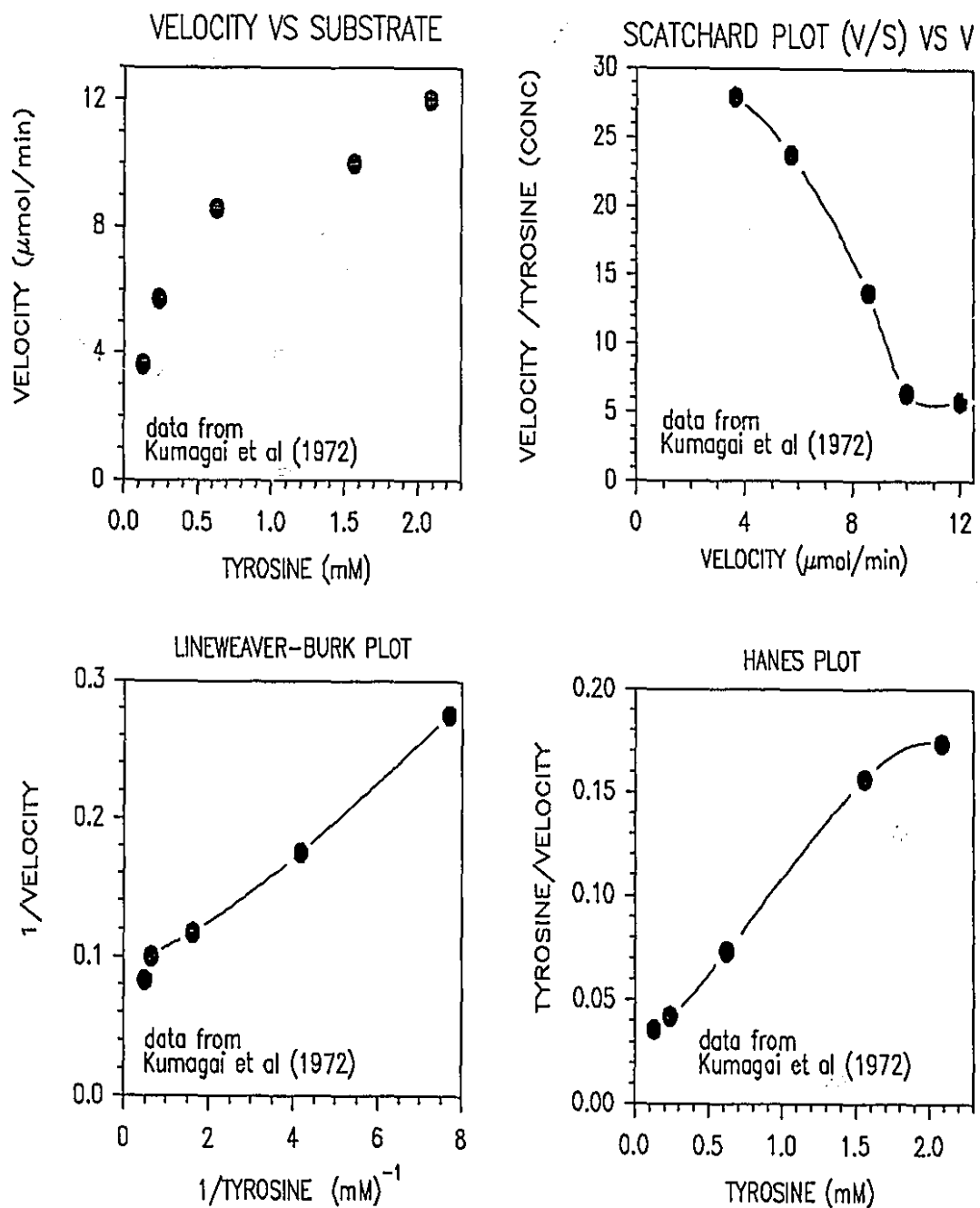


Figure 53. Replot of the data of Kumagai and Yamada (88) for cell free TPL. Note the curvature of the Scatchard plot.

The Eadie plot (155) which is the inverse of the Scatchard plot (156) has been shown to be the best plot for the detection of deviations from Michaelis-Menten behaviour (176, 177). The Scatchard rather than the Eadie plot of the data was presented since the Scatchard plot seems to be more popular and it mirrors the curvature of the Eadie plot.

The Lineweaver-Burk plot does not reliably detect deviations from Michaelis-Menten behaviour, nor does it reliably estimate V_{\max} and K_M (177). The Hanes plot is best for the estimation of V_{\max} and K_M but it does not highlight deviations from Michaelis-Menten behaviour (177).

It seems then, that the data obtained for TPL in this study is not truly at variance with the previous published studies on cell free TPL. The above reanalysis of the data in the literature indicate that an injudicious choice of substrate concentrations in these early studies (76, 88) obscured the complexity of the TPL system. Perhaps pronounced "bumps" or an intermediary plateau in the profiles would have occurred if they contained more data points.

Teipel and Koshland (162) have remarked on the fact that "bumpy curves would most likely have been dismissed in the past due to the large number of closely spaced points required to verify such curves and due to the tendency to average out such bumps assuming that they reflect experimental error".

4.6.3c (ii) Significance of the Initial Rate Data for the Degradation of Tyrosine.

"Every simplification is an over simplification."

-Alfred North Whitehead

"...God sets us nothing but riddles.."

-Fyodor Dostoyevski

The nonlinearity of Eadie plots of the initial rate kinetic data obtained in this study (Figures 39 and 42) for the degradation of tyrosine show that the system is non-Michaelis-Menten. If the velocity versus substrate profile of an enzyme has an intermediary plateau, the degree of the equation describing the kinetic mechanism must be of at least 3 (162, 178). If there is an initial sigmoidal rise followed then an intermediary plateau then the degree of the equation describing the mechanism must be at least four (178).

The Hill coefficient (n_H) in the whole cell TPL can be as high as 2 depending on the batch of the cells and the amount of cells in the system. These values imply that the degree of the kinetic mechanism is at least 3 since the number of subunits (n) or the degree of the steady state mechanism (z) must be greater than n_H (96, 175, 177).

The values obtained for the Hill coefficients and the general shape of the velocity versus substrate profiles indicate that the degree of the kinetic equation which describes the mechanism of TPL is at least 3.

Until 1991 the information that was available on the structure of TPL indicated that it was a dimer (73, 78, 86, 87, 88). If a quasi-equilibrium or rapid equilibrium analysis is applied to a dimer the degree of the equation of the mechanism cannot be greater than the number of binding sites for substrate. Therefore it was difficult to reconcile the complexity of the velocity versus substrate profiles with the structure of the enzyme.

One of the approaches that was used in an attempt to reconcile the data with the reported structure of TPL was to consider that there was an endogenous inhibitor interacting with the enzyme. If the binding or dissociation of an inhibitor is not rapid relative to the product forming steps then the rapid equilibrium or

Michaelis-Menten assumptions would not be valid. In this case the more rigorous steady state approximation (93, 164, 177, 179) would have to be applied.

The degree (in S substrate) of the kinetic equation which describes a steady state system is equal to the number of species which can react with S (180). Therefore a dimeric enzyme E with 2 sites for substrate in the presence of a competitive inhibitor I, could have E, ES, and EI react with S to form ES, ES₂ and EIS respectively. This system would then produce a mechanism described by an equation of degree 3 in the concentration of S. Since the E, EI, and ES could also react with I to form EI, EI₂ and ESI respectively, the equations would also be of degree 3 in the concentration of I. The solution of steady state systems are usually very difficult if more than 4 or 5 enzyme forms are present in the system (164, 177, 179).

The individual rate constant for each association and dissociation of substrate and inhibitor from the enzyme, plus the rate constants of product formation are parameters of the equation. Hence, in general steady state systems have a large number of parameters. Ricard *et al* has shown that by using the structural rate concept of enzyme kinetics (93, 181, 182, 183), the steady state equation describing the kinetics of polymeric enzymes can be simplified. The rate constants in polymeric enzymes are related to that of the "intrinsic process" which would occur if the enzyme subunit were isolated, and the subunit interactions which occur because in fact the subunits are not isolated. This approach reduces the number of parameters in a steady state mechanism. It also explains rigorously for the first time, by thermodynamic principles, why so many polymeric enzymes may display Michaelis-Menten kinetics, when in fact there is no a-priori reason why quasi equilibrium principles should apply (93, 182, 183).

The structural rate equations for the interaction of a dimeric enzyme with both substrate and an inhibitor have been developed by Ricard *et al* (183). These equations successfully described the behaviour of phenylalanine ammonia-lyase in the presence of various inhibitors (183). However when these equations were applied to the data obtained with TPL in this study, they did not fit the data well.

These equations have not been presented, but they are readily available in the literature (183), nor were the values obtained for the parameters of the fit discussed in the Results section. Indeed these equations were only used because it was reported that TPL was a dimer, hence they represent the only way in which the complex velocity substrate profiles obtained with whole cell TPL could be generated. Recent reports however suggest that this view is erroneous, and that TPL is likely to be a tetramer (89, 90, 91).

Oligomeric enzymes with 4 or more subunits, each with a binding site for substrate, may have velocity versus substrate profiles with an intermediary plateau. Notable examples of such enzymes are cytidine triphosphate (CTP) synthetase (184), phosphoenolpyruvate carboxylase (185) and glutamate dehydrogenase (GDH) (186).

Cytidine triphosphate synthetase catalyses the formation of CTP from UTP, ATP and glutamine. The reaction velocity versus glutamine concentration appears like 2 "stair-steps" when the concentration of the effector GTP is low. The region of the second stair-step becomes more hyperbolic at moderate concentrations of GTP. The region of the first stair-step also becomes more hyperbolic when the concentration of GTP is high. If the concentration of GTP is high enough the profile can appear to be Michaelis-Menten.

The behaviour of CTP synthetase and other enzymes shows clearly that the complex velocity versus substrate profiles displayed by whole cell TPL are not without precedent. The variation in the profiles observed in the whole cell TPL system, when the amount of cells in the system increase, probably reflects the effects of endogenous modifiers on TPL.

Ricard has reminded us that, "evolution occupies a key position in biology in the sense that any important problem may be considered in an evolutionary perspective" (93). We can then wonder, what would be the neo-Darwinian logic for the bacteria to have its TPL displaying mixed cooperativity in its kinetics?

Tyrosine phenol-lyase apparently evolved in some *Enterobacteria* to enable them to survive in conditions where tyrosine is the sole carbon source (86). The

enzyme serves this role by lysing phenol from tyrosine. The phenol can then be metabolised into other carbon compounds that the cells might require. Phenol is toxic to cells, therefore once TPL has been induced and if high concentrations of tyrosine are present the cell could kill itself. It is known that the cell growth and the induction of TPL are reduced if phenol is added during the growth of *Erwinia herbicola* and *Escherichia coli* (187).

It would therefore be of considerable survival value to the bacteria if the kinetics of TPL could display an intermediary plateau. This would mean that if the tyrosine concentration is low the rate of phenol production would be high enough to produce meaningful amounts of phenol. However if the tyrosine concentration was high the rate of phenol production would plateau, rather than being so high that the cells would produce enough phenol to inhibit their growth. It seems then that there is an evolutionary logic behind TPL exhibiting complicated kinetics.

The Adair equation for an enzyme with 4 or more subunits can fit mixed cooperativity data if the intrinsic binding constants (K_i') vary appropriately. For example binding constants which vary such that $K_1' < K_2' > K_3' < K_4'$ implies that:

- 1) the binding of the first substrate molecule induces conformational changes in the subunits with available active sites such that their average affinity for substrate increases;
- 2) the binding of the second substrate molecule induces conformational changes in the remaining subunits with available active sites such that their average affinity for substrate decreases; and
- 3) the binding of the third substrate molecule induces conformational changes in the remaining subunits such that their average affinity for substrate increases.

If the differences in the magnitude of the K_i' are substantial enough the velocity versus substrate profile could have an initial sigmoidal rise followed by an intermediary plateau, followed by a hyperbolic or sigmoidal rise.

The Adair equation was not able to fit the data obtained for the degradation of tyrosine with whole cell TPL. However this equation is not always able to fit data

which reflect mixed cooperativity; since it was able to fit the data of CTP synthetase and glutamate dehydrogenase, but not that of phosphoenol pyruvate decarboxylase. It has already been mentioned above that these enzymes have kinetic profiles with at least one intermediary plateau (162, 184, 185, 186).

The derivation of the Adair equation assumes that the system is at quasi-equilibrium, *i.e.* that the rate determining step is the rate of product formation. However if there are slow conformational changes or other transitions in the system, quasi-equilibrium cannot be assumed and the equation would be invalid. Slow conformational changes have been observed in enzyme systems (188, 189).

The general concerted allosteric model of Monod (94) and the interaction model of Koshland, Nemethy and Filmer (KNF) (163) can be shown to be equivalent to particular cases of the Adair equation when there are constraints on the values of K'_i (180, 96). For example the Monod model is consistent with a rapid equilibrium situation such that $K'_1 < K'_2 \dots < K'_i < K'_{i+1} \dots < K'_n$. Thus the inability of the Adair equation to fit the data implies that neither the Monod model nor the KNF model will fit the data. A reanalysis of the data in the literature on the kinetics of cell free TPL indicate that the kinetics of TPL is quite complicated; hence the appropriate assumptions required to build a valid kinetic model probably requires a detailed analysis of the cell free TPL.

The presence of endogenous inhibitors and the possible presence of an endogenous effector such as ammonia in the whole cell TPL system has been discussed previously. One possible effect of an effector on an enzyme would be to bind to the enzyme and force the subunits to all occupy the same conformation. This would then simplify the kinetics of the enzyme, because in that situation the affinity of the active sites for substrate would be a constant, regardless of the number of sites that were already occupied by substrate. The enzyme could then display Michaelis-Menten behaviour if there are saturating concentrations of the effector.

If there is an endogenous effector in the whole cell TPL system, as the amount of cells in the assay increases the amount of the endogenous effector

would likewise increase. The degree of cooperativity shown by TPL would then vary with the amount of cells in the assay. If the concentration of the effector reaches that required for saturation; the behaviour of the whole cell TPL system could then approximate Michaelis-Menten behaviour. This saturating condition could occur as the amount of cells in the assay increases; since the concentration of the effector would be proportional to the amount of cells. The results obtained in this study supports the idea that as the amount of cells in the assay increases the system becomes somewhat more Michaelis-Menten. Indeed at low protein concentrations the Michaelis-Menten parameters may not be significant but as the amount of cells in the assay was increased they become more so.

Kumagai used the data that was discussed in Figure 55 to calculate the K_M of tyrosine with "purified" cell free TPL as 0.278 mM (88). In the exploratory kinetic studies, when the amount of cells present in the assay, as measured by total cell protein, was 3.267, 4.086 and 4.904 mg the apparent K_M was 0.28, 0.25, and 0.39 mM respectively. These apparent K_M values are for the situation in which the Eadie plots were most linear and their average is 0.277 mM. The similarity of this average value to that obtained by Kumagai suggest that the transport system for tyrosine is still intact in these cells, and so there is perhaps little resistance to tyrosine transport across the cell membrane. There are endogenous modifiers in the whole cell system, hence it is only a coincidence that the value obtained for the K_M of the cell free enzyme is so close to the apparent K_M for the whole cell enzyme. The apparent K_M for another batch of cells would be somewhat different, depending on the amount of endogenous modifiers, whether inhibitor or effector, and the amount of cells in the assay.

The above discussion suggests that the kinetics displayed by tyrosine phenol-lyase is consistent with it being a tetrameric enzyme since the velocity versus substrate profiles indicate a high degree of complexity. If the published data on TPL is more thoroughly analyzed, it is clear that even the cell free purified enzyme displays cooperativity in its kinetics. Thus the cooperativity in the kinetics of the whole cell enzyme may be modulated by the presence of endogenous

modifiers, but it is not caused by them. The complex behaviour displayed by TPL however is not unlike that of other well known enzymes in the literature. Further when it is considered that a product of the TPL reaction is phenol, there are good evolutionary reasons why the enzyme would display mixed cooperativity in its kinetics.

4.6.4. Significance of the Comparative Studies on the TPL Activity of Free and Microencapsulated Whole Cell *E. herbicola*.

4.6.4 (a). Comparative Study of TPL Activity for Free and Microencapsulated Cells.

Microencapsulated *E. herbicola* did not exhibit TPL activity unless the microcapsules were stirred vigorously. A shake rate of 240 rpm was required before the TPL activity of microencapsulated cells approached that of the free cells.

A high stir rate was shown to be desirable in the determination of the TPL activity of free cells (109). Therefore the resistances to mass transfer observed with the microencapsulated cells are due to:

- 1) the "Nernst" or unstirred layer surrounding the microcapsules;
- 2) the finite permeability of the microcapsule membrane;
- 3) the "Nernst" or unstirred layer surrounding the cells; and
- 4) the finite permeability of the cell membrane.

The Nernst layer surrounding the microcapsules can be reduced by vigorous stirring. The permeability of the alginate-polylysine-alginate membrane of the microcapsule is high for small hydrophilic molecules, since the membrane can be considered to be a hydrogel (126, 127). The Nernst layer around the cells within the microcapsule would not be significant if it is assumed that the contents of the microcapsules are well mixed. Since in bacteria there is a transport system for tyrosine (69), the cell membrane is not likely to offer significant resistance to tyrosine. This discussion suggests that the bulk of the resistance to the mass

transfer would be due to the Nernst layer surrounding the microcapsule; hence with vigorous stirring this resistance can be minimised.

The fact that the apparent K_M , (assuming that TPL system was approximating Michaelis - Menten behaviour), was 0.8 mM for encapsulated cells and 0.2 mM for free cells from the same batch, suggest that there is still some resistance to mass transfer in the TPL system. However since the microcapsules are washed repeatedly during the process of making them, the higher K_M for the encapsulated cells could also be due to some endogenous effectors being washed from the system. Hence it is not clear whether all of the increase in the K_M of encapsulated cells relative to that of free cells can be attributed to mass transfer effects.

If the difference in the apparent K_M values for free and encapsulated cells are due to kinetic effects related to the loss of endogenous effectors the addition of ammonium ions or some other effector would lead to a reduction in K_M . The effect of ammonium addition on the initial rate kinetics of tyrosine degradation by whole cell TPL was not done, but this could prove to be a worthwhile experiment.

4.6.4(b). Significance of the Results Obtained in the Comparative Study for the Production of Tyrosine and Dopa.

The apparent K_M for the substrates of an enzyme are usually much higher for whole cell enzyme than for free enzyme. This is due to the presence of the cell membrane which can offer significant resistances to the transport of substrates and products to and from the cell. Permeabilization of the cell wall by toluene treatment or freezing and thawing are among the methods employed to facilitate the movement of substrates and cofactors across the cell membrane (190). It would therefore be interesting to compare the values obtained for the apparent K_M of the substrates of TPL for the whole cell enzyme, whether free or microencapsulated, to those for the cell free enzyme. The values obtained for the cell free enzyme by Kumagai (88) are not reliable, since the fact that there was cooperativity in the TPL system was not considered. Notwithstanding this fact they

will be used as the basis of comparison of whole cell enzyme to cell free enzyme since there are no other values available.

The similarity of the apparent K_M of tyrosine for both free enzyme and whole cell enzyme has already been discussed. In the production of tyrosine with 1.6 mg of whole cell *E. herbicola* protein (Table XVI), the value obtained for the apparent K_M of tyrosine was 0.18 mM. This value is less than the 0.277 mM obtained in the initial rate studies, and underlines the fact that there can be batch to batch variation in the apparent K_M because of the presence of endogenous inhibitors or effectors in the system.

The apparent K_M for phenol of cell free TPL enzyme is 1.1 mM (88). The values in Table XVI for whole cell enzyme are about 0.5 mM. The similarity between the whole cell enzyme and the free TPL enzyme is probably due to the fact that the rate of stirring was high. This helps to reduce the resistance to mass transport. Phenol is also lipid soluble and so it would travel rapidly through the lipid membrane of the cell (191).

The K_M for ammonia and pyruvate for free TPL is 20 and 12 mM respectively (88). The results of this study indicate values for K_M NH_3 that are much closer to 100 mM, hence the large values of $K_A K_B$, the apparent K_M of the TPL- NH_3 -Pyruvate complex. The ammonium ion and pyruvate are charged and so they will not readily cross the cell membrane. It is therefore reasonable that the apparent K_M for ammonia and pyruvate will be higher for whole cells than for free enzyme.

The value of V_{\max} obtained by the kinetic analysis of the production data at 6.6 mg of protein is twice what it is at 1.6 mg of protein (Table XVI). This shows that the specific activity is less at higher concentrations of protein. This conclusion is consistent with the activity versus total protein profile (Figure 34). However in that profile there was no information about the simultaneous change in K_M and V_{\max} .

If the specific activity decreases as the amount of protein increases there is an endogenous inhibitor in the system (173, 174). This means that the value of certain kinetic parameters obtained in an analysis could be a function of the

amount of whole cells present in the system. For Michaelis-Menten or rapid equilibrium type systems the effects of inhibitors are easily determined. A competitive inhibitor in the system will result in an apparent K_M that is higher than the true K_M , however the V_{max} will be unchanged. The presence of an uncompetitive inhibitor will result in an apparently lower value for V_{max} . A mixed type inhibitor increases K_M and may lower V_{max} (174). The fact that V_{max} per mg of protein is less at higher concentrations imply that uncompetitive inhibitor(s) are present in the whole cell TPL system.

Some of the inhibitors of TPL were discussed previously; for example phenylalanine and alanine are competitive inhibitors and phenol, resorcinol and pyrocatechol are mixed type inhibitors (78, 88). However no specific uncompetitive inhibitors of TPL have been described. *In-vivo* there are likely to be several inhibitors with varying mechanisms of inhibition; since this type of control of enzyme activity using the effects of a variety of inhibitors is known (192).

The cell free purified TPL enzyme is inhibited strongly by phenol (86, 88). These results show limited inhibition of whole cell TPL at the phenol concentrations present in these experiment (i.e. at concentrations less than 50 mM). A similar result was obtained by Para *et al* (107). This maybe due to the fact that the whole cell enzyme is stabilized in a conformation with a lower affinity for phenol by the high concentration of protein in the cell. Some the endogenous inhibitors in the cell may also be occupying the inhibitory site that would normally bind phenol. Such competition for the inhibitory site would increase the apparent value for K_i .

The similarity of the kinetic parameters for both free and microencapsulated cells imply that the reaction is kinetically controlled even for the microencapsulated cells; therefore the stir rate of 240 rpm is adequate. Therefore the hypothesis that the presence of ammonium ions in the assay would reduce the K_M of microencapsulated system is supported by this fact. It should also be noted that if ammonium ions are serving as an activator it would make the system more Michaelis-Menten, since it could lock the subunits into one particular conformation.

If this is the case the subunit effects would not manifest themselves as much and thus the model used for the estimation of the parameters would be more justified.

The parameters of the kinetic model of TPL were evaluated by using the integrated equation of the ter-uni mechanism for the conditions in this study. The use of the integrated form of the Michaelis-Menten equation is well established (193, 194, 195, 196); however the necessary algebra can be formidable for more complex systems and thus the method is not as widely used as it should be (197). The use of the integrated equation of the mechanism to analyse the kinetics of whole cell TPL is desirable since time dependent changes in the cells due to the permeabilization of the cells by phenol, or the effect of shear, could show up in a study where the reaction is followed for a long time. In a short term initial rate study such effects may not be discernible.

Less L-dopa is produced relative to the tyrosine when the same concentration of substrates *et cetera* are used. Enei (83) showed that L-dopa and pyruvate can react to form addition compounds. The formation of these compounds would deplete the net amount of L-dopa produced when the pyruvate concentration is high. High temperatures also increase the rate of the reaction to form undesired by products. Aqueous solutions of dopa and catechol are oxidised upon exposure to light. It is also known that TPL is inhibited by phenolic compounds. It is likely then that there could be substrate inhibition and decomposition of the L-dopa produced by light. Our results with microencapsulated cells (Table XV) showed that decreasing the catechol concentration from 40 to 10 mM did increase the amount of L-dopa produced. This suggests that the degree of substrate inhibition by catechol is severe relative to that due to phenol. If the reaction was conducted in the dark less L-dopa was produced. This probably means that in the light catechol is decomposed rapidly. This decomposition reduces the amount of catechol available to inhibit the reaction. If the concentration of catechol is high sufficient catechol can remain to inhibit the reaction and so the advantage in conducting the reaction in the light is lost at higher concentrations of L-dopa. This result shows that low concentrations of catechol are desirable in the production of L-dopa from

ammonia, pyruvate and catechol.

If microencapsulated cells are used for the production of L-tyrosine or L-dopa the behaviour of free and encapsulated cells are the same if the stir speed is adequate and the concentration of substrates are high. If the reaction is prolonged the free cells may no longer perform as well. It seems that free cells are broken down by prolonged stirring, hence microencapsulation protects the cells from shear. More data is required before a definitive statement on this point can be made.

The successful microencapsulation of the whole cell *E. herbicola* TPL activity offers another method for the removal of ammonia and phenol from the blood during liver failure. It also suggests another approach for the commercial production of tyrosine and L-dopa.

4.6.6. General Considerations and Suggestions for Further Work.

Tyrosine Phenol-lyase (TPL) is able to convert ammonia, phenol and pyruvate into tyrosine. This process can occur at 37 °C and at physiological pH (7.4) if the concentrations of ammonia, phenol and pyruvate are high enough.

In conditions such as liver failure where both phenol, ammonia and pyruvate are elevated in the blood, the microencapsulation of TPL activity offers a way of converting the toxic ammonia and phenol into the less toxic tyrosine. Further since tyrosine can be adsorbed by charcoal, charcoal haemoperfusion could be used to remove the tyrosine leading to a net removal of nitrogen from the blood. In kidney failure where urea concentrations are high, microencapsulated urease could be used to produce ammonia from the urea. Therefore by including an extra step the TPL system could also be used for the development of system for use in kidney failure.

Care has been taken to ensure that the microcapsules are able to maintain their integrity if they are shaken at 240 rpm. Extra vigilance is required in the use of bacteria for biomedical applications since the escape of viable cells into the blood could precipitate undesired consequences. Of course the cells could be

treated with an antibiotic such as chloramphenicol before their use. This antibiotic prevents cell growth without damaging the membranes of the cell, hence it is not difficult to keep the cells intact and in a resting state. This would reduce the chance of any escaped cells starting to proliferate in the biological fluid.

An alternative to the use of whole cell *E. herbicola* as the source of TPL would be to clone the TPL gene and insert it into a mammalian cell, using a retro-viral vector. If the mammalian cell is a fibroblast or an endothelial cell then it can divide in culture and so the new genetically engineered cell line can be maintained. Genetically engineered cells have found application in systems for drug delivery and in the treatment of some diseases due to inborn errors in metabolism (198, 199).

The use of a genetically engineered mammalian cells with TPL activity would increase the safety of a whole cell TPL enzyme system.

The analysis of the velocity versus substrate profiles for tyrosine degradation revealed that tyrosine phenol-lyase is not a simple Michaelis-Menten enzyme, but rather one that may display mixed cooperativity in its kinetics. Therefore a detailed study of the kinetics of the purified cell free enzyme should be done. There should also be an attempt to discover the most important endogenous modifiers in the whole cell TPL system, with this information the cells can then be grown or treated to produce the maximum possible specific activity. This would allow the use of smaller amounts of microcapsules for any desired application, and certain batch to batch variations in cell properties could probably be eliminated.

5.0 CONCLUSIONS

"The fact is the sweetest dream that labour knows".

-Robert Frost.

This project was undertaken to see whether the whole cell Tyrosine Phenol-lyase activity of *Erwinia herbicola* could be microencapsulated and used for the conversion of ammonia, phenol and pyruvate into tyrosine. This reaction is of relevance to the development of an alternative treatment for liver failure, since the microencapsulated cells could be incorporated in a device for the removal of ammonia and phenol from the blood during liver failure. The kinetics of the whole cell TPL was also examined so that the effects of microencapsulation could be better determined.

After reviewing the results obtained the following conclusions can be made:

- 1) The molecular weight of the alginate is a very important variable whose value affects significantly the final strength of the microcapsules; and so microcapsules made with heat sterilized Kelco-Gel® L.V. alginate cannot withstand shear as well as those made with heat sterilized Kelco-Gel® H.V. alginate.
- 2) If a high molecular weight alginate is not heat sterilised for much longer than the time required to kill all spores, it will have a degree of polymerization that is sufficient for it to form microcapsules of good quality with the capacity to withstand shear.
- 3) Increasing the polylysine reaction time results in an improvement of the shear strength of the microcapsules.
- 4) As the airflow to the droplet former is increased the frequency distribution of the microcapsule diameters become bimodal; and more importantly many of the microcapsules develop defects and are in fact empty.

- 5) Changes in the liquid flow to the droplet former does not change significantly the diameters of the microcapsules.
- 6) The entrapment of blue-dextran 2000 within microcapsules allows the visual assessment of the effects of process variables on the quality of the microcapsule.
- 7) The entrapment of blue-dextran 2000 also offers a rapid way to determine the relative ability of microcapsules to resist shear while variables such the molecular weight of the alginate or the polylysine reaction time used in their manufacture are varied.
- 8) The growth of *Erwinia herbicola* in nutrient broth is limited by the amount of oxygen available to the cells, but as the level of oxygen available is increased by increasing the agitation speed the growth rate plateaus.
- 9) The growth of *Erwinia herbicola* at temperatures from 22 °C to 32 °C is quite stable in that the cells grow up to the stationary phase and remain there for at least 10 hours. At 37 °C the cells grow rapidly but they also enter the death phase rapidly. There is only limited growth of *Erwinia herbicola* at 42 °C.
- 10) There are endogenous inhibitors and possible other modifiers in the whole cell tyrosine phenol lyase system; thus the specific activity observed is a function of the amount of cells present in the assay.
- 11) The external addition of excess pyridoxal phosphate to whole *Erwinia herbicola* cells can lower the TPL activity of the cells.
- 12) Tyrosine phenol-lyase displays mixed cooperativity in its kinetics; and the complexity of the cooperativity implies that it is at least a tetrameric enzyme.
- 13) Whole cells of *Erwinia herbicola* can be encapsulated within Alginate-PLL-alginate microcapsules, and the TPL activity of the cells used for the production of L-tyrosine or L-dihydroxyphenylalanine from ammonia, pyruvate and phenol or catechol respectively.

- 14) In the production of tyrosine from ammonia, phenol, and pyruvate an integrated equation of the ordered ter-uni mechanism can be used to estimate the kinetic parameters of the system. If the stir rate is adequate the kinetic parameters such as the apparent values of the K_M for tyrosine and phenol are equal for both free and microencapsulated cells.
- 15) Under those conditions where the whole cell TPL system is approximately Michaelis-Menten, the apparent K_M of tyrosine varies with the amount of whole cells in the system and the amount of endogenous modifiers present. However the apparent K_M typically ranges from 0.2 to 0.3 mM. This compares well with the value for cell free enzyme which is about 0.28 mM. The apparent K_M for phenol is 0.5 mM and this is similar to an apparent K_M of 1.0 mM for cell free enzyme. The apparent K_M for both pyruvate and ammonia are about 10 times higher for whole cells than it is for the cell free enzyme.

6.0 CLAIMS TO ORIGINALITY

In the attempt to prepare a micro-encapsulated whole cell tyrosine phenol-lyase enzyme with the ability to convert ammonia, phenol and pyruvate to tyrosine a number of original contributions were made. The chief of these were:

- 1) It was established for the first time, that tyrosine phenol-lyase (TPL) displays mixed cooperativity in its kinetics to such a degree that TPL is likely to be at least a tetrameric enzyme with 4 binding sites for substrate.
- 2) It was established for the first time, that the kinetics displayed by whole cell TPL can be affected by the amount of cells in the assay because of the presence of endogenous modifiers in the system.
- 3) It was established for the first time, that heat sterilized Kelco-Gel® high viscosity (H.V.) alginate can have a higher molecular weight than Kelco-Gel® low viscosity (L.V.) alginate. The use of the higher molecular weight alginate produces microcapsules which are much better able to resist shear.
- 4) For the first time, blue dextran 2000 was microencapsulated within alginate-PLL-alginate microcapsules, thus allowing the rapid assessment of the effect of variables such as PLL reaction time and alginate molecular weight on the relative strength of alginate-PLL-alginate microcapsules.
- 5) For the first time, the concept of using tyrosine phenol-lyase for the simultaneous detoxification of blood ammonia and phenol during liver failure was advanced.
- 6) For the first time, the effect of the agitation rate and temperature on the biomass versus time profiles of *E. herbicola* were determined.
- 7) For the first time, the tyrosine phenol-lyase activity of whole cells of *Erwinia herbicola* was microencapsulated. These microcapsules were

used for the conversion of ammonia, pyruvate and phenol or catechol into L-tyrosine or L-dihydroxy-phenylalanine.

- 8) For the first time the kinetic parameters of a model, which relates the tyrosine produced with time, have been evaluated. The parameters of the model compares well with the literature values obtained by other means.

7.0 REFERENCES

1. Jensen, David., *The Principles of Physiology*, Appleton-Century-Crofts, New York, (1976), pp 829-833
2. Wolpert, Enrique; Phillips, Sidney F.; Summerskill, W. H. J. "Transport of Urea and Ammonia Production in the Human Colon." *Lancet* (2):1387-1390 (1971).
3. Krebs, Hans A; Hems, Reginald; Lund, Patricia; Halliday, David; Read, Walter, W. C. "Sources of Ammonia for Mammalian Urea Synthesis." *Biochem. J.* **176**:733-737 (1978).
4. Geiger, Alexander. "Correlation of Brain Metabolism and Function by the Use of a Brain Perfusion Method *in-Situ*." *Physiological Reviews* **38**(1):1-20 (1958).
5. Bernuau, Jacques; Rueff, Bernard; Benhamou, Jean-Pierre. "Fulminant and Subfulminant Liver Failure: Definition and Causes." *Seminars in Liver Diseases* **6**(2):97-106 (1986).
6. Trey, Charles; Davidson, Charles S. "The Management of Fulminant Hepatic Failure." In : Popper, H; Schaffner, F. eds *Progress in Liver Diseases Vol 3*, Grune & Stratton, New York, pp 282-298 (1970)
7. Zieve, L. "Hepatic Encephalopathy." In: Schiff L, Schiff E. R. eds *Diseases of the Liver*, J. B. Lippincott Co., Philadelphia, pp 433-459 (1982).
8. Duffy, T. E.; Plum, F. "Hepatic Encephalopathy." In: Arias, I.; Popper, H; Schachter, D.; Shafritz, D. A. eds *The Liver: Biology and Pathobiology*, Raven Press, New York, pp 693-715 (1982).
9. Gimson, Alexander E. S.; O'Grady, John; Ede, Roland J.; Portmann, Bernard; Williams, Roger. "Late Onset Hepatic Failure: Clinical, Serological and Histological Features." *Hepatology* **6**(2):288-294 (1986).
10. Zieve, Leslie. "Metabolic Abnormalities in Hepatic Coma and Potential Toxins to be Removed." In: Williams, Roger and Murray-Lyon, Iain M eds

Artificial Liver Support, Pitman Medical Publ, Kent, pp 11-26 (1975).

11. Record, C. O.; Chase, R. A.; Curzon, G and Murray-Lyon, Iain M. "Amino Acids Changes in Hepatic Encephalopathy and Their Relationship to Disturbed Cerebral Neurotransmission." In: Williams, Roger and Murray-Lyon, Iain M eds *Artificial Liver Support*, Pitman Medical Publ, Kent, pp 27-30 (1975).
12. Shi, Z. Q.; Chang, T. M. S. "Amino Acid Disturbances in Experimental Hepatic Coma Rats." *Int J Artif Organs* 7:197-202 (1984).
13. Hughes, Robin; Williams, Roger. "Clinical Experience with Charcoal and Resin Haemoperfusion." *Seminars in Liver Disease* 6(2):164-173 (1986).
14. Chang, T. M. S.; Lister, C.; "Middle Molecules in Hepatic Coma and Uraemia." *Artif Organs* (suppl) 4:169-172 (1981).
15. Chang, T. M. S.; Migchelsen, M. "Characterization of Possible "Toxic" Metabolites in Uraemia and Hepatic Coma Based on the Clearance Spectrum for Larger Molecules by the ACAC Microcapsules Artificial Kidney." *Trans. Am. Soc. Artif. Intern. Organs* 19:314-319 (1973).
16. Zieve, L.; Doziaki, W. M.; Zieve, F. J. "Synergism Between Mercaptans and Ammonia or Fatty Acids in the Production of Coma: a Possible Role for Mercaptans in the Pathogenesis of Hepatic Coma." *J. Lab. Clin. Med.* 83:16-28 (1974).
17. Schafer, Daniel F.; Fowler, Jeffrey M.; Jones, E. Anthony. "Hepatic Encephalopathy and the γ -Aminobutyric-Acid Neurotransmitter System." *Lancet* (1):18-20 (1982).
18. Maddison, Jill E.; Dodd, Peter R.; Morrison, Murray; Johnston, Graham A. R.; Farrell, Geoffrey, C. "Plasma GABA, GABA-like Activity and the Brain GABA-Like Benzodiazepine Receptor Complex in Rats with Chronic Hepatic Encephalopathy." *Hepatology* 7(4):621-628 (1987).
19. Muting, D.; Perisoara A.; Baum, G.; Flasshoff, H. J.; Bucsis, L. "The Role of Protein Metabolism in 204 Liver Cirrhotics with and without Hepatic

- Encephalopathy II. Amino Acids, Free Phenols and Indoles." *Hepato-Gastroenterol* 33:66-70 (1986).
20. Chang, T.M.S. "Experimental Artificial Liver Support with Emphasis on Fulminant Hepatic Failure: Concepts and Review." *Seminars in Liver Disease* 6(2):148-158 (1986).
 21. Pappas, S. C.; Jones, E. A.; Schafer, D. F.; Berk, P. D. "Artificial Liver Support: Functional Requirements and Research Strategies for Future Development." In: Nose, Y.; Kjellstrand, C; Ivanovich, P.; *Progress in Artificial Organs - 1985*, ISAO Press, Cleveland, pp 721-725 (1986).
 22. Monaco, Anthony P.; Hallgrimsson, Jonas; McDermott, William V. "Multiple Adenoma (Hamartoma) of the Liver Treated by Subtotal (90 %) Resection: Morphological and Functional Studies of Regeneration." *Annals of Surgery* 150(4):513-519 (1964).
 23. Zieve, L.; Anderson, W. R.; Lindblad, S. "Course of Hepatic Regeneration After 80% to 90 % Resection of Normal Rat Liver." *J. Lab. Clin. Med.* 105:331-336 (1985).
 24. Chang, T.M.S. "Artificial Liver Support: Requirements and Approaches." *Intl. J. of Artif. Organs* 6(4):178-182 (1983).
 25. Yarmush, Martin L.; Dunn, James C. Y.; Tompkins, Ronald G.; "Assessment of Artificial Liver Support Technology." *Cell Transplantation* 1(5):323-341 (1992).
 26. Hoenig, Vojtech. "Management of Acute Liver Damage in Man." In: Popper, H; Schaffner, F. eds *Progress in Liver Diseases Vol 3*, Grune & Stratton, New York, pp 282-298 (1970).
 27. Redecker, Allan G.; Yamahiro, Harry S.; "Controlled Trial of Exchange-Transfusion Therapy in Fulminant Hepatitis." *Lancet* (1):3-6 (1973).
 28. Benhamou, J. P.; Rueff, B.; Sicot, C. "Severe Hepatic Failure: a Critical Study of Current Therapy." In: Orlandi, F., Zezequel, A. M. eds, *Liver and Drugs*, Academic Press, New York, pp 213-228 (1972).

29. Chang, T. M. S. "Haemoperfusion Over Microencapsulated Charcoal Adsorbent in a Patient with Hepatic Coma." *Lancet* (2):1371-1372 (1972).
30. Piskin, Erhan "Semipermeable Membranes Suitable for Haemoperfusion." In: Chang, T.M.S and Bing-Lin, He, eds, *Proceedings of the International Symposium on Haemoperfusion and Artificial Organs, Nov 20 to 22 (1983)*, China Academic Publishers, Bei-jing China (1984).
31. Gazzard, B. G.; Weston, M. J.; Murray-Lyon, I. M.; Flax, H.; Record, C. O.; Portmann, B.; Langley, P. G.; Dunlop, E. H.; Mellon, P. J.; Ward, M. B.; Williams, Roger. "Charcoal Haemoperfusion in the Treatment of Fulminant Hepatic Failure." (1974), *Lancet* (1):1301-1307 (1974).
32. Tabata, Y.; Chang, T. M. S.; "Comparison of Six Artificial Liver Support Regimes in Fulminant Hepatic Coma Rats." *Trans. Am. Soc. Artif. Intern. Organs* 26:394-399 (1980).
33. O'Grady; Gimson, A. E. S.; O'Brien, C. J.; Pucknell, A.; Hughes, R. D.; Williams, Roger; "Controlled Trials of Charcoal Haemoperfusion and Prognostic Factors in Fulminant Failure." *Gastroenterology* 94:1186-1192 (1988).
34. Zaki, A. E. O.; Wardle, E. N.; Canalese, J. et al "Potential Toxins of Acute Liver Failure and Their Effects on Blood-Brain Barrier Permeability." *Experientia* 39:988-991 (1983).
35. Zieve, Leslie; Shekleton, Michael; Lyftogt, Carolyn; Draves, Kay. "Ammonia, Octanoate and a Mercaptan Depress Regeneration of Normal Rat Liver Failure after Partial Hepatectomy." *Hepatology* 5(1):28-31 (1985).
36. Zeig, Steven and Friedmann, Eli A. "Potential for Oral Sorbent Treatment of Uraemia." In: Giordano, Carmelo ed, *Sorbents and Their Clinical Applications*, Pp 275-294 (1980).
37. Esposito, Renato and Giordano, Carmelo. "Polyaldehydes" In: Giordano, Carmelo ed, *Sorbents and Their Clinical Applications*, Pp 275-294 (1980).
38. Kjellstrand, Borges, H.; Pru, C.; Gardner, D. and Fink, D. "On the Clinical Use of Microencapsulated Zirconium Phosphate-Urease for the Treatment

- of Chronic Uraemia." In: Chang, T.M.S and Bing-Lin, He, eds, *Proceedings of the International Symposium on Haemoperfusion and Artificial Organs, Nov 20 to 22 (1983)*, China Academic Publishers, Bei-jing China (1984).
39. Zuidema, George D.; Cullen, David; Kowalczyk, Richard S. and Wolfman, Earl F. "Blood Ammonia Reduction by Potassium Exchange Resin." *Archives of Surgery* 87:296-300 (1963).
 40. Powers, Sue G.; Meister, Alton. "Urea Synthesis and Ammonia Metabolism." In: Arias, I.; Popper, H; Schachter, D.; Shafritz, D. A. eds *The Liver: Biology and Pathobiology*, Raven Press, New York, pp 251-263 (1982).
 41. Walser, Mackenzie. "Urea Metabolism: Regulation and Sources of In: Blackburn, George L.; Grant, John P; Young, Vernon R. eds, *Amino Acids: Metabolism and Medical Applications*, John Wright P S G Inc, Boston, pp 77-87 (1983).
 42. Kawamura, A.; Takahashi, T.; Kusumoto, K.; Kyuuno, K.; Kumagai, F.; Kushida, K.; Kuraoka, Y.; Sakao, N. "The Development of a New Hybrid Hepatic Support System Using Frozen Liver Pieces." *Jpn. J. Artif. Organs* 14:253-257 (1985).
 43. Kimura, K.; Gundermann, K. J.; Lie, T. S. "Haemoperfusion Over Small Liver Pieces for Liver Support." *Artif. Organs* 4:297-301 (1980).
 44. Hager, J. C.; Carman, R.; Stoller, R.; Panol, G.; Leduc, E. H.; Thayer, W. R.; Porter, L. E.; Galetti, P. M.; Calabresi, P.; "A Prototype for a Hybrid Artificial Liver." *Trans Am. Soc. Artif. Intern. Organs* 24:250-253 (1978).
 45. Arnaout, W. S.; Moscioni, A. D.; Barbour, R. L.; Demetriou, A. A. "Development of Bioartificial Liver: Bilirubin Conjugation in Gunn Rats." *J. Surg. Res.* 48:379-382 (1990).
 46. Wong, H; Chang, T. M. S. "Bioartificial Liver: Implanted Artificial Cells Living Hepatocytes Increases Survival of Liver Failure." *Intl J. Artif. Org* 9:335-336 (1986).
 47. Bruni, Silvia; Chang, T. M. S. "Hepatocytes Immobilised by Microencapsu-

- lation in Artificial Cells: Effects on Hyperbilirubinemia in Gunn Rats." *Biomat. Art. Cells, Art. Org.* **17**(4):403-411 (1989).
48. Cai, A.; Shi, Z.; Sherman, M.; Sun, A. M. "Development and Evaluation of a System of Microencapsulation of Primary Rat Hepatocytes." *Hepatology* **10**:855-860 (1989).
 49. Sun, A. M.; Cai, Z.; Shi, Z.; Ma, F.; O'Shea, G. M.; Gharapetian, M. "Microencapsulated Hepatocytes as a Bioartificial Liver." *Trans. Am. Soc. Artif. Intern. Organs* **32**:39-41 (1986).
 50. Chang, T.M.S.; "Semipermeable Microcapsules." *Science* **146**:524 (1964).
 51. Chang, T.M.S.; McIntosh, F.C. and Mason, F.G. "Semipermeable Aqueous Microcapsules: Preparation and Properties." *Can J. Physiol and Pharmacol.* **44**:115 (1966).
 52. Chang, T.M.S., *Artificial Cells*, Charles C. Thomas, Springfield IL (1972).
 53. Bissell, D. M.; Arens, D. M.; Maher, J. J.; Roll, F. J. "Support of Cultured Hepatocytes on a Laminin-Rich Gel." *J Clin. Invest.* **79**:801-812 (1987).
 54. Yu, Y.T.; Chang, T.M.S.; "Immobilization of Multienzymes and Cofactors Within Lipid-Polyamide Membrane Microcapsules for the Multistep Conversion of Lipophilic and Lipophobic Substrates." *Enzyme Microbial Technol* **4**:327-331 (1982).
 55. Cousineau, J.; and Chang, T.M.S. "Formation of Amino Acid from Urea and Ammonia by Sequential Enzyme Reaction Using Micro-Encapsulated Multi-Enzyme System." *Biochem Biophys Res. Com.* **79**(1):24-31 (1977).
 56. Chang, et al. "Artificial Cells Containing Multienzyme Systems for the Sequential Conversion of Urea into Ammonia, Glutamate then Alanine." *Artif. Organs.* **3**:244-287 (1979).
 57. Rudman, D.; Galambos, J. T.; Smith, R. B., III; Salam, A. A.; Warren, W. D.; "Comparison of Effect of Various Amino Acids Upon the Blood Ammonia Concentration of Patients with Liver Disease." *Am J Clin. Nutr.* **26**:916-925 (1973).

58. Grunwald, J.; and Chang, T.M.S. "Nylon Polyethyleneimine Microcapsules for Immobilising Multienzyme with Soluble Dextran-NAD⁺ for the Continuous Recycling of the Microencapsulated Dextran NAD⁺. *Biochem. Biophys. Res. Com.* **61**:565-570 (1978).
59. Grunwald, J.; and Chang, T.M.S. "Continuous Recycling of NAD⁺ Using an Immobilized System of Collodion Microcapsules Containing Dextran-Nad⁺, Alcohol Dehydrogenase and Malate Dehydrogenase." *J. of Applied Biochem.* **1**:104-114 (1979).
60. Gu, K.F.; Chang, T.M.S. "Conversion of Urea or Ammonia into Essential Amino Acids (L-Leucine, L-Valine, L-Isoleucine) Using Multienzyme Systems and NADH-Dextran Immobilised in Artificial Cells." *Biomat. Artif. Cells Artif. Organs* **15**(1):297-303 (1988).
61. Mosbach, K. "Immobilized AMP and NAD⁺ Analogs." *Methods in Enzymology* **34**:229-253 (1974).
62. Fischer, Josef E.; Rosen, Harvey M.; Ebeid, Amin M.; et al "The Effect of Normalization of Plasma Amino Acids on Hepatic Encephalopathy in Man." *Surgery*, **80**(1):77-91 (1976).
63. Miniuk, Gerald Y.; Sherman, Thomas A.; Shaffer, Eldon A.; Kelly, Seamus K. "A Comparative Study of the Effects of Insulin/Glucagon Infusions, Parenteral Amino Acids and High Dose Corticosteroids on Survival in a Rabbit Model of Acute Fulminant Hepatitis." *Hepatology* **6**(1):73-78 (1986).
64. Shi, Z.Q.; and Chang, T.M.S. "In Vitro Adsorption Spectrum of Plasma Amino Acids by Coated Charcoal Haemoperfusion." *Int J Artif Organs* **7**:197-202 (1984).
65. Abe, Shigeo.; and Takayama, Kenichiro; "Amino Acid Micro-organisms: Variety and Classification." In: Yamada, K.; Kinoshita, S.; Tsunoda, T.; Aida, K. eds, *The Microbial Production of Amino Acids.*, John Wiley and Sons, New York, pp 3-38 (1972).
66. Yoshinaga, Fumishiro; Nakamori, Seguru; "Production of Amino Acids. " In:

- Hermann, Klaus; and Somerville, Ronald L. eds, *Amino Acids: Biosynthesis and Genetic Regulation* (1983), Addison Wesley, pp 405-429 (1983).
67. Aida, Ko; "Control of Microbial Metabolism." In: Yamada, K.; Kinoshita, S.; Tsunoda, T.; Aida, K. eds, *The Microbial Production of Amino Acids*. John Wiley and Sons, New York, pp 91-122 (1972).
 68. Fukui, Sakuzo; "Biomembrane Permeability and Accumulation of Amino Acids." In: Yamada, K.; Kinoshita, S.; Tsunoda, T.; Aida, K. eds, *The Microbial Production of Amino Acids*. John Wiley and Sons, New York, pp 123-137 (1972).
 69. Ingraham, John L; Maaloe, Ole; Neidhardt, Frederick C., *Growth of the Bacterial Cell*, Sinauer Associates Inc pp 1-48 (1983).
 70. Karel, Steven F.; Libicki, Shari, B.; Robertson, Channing R. "The Immobilization of Whole Cells: Engineering Principles." *Chemical Engineering Science* **40**(8):1321-1353 (1985).
 71. Inloes, D. S.; Smith, W.S.; Taylor, D.P.; Cohen, C.N.; Michaels, A.S.; and Robertson, C.R. "Hollow-Fiber Membrane Bioreactors Using Immobilized *E. coli* for Protein Synthesis." *Biotechnol. Bioengng* **25**:2653 (1983).
 72. Mattiasson, B.; Ramstorp M., Nilsson, I. and Hahn-Hagerdal, B. "Comparison of the Performance of a Hollow-Fibre Microbe Reactor with a Reactor Containing Alginate Entrapped Cells: Denitrification of Water Using *Pseudomonas denitrificans*." *Biotechnol. Lett.* **3**:561 (1981).
 73. Miles, Edith Wilson; "Pyridoxal Phosphate Enzymes Catalyzing β -Elimination and β -Replacement Reactions." In: Dolphin, David; Poulson, Rozanne; Avramovic, Olga. eds, *Coenzymes and Cofactors*, pp 253-310 (1986).
 74. Enei, Hitoshi; Matsui, Hiroshi; Yamashita, Koichi; Okumura, Shinji; Yamada, Hideaki; "Distribution of Tyrosine Phenol-Lyase in Microorganisms." *Agr. Biol. Chem.* **36**(11):1861-1861 (1972).
 75. Riichi, Sakazaki; "*Citrobacter*." In: Krieg, Noel ed, *Bergey's Manual of Systematic Bacteriology, Vol 1.*, Williams & Wilkins, Baltimore/London pp

458-461 (1984).

76. Brot, Nathan; Smit, Zacharias; Weissbach, Herbert. "Conversion of L-Tyrosine to Phenol by *Clostridium tetanomorphum*." *Arch. Biochem. and Biophys.* **112**:1-6 (1965).
77. Enei, Hitoshi; Yamashita, Koichi; Okumura, Shinji; Yamada, Hideaki. "Culture Conditions for the Preparation of Cells Containing High Tyrosine Phenol-Lyase." *Agr. Biol. Chem* **37**(3):485-492 (1973).
78. Yamada, Hideaki and Kumagai, Hidehiko. "Synthesis of L-Tyrosine-Related Amino Acids by β -Tyrosinase." *Adv. in Appl. Microbiol.* **19**:249-288 (1975).
79. Yamada, Hideaki; Kumagai, Hidehiko; Kashima, Nobakazu; Torii, Hiroshi; Enei, Hitoshi; Okumura, Shinji. "Synthesis of L-Tyrosine from Pyruvate, Ammonia, and Phenol by Crystalline Tyrosine Phenol-Lyase." *Biochem. Biophys. Res. Commun.* **46**(2):370-374 (1972).
80. Enei, H.; Nakazawa, H.; Matsui, H.; Okumura, S.; and Yamada, H. "Enzymatic Preparation of L-Tyrosine or 3,4-Dihydroxyphenyl-L-Alanine from Pyruvate, Ammonia and Phenol or Pyrocatechol." *FEBS Let.* **21**(1):39-41 (1972).
81. Kumagai, H.; Matsui, H.; Ohgishu, H.; Ogata, K.; Yamada, H.; Ueno, T.; Fukami, H.; "Synthesis of 3,4-Dihydroxyphenyl-L-Alanine from L-Tyrosine and Pyrocatechol by Crystalline β -Tyrosinase." *Biochem. Biophys. Res Commun.* **34**(3):266-270 (1969).
82. Enei, Hitoshi; Matsui, Hiroshi; Nakazawa, Hidetsugu; Okumura, Shinji; Yamada, Hideaki. "Synthesis of L-Tyrosine or 3,4-Dihydroxyphenyl-L-Alanine from DL-Serine and Phenol or Pyrocatechol." *Agr. Biol. Chem.* **37**(3):493-499 (1973).
83. Enei, Hitoshi, Nakazawa, Hidetsugu; Okumura, Shinji; Yamada, Hideaki; "Synthesis of L-Tyrosine or 3,4-Dihydroxy-phenyl-L-Alanine from Pyruvic Acid, Ammonia, and Phenol or Pyrocatechol." *Agr. Biol. Chem* **37**(4):725-735 (1973).

84. Enei, Hitoshi; Matsui, Hiroshi; Okumura, Shinji and Yamada, Hideaki. "Enzymatic Preparation of L-Tyrosine and 3,4-Dihydroxy-phenyl-L-Alanine." *Biochem. Biophys. Res. Commun.* **43**(6):1345-1349 (1971).
85. Enei, Hitoshi; Matsui, Hiroshi; Okumura, Shinji; and Yamada, Hideaki. "Elimination, Replacement and Isomerization Reactions by Intact Cells Containing Tyrosine Phenol-Lyase." *Agr. Biol. Chem.* **36**(11):1869-1876 (1972).
86. Kumagai, Hidehiko; Yamada, Hideaki; Matsui, Hiroshi; Ohkishi, Haruyuki; Ogata, Koichi. "Tyrosine Phenol Lyase I: Purification, Crystallization, and Properties." *J. Biol. Chem.* **245**(7):1767-1772 (1970).
87. Kumagai, Hidehiko; Yamada, Hideaki; Matsui, Hiroshi; Ohkishi, Haruyuki; Ogata, Koichi. "Tyrosine Phenol Lyase II: Cofactor Requirements." *J. Biol. Chem.* **245**(7):1773-1777 (1970).
88. Kumagai, Hidehiko; Kashima, Nobukazu; Torii, Hiroshi; Yamada, Hideaki; Enei, Hitoshi; Okumura, Shinji. "Purification, Crystallization and Properties of Tyrosine Phenol-Lyase from *Erwinia herbicola*." *Agr. Biol. Chem.* **36**(3):472-482 (1972).
89. Antson, Alfred; Stropkopytov, Boris V.; Murshudov, Garib N.; Isupov, Michail N.; Harutyunyu, Emil H.; Demidkina, Tatyana V.; Vassylev, Dimitry G.; Dauter, Zbigniew; Terry, Howard; Wilson, Kieth S. "The Polypeptide Chain Fold in Tyrosine Phenol-Lyase, a Pyridoxal-5'-phosphate Dependent Enzyme." *FEBS* **302**(3):256-260 (1992).
90. Iwamori, Satoru; Yoshino, Sestuo; Ishiwata, Ken-ichi; and Makiguchi, Nobuyoshi; "Structure of Tyrosine Phenol-Lyase Genes from *Citrobacter freundii* and Structural Comparison with Tryptophanase from *Escherichia coli*." *Journal of Fermentation and Bioengineering* **72**(3):147-151 (1991).
91. Polak, Jacek; Brzeski, Henry; "Isolation of the Tyrosine Phenol-Lyase Genes from *Citrobacter freundii*." *Biotechnology Lett* **12**(11):805-810 (1990).
92. Kurusu, Yasurou; Fukushima, Makiko; Kohama, Keiko; Kobayashi, Miki;

- Terasawa, Masato; Kumagai, Hidehiko; Yukawa, Hideaki. "Cloning and Nucleotide Sequencing of the Tyrosine Phenol-Lyase Gene from *Escherichia intermedia*." *Biotechnology Lett.* **13**(11):769-772.
93. Ricard, Jacques. "Organized Polymeric Enzyme Systems: Catalytic Properties." In: Welch, G. Rickey ed, *Organized Multienzyme Systems*, Academic Press, New York, (1985), pp 177-240.
 94. Monod, Jacques; Wyman, Jeffries and Changeux, Jean-Pierre. "On the Nature of Allosteric Transitions: A Plausible Model." *J. Mol. Biol.* **12**:88-118 (1965).
 95. Koshland, E.E. "The Molecular Basis for Enzyme Regulation." In: Boyer, P.D. ed, *The Enzymes Vol 1*, second edition, Academic Press, New York, (1969), pp 341-396.
 96. Neet, Kenneth E. "Cooperativity in Enzyme Function: Equilibrium and Kinetic Aspects." In: *Contemporary Enzyme Kinetics and Mechanism*, Academic Press, New York, (1983), pp 267-320.
 97. Dunathan, H.C. and Voet, J.G. "Stereochemical Evidence for the Evolution of Pyridoxal-Phosphate Enzymes of Various Functions from a Common Ancestor." *Proc. Natl. Acad. Sci. USA*, **71**:3888-3891 (1974).
 98. Martell, Arthur E. "Reaction Pathways and Mechanisms of Pyridoxal Catalysis." *Advances in Enzymology* **53**:163-199 (1982).
 99. Axelson, B. Svante; Bjurling, Peter; Mattson, Olle; Langstrom, Bengt. "¹¹C/¹⁴C Kinetic Isotope Effects in Enzyme Mechanism Studies. ¹¹C/¹⁴C Kinetic Isotope Effect of the Tyrosine Phenol-Lyase Catalyzed α,β -Elimination of L-Tyrosine." *J. Am. Chem. Soc.* **114**:1502-1503 (1992).
 100. Faleev, N.G.; Ruvinov, S.B.; Bakhmutov, V.I.; Demidkina, T.V.; Myagkikh, I.V.; Belikov, V.M.; "Substrate Specificity of Tyrosine Phenol-Lyase. Electron and Steric Control at the Stage of Aromatic-Moiety Elimination." *Molecular Biology (translated from Molekulyarnaya Biologiya)* **21**(6):1636-1644 (1987).
 101. Kiick, Dennis M.; Phillips, Robert S.; "Mechanistic Deductions from Kinetic

Isotope Effects and pH Studies of Pyridoxal Phosphate Dependent Carbon-Carbon Lyases: *Erwinia herbicola* and *Citrobacter freundii* Tyrosine Phenol Lyase." *Biochemistry* **27**:7333-7338 (1988).

102. Palcic, M.M.; Shen, S.-J.; Scheicher, E.; Kumagai, H.; Sawada, S.; Yamada, H.; and Floss, H.G.; "Stereochemistry and Mechanism of Reactions Catalyzed by Tyrosine Phenol Lyase from *Escherichia intermedia*." *Z. Naturforsch*, **42c** pp 307-318 (1987).
103. Faleev, Nikolai, G.; Ruvinov, Sergei B.; Demidkina, Tatyana V.; Myagkikh, Igor V.; Gololobov, Michail Yu; Bakhmutoy, Vladimir I.; Belikov, Vasili M.; "Tyrosine Phenol-Lyase from *Citrobacter intermedium*: Factors Controlling Substrate Specificity." *Eur J. Biochem*, **177**:395-401 (1988).
104. Muro, Tetsuo; Nakatani, Hiroshi; Hiromi, Keitaro; Kumagai, Hidehiko and Yamada, Hideaki. "Elementary Processes in the Interaction of Tyrosine Phenol-Lyase with Inhibitors and Substrate." *J. Biochem* **84**:633-640 (1978).
105. Cleland, W.W. "The Kinetics of Enzyme-Catalyzed Reactions with Two or More Substrates or Products I. Nomenclature and Rate Equations." *Biochimica Et Biophysica Acta* **67**:104-137 (1963).
106. Nagasawa, Torii; Utagawa, Takashi; Goto, Joji; Kim, Chan-Jo; Tani, Yoshiki; Kumagai, Hidehiko and Yamada, Hideaki. "Synthesis of L-Tyrosine Related Amino Acids by Tyrosine Phenol-Lyase of *Citrobacter intermedium*." *Eur. J. Biochem* **117**:33-40 (1981).
107. Para, G.; Luciardi, P; Barratti, J. "Synthesis of L-Tyrosine by Immobilized *Escherichia intermedia* Cells." *Appl. Microbiol. Biotechnol.* **21**:273-279 (1985).
108. Fukui, Saburo; Ikeda, Sei-ichiro; Fujimara, Motoki; Yamada, Hideaki; Kumagai, Hidehiko. "Comparative Studies on the Properties of Tryptophanase and Tyrosine Phenol-Lyase Immobilized Directly on Sepharose or by the use of Sepharose-Bound Pyridoxal Phosphate." *Eur. J. Biochem.* **51**:156-164 (1975).

109. Tsyachnaya, I.V.; Rodrigues, M.Kh; Yakovlena, V.I.; Berezin, I.V. "Kinetic Peculiarities of Tyrosine Synthesis Catalyzed by Free Immobilized Bacterial Cells. Influence of Mass transport of Reagents on the Kinetics of Tyrosine Phenol-Lyase in Cells." *Biokhimiya* 51(11):1768-1775 (1986).
110. Nishida, Yutaka; Sato, Tadashi; Tosa, Tetsuya; Chibata, Ichiro; "Immobilization of *Escherichia coli* Cells Having Aspartase Activity with Carrageenan and Locust Bean Gum." *Enzyme Microb. Technol.* 1:95-99 (1979).
111. Chang, T.M.S. "A Comparison of Semipermeable Microcapsules and Standard Dialyzers for Use in Separation." *Separ. Purif. Methods* 3:245 (1974).
112. Chang, T.M.S. "Effects of Local Applications of Microencapsulated Catalase on the Response of Oral Lesions to Hydrogen Peroxide in Acatalasaemia." *J. Dent. Res.* 51:319 (1972).
113. Chang, T.M.S. and Poznansky, M.J. "Semipermeable Microcapsules Containing Catalase for Enzyme Replacement in Acatalasaemic Mice." *Nature (London)*, 218:243-245 (1968).
114. Bourget, Louis; and Chang, Thomas M.S. "Experimental Enzyme Therapy Replacement for Phenylketonuria using Phenylalanine ammonia-lyase Immobilized by Microencapsulation with Artificial Cells." *FEBS Lett* 180(1):5-8 (1985).
115. Chang, T.M.S.; Espinoza-Melendez, E.; Francoeur, T.E.; Eade, N.R. "Albumin-Collodion Activated Coated Charcoal Haemoperfusion in the Treatment of Severe Theophylline Intoxification in a 3 Year Old Patient." *Paediatrics* 65(4):811-814 (1980).
116. Winchester, James F. "Active Methods for Detoxification." In: Haddad, Lester M. and Winchester, James F. eds, *Clinical Management of Poisonings and Drug Overdose*, 2nd edition, W. B. Saunders Co, Pa (1990) Pp 148-167.
117. Klein, Joachim and Wagner, Fritz. "Methods for the Immobilization of

- Microbial Cells." *Applied Biochemistry and Bioengineering* 4:11-51 (1983).
118. Kennedy, John F.; Cabral, Joaquim M.S.; "Immobilized Living Cells and Their Applications." *Applied Biochemistry and Bioengineering* 4:189-280 (1983).
 119. Lim, Franklin and Sun, Anthony M. "Microencapsulated Islets as Bioartificial Endocrine Pancreas." *Science* 210:908-910 (1980).
 120. Lim, F. "Microencapsulation of Living Cells and Tissues: Theory and Practice." In: Lim, F ed, *Biomedical Applications of Microencapsulation*, CRC Press, Boca Raton Fl, Pp 138-154 (1984).
 121. Lim, Franklin. "Microencapsulation of Living Mammalian Cells." *Advances in Biotechnological Processes* 7:185-197 (1988).
 122. McKnight, C.A.; Ku, A.; Goosen, M.F.A.; Sun, D. and Penney, C.; "Synthesis of Chitosan-Alginate Microcapsule Membranes." *J Bioactive and Compatible Polymers* 3: 334-355 (1988).
 123. Stefuca, Vladimir; Gemeiner, Peter; Kurillova, Lubica; Dauntzenberg, Horst; Polakovic, Milan and Bales, Vladimir. "Polyelectrolyte Complex Capsules as a Material for Enzyme Immobilization: Catalytic Properties of Encapsulated Lactate Dehydrogenase." *Applied Biochemistry and Biotechnology* 30:313-324 (1991).
 124. Stevenson, W.T.K.; Evangelista, R.A.; Sugamori, M.E. and Sefton, M.V.; "Microencapsulation of Mammalian Cells in a Hydroxyethyl Methacrylate Co-Polymer: Preliminary Development." *Biomat. Art. Cells, Art Org* 16(4):747-769 (1988).
 125. Yoshioka, Toshimitsu; Hirano, Ryogo; Shioya, Toshiaki and Kako, Masatoshi. "Encapsulation of Mammalian Cell Chitosan-CMC Capsule." *Biotechnology and Bioengineering* 35:66-72 (1990).
 126. Goosen, Mattheus F.A.; O'Shea, Geraldine M.; Gharapetian, Hrre M.; Chou, Sheng and Sun, Anthony M. "Optimization of Microencapsulation Parameters: Semipermeable Microcapsules as Bioatificial Pancreas."

Biotechnology and Bioengineering XXVII Pp 146-150 (1985).

127. King, G.A.; Daugulis, A.J.; Faulkner, P. and Goosen, M.F.A. "Alginate-Polylysine Microcapsules of Controlled Membrane Molecular Weight Cut-Off for Mammalian Cell Culture Engineering." *Biotechnology Progress* **3**(4):231-240 (1987).
128. Goosen, M.F.A.; King, G.A.; McKnight, C.A.; Marcotte.; "Animal Cell Culture Engineering Using Alginate-Polycation Microcapsules of Controlled Membrane Molecular Weight Cut-Off." *J. Membrane Science* **41**:323-343 (1989).
129. Soon-Shiong, P.; Otterlie, M.; Skjak-Braek, G.; Smidsrod, O.; Heintz, R.; Lanzer, R.P. and Espevik, T. "An Immunologic Basis for the Fibrotic Reaction to Implanted Microcapsules." *Transplantation Proceedings* **23**(1):758-759 (1991).
130. Clayton, H.A.; London, N.J.M.; Colloby, P.S.; James, R.F.L. and Bell, P.R.F. "The Effect of Capsule Composition on the Viability and Biocompatibility of Sodium Alginate/Poly-L-Lysine Encapsulated Islets." *Transplantation Proceedings* **24**(3):956 (1992).
131. Clayton, H.A.; London, N.J.M.; Colloby, P.S.; Bell, P.R.F. and James, R.F.L. "The Effect of Capsule Composition on the Biocompatibility of Alginate-Poly-L-Lysine Capsules." *J of Microencapsulation* **8**(2):221-233 (1991).
132. Wong, H. and Chang, T.M.S. "A Novel Two-Step Procedure for Immobilizing Living Cells in Microcapsules for Improving Xenograft Survival." *Biomat. Art. Cells & Immob. Biotech.* **19**(4):687-697 (1991).
133. Wong, H. and Chang, T.M.S. "The Microencapsulation of Cells Within Alginate Poly-L-Lysine Microcapsules Prepared With the Standard Single Step Drop Technique: Histologically Identified Membrane Imperfections and the Associated Graft Rejection." *Biomat. Art. Cells & Immob. Biotech.* **19**(4):675-686 (1991).
134. Chang, T.M.S. "Biotechnological and Medical Applications Based on

- Immobilization of Hepatocytes, Microorganisms, or Enzyme Systems by Microencapsulation in Artificial Cells." *Annals of New York Academy of Sciences* **613**:109-115 (1990).
135. Aiba, Shuichi; Humphrey, Arthur E.; Mills, Nancy F., *Biochemical Engineering*, Academic Press N.Y.; Chapter 8: Media Sterilization, Pp 186-215 (1965).
 136. Deindorfer, F.H.; Humphrey, Arthur E.; "Analytical Method for Calculating Heat Sterilization Times." *Applied Microbiology* **7**:256-264 (1959).
 137. Geankoplis, Christie J., *Transport Processes and Unit Operations*, Allyn and Bacon Inc, (1978).
 138. Evans, L.B. and Stefany, N.E.; "An Experimental Study of Transient Heat Transfer to Liquids in Cylindrical Enclosures." *A.I.Ch.E Pap 4, Heat Transfer Conf. Los Angeles, August 1965*. (1965)
 139. Donnan, F.G. and Rose, R.C. "Osmotic Pressure, Molecular Weight, and Viscosity of Sodium Alginate." *Canadian J. of Research* **28 SEC B** Pp 105-113 (1950).
 140. Cook, W.H. and Smith, David B. "Molecular Weight and Hydrodynamic Properties of Sodium Alginate" *Canadian Journal of Biochemistry and Physiology* Vol **32** Pp 227-239 (1954).
 141. Greenwood, C.T. and Banks, W., *Synthetic High Polymers*, Oliver & Boyd, Edinburgh (1968).
 142. Sleesman, John P. and Leben, Curt. "Preserving Phytopathogenic Bacteria at -70 °C or with Silica Gel." *Plant Disease Reporter* **62**(10):910-913 (1978).
 143. Koch, Arthur L. "Growth Measurement" In: Gerhardt, Phillip et al, eds, *Manual of Methods for General Bacteriology*, American Society for Microbiology Pp 179-207 (1981).
 144. Koch, Arthur L. "Theory of the Angular Dependence of Light Scattered by Bacteria and Similar-sized Biological Objects." *J. Theoretical Biology* **18**:133-156 (1968).

145. Bradford, Marion. "A Rapid and Sensitive Method for the Quantitation of Microgram Quantities of Protein Utilizing the Principle of Protein-Dye Binding." *Analytical Biochemistry* **72**:248-254 (1976).
146. Porteous, J.W. and Williams, R.T. "The Metabolism of Benzene: I (a) The Determination of Phenol in Urine with 2:6-Dichloroquinone Chloroimide. (b) The Excretion of Phenol, Glucuronic Acid and Ethereal Sulphate by Rabbits Receiving Benzene and Phenol. (c) Observations on the Determination of Catechol, Quinol and Phenol and Muconic Acid in Urine." *Biochem J.* **44**:46-55 (1949).
147. Booman, K.A. and Niemann, C. *J. Am. Chem. Soc.* **78**, 3642 (1956).
148. Walter, Charles and Barrett, M.J. "The Information Content of Enzyme Kinetic Data III. A Comparison of 4 Methods for Fitting Kinetic Data to a Power Series." *Enzymologia* **38**:147-160 (1960).
149. Draper, Norman and Smith, Harry, *Applied Regression Analysis*, 2nd edition, John Wiley & Sons Pp 101-136 (1981).
150. Hill, D.W.; Walker, F.H.; Wilson, T.D. and Stuart, J.D. "High Performance Liquid Chromatography Determination of Amino Acids in the Picomole Range." *Analytical Chemistry* **51**(8):1338-1341 (1979).
151. Marquardt, D.W. "An Algorithm for Least Squares Estimation of Nonlinear Parameters," *Journal for the Society of Industrial and Applied Mathematics* **11**:431-441 (1963).
152. Ralston, M.L. and Jennrich, R.I. "DUD, A Derivative-Free Algorithm for Nonlinear Least Squares," *Technometrics* **20**:7-14 (1978).
153. Lineweaver, Hans; and Burk, Dean. "The Determination of Enzyme Dissociation Constants", *J. Am. Chem. Soc.* **56**:658-666 (1934)
154. Michaelis, L; and Menten, M.L. "Die Kinetik der Invertinwirkung", *Biochem Z* **49**:333-369 (1913).
155. Eadie, G.S. "The Inhibition of Cholinesterase by Physostigmine and Prostigmine", *J. Biol. Chem* **146**:85-93 (1942).

156. Scatchard, G. "The Attractions of Proteins for Small Molecules and Ions", *Ann. N.Y. Acad. Sci* **51**:660-672 (1949).
157. Hanes, C.S. "Studies on Plant Amylases I: The Effect of Starch Concentration Upon the Velocity of Hydrolysis by the Amylase of Germinated Barley" *Biochem J* **26**:1406-1421 (1932).
158. Hill, A.V. "The Possible Effects of the Aggregation of the Molecules of Haemoglobin on its Dissociation Curves", *J. Physiol. (London)* **40**, iv (1910).
159. Monod, Jacques; Wyman, J.; Changeux, J.-P. "On the Nature of Allosteric Transitions: A Plausible Model", *J. Mol. Biol.* **12**:88-118 (1965).
160. Draper, N.R. and Smith, H., *Applied Regression Analysis*, second edition John Wiley and Sons N.Y., Pp 458-517 (1981).
161. Adair, G.S. "The Hemoglobin System VI. The Oxygen Dissociation Curve of Hemoglobin." *J. Biol. Chem.* **63**:529-545 (1945).
162. Teipel, John; and Koshland, D.E., Jr "The Significance of Intermediary Plateau Regions in Enzyme Saturation Curves", *Biochemistry* **8**(11):4656-4663 (1969).
163. Koshland, D.E. Jr; Nemethy, G; and Filmer, D. "Comparison of Experimental Binding Data and Theoretical Models in Proteins Containing Subunits" *Biochemistry* **5**(1):365-385 (1966).
164. Segel, Irwin H. , *Enzyme Kinetics: Behaviour and Analysis of Rapid Equilibrium and Steady State Enzyme Systems*, John Wiley & Sons N.Y. (1975).
165. Weast, R.C; and Astle, M.J; editors, *CRC Handbook of Chemistry and Physics*, 60 th edition, CRC Press Inc, Boca Raton, Florida, (1979).
166. Leo, W.J.; Aichen, J.M.; and Malone, D.M. "Effects of Sterilization Treatments on Some Properties of Alginate Solutions and Gels." *Biotechnol. Prog.*, **6**:51-63 (1990).
167. Smidsrod, O; and Skjaek-Braek, G. "Alginate as Immobilization Matrix for Cells." *Tibtech* **8**:71-78 (1990).

168. Martinsen, A.; Skjak-Braek, G.; and Smidsrod, O. "Alginate as Immobilization Material: I. Correlation between Chemical and Physical Properties of Alginate Gel Beads" *Biotechnology and Bioengineering* 33:79-89 (1989).
169. Rehg, T.; Dorger, C.; and Chau, P.C. "Application of an Atomiser in Producing Small Alginate Gel Beads for Cell Immobilization." *Biotechnology Lett* 8(2):111-114 (1986).
170. Su, H.; Bajpai, R.; and Preckshot, G.W. "Characterization of Alginate Beads Formed by a Two-fluid Annular Atomizer.", *Applied Biochemistry and Biotechnology*, 20/21 Pp 561-569 (1969).
171. Poncelet, Denis; and Neufeld, Ronald J. "Shear-Breakage of Nylon Membrane Microcapsules in a Turbine Reactor", *Biotechnology and Bioengineering*, 33:95-103 (1989).
172. Marquis, R.E. "Permeability and Transport" in Gerhardt, P *et al* editors, *Manual of Methods for General Bacteriology*, American Society for Microbiology, Washington; Pp 393-404 (1981).
173. Reiner, John M., *Behaviour of Enzyme Systems*, second edition, Von Nostrand Reinhold Company, (1969) Pp 108-132.
174. Segel, Irwin H. , *Enzyme Kinetics: Behaviour and Analysis of Rapid Equilibrium and Steady State Enzyme Systems*, John Wiley & Sons N.Y. (1975).
175. Endrenyi, L.; Chan, M.S. and Wong, J. T-F. "Interpretation of Nonhyperbolic Behaviour in Enzymic Systems II. Quantitative Characteristics of Rate and Binding Functions" *Can. J. Biochem.* 49:581-598 (1971).
176. Walter, Charles "Graphical Procedures for the Detection of Deviations from the Classical Model of Enzyme Kinetics" *J. Biol. Chem* 249(3):699-703 (1974).
177. Wong, J, T-F, *Kinetics of Enzyme Mechanisms*, Academic Press, London (1975).
178. Bardsley, W.G. and Childs, R.E. "Sigmoid Curves, Non-linear Double Reciprocal Plots and Allostereism" *Biochem J* 149:313-328 (1975).

179. Huang, C.Y. "Derivation of Initial Velocity and Isotope Exchange Rate Equations." *Methods in Enzymology* **63** [4] Pp 54-84 (1979).
180. Wong, J. T-F.; and Endrenyi, L. "Interpretation of Nonhyperbolic Behaviour in Enzymic Systems I. Differentiation of Model Mechanisms" *Can J. Biochem* **49**:568-580 (1971).
181. Ricard, J.; Mouttet, C; and Nari, J. "Subunit Interactions in Enzyme Catalysis: Kinetic Models for one Substrate Polymeric Enzymes." *Eur. J. Biochem* **41**:479-497 (1974).
182. Ricard, J. and Noat, G. "Subunit Interactions in Enzyme Transition States- Antagonism Between Substrate Binding and Reaction Rate" *J. theor. Biol* **111**:737-753 (1984)
183. Nari, J; Mouttet, C.; Fouchier, F and Ricard, J. "Subunit Interactions in Enzyme Catalysis: Kinetic Analysis of Subunit Interactions in the Enzyme L-Phenylalanine Ammonia-Lyase" *Eur J. Biochem* **41**:499-515 (1974).
184. Levitzki, A.; and Koshland, D.E., Jr "Negative Cooperativity in Regulatory Enzymes" *Proc natl Acad Sci U.S.A.* **62**:1121-1128 (1969).
185. Corwin, L.M.; and Fanning, G.K. "Studies of Parameters Affecting the Allosteric Nature of Phosphoenol Pyruvate Carboxylase of *Escherichia coli*" *J. Biol. Chem.* **243**:3517 (1968).
186. Le John, H.B.; and Jackson, S. "Allosteric Interactions of a Regulatory Nicotinamide Adenine Dinucleotide Specific Glutamate Dehydrogenase from *Blastocladdia*: A Molecular Model for the Enzyme" *J. Biol. Chem.* **243**:3447 (1968).
187. Para, G.; and Baratti, J. "The Effect of Phenol on Growth and Induction of Tyrosine Phenol-Lyase of *Escherichia intermedia* and *Erwinia herbicola*" *Biotechnology Letters* **9**(6):399-404 (1987).
188. Hammes, G.G.; and Wu, C-W "Regulation of Enzyme Activity" *Science* **172**:1205-1211 (1971).
189. Hammes, G.G.; Lillford, P.J.; and Simplicio, J. "Mechanism of Nicotinamide-

- Adenine Dinucleotide Binding to Rabbit Muscle Glyceraldehyde 3-Phosphate Dehydrogenase." *Biochemistry* **10**(20):3686-3693 (1971).
190. Sols, Alberto; Reeves, A.E.; and Gancedo, C. "Regulation of Enzymes *in situ*" in Fischer, E.H.; Krebs, E.G.; Neurath, H. and Stadtman, E.R. eds, *Metabolic Interconversion of Enzymes*, Springer Verlag, Berlin (1973) Pp 393-399.
 191. Stein, Wilfred., *Transport and Diffusion Across Cell Membranes*, Academic Press, London, (1986) Chapter 2.
 192. Pardee, Arthur, B. "The Control of Enzyme Activity" in Boyer, Paul ed , *The Enzymes Vol II : Kinetics and Mechanisms*, pp 681-716.
 193. Atkins, G.L; and Nimmo, Ian A "The Reliability of Michaelis Constants and Maximum Velocities Estimated by Using the Integrated Michaelis-Menten Equation" *Biochem. J.* **135**:779-784 (1973).
 194. Philo, R.D.; and Selwyn, M.J. "Use of Progress Curves to Investigate Product Inhibition in Enzyme-Catalysed Reactions: Application to the Soluble Mitochondrial Adenosine Triphosphatase" *Biochem. J.* **135**:525-530 (1973).
 195. Bizzozero, S.; Kaiser, A.W.; and Dutler, H. "A Numerical Method for Acquisition and Processing of Steady-State Kinetic Data Contained in an Entire Progression Curve: Application to the Study of α -Chymotrypsin-Catalyzed Hydrolysis." *Eur. J. Biochem.* **33**:292-300 (1973).
 196. Darvey, I.G.; and Williams, J.F. "Integrated Steady-State Rate Equations for Enzyme-Catalyzed Reactions" *Biochimica et Biophysica Acta* **85**:1-10 (1964).
 197. Duggleby, D.G; and Morrison, J.F."The Analysis of Progress Curves for Enzyme-Catalyzed Reactions by Non-Linear Regression" *Biochimica et Biophysica Acta* **481**:297-312 (1977).
 198. Anderson, W.F."Prospects for Human Gene Therapy." *Science* **226**(4673):401-409 (1984).

199. Temin, H.M. "Retrovirus Vectors for Gene Transfer: Efficient Integration into and Expression of Exogenous DNA in Vertebrate Cell Genomes" *In* Gene Transfer. R. Kucherlapati, editor, Plenum Press. New York, N.Y. Pp 149-187 (1986).

8.0 APPENDICES

8.1 APPENDIX I.

8.1.1. Source of And Purity of Chemicals.

The components of the medium for the induction of tyrosine phenol-lyase activity in *Erwinia herbicola* is given in the Table XVII. The chemicals from Sigma Chemicals (St Louis, Mo) were of the "microbiologically tested for cell culture grade". Chemicals from Fisher Scientific (Fairlawn, New Jersey) and BDH (British Drug Houses) were of analytical grade. The hydrolysed soy protein was obtained in powder form from ICN (Cleveland, Ohio).

Table XVII. Components of the Tyrosine Phenol-Lyase Induction Medium		
Chemical	Amount per 4.0 l of Medium (g)	Source
Tyrosine	2.0	Sigma
KH ₂ PO ₄	8.0	B.D.H
FeSO ₄	4.0	Fisher
Pyridoxine	0.004	Sigma
Glycerol	24.0	Fisher
Succinate	20.0	Sigma
L-Methionine	4.0	Sigma
L-Alanine	8.0	Sigma
Glycine	2.0	Sigma
Phenyl-L-Alanine	4.0	Sigma
Hydrolysed Soy Protein	48.0	I.C.N.

8.1.2. Chemicals used in Microencapsulation.

Alginate was obtained from Kelco, Division of Merck & Co Inc (Clark, NJ). The 2 types of alginate used were Kelco-Gel[®] L.V. (low viscosity) alginate and Kelco-Gel[®] H.V. (high viscosity). Poly-L-lysine was obtained from Sigma with a nominal molecular weight of 25000, but the actual molecular weight varied from 20000 to about 26000. The true molecular weight used in a particular experiment is indicated in the text at the appropriate place. HEPES (N-2-Hydroxyethyl piperazine-N-2-ethanesulfonic acid) was obtained from Boehringer Manneheim

(Montreal, QC). Sodium chloride, calcium chloride and other chemicals were obtained from various sources but were of at least 98 percent purity.

8.2 APPENDIX II

8.2.1. Scans of Blue-Dextran and Alginate Solutions.

The following scans (Figures 54 and 55) show that alginate does not interfere at either at $\lambda = 616.1$ nm or $\lambda = 257.9$ nm the absorbance maxima of blue dextran 2000 (Mwt 2.0×10^6).

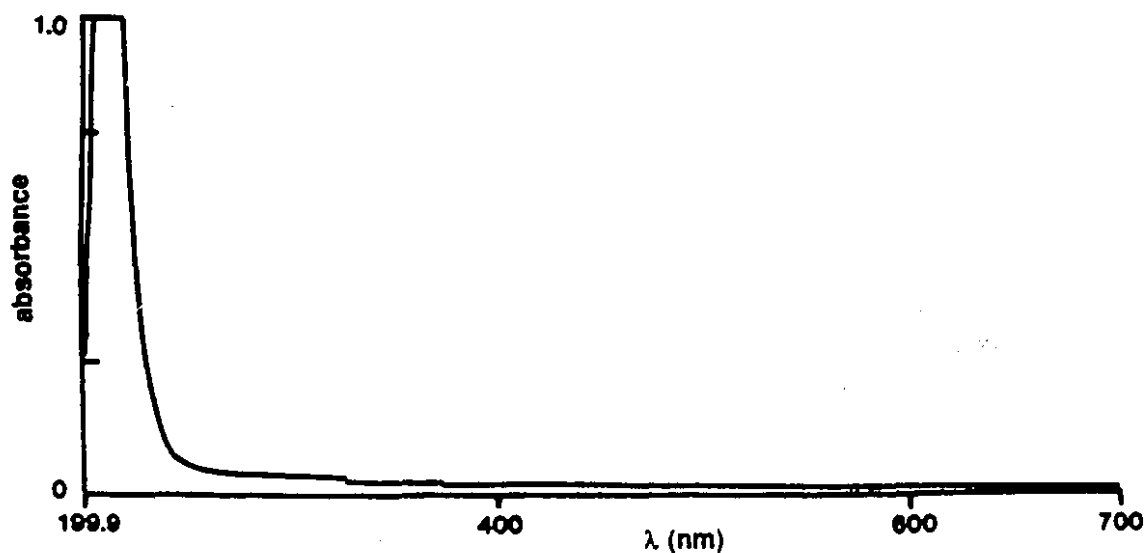


Figure 54. Scan of 0.1 percent alginate in HEPES buffered saline.

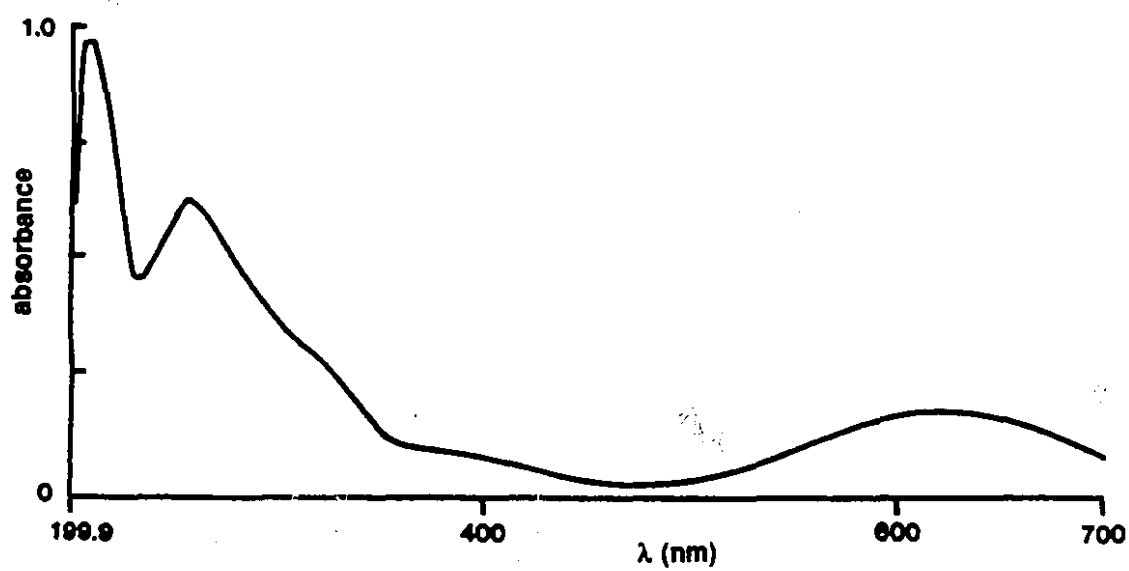


Figure 55. Scan of blue dextran 0.2 mg per ml in HEPES buffered saline (pH 7.4).

8.3 APPENDIX III

8.3.1 Development of Rapid Equilibrium Kinetic Models Used.

A number of models of enzyme behaviour were discussed in the body of the thesis. In this appendix some of these equations will be developed. The Michaelis-Menten equation (154) is well known, hence it was only developed for the sake of completion; and because some of the assumptions underlying this model are common to all the models presented.

The Michaelis-Menten Equation for Enzyme Kinetic Data.

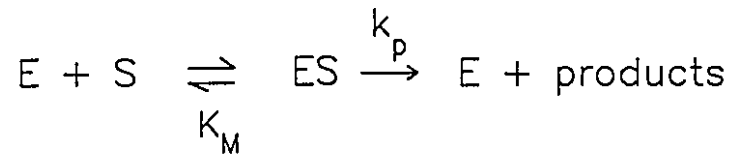
If it is assumed that the enzyme interacts in a rapid equilibrium or quasi-equilibrium manner with substrate a simplified derivation of the Michaelis-Menten equation (154) is possible. The more rigorous analysis by Briggs and Haldane gives a steady state solution of similar form (164, 177), but the rapid equilibrium derivation will be presented here.

The following assumptions are required for the derivation of the Michaelis-Menten equation under rapid equilibrium conditions:

- 1) The enzyme is a catalyst;
- 2) The enzyme and substrate complex react rapidly to form an enzyme substrate complex;
- 3) Only a single substrate and a single enzyme-substrate complex are involved and the enzyme substrate breaks down directly to form free enzyme and product;
- 4) Enzyme (E), substrate (S), and the enzyme-substrate complex (ES) are at equilibrium, and further the rate at which ES dissociates to E and S is much faster than the rate at which ES breaks down to form product;
- 5) The overall reaction rate is limited by the breakdown of the ES complex to form free enzyme and product;

- 6) The reverse reaction is insignificant; i.e. the system is far from equilibrium.

The above assumptions suggest the following mechanism for a Michaelis-Menten system:



Further the assumptions imply that the reaction rate or velocity is given by equation 8.1:

$$v = k_p[ES] \quad \dots 8.1$$

where v is the rate or velocity; k_p is the rate constant for product formation; $[ES]$ is the concentration of the ES complex. A mass balance on the total amount of enzyme implies equation 8.2:

$$[E]_t = [E] + [ES] \quad \dots 8.2$$

where $[E]_t$ is the total concentration of enzyme. The reaction rate per total enzyme concentration is given by 8.3:

$$\frac{v}{[E]_t} = \frac{k_p[ES]}{[E] + [ES]} \quad \dots 8.3$$

By defining an equilibrium constant K_M for the dissociation of the ES complex to E and S we can substitute for $[ES]$ in terms of $[E]$ as shown in equation 8.4; which gives immediately 8.5 the Michaelis-Menten equation. If the product of k_p and $[E]_t$ is called V_{\max} ; the maximum rate which occurs when all the enzyme is in the form of ES; equation 8.6 an alternative of the Michaelis-Menten equation results as shown below.

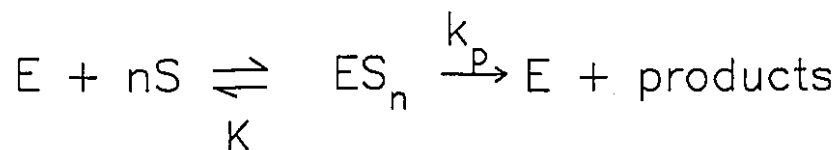
$$\frac{v}{[E]_t} = \frac{\frac{k_p[E][S]}{K_M}}{[E] + \frac{[E][S]}{K_M}} \quad \dots 8.4$$

$$\frac{v}{[E]_t} = \frac{k_p[S]}{K_M + [S]} \quad \dots 8.5$$

$$\frac{v}{V_{\max}} = \frac{[S]}{K_M + [S]} \quad \dots 8.6$$

The Hill Equation for Kinetic Data.

Hill (158, 96) assumed that for a polymeric protein the binding of ligand could be considered to occur in one step. Therefore for a multisubunit enzyme E binding with S the following one step reaction is envisioned:



It is assumed that the rate of product formation is the slowest step hence E and ES_n are at equilibrium, and further other complexes of E with S occur to a negligible extent. These assumptions are similar to those made in the Michaelis-Menten system and will not restated in detail. The nomenclature is also similar and

will be considered to be self explanatory. The rate of reaction is:

$$v = nk_p[ES_n] \quad \dots 8.7$$

therefore:

$$\frac{v}{[E]_t} = \frac{nk_p[ES_n]}{[E] + [ES_n]} \quad \dots 8.8$$

If K, a dissociation constant for the breakdown of ES_n to E and S is defined, then

$$\frac{v}{[E]_t} = \frac{\frac{nk_p[E][S]^n}{K}}{[E] + \frac{[E][S]^n}{K}} \quad \dots 8.9$$

and immediately:

$$\frac{v}{[E]_t} = \frac{nk_p[S]^n}{K + [S]^n} \quad \dots 8.10$$

If $nk_p[E]_t$ is defined as V_{\max} , the rate of reaction when all the enzyme is in the form of ES_n , then equation 8.11 results:

$$\frac{v}{V_{\max}} = \frac{[S]^n}{K + [S]^n} \quad \dots 8.11$$

The coefficient n is only equal to the number of subunits if the binding of S to E occurs in essentially one step. This situation would occur if the binding of the first molecule of S changes the conformation of the enzyme such that the affinity of the remaining sites for substrate was infinite. The binding would then be highly cooperative. In general the binding of the first molecule of S does not lead to an

infinite increase in the affinity of the other sites for substrate; hence n is actually less than the total number of subunits. Thus 8.11 is usually written as 8.12 where n the number of subunits is replaced by n_H the Hill coefficient.

$$\frac{v}{V_{\max}} = \frac{[S]^{n_H}}{K + [S]^{n_H}} \quad \dots 8.12$$

The Adair Equation

Adair (161, 162) assumed that the binding of ligand with a multisubunit protein did not necessarily occur in one step. Therefore the following equilibria is envisioned for a polymeric enzyme with n sites for substrate per molecule of enzyme.



$K_1, K_2, \dots, K_i, \dots$ and K_n are association (binding) constants of substrate to E and they include statistical factors which depend on the total number of binding sites as shown equation 8.13:

$$K_1 = \frac{[ES]}{[E][S]}; \quad K_2 = \frac{[ES_2]}{[ES][S]}$$

$$K_i = \frac{[ES_i]}{[ES_{i-1}][S]}; \quad K_n = \frac{[ES_n]}{[ES_{n-1}][S]} \quad \dots 8.13$$

The intrinsic binding constants, which express directly the inherent affinity of the individual binding sites for substrate, allows the assessment of what occurs after each substrate molecule binds. The K_i can be replaced by the intrinsic binding constants by using equation 8.14:

$$K_i = \frac{(n+1-i)}{i} K'_i \quad \dots 8.14$$

The net rate of reaction by the multisite enzyme is:

$$v = \sum_{i=1}^n i k_i [ES_i] \quad \dots 8.15$$

where k_i is the average rate of product formation from each site of a particular ES_i complex. Therefore:

$$\frac{v}{[E]_t} = \frac{k_1[ES] + 2k_2[ES_2] + \dots + i k_i [ES_i] + \dots + n k_n [ES_n]}{[E] + [ES] + \dots + [ES_i] + \dots + [ES_n]} \quad \dots 8.16$$

Hence in general, for a multisubunit enzyme the reaction rate is given by:

$$\frac{v}{[E]_t} = \frac{\sum_{i=1}^n i k_i \psi_i [S]^i}{1 + \sum_{i=1}^n \psi_i [S]^i} \quad \dots 8.17$$

where the ψ are products of the binding constants as shown in equation 8.18 below:

$$\psi_i = \prod_{j=1}^i \left(\frac{n+1-j}{j} \right) K'_j \quad \dots 8.18$$

For an enzyme with 4 binding sites the application of equations 8.17 and 8.18 give:

$$\frac{v_0}{[E]_t} = \frac{[4k_1 K'_1 S + 12k_2 K'_1 K'_2 S^2 + 12k_3 K'_1 K'_2 K'_3 S^3 + 4k_4 K'_1 K'_2 K'_3 K'_4 S^4]}{1 + 4K'_1 S + 6K'_1 K'_2 S^2 + 4K'_1 K'_2 K'_3 S^3 + K'_1 K'_2 K'_3 K'_4 S^4} \quad \dots 8.19$$

If $k_1 = k_2 = k_3 = k_4 = k_p$ and $4k_p[E]_t$ is replaced by V_{\max} , then 8.19 becomes 8.20 which is identical in form to the equation for the fractional saturation of a tetramer by a ligand. This form of the Adair equation is often used for the analysis of protein-ligand systems such as the haemoglobin-oxygen system.

$$\frac{v_0}{V_{\max}} = \frac{[K'_1 S + 3K'_1 K'_2 S^2 + 3K'_1 K'_2 K'_3 S^3 + K'_1 K'_2 K'_3 K'_4 S^4]}{1 + 4K'_1 S + 6K'_1 K'_2 S^2 + 4K'_1 K'_2 K'_3 S^3 + K'_1 K'_2 K'_3 K'_4 S^4} \quad \dots 8.20$$

Note that when the K'_i are equal to each other and thus are replaced by K' ; and the k_i are also equal to each other and thus are replaced by k_p , the system can be simplified to a form that is identical to the Michaelis-Menten equation. Since 8.20 then simplifies to:

$$\frac{v}{V_{\max}} = \frac{[S]}{\frac{1}{K'} + [S]} \quad \dots 8.21$$

where V_{\max} is $4k_p[E]_t$ and $1/K'$ is K_M .

The Concerted Allosteric Model of Monod, Wyman and Changeux.

The assumptions in the model of Monod et al (159) are that:

- 1) The protein is an oligomer which has at least 2 conformations and changes reversibly between both conformations;
- 2) All subunits occupy equivalent positions in the oligomer i.e. there must be at least one axis of symmetry in the oligomer;
- 3) There is only binding site per subunit;
- 4) The various conformations of the protein have different affinities for the substrate; and
- 5) The symmetry of the protein is conserved during conformation change, thus the conformation change must be a "concerted" all or nothing change in all subunits.

In the simpler allosteric model only 2 conformations the relaxed (**R**) and the tense (**T**) conformation are considered. The R state has the higher affinity for substrate. In this model K_R and K_T are the intrinsic dissociation constant for substrate from the R state and T state respectively. L is the equilibrium constant which describes the ratio of the T state to the R state in the absence of substrate. The following equilibria (Figure 56) then exists for a 4 subunit oligomer where $K_R/K_T = c$.

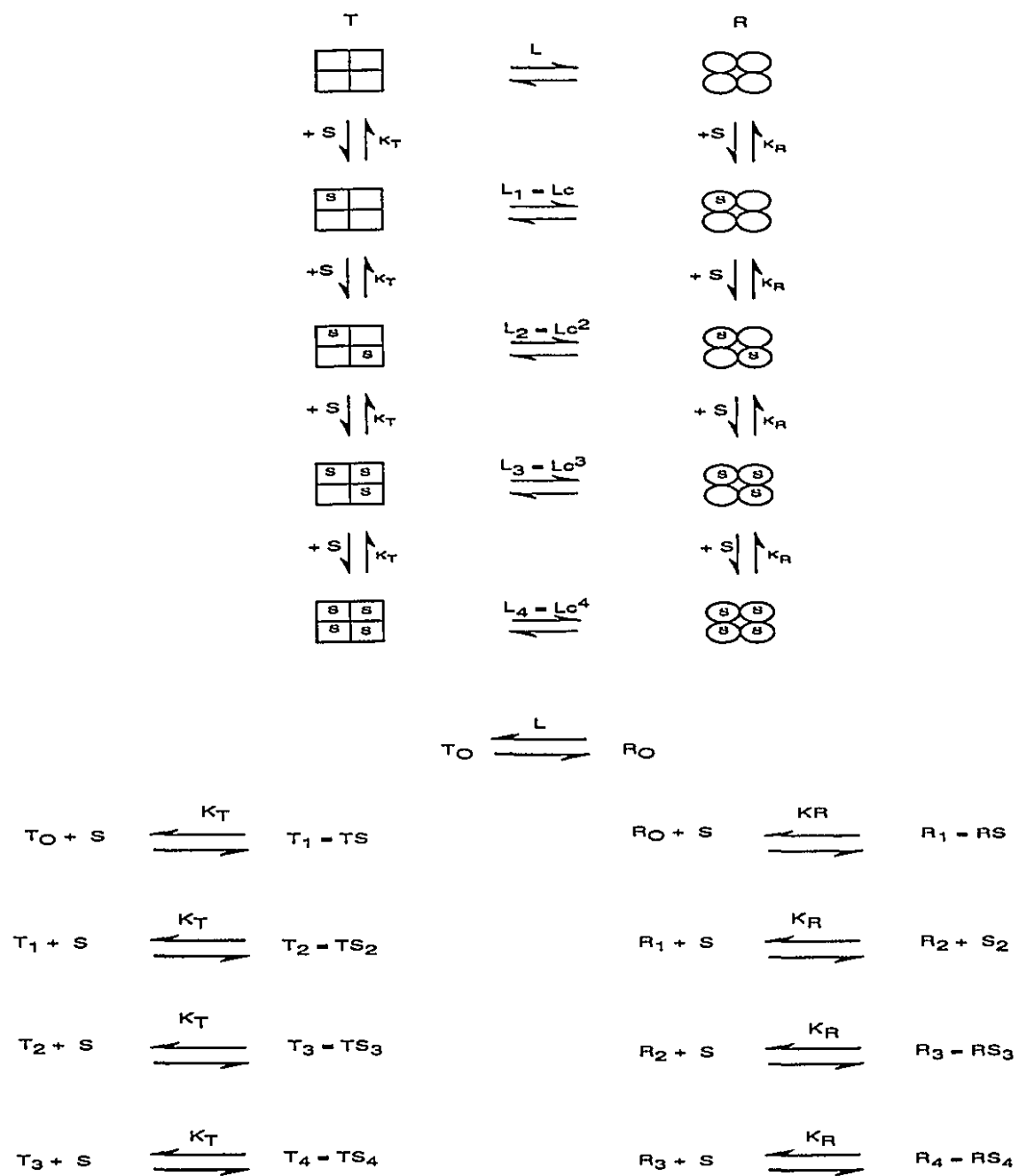


Figure 56. Equilibria visualized in the allosteric model of Monod, Wyman and Changeux.

The fraction of total sites occupied by S (the "saturation function") Y_s is:

$$\overline{Y}_s = \frac{([T_1] + 2[T_2] + 3[T_3] + 4[T_4]) + ([R_1] + 2[R_2] + 3[R_3] + 4[R_4])}{4([T_0] + [T_1] + [T_2] + [T_3] + [T_4]) + 4([R_0] + [R_1] + [R_2] + [R_3] + [R_4])} \quad \dots 8.22$$

The equilibrium relationships allow the substitution for the T_i and R_i , where the statistical values related to the different ways of forming a particular R_i or T_i complex must be considered. Therefore :

$$\begin{aligned} [R_i] &= \left(\frac{n-(i-1)}{i} \right) \frac{[R_{i-1}][S]}{K_R} \\ [T_i] &= \left(\frac{n-(i-1)}{i} \right) \frac{[T_{i-1}][S]}{K_T} \quad \dots 8.23 \end{aligned}$$

The equations are more readable if the following abbreviations are used:

$$\frac{[S]}{K_R} = \alpha; \quad \frac{K_R}{K_T} = c \quad \text{and} \quad \frac{[T_0]}{[R_0]} = L.$$

After substitution for R_i and T_i into equation 8.22 we get a more usable expression for Y_s the fractional saturation:

$$\overline{Y}_s = \frac{Lc\alpha(1 + c\alpha)^3 + \alpha(1 + \alpha)^3}{4L(1 + c\alpha)^4 + 4(1 + \alpha)^4} \quad \dots 8.24$$

In general for an n-sited oligomer:

$$\overline{Y}_s = \frac{Lc\alpha(1 + c\alpha)^{n-1} + \alpha(1 + \alpha)^{n-1}}{nL(1 + c\alpha)^n + n(1 + \alpha)^n} \quad \dots 8.25$$

If the protein is an enzyme and all sites with substrate release product at the same

rate whether the other sites are occupied or vacant; and further the rate of product formation is the rate limiting step then under this quasi-equilibrium condition:

$$\frac{v}{V_{\max}} = \overline{Y}_S = \frac{Lc\alpha(1 + c\alpha)^{n-1} + \alpha(1 + \alpha)^{n-1}}{nL(1 + c\alpha)^n + n(1 + \alpha)^n} \quad \dots 8.26$$

where v is the velocity or reaction rate, $V_{\max} = nk_p[E]_t$ is the maximum velocity which occurs when the enzyme is saturated with substrate, and n is the number of subunits.

Equation 8.26 shows clearly that if $c = 1$ or if L is very small the system becomes Michaelis-Menten. If the rate constant for product formation for the R state is different from that of the T state, the velocity relationship becomes:

$$v = \frac{k_T[E]_t Lc\alpha(1 + c\alpha)^{n-1} + k_R[E]_t \alpha(1 + \alpha)^{n-1}}{nL(1 + c\alpha)^n + n(1 + \alpha)^n} \quad \dots 8.27$$

The Induced Fit Interaction Model of Koshland, Nemethy and Filmer (KNF).

The assumptions of the interaction model of Koshland, Nemethy and Filmer (KNF) are that:

- 1) The subunits of the protein can exist in at least two different conformations. in the simplest scenario there are only 2 conformations **A** and **B** such that the subunit prefers conformation A in the absence of ligand and only B will bind ligand S. Symmetry does not need to be conserved, hence some subunits can be in the A conformation while others are in the B conformation;
- 2) Cooperativity in the system results from conformation changes as the protein becomes saturated with substrate;
- 3) When the protein is an enzyme, the usual quasi-equilibrium assumption

tions apply; that is the system is far from equilibrium; and the rate limiting step is the rate of product formation from the various complexes of enzyme with substrate.

The constants K_S , K_t , K_{AB} , and K_{BB} are defined for the KNF model as shown below:

$$K_S = \frac{[BS]}{[B][S]}$$

$$K_t = \frac{[B]}{[A]}$$

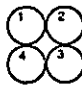
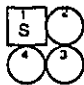
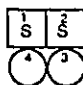
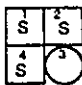
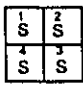
$$K_{AB} = \frac{[AB][A]}{[AA][B]}$$

$$K_{BB} = \frac{[BB][A][A]}{[AA][B][B]}$$

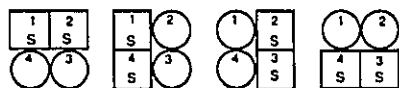
K_S is the substrate binding constant and represents the intrinsic affinity of the ligand for an individual subunit. K_t is the transformation constant for a subunit change from conformation A to conformation B. K_{AB} is the equilibrium constant which measures the strength of the interaction between two subunits when the active site of one is occupied, and the active site of the other is vacant. K_{BB} is an equilibrium constant measures the strength of the interaction between two subunits when both their active sites are occupied. K_{AA} which measures the strength of interaction between 2 subunits when their active sites are vacant, is set equal to one.

The possible subunit interactions which can occur in a protein depend on the arrangement of the subunits. For a tetramer arranged as a "square" the possible interactions are shown below (Figure 57). Note that the "square" arrangement does not imply a particular arrangement in space, other than that

each subunit interacts with only 2 others, and that diagonal interactions are not being considered.

		\xrightarrow{S}		\xrightarrow{S}		\xrightarrow{S}		\xrightarrow{S}	
Complex	A_4		A_3BS		$A_2B_2S_2$		AB_3S_3		B_4S_4
Number of modes of binding S		1		2		1		1	
Number of ways of arranging S		4		4 [*] 2 ^{**}		4		1	
Number of possible AB interactions		2		2 2		2		0	
Number of possible BB interactions		0		1 0		2		4	
Term for species (concentration relative to A_4)		$4K_{AB}^2(K_S K_d S)$		$(4K_{AB}^2 K_{BB} + 2K_{AB}^4)(K_S K_d S)^2$		$4K_{AB}^2 K_{BB}^2 (K_S K_d S)^3$		$K_{BB}^4 (K_S K_d S)^4$	
Effective catalytic rate constant of complex (k_p)		$1k_p$		$2k_p$		$3k_p$		$4k_p$	

*Four cis arrangements of ES_2



** Two "trans" arrangements of ES_2

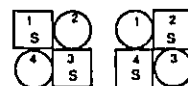


Figure 57.

Scheme of subunit interactions which occur in the sequential interaction model of Koshland, Nemethy and Filmer for the square arrangement.

Assuming that the rapid equilibrium assumption holds, and that the rate limiting steps are the product forming steps; then the following expression for the velocity of the tetrameric enzyme is:

$$\frac{v}{[E]_i} = \frac{k_p[ES] + 2k_p[ES_2] + 3k_p[ES_3] + 4k_p[ES_4]}{4([E] + [ES] + [ES_2] + [ES_3] + [ES_4])} \quad \dots 8.28$$

where it is assumed that the average rate constant for product formation per occupied active site is equal to k_p for all species.

The concentration of each enzyme specie can be expressed in terms of the equilibrium constants defined for the KNF model by referring to the above illustration, hence:

$$[ES] = [A_3BS] = 4K_{AB}^2(K_S K_i[S])[A_4]$$

$$[ES_2] = [A_2B_2S_2] = (4K_{AB}^2K_{BB} + 2K_{AB}^4)(K_S K_i[S])^2[A_4]$$

$$[ES_3] = [AB_3S_3] = 4K_{AB}^2K_{BB}^2(K_S K_i[S])^3[A_4]$$

$$[ES_4] = [B_4S_4] = K_{BB}^4(K_S K_i[S])^4[A_4]$$

If $4k_p[E]_i$ is set equal to V_{max} and the expressions for the various complexes are substituted into equation 8.28 the following expression for the rate results:

$$\frac{V_0}{V_{max}} = \frac{K_{AB}^2(K_S K_i[S]) + (2K_{AB}^2K_{BB} + K_{AB}^4)(K_S K_i[S])^2 + 3K_{AB}^2K_{BB}^2(K_S K_i[S])^3 + K_{BB}^4(K_S K_i[S])^4}{1 + 4K_{AB}^2(K_S K_i[S]) + (4K_{AB}^2K_{BB} + 2K_{AB}^4)(K_S K_i[S])^2 + 4K_{AB}^2K_{BB}^2(K_S K_i[S])^3 + K_{BB}^4(K_S K_i[S])^4} \quad \dots 8.29$$

If K_{AB} is equal to the square root of K_{BB} in the square sequential interaction model, then the system simplifies to:

$$\frac{v}{V_{\max}} = \frac{K_{BB}K_S K_I [S]}{1 + K_{BB}K_S K_I [S]} \quad \dots 8.30$$

which is Michaelis-Menten in form.

8.4 APPENDIX IV

8.4.1. Photomicrographs of Microcapsules Prepared Similarly to Those Used in Comparative (Free Versus Microencapsulated) Kinetic Studies.

The following photographs (Figures 58 and 59) show freshly prepared microcapsules, and microcapsules from the same batch after 2 months of storage in the cold-room (4 °C). The microcapsules were made with a polylysine reaction time of 10 minutes, and with Kelco-Gel® HV (high viscosity) alginate that had been sterilized for 5 minutes as described previously. The airflow to the droplet former was 2.5 l/min. Note that after 2 months the microcapsules still maintain their integrity.

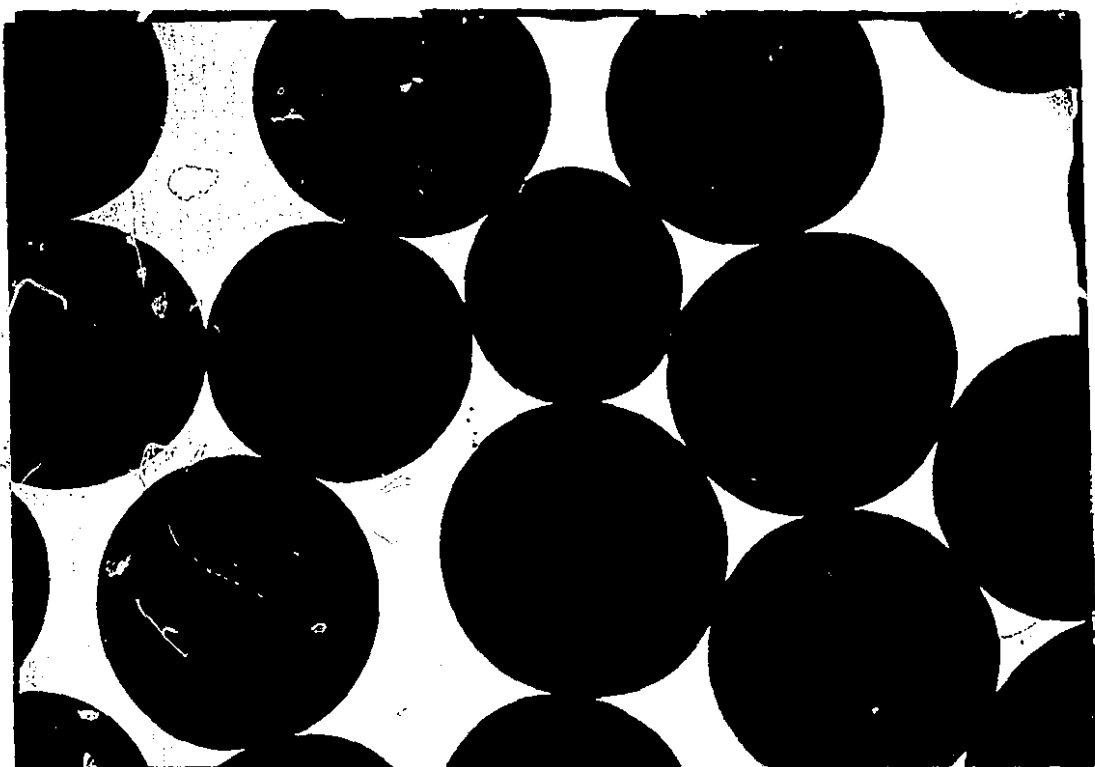


Figure 58. Freshly prepared microcapsules made with Kelco-Gel® HV alginate

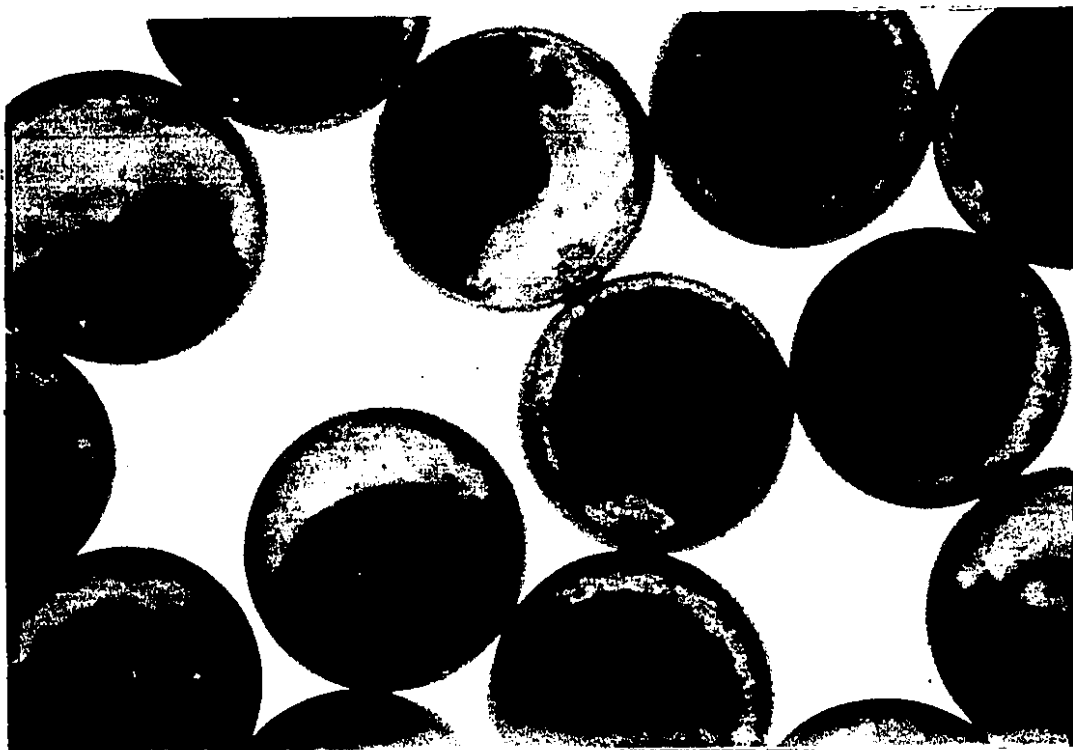


Figure 59. Microcapsules from the same batch as those shown in Figure 58 after 2 months of storage at 4°C.

8.5 APPENDIX V.

4.5.2 Development of an Approximate Kinetic Model for the Conversion of Ammonia, Phenol and Pyruvate into Tyrosine.

Model Development

Mechanistic Considerations.

The postulated mechanism for the degradation of tyrosine by tyrosine phenol-lyase (73, 99) implies that the production of tyrosine occurs by an ordered ter-uni mechanism. A simplified scheme of the process is shown as Figure 60, in

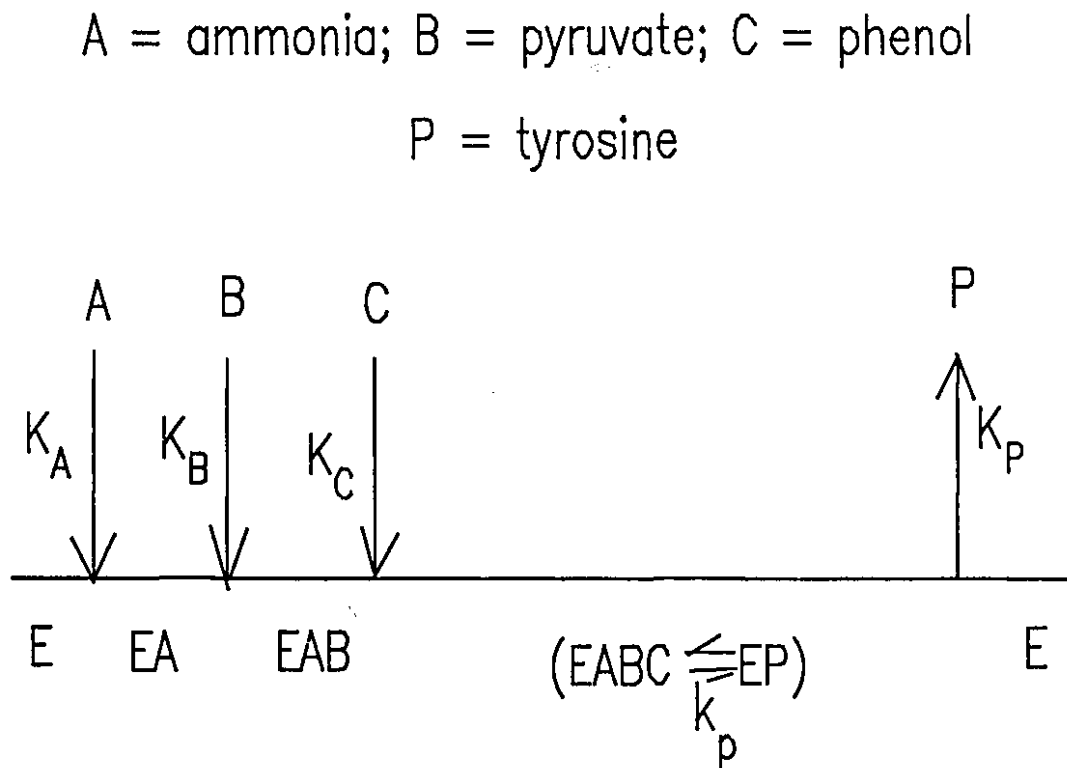


Figure 60. Scheme of the steps in the formation of tyrosine from ammonia, phenol and pyruvate by tyrosine phenol lyase (assuming the enzyme has identical and equivalent active sites).

which ammonia, phenol and pyruvate are bound by the enzyme in that order, before the release of phenol.

This reaction scheme implies that under rapid equilibrium conditions (164) the reaction rate when the system is far from equilibrium is given by:

$$\frac{v}{[E]_{total}} = \frac{k_p[EABQ]}{[E] + [EA] + [EAB] + [EABQ] + [EP]} \quad \dots(8.31)$$

This equation assumes that subunit interactions are negligible *i.e.* each active site is identical, and equivalent. After substitution for the concentration of each enzyme specie by the appropriate equilibrium relationships (using the nomenclature from Figure 60), and replacing $k_p[E]_i$ by V_{max} , equation 8.32 results:

$$\frac{v}{V_{max}} = \frac{\frac{[A][B][Q]}{K_A K_B K_C}}{1 + \frac{[A]}{K_A} + \frac{[A][B]}{K_A K_B} + \frac{[A][B][Q]}{K_A K_B K_C} + \frac{[P]}{K_P}} \quad \dots(8.32)$$

Therefore if the concentration of ammonia and pyruvate are equal, and greater than the concentration of phenol then equation 8.33, an integral form of equation 8.32, can be readily derived.

$$\begin{aligned} V_{max} \int_0^t dt = & - C_1 \int_{S_0}^S dS - C_2 \int_{S_0}^S \frac{S dS}{S} \\ & - C_3 \int_{S_0}^S \frac{S dS}{(H+S)S} - C_4 \int_{S_0}^S \frac{S dS}{(H+S)^2 S} + C_5 \int_{S_0}^S \frac{S dS}{(H+S)^2} \end{aligned} \quad \dots(8.33)$$

where:

$$C_1=1; \quad C_2=K_Q; \quad C_3=K_B K_Q; \quad C_4=K_A K_B K_C \left(1 + \frac{S_0}{K_P}\right);$$

$$\text{and } C_5 = K_A K_B \frac{K_C}{K_P}$$

S has been substituted for the concentration of phenol, therefore $[A] = [B] = H + S$, where $H = [A]_0 - [C]_0$ and it is assumed that the concentration of tyrosine $[P]$ is $S_0 - S$ since $[P]_0$ is equal to zero. After integration, equation 8.33 gives equation 8.34.

$$t = \frac{1}{V_{\max}} \left(C_1(S_0 - S) + \left(C_2 + \frac{C_3}{H} + \frac{C_4}{H^2} \right) \ln \frac{S_0}{S} - \left(\frac{C_3}{H} + \frac{C_4}{H^2} \right) \ln \frac{H+S_0}{H+S} + \left(C_5 + \frac{C_4}{H} \right) \left(\frac{1}{(H+S_0)} - \frac{1}{(H+S)} \right) \right) \quad \dots(8.34)$$

Mixed Type Inhibition by Phenol Considerations.

It has been reported that phenol inhibits tyrosine phenol-lyase (78, 86, 107). In the degradation of tyrosine by TPL, phenol inhibits the reaction with mixed type kinetics (78, 86). Therefore we may imagine that the following equilibria (Figure 61) also occur in the system outlined in Figure 60 for the production of tyrosine. K_i is the inhibition constant for phenol, and the notation of Figure 61 is the same as that in Figure 60, *i.e.* C is phenol, and P is tyrosine. This represents the simplest mixed type inhibition mechanism by phenol; and it presumes that there is a site for phenol other than the active site (where tyrosine or ammonia, pyruvate and phenol in that order binds).

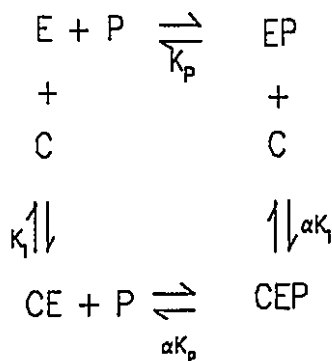


Figure 61. A simple mechanism which accounts for the mixed type inhibition of TPL by phenol reported by Kumagai (1972).

Consideration of this equilibria leads to a rapid equilibrium relationship for the reaction rate as shown below:

$$\frac{v}{V_{\max}} = \frac{\frac{[A][B][C]}{K_A K_B K_C}}{1 + \frac{[A]}{K_A} + \frac{[A][B]}{K_A K_B} + \frac{[A][B][C]}{K_A K_B K_C} + \frac{[P]}{K_P} + \frac{[C]}{K_I} + \frac{[C][P]}{\alpha K_I K_P}} \quad \dots(8.35)$$

After separation of variables and integration (from S_0 to S) equation 8.36 is obtained. It is assumed that as in equation 8.33 the concentrations of ammonia and pyruvate are equal and greater than the concentration of phenol.

$$t = \frac{1}{V_{\max}} \left(C_1(S_0 - S) + (C_2 + \frac{C_3}{H} + \frac{C_4}{H^2}) \ln \frac{S_0}{S} - (\frac{C_3}{H} + \frac{C_4}{H^2} + C_6) \ln \frac{H+S_0}{H+S} + \right. \\ \left. (\frac{C_4}{H} - C_5 - C_6 H) (\frac{1}{(H+S_0)} - \frac{1}{(H+S)}) \right) \quad \dots(8.36)$$

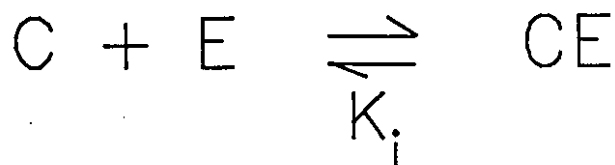
where:

$$C_1=1; \quad C_2=K_C; \quad C_3=K_B K_C; \quad C_4=K_A K_B K_C; \quad C_5=K_A K_B K_C \left(\frac{1}{K_I} - \frac{1}{K_P} + \frac{S_0}{\alpha K_I K_P} \right)$$

$$\text{and } C_6 = \frac{K_A K_B K_C}{\alpha K_I K_P}$$

Simple Inhibition by Phenol Considerations.

Para, Luciardi and Barrati (107) claimed that the inhibition by phenol of whole cell TPL was analyzable by "classical" inhibition kinetics. This results conflicts with that reported by Kumagai et al (78, 86) which suggest mixed inhibition by phenol. If Para *et al* are correct the only equilibrium (in addition to those in Figure 60) that needs to be considered is:



where phenol (C) binds to the inhibitory site, with dissociation constant K_i . The rapid equilibrium expression for the reaction rate of this system (again using the notation of Figure 60) is :

$$\frac{v}{V_{\max}} = \frac{\frac{[A][B][C]}{K_A K_B K_C}}{1 + \frac{[A]}{K_A} + \frac{[A][B]}{K_A K_B} + \frac{[A][B][C]}{K_A K_B K_C} + \frac{[A]}{K_P} + \frac{[C]}{K_I}} \quad \dots(8.37)$$

After separation of variables and integration, this equation gives 8.38.

$$t = \frac{1}{V_{\max}} \left(C_1(S_0 - S) + \left(C_2 + \frac{C_3}{H} + \frac{C_4}{H^2} \right) \ln \frac{S_0}{S} - \left(\frac{C_3}{H} + \frac{C_4}{H^2} \right) \ln \frac{H+S_0}{H+S} + \left(\frac{C_4}{H} - C_5 \right) \left(\frac{1}{(H+S_0)} - \frac{1}{(H+S)} \right) \right) \quad \dots(8.38)$$

where:

$$C_1=1; \quad C_2=K_C; \quad C_3=K_B K_C; \quad C_4=K_A K_B K_C \left(1 + \frac{S_0}{K_P} \right) \quad \text{and} \quad C_5=K_A K_B K_C \left(\frac{1}{K_I} - \frac{1}{K_P} \right)$$

Saturation by Phenol Considerations

If K_A is large relative to K_B and K_C then when small amounts of ammonia are in the system (relative to its K_A i.e. pseudo K_M) as soon as EA is formed it will be transformed to EAB and EABC. Therefore [E] and [EA] will be small relative to [EAB], [EABC] and [EP], hence equation 8.31, 8.32, and 8.34 become 8.39, 8.40 and 8.41 respectively.

$$\frac{v}{[E]_{total}} = \frac{k_p[EABC]}{[EAB] + [EABC] + [EP]} \quad \dots(8.39)$$

$$\frac{v}{V_{max}} = \frac{\frac{[A][B][C]}{K_A K_B K_C}}{\frac{[A][B]}{K_A K_B} + \frac{[A][B][C]}{K_A K_B K_C} + \frac{[P]}{K_P}} \quad \dots(8.40)$$

$$t = \frac{1}{V_{max}} \left(C_1(S_0 - S) + \left(C_2 + \frac{C_4}{H^2} \right) \ln \frac{S_0}{S} - \left(\frac{C_4}{H^2} \right) \ln \frac{H+S_0}{H+S} + \right. \\ \left. \left(C_5 + \frac{C_4}{H} \right) \left(\frac{1}{(H+S_0)} - \frac{1}{(H+S)} \right) \right) \quad \dots(8.41)$$

$$\text{where } C_1=1; C_2=K_C; C_4=(K_A K_B) K_C \frac{S_0}{K_P}; C_5=(K_A K_B) \frac{K_C}{K_P}$$

8.6 APPENDIX VI

8.6.1 Data Obtained After Prolonged Reaction at 37 °C.

Figure 62 show data for the conversion of ammonia, pyruvate and phenol to tyrosine by the TPL activity of microencapsulated whole cell *Erwinia herbicola*. Note the microcapsules can survive after vigorous shaking for 24 hours.

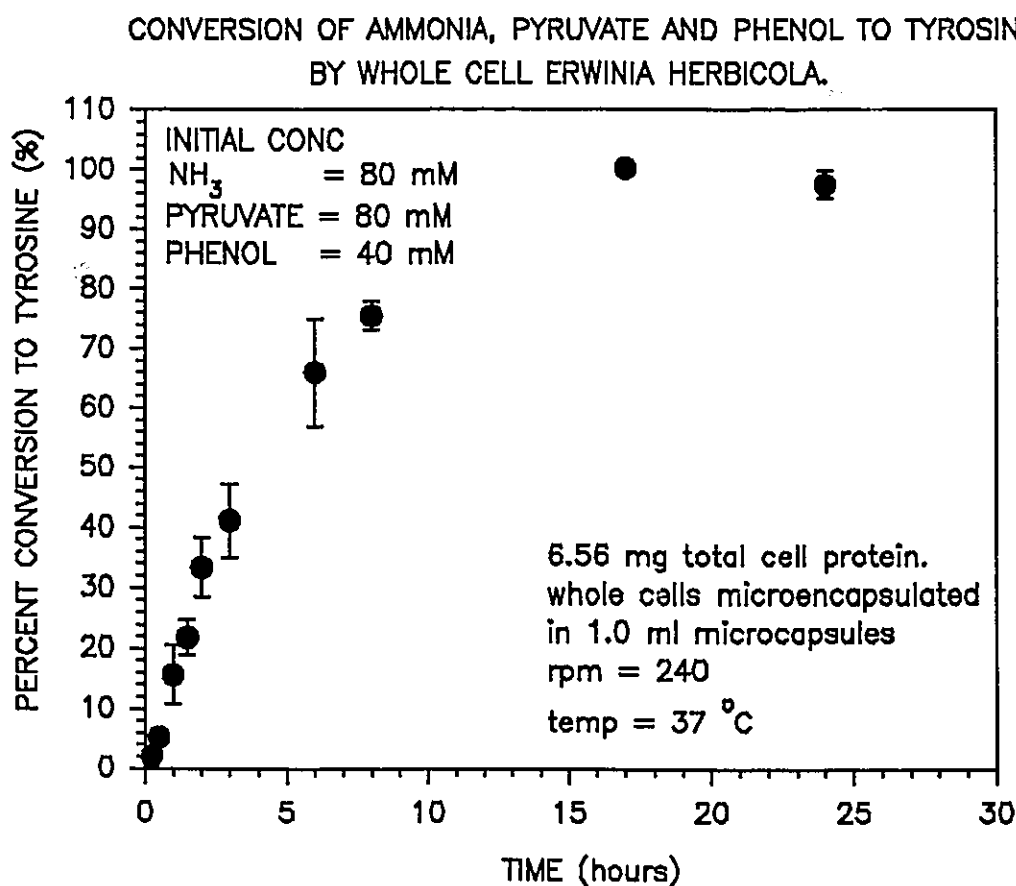


Figure 62. One example of the conversion of ammonia, phenol and pyruvate to tyrosine (Initial phenol concentration 50mM).